CC2 response method using local correlation and density fitting approximations for the calculation of the electronic g-tensor of extended open-shell molecules

Dissertation zur Erlangung des akademischen Grades
doctor rerum naturalium
(Dr. rer. nat.)

Im Fach Chemie
Spezialisierung Physikalische und Theoretische Chemie

eingereicht an der
Mathematisch-Naturwissenschaftlichen Fakultät der Humboldt-Universität zu Berlin
von
M. Sc. Evelin Martine Christlmaier
geb. Martin Josef Adolf Christlmaier

Präsidentin der Humboldt-Universität zu Berlin
Prof. Dr.-Ing. habil. Dr. Sabine Kunst

Dekan der Mathematisch-Naturwissenschaftlichen Fakultät
Prof. Dr. Elmar Kulke

Gutachter_innen:

1. PD Dr. Denis Usvyat
2. Ph.D. D.Sc. Tatiana Korona
3. Prof. Dr. Martin Kaupp

Tag der mündlichen Prüfung: 10.05.2021

Selbständigkeitserklärung

Ich erkläre, dass ich die Dissertation selbständig und nur unter Verwendung der von mir gemäß § 7 Abs. 3 der Promotionsordnung der Mathematisch-Naturwissenschaftlichen Fakultät, veröffentlicht im Amtlichen Mitteilungsblatt der Humboldt-Universität zu Berlin Nr. 42/2018 am 11.07.2018 angegebenen Hilfsmittel angefertigt habe.

Berlin, den 02.12.2020

Evelin Martine Christlmaier
(juristisch: Martin Josef Adolf Christlmaier)

Summary

This work presents an unrestricted coupled-cluster CC2 response method using local correlation and density fitting approximations for the calculation of first and second order properties with particular focus on the electronic g-tensor. The fundamental concepts related to coupled-cluster theory, density fitting, local correlation, general coupled-cluster properties and the electronic g-tensor are discussed. The calculated g-tensors are benchmarked against those obtained from coupled-cluster singles and doubles, density functional theory and experiment. Efficiency and accuracy of the approximations is investigated. A detailed appendix covers the fundamentals of diagrammatic coupled-cluster and its application to the derivation of the working equations. The method presented in this thesis enables the quantitative prediction of the electronic g-tensor of extended systems with a method other than density functional theory. It represents an important step towards the development of low-scaling higher order coupled-cluster methods for this type of problem.

Zusammenfassung

In dieser Arbeit wird eine unrestricted Coupled-Cluster CC2 Response-Methode für die Berechnung von Eigenschaften erster und zweiter Ordnung, mit dem elektronischen g-Tensor als Schwerpunkt, präsentiert. Lokale Korrelations- und Dichtefittingnäherungen wurden verwendet. Die fundamentalen Konzepte notwendig für das Verständnis von Coupled-Cluster-Theorie, Dichtefitting, lokaler Korrelation, allgemeinen Coupled-Cluster Eigenschaften und dem elektronischen g-Tensor werden diskutiert. Die berechneten g-Tensoren werden mit denen durch Coupled-Cluster Singles and Doubles, Dichtefunktionaltheorie und Experiment erhaltenen verglichen. Effizienz und Genauigkeit der Näherung wird untersucht. Ein detailierter Anhang beschreibt die diagrammatische Coupled-Cluster-Theorie sowie ihre Anwendung zur Herleitung der verwendeten Arbeitsgleichungen. Die in dieser Arbeit entwickelte Methode ermöglicht es, den elektronischen g-Tensor von ausgedehnten Systemen mit einer Methode, die nicht auf Dichtefunktionaltheorie basiert, quantitativ vorherzusagen. Damit ist sie ein wichtiger Schritt hin zur Entwicklung von niedrig skalierenden Coupled-Cluster-Methoden höherer Ordnung für diese Art von Problem.

Acknowledgements

Completion of this work was made possible by the support of various people. In the following, I offer my thanks and appreciation to them.

To my advisor Denis Usvyat for taking over when my initial advisor became unavailable and investing significant time and effort into helping me finish my project. He is not just willing to tolerate my endless questions and discussions about pretty much everything, but also provides an environment very conducive to the well-being of his students.

To David David for his help in understanding his underlying open-shell code and theory as well as interesting discussions about sometimes unrelated issues.

To Daniel Kats for answering questions regarding the closed-shell code, providing a custom LaTeX package for drawing coupled-cluster diagrams and writing a simplified canonical implementation of my equations for debugging purposes.

To our system administrator Thomas Dargel for his support in technical questions.

To Cornelia Krell for taking over as much of the administrative affairs as was possible.

To my remaining colleagues in Regensburg and Berlin for providing a good work environment. In no particular order Stefan Loibl, Gero Wälz, Matthias Hinreiner, Oliver Masur, Alexander Krach, Jakob Kottmann, Ernst-Christian Flach, Thomas Mullan, Elizaveta Rogozina and anyone else who thinks they should be on this list but has slipped my mind right now. Additional thanks go to Ernst-Christian Flach and especially Alexander Krach for putting up with the worst of my idiosyncracies for multiple years and proofreading this thesis. Many typos have been squashed thanks to their efforts.

To my immediate family, my mother Monika and my sisters Christina and Nicole, for their support and understanding and for being a source of strength and persistence for me.

To my friends Roland Trepesch and Sybille Heintz who accepted me despite all my faults and provided vital support when I needed it most.

Posthumously to my father Josef Christlmaier and my initial advisor Prof. Dr. Martin Schütz for doing their part in setting me on the path that led me here.

To Ahjith Perera and Jorge Morales for kindly providing not just their geometries but also their raw data, allowing for some interesting comparisons with my own results.

Finally, I want to express my gratitude to the people in my life for just accepting me the way I am when after almost two decades of internal struggles I finally decided to be honest with myself and the rest of the world and started my transition in the middle of 2020. Aside from the expected resistance from the bureaucracy and some unexpected but fortunately not very relevant gatekeeping from unhelpful medical professionals, I have met virtually no resistance or judgment so far. This is unfortunately far from the norm, and I am very grateful for the positive response to my revelation. It has made my endeavor so much easier than I ever hoped it could be.

Contents

Chapter 1

Introduction

Spin is the angular momentum of a particle at rest[1] and is a purely quantum mechanical phenomenon with no classical analogue. Stern and Gerlach[2,3] first observed its effects in their famous experiment on the anomalous Zeeman splitting of a beam of silver atoms into two well-defined peaks when directed through a heterogeneous magnetic field. The theoretical interpretation of the spin as an additional degree of freedom of an electron next to the spatial coordinates with two discrete values followed shortly afterwards by Pauli.[4]

The observations made by Stern and Gerlach are the foundation for the field of electron spin resonance (ESR) spectroscopy, which was pioneered by Zavoisky.[5] The magnitude of the splitting is not just governed by the direct interaction of the electronic spin with an external magnetic field, but also by spin-orbit coupling and additional relativistic corrections. This leads to a generally anisotropic splitting represented by the so-called electronic g-tensor, a 3×3 matrix that reduces to the free electron g-value in the case of an isolated electron. In addition to the g-tensor, ESR spectroscopy also measures additional hyperfine splittings due to interactions of the nuclear spins with the electronic spin and zero-field splitting in triplet states and higher due to interactions of the electronic spins of the unpaired electrons.

ESR spectroscopy, also called electronic paramagnetic resonance (EPR) spectroscopy when applied to transition metal compounds, has become a vital experimental tool. Applications include the study of organic radicals, open-shell transition ions and complexes, inorganic radicals, radical and metal active sites in proteins and short-lived charge separated states in photosynthesis.[6–9] A reliable theoretical prediction of the observable constants is therefore very desirable. A thorough review of the historical development of ESR calculations including an overview of the experimental developments has been given by Neese and Munzurová.[6]

The interface between theory and experiment is provided by the spin Hamiltonian, which depends only on electronic and nuclear spins, the magnetic field and observable coupling constants. The first clean derivation has been presented by McWeeny in 1965[10], who in the same work also showed that the g-tensor can be obtained via simple contraction of spatial integrals with normalized spin densities. Together with Moores[11], he reported the first ab initio calculations of the electronic g-tensor about a decade later, although with neglect of the Zeeman kinetic energy correction. A very exhaustive and consistent description of the theoretical foundations of electron spin resonance has been published by Harriman in 1978.[12]

Not much happened in the field of ab initio g-tensor calculation after that until the

1990s, when Lushington and Grein employed Hartree-Fock (HF)[13–15] and multi-reference configuration interaction (MRCI)[16–18] to evaluate the g-tensor. Their later work included all contributions to the g-tensor up to second order in the fine structure constant α, but they employed only a truncated sum-over-states formalism and did not rigorously solve the gauge origin problem. Shortly thereafter, Vahtras *et al.* developed a multi-reference treatment using response theory.[19–25] Simultaneously, Ziegler *et al.* developed a density functional theory (DFT) treatment using double perturbation theory and gauge-including atomic orbitals (GIAOs).[26–32]

More recently, Gauss *et al.*[33] have provided a gauge invariant coupled-cluster singles and doubles (GIAO-CCSD) method using effective charges to approximate the two-electron contributions which has since been enhanced by Perera *et al.*[34] to provide the first g-tensor implementation using exact two-electron contributions. This provides a high-quality benchmark for the evaluation of the quality of lower order methods. A density functional theory method using a spin-orbit mean-field (SOMF) operator for extended molecules has recently been developed by Glasbrenner *et al.*[35] They showed not only that it is necessary to address the gauge issue for calculations on extended systems, but that for systems with a single spin-center this can be achieved via a common gauge origin at that center. Using this insight, they implemented a DFT method that only evaluates the perturbed densities in regions of significant spin density, thus achieving sublinear scaling with molecular size.[36]

Aside from treating the spin-orbit coupling as a perturbation in a one-component calculation, as has been the case in the studies cited so far, it is also possible to use multi-component relativistic approaches instead.[37–42] They have the advantage of being able to include the full spin-orbit coupling instead of only keeping the lowest order contribution in the fine structure constant α, which is especially important if heavy atoms or near-degeneracies are involved.

So far, DFT is the only practical option for g-tensor calculations on extended systems. Hartree-Fock is not even qualitatively correct[33] and more advanced wave function based methods scale very unfavorably with the system size in their canonical implementations. Local correlation methods however can achieve quantitative description of even extended systems with acceptable computational effort.[43,44] They have been successfully employed for the treatment of closed-shell ground as well as singlet and triplet excited states and their first order properties[45–51], nuclear magnetic resonance shielding tensors[52], magnetizabilites and rotational g-tensors[53], ionization potentials[54], excited states of open-shell molecules[55] and more. In this work, their reach is extended to first and second order properties of open-shell molecules, with particular focus on the electronic g-shift. This represents an important step towards a low-scaling coupled-cluster hierarchy for the treatment of the g-shift and other spin dependent properties of extended open-shell systems, e. g. the hyperfine coupling tensors.

This thesis is structured as follows: In chapter 2 we introduce the underlying theoretical concepts, i.e. coupled-cluster theory, density fitting, local correlation, general coupled-cluster properties, specific considerations for the g-tensor and the working equations. In chapter 3 we compare the obtained g-shifts with other quantum chemical methods and experiment and investigate the effect of varying the internal degrees of freedom in the employed approximations on both the efficiency of the calculations and the quality of the results. Appendix A contains a brief description of the connection between the proper quantum mechanical treatment and the spin Hamiltonian and demonstrates that evaluation of the g-tensor can be achieved via contraction of purely spatial integrals with

spin density matrices. Appendix B gives a detailed review of second quantization and its relevance to diagrammatic coupled-cluster followed by an extensive derivation of the working equations. Finally, appendix C contains the tabulated values employed for the comparisons in chapter 3.

Chapter 2

Theory

2.1 DF-LUCC2

2.1.1 Coupled-cluster theory

2.1.1.1 Coupled-cluster ansatz

The coupled-cluster ansatz (CC)[56–60] is a multi-determinant ansatz that generates additional determinants from a reference determinant $|0\rangle$, usually a Hartree-Fock wave function, via application of an exponential substitution operator

$$|CC\rangle = exp(T)|0\rangle. \tag{2.1}$$

We deliberately avoid here the usual terminology of "excitations" since it incorrectly implies an equivalency of "excited" determinants and electronically excited states. This mistake is often appealing to beginning students of quantum chemistry due to widely spread misconceptions[61] about orbitals in applied chemistry and should be addressed as early as possible.
The cluster operator T is just the sum over all possible orbital substitutions

$$T = \sum_{\mu} t_\mu \tau_\mu, \tag{2.2}$$

with τ_μ being the substitution operator for a specific orbital substitution and t_μ the corresponding probability amplitude.
Similar to configuration-interaction theory (CI), the cluster operator can be partitioned into different substitution classes

$$T = \sum_{n=1}^{min(N_{\text{elec}},N_{\text{virt}})} T_n, \tag{2.3}$$

where T_n contains all operators that substitute n occupied orbitals in the reference determinant with n unoccupied, also called virtual, orbitals.
Unlike CI, CC maintains size consistency, i.e. the additivity of the energies of non-interacting systems, and size extensivity, i.e. the proper scaling of the energy with the system size, when truncating the cluster operator.

2.1.1.2 Linked coupled-cluster

The CC energy expectation value

$$\langle CC|H|CC\rangle = \langle 0|\exp(T^\dagger)H\exp(T)|0\rangle \tag{2.4}$$

involves substitution operators acting on the determinants to the left and right and results into a computationally inconvenient formalism. Solving the CC equations via projection onto the reference determinant $|0\rangle$ and the "excited" determinants $|\mu\rangle$

$$\langle 0|H\exp(T)|0\rangle = E \tag{2.5}$$
$$\langle \mu|H\exp(T)|0\rangle = E\langle \mu|exp(T)|0\rangle \tag{2.6}$$

circumvents this issue.
In order to avoid the appearance of the energy in the amplitude equations, an additional factor of $\exp(-T)$ is included in the projection

$$\langle 0|\exp(-T)H\exp(T)|0\rangle = E \tag{2.7}$$
$$\Omega_\mu = \langle \mu|\exp(-T)H\exp(T)|0\rangle = 0, \tag{2.8}$$

where we have assumed orthogonality of occupied and virtual orbitals and therefore reference and "excited" determinants.
Aside from the disappearance of the energy from the amplitude equations Ω_μ, these so-called linked CC equations have the advantage that one can use the Baker-Campbell-Hausdorff expansion (BCH)

$$\begin{aligned}\exp(-T)H\exp(T) &= \sum_{n=0}^{4}\frac{1}{n!}\big([\,]\big)^n H\big(,T]\big)^n \\ &= H + [H,T] + \frac{1}{2}[[H,T],T] + \frac{1}{6}[[[H,T],T],T] + \frac{1}{24}[[[[H,T],T],T],T].\end{aligned} \tag{2.9}$$

This similarity transformation terminates after $n = 4$ due to reasons discussed in appendix B.2.5. Furthermore, each individual term arising from the BCH-expansion leads to a size consistent and extensive contribution. This in turn allows for easy introduction of approximate models neglecting some of the more expensive contributions.
Note that use of the linked CC formalism is equivalent to optimizing the Lagrangian

$$L = E + \sum_\mu \lambda_\mu \Omega_\mu, \tag{2.10}$$

which will become important for the derivation of properties.

2.1.1.3 Similarity transformed Hamiltonian

In many CC methods the singles are included with all terms arising form the BCH-expansion. In order to reduce the complexity of the theory it is thus convenient to introduce the similarity transformed Hamiltonian

$$\hat{H} = \exp(-T_1)H\exp(T_1), \tag{2.11}$$

where the hat in $\hat{H}$ is used here and in the following to signify an operator (or integral) transformed in this way. This allows implicit inclusion of the singles substitutions T_1 via transformation of the integrals (see appendix B.2.6). These transformed operators and integrals are in the following referred to as "dressed".

2.1.1.4 CC2 approximation

This work employs the CC2 approximation[62] to the coupled-cluster singles and doubles (CCSD) method, which reduces the scaling with the system size from $\mathcal{O}(\mathcal{N}^6)$ to $\mathcal{O}(\mathcal{N}^5)$. In order to introduce this method we first partition the Hamiltonian

$$H = F^{(0)} + V^{(1)}, \tag{2.12}$$

where $F^{(0)}$ is the Fock operator and the fluctuation potential $V^{(1)}$ describes the deviation from the Hartree-Fock mean-field of the actual field experienced by the electrons due to each other.
Like CCSD, the CC2 model truncates the cluster operator to singles and doubles substitutions. The singles amplitude equations Ω_{μ_1} contain no further approximations and the singles substitutions T_1 are treated as zeroth order parameters. This ensures that approximate orbital relaxation is effectively included via the singles substitutions even in orbital-unrelaxed property calculations like those reported in this thesis.
The doubles amplitude equations Ω_{μ_2} on the other hand are restricted to contributions of first order in $V^{(1)}$, thus removing some of the more expensive CCSD terms.
Enforcing these approximations and using the previously introduced dressed operators yields the CC2 energy and amplitude equations

$$\langle 0|\hat{H} + [\hat{H}, T_2]|0\rangle = E \tag{2.13}$$

$$\Omega_{\mu_1} = \langle \mu_1|\hat{H} + [\hat{H}, T_2]|0\rangle = 0 \tag{2.14}$$

$$\Omega_{\mu_2} = \langle \mu_2|\hat{H} + [F^{(0)}, T_2]|0\rangle = 0. \tag{2.15}$$

Note that the Fock operator appears undressed in the second part of the doubles equations. This is justified by the corresponding term disappearing if a closed-shell Hartree-Fock reference is used. For open-shell molecules, this is no longer the case, and the off-diagonal elements of the Fock matrix are instead considered to be of higher order[55], which leads to their exclusion from the commutator for the same reason as the fluctuation potential. Further note that multi-reference systems are challenging for coupled-cluster methods in general and in particular when they are restricted to lower classes of orbital substitutions. Therefore, we cannot expect reasonable results when applying the method presented here to systems with degeneracies beyond that due to the electronic net spin.

2.1.2 Reference determinant

The reference determinant for the treatment of open-shell systems can be provided by two approaches: unrestricted Hartree-Fock (UHF)[63] or restricted open-shell Hartree-Fock (ROHF).[64]
UHF varies the α and β spatial orbitals separately and provides orbitals that are eigenfunctions of the spin-specific Fock matrices F^α and F^β, respectively. This is achieved at the cost of introducing spin contamination into the wave function, i.e. the UHF determinant is in general not an eigenfunction of the square of the electronic net spin operator.
ROHF shares the same spatial orbitals for both spins and does not suffer from spin contamination. However, the conventional separation of the spatial orbitals into doubly (d) occupied, singly (s) occupied and empty (e) orbitals leads to orbitals that cannot be eigenfunctions of F^α and F^β at the same time.[65]
To provide well-defined and unique orbitals and orbital energies, Knowles *et al.*[65] suggested the use of so-called semi-canonical orbitals, which diagonalize the occupied-occupied

and virtual-virtual parts of the spin-specific Fock matrices. They are obtained by the following algorithm:

1. Construct the spin-specific Fock matrices F^α and F^β in the conventional d-s-e scheme.
2. Diagonalize the [d-s]-block of F^α to obtain the occupied α spatial orbitals and orbital energies.
3. Diagonalize the [e]-block of F^α to obtain the virtual α spatial orbitals and orbital energies.
4. Diagonalize the [d]-block of F^β to obtain the occupied β spatial orbitals and orbital energies.
5. Diagonalize the [s-e]-block of F^β to obtain the virtual β spatial orbitals and orbital energies.

For a system with a basis of N_{AO} atomic orbitals and N_α and N_β electrons of α or β spin respectively, this leads to a set of N_σ occupied orbitals and $N_{\mathrm{AO}} - N_\sigma$ virtual orbitals with $\sigma \in \alpha, \beta$. This mirrors the behavior found in UHF, but since the occupied β-space is spanned by linear combinations of occupied α-orbitals, there is no spin contamination for the reference function itself. There may however still be some slight spin contamination for correlation methods based on these orbitals.
Furthermore, the occupied-virtual and virtual-occupied blocks of the Fock matrices in semi-canonical basis are non-zero. This does not have any effect on the method presented here, since use of dressed Fock matrices already ensures that the off-diagonal blocks are in general non-zero. The only term that uses the undressed Fock operator appears in the doubles amplitude equations (2.15), but there only the occupied-occupied and virtual-virtual blocks are relevant since we consider the contributions from the off-diagonal elements to be of higher order. That being said, the effect of using the dressed Fock operator in all terms of the doubles amplitude equations might be worth investigating in future work.
The observations made in the previous paragraphs enable us to treat the case of a UHF and a ROHF reference in semi-canonical basis in an identical manner and we will not have to distinguish between them in the rest of the theory.
At first glance it may seem like a very bad idea indeed to use a spin contaminated reference function for the calculations of explicitly spin dependent properties. However, a previous study by Gauss *et al.*[33] of electronic g-tensor calculations has found the choice of reference determinant to have in general only an insignificant impact on their CCSD results, although there may be exceptions. For this reason - and to be able to compare results with later work using UHF reference functions by Perera *et al.*[34] - both possibilities listed above have been implemented in this work.

2.1.3 Local correlation method

2.1.3.1 Localized orbitals

The converged Hartree-Fock molecular orbitals (MOs), which are usually delocalized over the entire system, are unsuited to the exploitation of the short-range character of electron-electron interactions. Instead we will employ the local correlation method of Saebø and

Pulay[43] which requires first the introduction of localized molecular orbitals (LMOs) for the occupied space (indices I, J, K, ...) and a local basis for the virtual space (indices A, B, C, ...).
There are several possible choices for the LMOs. They can be obtained by applying one of the well-known orbital localization algorithms like those of Pipek and Mezey[66] (maximization of Mulliken orbital populations) or Boys[67–69] (minimization of spatial extension of orbitals) to the occupied Hartree-Fock orbitals. Alternatively, Knizia's intrinsic molecular orbitals (IMO) could be used, which replace the Mulliken charges with intrinsic atomic orbital (IAO) charges in the localization algorithm.[70] For consistency with the underlying DF-LUCC2 ground state method,[55] we employ the Pipek-Mezey localization for the occupied space used in this thesis.
The virtual Hartree-Fock orbitals are inherently meaningless. Thus, we can discard them and use an arbitrary basis to span the virtual space instead. Just like for the occupied space, several choices for a localized virtual space have been proposed. Among them are pair natural orbitals (PNOs)[71,72] and orbital specific virtuals (OSVs).[73] In this work however, we are using projected atomic orbitals (PAOs)[43,74,75], again primarily for consistency with the ground state code.
The PAOs – which are centered on the corresponding atoms – are obtained by requiring orthogonality between virtual and occupied orbitals. This is achieved via the projection

$$|A\rangle = \left(1 - \sum_I |I\rangle\langle I|\right)|\mu\rangle\Big|_{\mu=A}. \tag{2.16}$$

The PAOs share the dimension of the AOs, but conventionally they are labeled with indices that emphasize the orthogonality to the occupied space instead of their derivation from the AOs. Note that just like AOs, PAOs are non-orthonormal to each other. Consequently, the PAO overlap matrix will appear in the working equations (for details see appendices B.1.5, B.2.6 and B.2.7). Moreover, the PAOs form a redundant set meaning the overlap matrix has eigenvalues numerically equal to zero. Therefore, we cannot use the inverse of the overlap and have to use a pseudo inverse matrix instead[76] (see section 2.3.5).
Integrals in the local basis are obtained via transformation from the AO basis to the LMO and PAO basis

$$|I\rangle = \sum_\mu |\mu\rangle L_{\mu I} \tag{2.17}$$

$$|A\rangle = \sum_\mu |\mu\rangle P_{\mu A}. \tag{2.18}$$

If the target integrals are dressed, we can further combine this transformation with the T_1-transformation (2.11). This is accomplished by use of the matrices

$${}^{P}\Lambda^{\text{occ}}_{\mu I} = L_{\mu I} \tag{2.19}$$

$${}^{H}\Lambda^{\text{occ}}_{\mu I} = L_{\mu I} + \sum_A P_{\mu A} t^I_A \tag{2.20}$$

$${}^{P}\Lambda^{\text{virt}}_{\mu A} = P_{\mu A} - \sum_{IB} S_{AB} t^I_B L_{\mu I} \tag{2.21}$$

$${}^{H}\Lambda^{\text{virt}}_{\mu A} = P_{\mu A} \tag{2.22}$$

with the PAO overlap S_{AB} and the singles amplitudes t^I_A. The superscripts P and H refer here to transformation of "particle", i.e. bra, and "hole", i.e. ket, indices of integrals, respectively.

Special care has to be taken when transforming mean-field operators like the Fock operator due to the internal dressing of the two-electron integrals.

2.1.3.2 LMO domains

Including all virtual orbitals in the calculations of extended molecules is prohibitively expensive. On the other hand, due to the local nature of the LMO and PAO basis many integrals are negligible. In order to systematically exploit this fact, Boughton and Pulay[77] developed an algorithm based on a population analysis of the LMOs that assigns each LMO a so-called "domain" of atoms. The virtual space for each LMO is then restricted to the PAOs centered on these atoms.
For each LMO, the algorithm has the following steps:

1. Rank atoms according to their contribution to the Löwdin or Mulliken orbital population of the LMO.

2. Add atoms until the sum of their contributions is larger than a predetermined threshold.

3. Optionally, the domains can be expanded via a distance or bond connectivity criterion.

The correlation energy captured by this choice of virtual space generally deviates by less than 2 % from the correlation energy calculated with canonical methods. This deviation tends to decrease on progression towards the basis set limit. Note that the larger deviations from the canonical result for smaller basis sets can be considered an improvement due to partial correction of the basis set superposition error when using localized orbitals and domains.[43]
Finally, note that unlike for local CCSD[74,75] we use full domains for the virtual space of the singles amplitudes and multipliers following the example of closed-shell CC2[45] and the underlying open-shell CC2 method.[55]

2.1.3.3 LMO pair list

To further exploit the short-range character of electron-electron interactions, Saebø and Pulay[43] suggested the restriction of doubles quantities to relevant pairs $[IJ]$ of LMOs. The importance of a given pair can be estimated for example via the inter-orbital distance of the LMOs I and J or the contribution of the pair to the second order Møller-Plesset perturbation theory (MP2) correlation energy ("MP2 pair energy" $E^{[IJ]}$).
Based on either criterion, the individual pairs can then be categorized as strong, weak or very distant. A common approach is to simplify the treatment of weak pairs by evaluating their contribution with a simpler model, e.g. MP2, while neglecting the very distant pairs. However, in his pursuit of excited state calculations for open-shell molecules, David[55] discovered that use of the distance criterion provides an insufficient description of the ground state for this purpose. Instead he employed the pair energy criterion or treated all (valence) pairs as strong.
The restriction of the pair list based on MP2 pair energies is unlikely to be the optimal choice for strongly localized, spin density dependent properties like the electronic g-tensor. Nevertheless, investigating the effect on the quality and efficiency of the calculations is worthwhile (see section 3.3.4).

Finally, we note that due to the antisymmetry of the doubles vectors in the spin-orbital formalism, i.e.

$$t_{AB}^{IJ} = -t_{AB}^{JI} = -t_{BA}^{IJ} = t_{BA}^{JI}, \tag{2.23}$$

it is sufficient to only explicitly evaluate pairs $[IJ]$ with $I > J$. The matrices for the pairs $[II]$ are zero, while the matrices for pairs $[JI]$ with $I > J$ can be obtained via transposition of the virtual indices of the matrix for the pair $[IJ]$.

2.1.3.4 Pair-domains and united pair-domains

In order to obtain reasonable results, we need to ensure that "excitations" are possible from both LMOs in a given LMO pair to the PAOs belonging to either domain. Hampel and Werner[74] achieved this by simply uniting the individual LMO domains to a "pair-domain".
Finally, we will encounter intermediates to the doubles vectors that only depend on a single LMO index. To ensure that all relevant matrix elements are kept, we need to extend the domains of the individual LMOs to also include all centers of potential partners in the LMO pair list. This yields the so-called "united pair-domains".

2.1.4 Density fitting

Transformation of the four-center two-electron electron repulsion integrals (ERIs)

$$(UV|WX) = \int \varphi_U^*(r_1)\varphi_V(r_1)r_{12}^{-1}\varphi_W^*(r_2)\varphi_X(r_2)dr_1dr_2 \tag{2.24}$$

from the AO basis to the MO basis is one of the bottlenecks in local correlation methods.[78] Here U,V,W and X are general MO indices representing either LMOs or PAOs. Introducing the orbital densities

$$\rho_{UV}(r_1) = \varphi_U^*(r_1)\varphi_V(r_1) \tag{2.25}$$

we can rewrite the ERIs as

$$(UV|WX) = \int \rho_{UV}(r_1)r_{12}^{-1}\rho_{WX}(r_2)dr_1dr_2 = (\rho_{UV}|\rho_{WX}). \tag{2.26}$$

Instead of evaluating the four-index integrals directly from the AOs, we can now fit[79] the density in MO basis via expansion in an auxiliary basis set Φ_P

$$\rho_{UV}(r_1) \approx \tilde{\rho}_{UV}(r_1) = \sum_P^{N_{\text{aux}}} C_P^{UV}\Phi_P(r_1). \tag{2.27}$$

An accurate approximation of the four-index ERIs is obtained via Dunlap's robust-variational fit[80,81]

$$(\rho_{UV}|\rho_{XY}) \approx (\rho_{UV}|\tilde{\rho}_{XY}) + (\tilde{\rho}_{UV}|\rho_{XY}) - (\tilde{\rho}_{UV}|\tilde{\rho}_{XY}). \tag{2.28}$$

This choice of fit ensures that a small error

$$\Delta\rho_{UV}(r) = \rho_{UV}(r) - \tilde{\rho}_{UV}(r) \tag{2.29}$$

in the fitted density results in at most a quadratic error in the integrals

$$\Delta_{UV} = \int \Delta\rho_{UV}(r_1) r_{12}^{-1} \Delta\rho_{UV}(r_2) dr_1 dr_2. \tag{2.30}$$

Optimizing the positive definite error functional Δ_{UV} as a function of the fit-coefficients C_P^{UV} we obtain the system of linear equations[78]

$$C_P^{UV} = \sum_Q^{N_{\text{aux}}} [J^{-1}]_{PQ} (UV|Q) \tag{2.31}$$

with the three-center two-electron ERIs

$$(UV|Q) = \int \varphi_U(r_1) \varphi_V(r_1) r_{12}^{-1} \Phi_Q(r_2) dr_1 dr_2 \tag{2.32}$$

and the inverse $[J_{PQ}]^{-1}$ of the matrix of the two-center two-electron ERIs

$$J_{PQ} = \int \Phi_P(r_1) r_{12}^{-1} \Phi_Q(r_2) dr_1 dr_2. \tag{2.33}$$

Thus, the four transformations of the four-index ERIs to the MO basis are replaced by two transformations of the three-index ERIs and solving a system of linear equations.
Density fitting alone does not necessarily change the scaling of the assembly of the explicitly needed four-electron integrals, but it significantly reduces the prefactor. Furthermore, it allows the introduction of intermediates resulting from the contraction with either the three-index or two-index ERIs, and we will make significant use of this in the working equations of the method presented here.
Further computational savings could be achieved by applying the local correlation method not just to the PAOs, but also to the fitting basis.[78] However, this option has not been pursued in this work and three-index quantities will only be restricted due to the previously introduced united pair-domains or prescreening.
Density fitting is known to introduce only minor errors in the final results, especially compared to the basis set incompleteness error.[78] This is confirmed in our test calculations (see section 3.3.2).

2.2 First and second order properties

2.2.1 General coupled-cluster properties up to second order

For detailed reviews of properties in general or use of coupled-cluster response theory in particular we refer to the very extensive review of Helgaker *et al.*[82] or the book by Shaviit and Bartlett.[60] In the following, the essentials are briefly summarized.

2.2.1.1 Perturbative expansion

When applying a perturbation with perturbation strength α to a system we can expand the energy around $\alpha = 0$

$$E = E^{[0]} + \alpha E^{[1]} + \frac{1}{2}\alpha^2 E^{[2]} + ... = \sum_{n=0} \frac{1}{n!} \alpha^n E^{[n]}. \tag{2.34}$$

Taking the derivative of the n-th order at zero perturbation strength

$$E^{[n]} = \left.\frac{d^n E}{d\alpha^n}\right|_{\alpha=0} \tag{2.35}$$

corresponds to an n-th order property of the system. If we apply an external electric field as the perturbation, the first and second order properties are the electric dipole moment and polarizability, respectively.
Similarly, when considering two perturbations we get the expansion

$$E = \sum_{m,n=0} \frac{1}{m!n!}\alpha^m \beta^n E^{[m,n]} \tag{2.36}$$

with

$$E^{[m,n]} = \left.\frac{d^{m+n} E}{d\alpha^m d\beta^n}\right|_{\alpha,\beta=0}. \tag{2.37}$$

The property of interest to us in this work is the electronic g-tensor, where α corresponds to an external magnetic field and β to the magnetic moment of the system due to its (effective) electronic net spin.
In order to simplify the equations, we will employ the following shorthand notation for derivatives

$$f^{[m,n]} = \left.\frac{d^{m+n} f}{d\alpha^m d\beta^n}\right|_{\alpha,\beta=0} \tag{2.38}$$

$$f^{(m,n)} = \left.\frac{\partial^{m+n} f}{\partial\alpha^m \partial\beta^n}\right|_{\alpha,\beta=0}. \tag{2.39}$$

Here, square brackets indicate total derivatives while round brackets correspond to partial derivatives, both taken at zero perturbation strength.
In analogy to the energy, expansions can be carried out for Hamiltonian and wave function

$$H = \sum_{m,n=0} \frac{1}{m!n!}\alpha^m \beta^n H^{[m,n]} \tag{2.40}$$

$$|\Psi\rangle = \sum_{m,n=0} \frac{1}{m!n!}\alpha^m \beta^n |\Psi^{[m,n]}\rangle. \tag{2.41}$$

2.2.1.2 Coupled-cluster Lagrangian

The linked coupled-cluster Lagrangian as a function of the amplitudes t and multipliers λ is

$$L(t,\lambda) = E(t) + \lambda_\mu \Omega_\mu(t), \tag{2.42}$$

where we have used Einstein's convention for summation over repeated indices.
At convergence, the CC-Lagrangian has to be stationary with respect to variation of amplitudes and multipliers

$$\Omega_\mu(t) = \frac{\partial L}{\partial \lambda_\mu} \stackrel{!}{=} 0 \tag{2.43}$$

$$\Lambda_\nu(t,\lambda) = \frac{\partial L}{\partial t_\nu} = \eta_\nu(t) + \lambda_\mu A_{\mu\nu}(t) \stackrel{!}{=} 0. \tag{2.44}$$

Note that since we know the analytical dependence of the Lagrangian on the amplitudes and multipliers, we do not have any implicit dependencies on those and can use partial derivatives. We have introduced here the energy derivative

$$\eta_\nu = \frac{\partial E}{\partial t_\nu} \tag{2.45}$$

and the Jacobian

$$A_{\mu\nu} = \frac{\partial \Omega_\mu}{\partial t_\nu} = \frac{\partial^2 L}{\partial \lambda_\mu \partial t_\nu}. \tag{2.46}$$

Solving the amplitude equations (2.43) and multiplier equations (2.44) yields values for amplitudes and multipliers, respectively.
Properties are obtained as the derivatives of the Lagrangian. To this purpose, we again carry out an expansion in orders of the perturbations of the equations

$$L(t,\lambda) = \sum_{mn} \frac{1}{m!n!} \alpha^m \beta^n L^{[m,n]} \tag{2.47}$$

$$\Omega_\mu = \sum_{mn} \frac{1}{m!n!} \alpha^m \beta^n \Omega_\mu^{[m,n]} \stackrel{!}{=} 0 \tag{2.48}$$

$$\Lambda_\mu = \sum_{mn} \frac{1}{m!n!} \alpha^m \beta^n \Lambda_\mu^{[m,n]} \stackrel{!}{=} 0, \tag{2.49}$$

the wave function parameters

$$t_\mu = \sum_{mn} \frac{1}{m!n!} \alpha^m \beta^n t_\mu^{(m,n)} \tag{2.50}$$

$$\lambda_\mu = \sum_{mn} \frac{1}{m!n!} \alpha^m \beta^n \lambda_\mu^{(m,n)} \tag{2.51}$$

and the cluster operator

$$T = \sum_{mn} \frac{1}{m!n!} \alpha^m \beta^n T^{(m,n)} = \sum_{mn} \frac{1}{m!n!} \alpha^m \beta^n t_\mu^{(m,n)} \tau_\mu. \tag{2.52}$$

Note that the amplitude and multiplier equations must be fulfilled for any perturbation strength, and therefore each order must be individually zero

$$\Omega_\mu^{[m,n]} = \left[\frac{d^2}{d\alpha^m d\beta^n} \frac{\partial L}{\partial \lambda_\mu} \right]_{\alpha,\beta=0} \stackrel{!}{=} 0 \tag{2.53}$$

$$\Lambda_\nu^{[m,n]} = \left[\frac{d^2}{d\alpha^m d\beta^n} \frac{\partial L}{\partial t_\nu} \right]_{\alpha,\beta=0} \stackrel{!}{=} 0. \tag{2.54}$$

2.2.1.3 Zeroth order property

Considering the energy of the unperturbed system to be the zeroth order property, we obtain it via the zeroth order Lagrangian

$$L^{[0,0]} = E^{[0,0]} + \lambda_\mu^{(0,0)} \Omega_\mu^{[0,0]}. \tag{2.55}$$

Note that we do not need to solve the zeroth order multiplier equations, since dependence on the multipliers disappears on solution of the zeroth order amplitude equations

$$\Omega_\mu^{[0,0]} \stackrel{!}{=} 0. \tag{2.56}$$

2.2.1.4 First order properties

When examining the first order Lagrangian

$$L^{[1,0]} = E^{[1,0]} + \lambda_\mu^{(0,0)}\Omega_\mu^{[1,0]} + \lambda_\mu^{(1,0)}\Omega_\mu^{[0,0]} \tag{2.57}$$

we can immediately eliminate the dependence on the perturbed multipliers $\lambda_\mu^{(1,0)}$ due to fulfillment of the zeroth order amplitude equations $\Omega_\mu^{[0,0]}$. Expanding the remaining total derivatives leads us to

$$L^{[1,0]} = E^{(1,0)} + \eta_\nu^{[0,0]} t_\nu^{(1,0)} + \lambda_\mu^{(0,0)}\Omega_\mu^{(1,0)} + \lambda_\mu^{(0,0)} A_{\mu\nu}^{(0,0)} t_\nu^{(1,0)}. \tag{2.58}$$

Enforcing the zeroth order multiplier equation

$$\Lambda_\nu^{[0,0]} = \eta_\nu^{[0,0]} + \lambda_\mu^{(0,0)} A_{\mu\nu}^{[0,0]} \stackrel{!}{=} 0 \tag{2.59}$$

removes the dependence on the perturbed amplitudes $t_\nu^{(1,0)}$ and we arrive at

$$L^{[1,0]} = E^{(1,0)} + \lambda_\mu^{(0,0)}\Omega^{(1,0)}. \tag{2.60}$$

This is consistent with the 2n+1 and 2n+2 rules for amplitudes and multipliers respectively, which state that we only require amplitudes and multipliers up to order n if we want to obtain properties up to order 2n+1 and 2n+2, respectively. Furthermore, it agrees with the generalized Hellmann-Feynman theorem

$$L^{[1,0]} = L^{(1,0)}, \tag{2.61}$$

which states that first order properties only depend on the perturbed Hamiltonian, but not on the perturbed wave function. In the coupled-cluster case, this is just

$$L^{[1,0]} = \left(\langle 0| + \lambda_\mu^{(0,0)}\langle\mu|\right) \exp(-T^{(0,0)}) H^{(1,0)} \exp(T^{(0,0)})|0\rangle. \tag{2.62}$$

For a one-electron perturbation, this corresponds to the contraction of the perturbation integrals $h_{\mu\nu}^{(1,0)}$ with the unperturbed coupled-cluster density matrix $D_{\nu\mu}^{[0,0]}$

$$L^{[1,0]} = h_{\mu\nu}^{(1,0)} D_{\nu\mu}^{[0,0]} \tag{2.63}$$

μ and ν referring here to atomic orbitals (note that these indices should not be confused with "excited" determinants).

2.2.1.5 Second order properties

The second order Lagrangian for two (at least formally) independent perturbations is

$$L^{[1,1]} = E^{[1,1]} + \lambda_\mu^{(0,0)}\Omega_\mu^{[1,1]} + \lambda_\mu^{(1,0)}\Omega_\mu^{[0,1]} + \lambda_\mu^{(0,1)}\Omega_\mu^{[1,0]} + \lambda_\mu^{(1,1)}\Omega_\mu^{[0,0]}. \tag{2.64}$$

The last term of this expansion can be dropped immediately due to fulfillment of the zeroth order amplitude equations (2.56), thus eliminating dependence on the doubly perturbed multipliers. Introducing the derivatives

$$\xi_{\mu\nu} = \frac{\partial^2 E}{\partial t_\mu \partial t_\nu} = \frac{\partial \eta_\nu}{\partial t_\mu} = \frac{\partial \eta_\mu}{\partial t_\nu} \tag{2.65}$$

$$B_{\mu\rho\nu} = \frac{\partial^3 L}{\partial \lambda_\mu \partial t_\rho \partial t_\nu} = \frac{\partial^2 \Omega_\mu}{\partial t_\rho \partial t_\nu} = \frac{\partial A_{\mu\rho}}{\partial t_\nu} = \frac{\partial A_{\mu\nu}}{\partial t_\rho}, \tag{2.66}$$

expansion of the remaining doubly perturbed terms yields

$$E^{[1,1]} = E^{(1,1)} + \eta^{(1,0)}_\nu t^{(0,1)}_\nu + \eta^{(0,1)}_\nu t^{(1,0)}_\nu + \eta^{(0,0)}_\nu t^{(1,1)}_\nu + \xi^{(0,0)}_{\mu\nu} t^{(1,0)}_\mu t^{(0,1)}_\nu \tag{2.67}$$

$$\Omega^{[1,1]}_\mu = \Omega^{(1,1)}_\mu + A^{(1,0)}_{\mu\nu} t^{(0,1)}_\nu + A^{(0,1)}_{\mu\nu} t^{(1,0)}_\nu + A^{(0,0)}_{\mu\nu} t^{(1,1)}_\nu + B^{(0,0)}_{\mu\rho\nu} t^{(1,0)}_\rho t^{(0,1)}_\nu. \tag{2.68}$$

The terms depending on the doubly perturbed amplitudes vanish since they correspond to contraction of the doubly perturbed amplitudes with the zeroth order multiplier equations (2.59), i.e. they are multiplied by zero. This leads us to

$$\begin{aligned} L^{[1,1]} =& E^{(1,1)} + \eta^{(1,0)}_\nu t^{(0,1)}_\nu + \eta^{(0,1)}_\nu t^{(1,0)}_\nu + \xi^{(0,0)}_{\mu\nu} t^{(1,0)}_\mu t^{(0,1)}_\nu \\ &+ \lambda^{(0,0)}_\mu \left(\Omega^{(1,1)}_\mu + A^{(1,0)}_{\mu\nu} t^{(0,1)}_\nu + A^{(0,1)}_{\mu\nu} t^{(1,0)}_\nu + B^{(0,0)}_{\mu\rho\nu} t^{(1,0)}_\rho t^{(0,1)}_\nu \right) \end{aligned} \tag{2.69}$$

where we have assumed solution of the perturbed amplitude equations

$$\Omega^{[1,0]}_\mu = \Omega^{(1,0)}_\mu + A^{(0,0)}_{\mu\nu} t^{(1,0)}_\nu \stackrel{!}{=} 0 \tag{2.70}$$

$$\Omega^{[0,1]}_\mu = \Omega^{(0,1)}_\mu + A^{(0,0)}_{\mu\nu} t^{(0,1)}_\nu \stackrel{!}{=} 0 \tag{2.71}$$

removing them from (2.64). This symmetric treatment of the perturbations ensures agreement with the 2n+2 rule for multipliers, can however be disadvantageous from an implementation perspective. An example for such disadvantages is encountered when treating nuclear magnetic shieldings, where the perturbations are an external magnetic field and the magnetic moments of the nuclei. This would require solution of three sets of amplitude equations for each nucleus in addition to the three equations for the magnetic field. Similarly, in the case of g-tensors it may be desirable to avoid dealing with the magnetic moment due to the (effective) net electronic spin, since it involves spin dependent operators.
Rearranging the second order Lagrangian without enforcing (2.71) to

$$\begin{aligned} L^{[1,1]} =& E^{(1,1)} + \lambda^{(0,0)}_\mu \Omega^{(1,1)}_\mu + \eta^{(0,1)}_\nu t^{(1,0)}_\nu + \lambda^{(0,0)}_\mu A^{(0,1)}_{\mu\nu} t^{(1,0)}_\nu + \lambda^{(1,0)}_\mu \Omega^{(0,1)}_\mu \\ &+ \left(\eta^{(1,0)}_\nu + \xi^{(0,0)}_{\mu\nu} t^{(1,0)}_\mu + \lambda^{(0,0)}_\mu A^{(1,0)}_{\mu\nu} + \lambda^{(0,0)}_\mu B^{(0,0)}_{\mu\rho\nu} t^{(1,0)}_\rho + \lambda^{(1,0)}_\mu A^{(0,0)}_{\mu\nu} \right) t^{(0,1)}_\nu, \end{aligned} \tag{2.72}$$

we see that the terms depending on the second set of perturbed amplitudes $t^{(0,1)}$ are multiplied by the equations for the perturbed multipliers $\lambda^{(1,0)}$ of the first perturbation

$$\Lambda^{[1,0]}_\nu \stackrel{!}{=} 0 = \eta^{[1,0]}_\nu + \lambda^{(0,0)}_\mu A^{[1,0]}_{\mu\nu} + \lambda^{(1,0)}_\mu A^{[0,0]}_{\mu\nu} \tag{2.73}$$

$$= \eta^{(1,0)}_\nu + \xi^{(0,0)}_{\mu\nu} t^{(1,0)}_\mu + \lambda^{(0,0)}_\mu \left(A^{(1,0)}_{\mu\nu} + B^{(0,0)}_{\mu\nu\rho} t^{(1,0)}_\rho \right) + \lambda^{(1,0)}_\mu A^{[0,0]}_{\mu\nu}. \tag{2.74}$$

Thus, we can avoid solution of the second set of perturbed amplitude equations by solving for the perturbed multipliers of the first perturbation instead, which is the option we will pursue in the rest of this work.
A second order coupled-cluster property is then evaluated according to

$$\begin{aligned} L^{[1,1]} =& \left(\langle 0| + \lambda^{(0,0)}_\mu \langle \mu| \right) \exp(-T^{(0,0)}) H^{(1,1)} \exp(T^{(0,0)}) |0\rangle \\ &+ \lambda^{(1,0)}_\mu \langle \mu| \exp(-T^{(0,0)}) H^{(0,1)} \exp(T^{(0,0)}) |0\rangle \\ &+ \lambda^{(0,0)}_\mu \langle \mu| \exp(-T^{(0,0)}) [H^{(0,1)}, T^{(1,0)}] \exp(T^{(0,0)}) |0\rangle. \end{aligned} \tag{2.75}$$

This corresponds to contraction of the perturbation integrals with density matrices as in (2.63). For a one-electron perturbation with first and second order perturbation integrals $h^{(0,1)}_{\nu\mu}$ and $h^{(1,1)}_{\nu\mu}$ we have

$$L^{[1,1]} = h^{(1,1)}_{\mu\nu} D^{[0,0]}_{\nu\mu} + h^{(0,1)}_{\mu\nu} D^{[1,0]}_{\nu\mu}, \tag{2.76}$$

with μ and ν here again referring to atomic orbitals instead of "excited" determinants. Note that the unperturbed density matrix $D^{[0,0]}_{\nu\mu}$ is the same as in (2.63) and only the perturbed density matrix $D^{[1,0]}_{\nu\mu}$ is new. Furthermore, there is no explicit dependence on the perturbation integrals $h^{(1,0)}_{\mu\nu}$. Instead, they appear in the perturbed amplitude and multiplier equations used to derive $D^{[1,0]}_{\nu\mu}$.

2.2.2 Electronic g-tensor

The electronic g-tensor is the second order response

$$g_{xy} = \left.\frac{d^2E}{dB_x d(\mu_S)_y}\right|_{\mathbf{B},\mu_S=0} = \frac{1}{\mu_B}\left.\frac{d^2E}{dB_x dS_y}\right|_{\mathbf{B},\mathbf{S}=0} \tag{2.77}$$

of the energy to an external magnetic field

$$\mathbf{B} = \begin{pmatrix} B_x \\ B_y \\ B_z \end{pmatrix} \tag{2.78}$$

and the magnetic moment due to the (effective) net spin of the electrons

$$\mu_S = \mu_B \mathbf{S} = \mu_B \begin{pmatrix} S_x \\ S_y \\ S_z \end{pmatrix}. \tag{2.79}$$

The magnetic moment depends on the Bohr magneton

$$\mu_B = \frac{\alpha}{2} \tag{2.80}$$

with the fine structure constant[83]

$$\alpha = 7.2973525693(11) \times 10^{-3}. \tag{2.81}$$

For a free electron, the g-tensor takes the form

$$g_{xy} = \delta_{xy} g_e, \tag{2.82}$$

with the free electron g-value[83]

$$g_e = 2.00231930436256(35). \tag{2.83}$$

In many-electron systems, there are generally anisotropic deviations from this value due to spin-orbit coupling and other relativistic effects. They are conventionally expressed as a shift $\Delta\mathbf{g}$ to the free electron g-tensor

$$g_{xy} = \delta_{xy} g_e + \Delta g_{xy}. \tag{2.84}$$

2.2.2.1 Perturbation operators

The perturbation operators relevant for electronic g-tensor calculations are obtained by reducing the Dirac-Coulomb-Breit Hamiltonian to the non-relativistic limit. The only relevant terms are those with linear dependence on one or both of the external magnetic field $\mathbf{B}$ and the one-electron spin operator $\mathbf{s}(s_i)$ acting on the spin-coordinates s_i of the electron, while being independent of other fields and the nuclear moments. Detailed reviews can be found in the literature[82,84], particularly Harriman's book[12] on the theoretical foundations of electron spin resonance, which provides a very thorough discussion. Here, we will only state the final expressions for these operators.

2.2.2.1.1 Spin and magnetic field perturbed operators

The perturbation operator with dependence on both spin and field can be written as a sum of four contributions

$$H^{(1,1)} = H^{\mathrm{SB}} + H^{\mathrm{ZKE}} + H^{\text{1el-DSO}} + H^{\text{2el-DSO}}. \tag{2.85}$$

Note that the superscript in $H^{(1,1)}$ implies here dependence on both the magnetic field $\mathbf{B}$ and the electron spin operators $\mathbf{s}(s_i)$ and not a partial derivative as in (2.40).
The first of these is the electronic Zeeman term

$$H^{\mathrm{SB}} = \frac{\alpha}{2} g_e \sum_i \mathbf{s}(s_i) \cdot \mathbf{B} = g_e \mu_B \mathbf{S} \cdot \mathbf{B}, \tag{2.86}$$

which provides the free-electron part of the g-tensor. Since we only want to obtain the g-shift relative to this value, we can ignore this contribution. The second contribution is the kinetic energy correction to the electronic Zeeman term

$$H^{\mathrm{ZKE}} = \frac{\alpha}{2} \alpha^2 g_e \sum_i (\mathbf{s}(s_i) \cdot \mathbf{B}) p_i^2 \tag{2.87}$$

with

$$\mathbf{p}_i = -i\nabla_i = -i \begin{pmatrix} \frac{\partial}{\partial x_i} \\ \frac{\partial}{\partial y_i} \\ \frac{\partial}{\partial z_i} \end{pmatrix} \tag{2.88}$$

being the momentum operator acting on the i-th electron. Unlike the subsequent contributions, it only provides an isotropic correction to the diagonal elements of the g-tensor. The third contribution is the one-electron diamagnetic spin-orbit operator

$$H^{\text{1el-DSO}} = \frac{\alpha}{2} \frac{\alpha^2 g_e}{4} \sum_{iK} \frac{Z_K}{r_{iK}^3} \Big[\big(\mathbf{r}_{iK} \cdot \mathbf{r}_{i0}\big)\big(\mathbf{B} \cdot \mathbf{s}(s_i)\big) - \big(\mathbf{s}(s_i) \cdot \mathbf{r}_{i0}\big)\big(\mathbf{r}_{iK} \cdot \mathbf{B}\big) \Big] \tag{2.89}$$

with the charge of the K-th nucleus Z_K and the distances

$$\mathbf{r}_{iK} = \mathbf{r}_i - \mathbf{R}_K \tag{2.90}$$

$$\mathbf{r}_{i0} = \mathbf{r}_i - \mathbf{R}_0 \tag{2.91}$$

of the i-th electron from the position $\mathbf{R}_K$ of the K-th nucleus and from the origin $\mathbf{R}_0$. Finally, the two-electron diamagnetic spin-orbit operator is given as

$$\begin{aligned} H^{\text{2el-DSO}} = -\frac{\alpha}{2} \frac{\alpha^2 g_e}{4} {\sum_{ij}}' r_{ij}^{-3} \Big[& \big(\mathbf{r}_{ij} \cdot \mathbf{r}_{j0}\big)\big((\mathbf{s}(s_j) + 2\mathbf{s}(s_i)) \cdot \mathbf{B}\big) \\ & - \big((\mathbf{s}(s_j) + 2\mathbf{s}(s_i)) \cdot \mathbf{r}_{j0}\big)\big(\mathbf{r}_{ij} \cdot \mathbf{B}\big) \Big] \end{aligned} \tag{2.92}$$

with the distance between the electrons

$$\mathbf{r}_{ij} = \mathbf{r}_i - \mathbf{r}_j. \tag{2.93}$$

2.2.2.1.2 Spin perturbed operators

The with respect to spin perturbed operator has only two contributions

$$H^{(0,1)} = H^{\text{1el-PSO}} + H^{\text{2el-PSO}}. \tag{2.94}$$

The one-electron paramagnetic spin-orbit operator is defined as

$$H^{\text{1el-PSO}} = \frac{\alpha^2 g_e}{4} \sum_{iK} \frac{Z_K}{r_{iK}^3} \mathbf{s}(s_i) \cdot \mathbf{l}_{iK} \tag{2.95}$$

with the angular momentum operator of the i-th electron around the K-th nucleus being

$$\mathbf{l}_{iK} = \mathbf{r}_{iK} \times \mathbf{p}_i = -i\mathbf{r}_{iK} \times \nabla_i. \tag{2.96}$$

and the two-electron paramagnetic spin-orbit operator is

$$H^{\text{2el-PSO}} = -\frac{\alpha^2 g_e}{4} \sum_{ij}{}' r_{ij}^{-3} \big(\mathbf{s}(s_i) + 2\mathbf{s}(s_j)\big) \cdot \mathbf{l}_{ij} \tag{2.97}$$

with

$$\mathbf{l}_{ij} = \mathbf{r}_{ij} \times \mathbf{p}_i = -i\mathbf{r}_{ij} \times \nabla_i. \tag{2.98}$$

Note that according to Harriman[12] the g-factors in the spin-orbit operators are not exactly the same as the free-electron g-value, but in much of the literature on g-tensors this small difference is neglected. Occasionally, the free electron g-value is replaced by the Dirac value of $g_e = 2$, which leads to an error of approximately 0.2 % in the calculated g-shifts. Since this is a negligible error, the results reported in this thesis have been obtained with this choice as well.

2.2.2.1.3 Magnetic field perturbed operators

The magnetic field perturbed operator used in this work has only a single contribution

$$H^{(1,0)} = H^{\text{LB}}, \tag{2.99}$$

the orbital Zeeman term

$$H^{\text{LB}} = \frac{\alpha}{2} \mathbf{B} \sum_i \cdot \mathbf{l}_{i0} = \frac{\alpha}{2} \mathbf{B} \cdot L_{i0}. \tag{2.100}$$

There is also a relativistic correction[12] to this Zeeman term similar to H^{ZKE}, but since it is of higher order in α it will be neglected.

2.2.2.2 Approximate spin-orbit operators

Explicit use of the two-electron spin-orbit operators (2.92) and (2.97) is undesirable for several reasons. It requires nine or three distinct sets of four-index integrals for the diamagnetic and paramagnetic contribution, respectively, as well as construction of the unperturbed and all three Cartesian components of the perturbed two-electron density matrices. This is especially problematic for extended molecules. To avoid these problems we use an effective one-electron operator instead. A comprehensive review of spin-orbit coupling including a section about effective one-electron spin-orbit operators has been published by Marian.[1]

2.2.2.2.1 Effective nuclear charges

One of the simplest options is the use of empirically determined effective nuclear charges in the one-electron spin-orbit operators (2.89) and (2.95)

$$H^{\text{1el-DSO}} + H^{\text{2el-DSO}} \approx \frac{\alpha}{2}\frac{\alpha^2 g_e}{4}\sum_{iK}\frac{Z_K^{\text{eff}}}{r_{iK}^3}\Big[\big(\mathbf{r}_{iK}\cdot\mathbf{r}_{i0}\big)\big(\mathbf{B}\cdot\mathbf{s}(s_i)\big) - \big(\mathbf{s}(s_i)\cdot\mathbf{r}_{i0}\big)\big(\mathbf{r}_{iK}\cdot\mathbf{B}\big)\Big] \tag{2.101}$$

$$H^{\text{1el-PSO}} + H^{\text{2el-PSO}} \approx \frac{\alpha^2 g_e}{4}\sum_{iK}\frac{Z_K^{\text{eff}}}{r_{iK}^3}\mathbf{s}(s_i)\cdot\mathbf{l}_{iK}. \tag{2.102}$$

The method presented in this work employs this approach and uses the parametrization developed by Koseki *et al.*[85,86]

$Z_K^{\text{eff}} = f_K Z_K$	$f_K = a + bN_{\text{val}}$	(2.103)
Li-F:	$a = 0.4,\ b = 0.05$	(2.104)
Na-Cl:	$a = 0.925,\ b = -0.0125$	(2.105)
K, Ca, Ga-Br:	$a = 1.21,\ b = -0.03$	(2.106)
Rb, Sr, In-I:	$a = 1.24,\ b = 0.0$	(2.107)
else:	$a = 1.0,\ b = 0.0,$	(2.108)

with the element dependent coefficients a and b and the number of valence electrons N_{val}. For the transition metals, we have

$Z_K^{\text{eff}} = f_K Z_K$	$f_K = a + b(m-2)$	(2.109)
Sc-Zn:	$a = 0.385,\ b = 0.025$	(2.110)
Y-Cd:	$a = 4.680,\ b = 0.060$	(2.111)
La,Hf-Hg:	$a = 13.960,\ b = 0.140$	(2.112)

with m being the number of nd- and $(n+1)$sp-electrons.
The equations for the effective charges have been determined empirically for the prediction of fine structure splittings, not for g-tensor calculations. However, Perera *et al.*[34] reported that the g-shifts obtained using effective charges by Gauss *et al.*[33] deviate by only approximately ± 200 ppm from their own results using exact two-electron operators, which is still well below the experimental uncertainty of ± 1000 ppm.

2.2.2.2.2 Spin-orbit mean-field operator

A more sophisticated, non-empirical approach is use of the spin-orbit mean-field (SOMF) operator proposed by Heß *et al.*[87]

$$H^{\text{1el-PSO}} + H^{\text{2el-PSO}} \approx H^{\text{SOMF}} = \sum_i \mathbf{h}^{\text{SOMF}}(\mathbf{r}_i)\cdot\mathbf{s}(s_i). \tag{2.113}$$

The mean-field ansatz in Hartree-Fock yields upwards of 99 % of the electronic energy, which is usually not enough for chemical accuracy. However, the spin-orbit coupling is four orders of magnitude smaller due to its proportionality to α^2 and an accuracy of 99 % would correspond to a much smaller absolute error. In their calculations of spin-orbit coupling matrix elements, Heß[87] *et al.* observed absolute errors of only a few cm^{-1} corresponding

to relative errors of at most 0.2 %. The integrals between AO basis functions of the spin-orbit mean-field operator are then given by[88]

$$\langle\nu|\mathbf{h}^{\text{SOMF}}|\rho\rangle = \langle\nu|\mathbf{h}^{\text{1el-PSO}}|\rho\rangle + \sum_{\sigma\xi} P_{\sigma\xi}\Bigg(\langle\nu\sigma|\mathbf{h}^{\text{2el-PSO}}|\rho\xi\rangle \tag{2.114}$$

$$- \frac{3}{2}\langle\nu\xi|\mathbf{h}^{\text{2el-PSO}}|\sigma\rho\rangle - \frac{3}{2}\langle\xi\nu|\mathbf{h}^{\text{2el-PSO}}|\rho\sigma\rangle\Bigg) \tag{2.115}$$

with the spatial operators

$$h^{\text{1el-PSO}}(\mathbf{r}_1) = \frac{\alpha^2 g_e}{4}\sum_K Z_K \frac{\mathbf{l}_{1K}}{r_{1K}^3} \tag{2.116}$$

$$\mathbf{h}^{\text{2el-PSO}}(\mathbf{r}_1, \mathbf{r}_2) = -\frac{\alpha^2 g_e}{4}\frac{\mathbf{l}_{12}}{r_{12}^3} \tag{2.117}$$

and the one particle density matrix $P_{\sigma\xi}$.
Use of the SOMF operator does not reduce the number of two-electron integrals that need to be calculated. However, additional approximations can vastly reduce the number of integrals to be included. For example, replacing the molecular mean-field with a sum of atomic mean-fields, i.e. inclusion of only those two-electron integrals with all basis functions belonging to the same atom, leads to linear scaling of the number of integrals with molecular size, thus greatly improving efficiency for large molecules.[1] This approximation works well for heavy atoms, but for smaller atoms a balanced neglect of multi-center contributions in the one- and two-electron spin-orbit contributions yields better results.[1] A further approximation worth investigating is the application of density fitting to the spin-orbit integrals in addition to the electron-repulsion integrals.[80,81,89]
Usually only the paramagnetic contribution is approximated in this way, since it dominates the g-shift in many systems (see section 3.2.1.1). The diamagnetic spin-orbit contribution not only requires three times as many integrals, but also tends to have only a very small contribution to the g-shift. Therefore, the two-electron diamagnetic spin-orbit coupling is sometimes - for instance in the density functional theory (DFT) method of Glasbrenner *et al.*[35,36] - only approximated by effective nuclear charges.

2.2.2.3 Gauge variance

The diamagnetic spin-orbit operators (2.89) and (2.92) as well as the orbital Zeeman operator (2.100) depend on the position $\mathbf{R}_0$ of the origin. This leads at first glance to a dependence of the results on the choice of this so-called gauge origin. However, in exact methods the origin dependence in the diamagnetic spin-orbit operators cancels exactly with the origin dependence in the contribution from the product of the orbital Zeeman term with the paramagnetic spin-orbit operators.[12] For this reason, the diamagnetic spin-orbit contributions are sometimes referred to as "gauge correction" terms in the literature. But for approximate methods, this correction is no longer sufficient.

2.2.2.3.1 Gauge origin and shifts

The origin dependence enters into the Dirac equation via the vector potential $\mathbf{A}$ used to define the magnetic field $\mathbf{B}$ (see for instance the book by Harriman[12])

$$\mathbf{B} = \nabla \times \mathbf{A}(\mathbf{r}). \tag{2.118}$$

Defining the magnetic field via the rotation of a vector guarantees fulfillment of the Maxwell equation

$$\nabla \cdot \mathbf{B} = 0, \tag{2.119}$$

since the divergence of a rotation always equals zero. Since the rotation of a gradient vanishes as well, the magnetic field does not change after application of a gauge shift in accordance with

$$\mathbf{A}(\mathbf{r}) \to \mathbf{A}'(\mathbf{r}) = \mathbf{A}(\mathbf{r}) + \nabla f(\mathbf{r}), \tag{2.120}$$

i.e. both the old and the new potential yield the same magnetic field.
The vector potential enters the Dirac equation via the gauge invariant momentum operator

$$\pi = \mathbf{p} - \frac{q}{c}\mathbf{A} = \mathbf{p} + \frac{e}{c}\mathbf{A}, \tag{2.121}$$

where we have assumed an electron with the charge of $q = -e$. Since only the magnetic field has any physical significance, a shift of the origin of the vector potential must not change the result, e.g. the expectation value of the gauge invariant momentum operator must be the same for both potentials if we have an exact wave function

$$\langle \Psi | \pi | \Psi \rangle = \langle \Psi' | \pi' | \Psi' \rangle. \tag{2.122}$$

As can easily be shown by application of the shifted operator

$$\pi' = \pi + \nabla f(\mathbf{r}) \tag{2.123}$$

to the corresponding wave function

$$\Psi' = e^{i\lambda(\mathbf{r})}\Psi, \tag{2.124}$$

the introduction of an unobservable phase shift with

$$\lambda(\mathbf{r}) = -f(\mathbf{r}) \tag{2.125}$$

fulfills this condition, since

$$\pi'\Psi' = e^{i\lambda}\big(\pi - i^2(\nabla\lambda) + (\nabla f)\big)\Psi \stackrel{!}{=} e^{i\lambda}\Psi \qquad \Leftrightarrow \qquad \lambda(\mathbf{r}) = -f(\mathbf{r}). \tag{2.126}$$

For approximate wave functions this is no longer the case.
A convenient choice for the vector potential for a constant, homogeneous external magnetic field is given by

$$\mathbf{A}(\mathbf{r}) = \frac{1}{2}\mathbf{B} \times (\mathbf{r} - \mathbf{R}_0). \tag{2.127}$$

It has the additional property of fulfilling the criteria

$$\nabla \cdot \mathbf{A}(\mathbf{r}) = 0 \tag{2.128}$$

of being a so-called Coulomb gauge, which leads to additional simplifications when dealing with products of the momentum operator and the vector potential.

2.2.2.3.2 Gauge including atomic orbitals

A rigorous approach to eliminating the dependence on the gauge origin is achieved via use of gauge including atomic orbitals (GIAOs)[90] originally proposed by London[91], which have since been used in several methods[34,35,52,53,82,92,93] for the calculations of magnetic field dependent properties. Each GIAO is derived from an AO via multiplication with an explicitly field dependent phase factor

$$|\varphi_\nu^{\mathrm{GIAO}}\rangle = \exp\big(-i\mathbf{A}_\nu \cdot \mathbf{r}\big)|\varphi_\nu^{\mathrm{AO}}\rangle = \exp\big(-i\mathbf{B}\cdot(\mathbf{R}_{\nu 0}\times\mathbf{r})\big)|\varphi_\nu^{\mathrm{AO}}\rangle \tag{2.129}$$

$$\mathbf{A}_\nu = \frac{1}{2}\mathbf{B}\times(\mathbf{R}_\nu - \mathbf{R}_0) = \frac{1}{2}\mathbf{B}\times\mathbf{R}_{\nu 0}. \tag{2.130}$$

When taking the derivative with respect to the external magnetic field at the point $\mathbf{B}=0$, additional correction terms arise and the GIAOs reduce to simple AOs. This means that in addition to the perturbation integrals due to the orbital Zeeman term, perturbed overlap integrals, Fock-integrals and electron repulsion integrals will appear in the non-iterative part of the perturbed equations, which of course increases the computational effort.

2.2.2.3.3 Effect on g-tensor calculations

Much of the literature (see references in Glasbrenner *et al.*[35]) assumes that the gauge error does not affect the electronic g-tensor to the same degree as it does for example the nuclear magnetic shieldings. This has lead to wide-spread use of common gauge origins like the center of mass or charge[15] as origins for small molecule g-tensor calculations, despite them not being related to the electronic g-tensor in any particular way. However, Glasbrenner *et al.*[35] showed that even for small molecules a shift of the gauge origin by 10 Å in all directions can lead to significant deviations in the obtained g-tensors.
While the gauge error may be negligible in many small molecule calculations, this is in general no longer the case for extended molecules. However, the spin density matrix $D_{\mu\nu}$ in AO basis is defined as the difference

$$D_{\mu\nu} = P_{\mu\nu}^{\alpha} - P_{\mu\nu}^{\beta} \tag{2.131}$$

between the spatial density matrices $P_{\mu\nu}^{\alpha}$ and $P_{\mu\nu}^{\beta}$ for α- and β-electrons, respectively. It is often localized to only a small region of the molecule. Since the gauge error grows with distance from the origin, Glasbrenner *et al.*[35] proposed choosing the spin density center (SDC) as the gauge origin

$$\mathbf{R}_0^{\mathrm{SDC}} = \frac{1}{\mathrm{Tr}(|DS|)}\sum_{\mu\nu}|D_{\mu\nu}|\langle\mu|\mathbf{r}|\nu\rangle \tag{2.132}$$

with S being the AO overlap matrix. This was found to be a reasonable compromise between efficiency and accuracy, even for extended molecules, and it is the approach chosen for the method developed in this thesis, with $D_{\mu\nu}$ being the unperturbed DF-LUCC2 spin density matrix. Note however that this choice can only provide reliable results when the spin density has a single, well localized area with non-zero contribution. For triplet states or higher this may no longer be the case and use of GIAOs or other distributed gauge origins would be preferable.

2.3 Working equations

Derivation of the working equations is covered in excruciating detail in appendix B. Therefore, only the final results will be repeated in this section.

The equations given here use spin-specific spatial orbitals to span the LMO and PAO spaces, which are indicated by lower case Latin letters with Greek spin indices (e.g. i_σ, a_τ). We use the Einstein convention for summation over repeated indices except for sums over spin, which are included explicitly for clarity. Furthermore, restriction of virtual orbitals to (united) pair-domains are left implicit.
As mentioned previously, doubles vectors only have to be explicitly evaluated for pairs with $I > J$. For spin-specific LMO indices i_σ, this implies inclusion of the upper triangles of the $\alpha\alpha$- and $\beta\beta$-blocks as well as the entirety of the $\beta\alpha$-block. That still leaves us with roughly three times as many doubles equations to solve as for restricted closed-shell calculations.
Many intermediates are shared between different sets of amplitude and multiplier equations and will only be defined the first time they appear. A trivial but nevertheless important example would be the contractions of the amplitudes and multipliers with the PAO overlap matrix, e.g.

$$[St]^{i_\sigma\,(m,n)}_{a_\sigma} = S_{a_\sigma b_\sigma} t^{i_\sigma\,(m,n)}_{a_\sigma} \tag{2.133}$$

$$[St]^{i_\sigma j_\tau\,(m,n)}_{a_\sigma b_\tau} = S_{a_\sigma c_\sigma} t^{i_\sigma j_\tau\,(m,n)}_{c_\sigma b_\tau} \tag{2.134}$$

$$[tS]^{i_\sigma j_\tau\,(m,n)}_{a_\sigma b_\tau} = t^{i_\sigma j_\tau\,(m,n)}_{a_\sigma d_\tau} S_{d_\tau b_\tau} \tag{2.135}$$

$$[StS]^{i_\sigma j_\tau\,(m,n)}_{a_\sigma b_\tau} = S_{a_\sigma c_\sigma} t^{i_\sigma j_\tau\,(m,n)}_{c_\sigma d_\tau} S_{d_\tau b_\tau}. \tag{2.136}$$

Generally, the residual vectors can be separated into a part independent of the target vectors and one that depends on them. The first part has to be evaluated only once before the first iteration while the second has to be treated iteratively.

2.3.1 Unperturbed amplitude equations

The unperturbed amplitude equations have been discussed in detail by David[55] and will not be repeated here. The interested reader can construct them from (B.158) and (B.170) given in appendix B.

2.3.2 Unperturbed multiplier equations

The unperturbed multiplier equations (2.59) for the DF-LUCC2 model have been derived in appendix B.3.2.1 and B.3.2.2.

2.3.2.1 Unperturbed singles multiplier equations

The residual vector for the unperturbed singles multiplier equations is

$$\begin{aligned} v^{a_\sigma}_{i_\sigma} =& \eta^{a_\sigma\,(0,0)}_{i_\sigma} + \lambda^{c_\sigma\,(0,0)}_{i_\sigma} \hat{f}_{c_\sigma a_\sigma} - \hat{f}_{i_\sigma k_\sigma} [S\lambda]^{a_\sigma\,(0,0)}_{k_\sigma} + [S\lambda]^{a_\sigma\,(0,0)}_{k_\sigma} Z^{(0,0)}_{i_\sigma k_\sigma} \\ &+ \tilde{C}^{(0,0)}_P (P|i_\sigma a_\sigma) + \left(\tilde{Y}^{k_\sigma i_\sigma\,(0,0)}_P + \Delta\tilde{Y}^{k_\sigma i_\sigma\,(0,0)}_P \right) (P|k_\sigma a_\sigma) \\ &+ \left(-\lambda^{c_\sigma\,(0,0)}_{k_\sigma} \hat{C}^{i_\sigma k_\sigma}_P + \tilde{A}^{i_\sigma c_\sigma\,(0,0)}_P \right) (P\hat{|}c_\sigma a_\sigma) - S_{c_\sigma a_\sigma} \tilde{A}^{k_\sigma c_\sigma\,(0,0)}_P (P\hat{|}i_\sigma k_\sigma) \end{aligned} \tag{2.137}$$

with the intermediates

$$\eta^{a_\sigma\,(0,0)}_{i_\sigma} = \hat{f}_{i_\sigma a_\sigma} \tag{2.138}$$

$$Z_{i_\sigma j_\sigma}^{(0,0)} = -(P|i_\sigma b_\sigma) A_P^{j_\sigma b_\sigma (0,0)} \tag{2.139}$$

$$A_P^{i_\sigma a_\sigma (0,0)} = \sum_\tau t_{a_\sigma b_\tau}^{i_\sigma j_\tau\ (0,0)} C_P^{j_\tau b_\tau} \tag{2.140}$$

$$\tilde{C}_P^{(0,0)} = \Delta\tilde{C}_P^{(0,0)} - \sum_\tau \tilde{Y}_P^{j_\tau j_\tau (0,0)} \tag{2.141}$$

$$\Delta\tilde{C}_P^{(0,0)} = \sum_\tau C_P^{b_\tau j_\tau} \lambda_{j_\tau}^{b_\tau (0,0)} \tag{2.142}$$

$$\tilde{Y}_P^{k_\sigma i_\sigma (0,0)} = -\tilde{X}_{k_\sigma c_\sigma}^{(0,0)} C_P^{i_\sigma c_\sigma} \tag{2.143}$$

$$\tilde{X}_{k_\sigma c_\sigma}^{(0,0)} = \sum_\tau [S\lambda]_{j_\tau}^{b_\tau (0,0)} t_{b_\tau c_\sigma}^{j_\tau k_\sigma (0,0)} \tag{2.144}$$

$$\Delta\tilde{Y}_P^{j_\sigma i_\sigma (0,0)} = -A_P^{j_\sigma b_\sigma (0,0)} [S\lambda]_{i_\sigma}^{b_\sigma (0,0)} \tag{2.145}$$

$$\tilde{A}_P^{k_\sigma c_\sigma (0,0)} = \sum_\tau \lambda_{k_\sigma j_\tau}^{c_\sigma b_\tau (0,0)} \hat{C}_P^{b_\tau j_\tau}. \tag{2.146}$$

2.3.2.2 Unperturbed doubles multiplier equations

The doubles residual vector is

$$\begin{aligned} v_{i_\sigma j_\tau}^{a_\sigma b_\tau} =& \eta_{i_\sigma j_\tau}^{a_\sigma b_\tau (0,0)} + \hat{f}_{j_\tau b_\tau} [S\lambda]_{i_\sigma}^{a_\sigma (0,0)} + \hat{f}_{i_\sigma a_\sigma} [S\lambda]_{j_\tau}^{b_\tau (0,0)} \\ & - \delta_{\sigma\tau} \hat{f}_{j_\sigma a_\sigma} [S\lambda]_{i_\sigma}^{b_\sigma (0,0)} - \delta_{\sigma\tau} \hat{f}_{i_\sigma b_\sigma} [S\lambda]_{j_\sigma}^{a_\sigma (0,0)} \\ & + \tilde{B}_P^{i_\sigma a_\sigma (0,0)} C_P^{j_\tau b_\tau} + \tilde{B}_P^{j_\tau b_\tau (0,0)} C_P^{i_\sigma a_\sigma} \\ & - \delta_{\sigma\tau} \tilde{B}_P^{i_\sigma b_\sigma (0,0)} C_P^{j_\sigma a_\sigma} - \delta_{\sigma\tau} \tilde{B}_P^{j_\sigma a_\sigma (0,0)} C_P^{i_\sigma b_\sigma} \\ & + [S\lambda]_{i_\sigma j_\tau}^{a_\sigma d_\tau (0,0)} f_{d_\tau b_\tau} + f_{c_\sigma a_\sigma} [\lambda S]_{i_\sigma j_\tau}^{c_\sigma b_\tau (0,0)} \\ & - [S\lambda S]_{i_\sigma k_\tau}^{a_\sigma b_\tau (0,0)} f_{j_\tau k_\tau} - [S\lambda]_{k_\sigma j_\tau}^{a_\sigma b_\tau (0,0)} f_{i_\sigma k_\sigma} \end{aligned} \tag{2.147}$$

with the additional intermediates

$$\eta_{i_\sigma j_\tau}^{a_\sigma b_\tau (0,0)} = K_{a_\sigma b_\tau}^{i_\sigma j_\tau} - \delta_{\sigma\tau} K_{b_\sigma a_\sigma}^{i_\sigma j_\sigma} \tag{2.148}$$

$$K_{a_\sigma b_\tau}^{i_\sigma j_\tau} = C_P^{i_\sigma a_\sigma} (P|j_\tau b_\tau) \tag{2.149}$$

$$\tilde{B}_P^{i_\sigma a_\sigma (0,0)} = \lambda_{i_\sigma}^{c_\sigma (0,0)} (P\hat{|}c_\sigma a_\sigma) - [S\lambda]_{k_\sigma}^{a_\sigma (0,0)} (P\hat{|}i_\sigma k_\sigma). \tag{2.150}$$

2.3.3 Perturbed amplitude equations

Solution of the perturbed amplitude equations (2.70) is the first time we actually need to refer to the perturbation integrals $h_{p_\sigma q_\sigma}^{(1,0)}$. Since we are choosing to solve for the magnetic field perturbed amplitudes and multipliers, we only have to deal with spin-independent one-electron operators. If we were to use GIAOs, we would have additional perturbed one- and also two-electron integrals to consider.

Note that some of the "new" intermediates required for the perturbed amplitude equations are just higher order equivalents of already available intermediates, which allows a significant amount of code sharing.

A detailed derivation of the equations given below can be found in appendix B.3.2.4 and B.3.2.5.

2.3.3.1 Perturbed singles amplitude equations

For the residual vector of the perturbed singles amplitude equations, we have

$$\begin{aligned} v_{i_\sigma}^{a_\sigma} =& \Omega_{i_\sigma}^{a_\sigma\,(1,0)} + t_{b_\sigma}^{i_\sigma\,(1,0)} \hat{f}_{a_\sigma b_\sigma} - [St]_{a_\sigma}^{j_\sigma\,(1,0)} \hat{f}_{j_\sigma i_\sigma} + [St]_{a_\sigma}^{k_\sigma\,(1,0)} Z_{k_\sigma i_\sigma}{}^{(0,0)} \\ &+ S_{a_\sigma d_\sigma} \left(C_P^{(1,0)} A_P^{i_\sigma d_\sigma\,(0,0)} + Y_P^{j_\sigma i_\sigma\,(1,0)} A_P^{j_\sigma d_\sigma\,(0,0)} \right) \\ &+ S_{a_\sigma d_\sigma} \sum_\tau X_{k_\tau c_\tau}{}^{(1,0)} t_{c_\tau d_\sigma}^{k_\tau i_\sigma\,(0,0)} + C_P^{(1,0)} \hat{C}_P^{a_\sigma i_\sigma} + S_{a_\sigma c_\sigma} \sum_\tau t_{c_\sigma b_\tau}^{i_\sigma j_\tau\,(1,0)} \hat{f}_{j_\tau b_\tau} \\ &+ \left(A_P^{i_\sigma c_\sigma\,(1,0)} - t_{c_\sigma}^{k_\sigma\,(1,0)} \hat{C}_P^{k_\sigma i_\sigma} \right) (P\hat{|} a_\sigma c_\sigma) - \sum_\tau S_{a_\sigma c_\sigma} A_P^{k_\sigma c_\sigma\,(1,0)} (P\hat{|} k_\sigma i_\sigma), \end{aligned} \tag{2.151}$$

with the additional intermediates

$$\Omega_{i_\sigma}^{a_\sigma\,(1,0)} = \hat{h}_{a_\sigma i_\sigma}^{(1,0)} + S_{a_\sigma c_\sigma} \sum_\tau t_{c_\sigma b_\tau}^{i_\sigma j_\tau\,(0,0)} h_{j_\tau b_\tau}^{(1,0)} \tag{2.152}$$

$$C_P^{(1,0)} = \sum_\tau (P|k_\tau c_\tau) t_{c_\tau}^{k_\tau\,(1,0)} \tag{2.153}$$

$$Y_P^{k_\sigma i_\sigma\,(1,0)} = -(P|k_\sigma c_\sigma) t_{c_\sigma}^{i_\sigma\,(1,0)} \tag{2.154}$$

$$X_{k_\tau c_\tau}{}^{(1,0)} = Y_P^{k_\tau j_\tau\,(1,0)} C_P^{j_\tau c_\tau} \tag{2.155}$$

$$A_P^{i_\sigma a_\sigma\,(1,0)} = \sum_\tau t_{a_\sigma b_\tau}^{i_\sigma j_\tau\,(1,0)} C_P^{j_\tau b_\tau}. \tag{2.156}$$

2.3.3.2 Perturbed doubles amplitude equations

For the residual vector of the doubles equations we have

$$\begin{aligned} v_{i_\sigma j_\tau}^{a_\sigma b_\tau} = \Omega_{i_\sigma j_\tau}^{a_\sigma b_\tau\,(1,0)} &+ B_P^{i_\sigma a_\sigma\,(1,0)} \hat{C}_P^{b_\tau j_\tau} + B_P^{j_\tau b_\tau\,(1,0)} \hat{C}_P^{a_\sigma i_\sigma} \\ &- \delta_{\sigma\tau} B_P^{i_\sigma b_\sigma} C_P^{a_\sigma j_\sigma} - \delta_{\sigma\tau} B_P^{j_\sigma a_\sigma} C_P^{b_\sigma i_\sigma} \\ &+ [St]_{a_\sigma d_\tau}^{i_\sigma j_\tau\,(1,0)} f_{b_\tau d_\tau} + f_{a_\sigma c_\sigma} [tS]_{c_\sigma b_\tau}^{i_\sigma j_\tau\,(1,0)} \\ &- [StS]_{a_\sigma b_\tau}^{i_\sigma k_\tau\,(1,0)} f_{k_\tau j_\tau} - [StS]_{a_\sigma b_\tau}^{k_\sigma j_\tau\,(1,0)} f_{k_\sigma i_\sigma} \end{aligned} \tag{2.157}$$

with the intermediates

$$\begin{aligned} \Omega_{i_\sigma j_\tau}^{a_\sigma b_\tau\,(1,0)} =& [St]_{a_\sigma c_\tau}^{i_\sigma j_\tau\,(0,0)} \hat{h}_{b_\tau c_\tau}^{(1,0)} + \hat{h}_{a_\sigma d_\sigma}^{(1,0)} [tS]_{d_\sigma b_\tau}^{i_\sigma j_\tau\,(0,0)} \\ &- [StS]_{i_\sigma k_\tau}^{a_\sigma b_\tau\,(0,0)} \hat{h}_{k_\tau j_\tau}^{(1,0)} - \hat{h}_{k_\sigma i_\sigma}^{(1,0)} [StS]_{k_\sigma j_\tau}^{a_\sigma b_\tau\,(0,0)} \end{aligned} \tag{2.158}$$

$$B_P^{i_\sigma a_\sigma\,(1,0)} = t_{c_\sigma}^{i_\sigma\,(1,0)} (P\hat{|} a_\sigma c_\sigma) - S_{a_\sigma c_\sigma} t_{c_\sigma}^{k_\sigma\,(1,0)} (P\hat{|} k_\sigma i_\sigma). \tag{2.159}$$

2.3.4 Perturbed multiplier equations

The iterative part of the perturbed multiplier equations (2.73) is essentially the same as for the unperturbed multiplier equations(2.59). All we have to do is change the constant part of the equations – i.e. replace $\eta^{(0,0)}$ with $\zeta^{[1,0]}$ (see below) – and solving them will yield the perturbed instead of the unperturbed multipliers.
A detailed derivation of $\zeta^{[1,0]}$ can be found in appendix B.3.2.6 and B.3.2.7.

2.3.4.1 Perturbed singles multiplier equations

For the non-iterative part of the residuum for the perturbed singles multipliers we have

$$\begin{aligned}
\zeta_{i_\sigma}^{a_\sigma\,[1,0]} =& \bar{\eta}_{i_\sigma}^{a_\sigma\,(1,0)} + \lambda_{i_\sigma}^{b_\sigma\,(0,0)} \hat{h}_{b_\sigma a_\sigma}^{(1,0)} - \hat{h}_{i_\sigma j_\sigma}^{(1,0)} [S\lambda]_{j_\sigma}^{a_\sigma\,(0,0)} \\
&+ D_{i_\sigma j_\sigma}{}^{[0,0]} h_{j_\sigma a_\sigma}^{(1,0)} - S_{a_\sigma d_\sigma} D_{b_\sigma d_\sigma}{}^{[0,0]} h_{i_\sigma b_\sigma}^{(1,0)} \\
&- \hat{f}_{i_\sigma b_\sigma} t_{b_\sigma}^{j_\sigma\,(1,0)} [S\lambda_{j_\sigma}^{a_\sigma}]^{(0,0)} - \bar{y}_{i_\sigma j_\sigma}{}^{(1,0)} \hat{f}_{j_\sigma a_\sigma} \\
&+ \bar{C}_P^{(1,0)} \tilde{B}_P^{i_\sigma a_\sigma\,(0,0)} - \bar{C}_P^{i_\sigma j_\sigma\,(1,0)} \tilde{B}_P^{j_\sigma a_\sigma\,(0,0)} \\
&+ \bar{B}_P^{(1,0)} C_P^{i_\sigma a_\sigma} - \bar{B}_P^{i_\sigma j_\sigma\,(1,0)} C_P^{j_\sigma a_\sigma} \\
&+ [S\lambda]_{j_\sigma}^{a_\sigma\,(0,0)} Z_{i_\sigma j_\sigma}^{(1,0)} - (P|i_\sigma a_\sigma) \sum_\tau \Delta\tilde{Y}_P^{j_\tau j_\tau\,(1,0)} \\
&+ \left(\tilde{Y}_P^{k_\sigma i_\sigma\,(1,0)} + \Delta\tilde{Y}_P^{k_\sigma i_\sigma\,(1,0)} \right) (P|k_\sigma a_\sigma) \\
&+ (P\hat{|}c_\sigma a_\sigma) W_P^{i_\sigma c_\sigma\,(1,0)} - S_{c_\sigma a_\sigma} (P\hat{|}i_\sigma k_\sigma) W_P^{k_\sigma c_\sigma\,(1,0)} \\
&+ S_{c_\sigma a_\sigma} Y_P^{i_\sigma k_\sigma\,(1,0)} \tilde{A}_P^{k_\sigma c_\sigma\,(0,0)} + \bar{A}_P^{i_\sigma k_\sigma\,(1,0)} (P|k_\sigma a_\sigma)
\end{aligned} \tag{2.160}$$

with the new intermediates

$$\bar{\eta}_{i_\sigma}^{a_\sigma\,(1,0)} = h_{i_\sigma a_\sigma}^{(1,0)} + C_P^{(1,0)} C_P^{i_\sigma a_\sigma} + Y_P^{i_\sigma j_\sigma\,(1,0)} C_P^{j_\sigma a_\sigma} \tag{2.161}$$

$$D_{j_\sigma i_\sigma}^{[0,0]} = -\sum_\tau (1 - \frac{\delta_{\sigma\tau}}{2}) \lambda_{k_\tau j_\sigma}^{c_\tau b_\sigma\,(0,0)} [StS]_{c_\tau b_\sigma}^{k_\tau i_\sigma\,(0,0)} \tag{2.162}$$

$$D_{b_\sigma a_\sigma}^{[0,0]} = \sum_\tau (1 - \frac{\delta_{\sigma\tau}}{2}) \lambda_{k_\tau j_\sigma}^{c_\tau a_\sigma\,(0,0)} [St]_{c_\tau b_\sigma}^{k_\tau j_\sigma\,(0,0)} \tag{2.163}$$

$$\bar{y}_{i_\sigma j_\sigma}{}^{(1,0)} = [S\lambda]_{i_\sigma}^{b_\sigma\,(0,0)} t_{b_\sigma}^{j_\sigma\,(1,0)} \tag{2.164}$$

$$\bar{C}_P^{(1,0)} = \sum_\tau C_P^{j_\tau b_\tau} t_{b_\tau}^{j_\tau\,(1,0)} \tag{2.165}$$

$$\bar{C}_P^{i_\sigma j_\sigma\,(1,0)} = C_P^{i_\sigma b_\sigma} t_{b_\sigma}^{j_\sigma\,(1,0)} \tag{2.166}$$

$$\bar{B}_P^{(1,0)} = \sum_\tau t_{b_\tau}^{j_\tau\,(1,0)} \tilde{B}_P^{j_\tau b_\tau\,(0,0)} \tag{2.167}$$

$$\bar{B}_P^{i_\sigma j_\sigma\,(1,0)} = \tilde{B}_P^{i_\sigma b_\sigma\,(0,0)} t_{b_\sigma}^{j_\sigma\,(1,0)} \tag{2.168}$$

$$Z_{i_\sigma j_\sigma}^{(1,0)} = -(P|i_\sigma c_\sigma) A_P^{j_\sigma c_\sigma\,(1,0)} \tag{2.169}$$

$$\Delta\tilde{Y}_P^{j_\sigma i_\sigma\,(1,0)} = -A_P^{j_\sigma b_\sigma\,(1,0)} [S\lambda]_{i_\sigma}^{b_\sigma\,(0,0)} \tag{2.170}$$

$$\tilde{Y}_P^{k_\sigma i_\sigma\,(1,0)} = -\tilde{X}_{k_\sigma c_\sigma}^{(1,0)} C_P^{i_\sigma c_\sigma} \tag{2.171}$$

$$\tilde{X}_{k_\sigma c_\sigma}^{(1,0)} = \sum_\tau [S\lambda]_{j_\tau}^{b_\tau\,(0,0)} t_{b_\tau c_\sigma}^{j_\tau k_\sigma\,(1,0)} \tag{2.172}$$

$$W_P^{i_\sigma c_\sigma\,(1,0)} = \sum_\tau \lambda_{i_\sigma j_\tau}^{c_\sigma b_\tau\,(0,0)} V_P^{j_\tau b_\tau\,(1,0)} \tag{2.173}$$

$$V_P^{j_\tau b_\tau\,(1,0)} = [J^{-1}]_{PQ} B_P^{j_\tau b_\tau\,(1,0)} \tag{2.174}$$

$$\bar{A}_P^{i_\sigma k_\sigma\,(1,0)} = -\tilde{A}_P^{i_\sigma c_\sigma\,(0,0)} [St]_{c_\sigma}^{k_\sigma\,(1,0)}. \tag{2.175}$$

Again, there is often a similarity or outright identity except for the order of the involved amplitudes and multipliers with previously introduced intermediates which can easily be exploited. One of the more important sources of new intermediates is the explicit inclusion

of the perturbed singles amplitudes. Recall that the unperturbed singles amplitudes do not occur explicitly in amplitude and multiplier equations due to the use of dressed integrals.

2.3.4.2 Perturbed doubles multiplier equations

The non-iterative part of the perturbed doubles multipliers is significantly simpler

$$\begin{aligned}\zeta_{i_\sigma j_\tau}^{a_\sigma b_\tau\,[1,0]} =& [S\lambda]_{i_\sigma}^{a_\sigma\,(0,0)} \bar{\eta}_{j_\tau}^{b_\tau\,(1,0)} + [S\lambda]_{j_\tau}^{b_\tau\,(0,0)} \bar{\eta}_{i_\sigma}^{a_\sigma\,(1,0)} \\ & - \delta_{\sigma\tau} [S\lambda]_{i_\sigma}^{b_\sigma\,(0,0)} \bar{\eta}_{j_\sigma}^{a_\sigma\,(1,0)} - \delta_{\sigma\tau} [S\lambda]_{j_\sigma}^{a_\sigma\,(0,0)} \bar{\eta}_{i_\sigma}^{b_\sigma\,(1,0)} \\ & + [S\lambda]_{i_\sigma j_\tau}^{a_\sigma d_\tau\,(0,0)} \hat{h}_{d_\tau b_\tau}^{(1,0)} + \hat{h}_{c_\sigma a_\sigma}^{(1,0)} [\lambda S]_{i_\sigma j_\tau}^{c_\sigma b_\tau\,(0,0)} \\ & - [S\lambda S]_{i_\sigma k_\tau}^{a_\sigma b_\tau\,(0,0)} \hat{h}_{j_\tau k_\tau}^{(1,0)} - [S\lambda S]_{k_\sigma j_\tau}^{a_\sigma b_\tau\,(0,0)} \hat{h}_{i_\sigma k_\sigma}^{(1,0)} \\ & + C_P^{i_\sigma a_\sigma} \bar{V}_P^{j_\tau b_\tau\,(1,0)} - \delta_{\sigma\tau} C_P^{i_\sigma b_\sigma} \bar{V}_P^{j_\sigma a_\sigma\,(1,0)} \\ & - \delta_{\sigma\tau} C_P^{j_\sigma a_\sigma} \bar{V}_P^{i_\sigma b_\sigma\,(1,0)} + C_P^{j_\tau b_\tau} \bar{V}_P^{i_\sigma a_\sigma\,(1,0)} \end{aligned} \tag{2.176}$$

with the intermediate

$$\bar{V}_P^{i_\sigma a_\sigma\,(1,0)} = [S\lambda]_{k_\sigma}^{a_\sigma\,(0,0)} Y_P^{i_\sigma k_\sigma\,(1,0)} - \bar{y}_{i_\sigma k_\sigma}{}^{(1,0)}(P|k_\sigma a_\sigma). \tag{2.177}$$

2.3.5 Updates

The updates are carried out via first order perturbation theory.[74] Since this update depends on the inverse of the Fock matrix, convergence is fastest if the Fock matrix is diagonal in the occupied-occupied and virtual-virtual blocks. This is the case for both canonical UHF and semi-canonical ROHF orbitals.
The equations are considered converged when the square of the norm of the entire update vector applied to the singles and doubles vectors drops below a predetermined threshold. For the calculations presented in later sections of this work we have used the default value of 10^{-8} atomic units.
To accelerate convergence, direct inversion of the iterative subspace (DIIS)[45,94,95] is employed.

2.3.5.1 Singles vectors

In order to obtain the update vector, we need to transform the singles residuum to the (semi-)canonical basis.
The unitary transformation of the occupied (semi-)canonical orbitals $|\bar{i}_\sigma\rangle$ to the LMOs $|i_\sigma\rangle$ is defined by[76]

$$W_{\bar{i}_\sigma i_\sigma} = C^*_{\mu \bar{i}_\sigma} S^{\mathrm{AO}}_{\mu\nu} L_{\nu i_\sigma}, \tag{2.178}$$

with $C_{\mu\bar{i}_\sigma}$ being the coefficients for the linear combination of AOs to the (semi-)canonical MOs and $L_{\nu i_\sigma}$ the transformation from AOs to LMOs introduced in (2.17).
Transformation of the (semi-)canonical virtual MOs to the PAO basis is given by the transformation[76]

$$Q_{\bar{a}_\sigma a_\sigma} = C^*_{\nu \bar{a}_\sigma} S^{\mathrm{AO}}_{\nu\mu}\Big|_{\mu=a_\sigma}, \tag{2.179}$$

with $C_{\mu\bar{a}_\sigma}$ defining the transformation from the AOs to the virtual (semi-)canonical MOs. For transformation of the residual vectors we need the inverse of (2.178) and (2.179). The transformation of the occupied orbitals (2.178) is unitary and inversion is therefore trivial. For the transformation of the virtual orbitals however we have to deal with the complication of redundancies in the PAO basis. These redundancies lead to some eigenvalues in the PAO overlap matrix being (numerically) zero, thus preventing inversion of this matrix. Instead a pseudo-inverse matrix $V_{a_\sigma b_\sigma}$ with the property

$$S^{\mathrm{PAO}}_{a_\sigma c_\sigma} V_{c_\sigma d_\sigma} S^{\mathrm{PAO}}_{d_\sigma b_\sigma} = S^{\mathrm{PAO}}_{a_\sigma b_\sigma} \tag{2.180}$$

is introduced[47,76] via the following procedure:

1. Diagonalize the PAO overlap matrix S^{PAO}.
2. Invert the diagonal elements of the obtained matrix if they are above a certain threshold or set them to zero otherwise.
3. Transform back.

The transformation of the singles residuum to the (semi-)canonical basis is then given by[47]

$$v^{\bar{a}_\sigma}_{\bar{i}_\sigma} = Q_{\bar{a}_\sigma b_\sigma} [V^\dagger]_{b_\sigma a_\sigma} v^{a_\sigma}_{i_\sigma} [W^\dagger]_{i_\sigma \bar{i}_\sigma}. \tag{2.181}$$

The first order perturbative update is obtained via

$$\Delta u^{\bar{a}_\sigma}_{\bar{i}_\sigma} = -\frac{v^{\bar{a}_\sigma}_{\bar{i}_\sigma}}{\epsilon_{\bar{a}_\sigma} - \epsilon_{\bar{i}_\sigma}} \tag{2.182}$$

with $\epsilon_{\bar{q}_\sigma}$ being the (semi-)canonical orbital energies. Since the amplitudes and updates always transform conversely to the residuals and integrals, i.e. they transform as covariant and contravariant objects,[76] the transformation of the update back to the local basis is identical to the transformation in (2.181). The update is then transformed according to[47]

$$\Delta u^{a_\sigma}_{i_\sigma} = Q_{\bar{a}_\sigma b_\sigma} [V^\dagger]_{b_\sigma a_\sigma} \Delta u^{\bar{a}_\sigma}_{\bar{i}_\sigma} [W^\dagger]_{\bar{i}_\sigma i_\sigma} \tag{2.183}$$

and added to the singles amplitudes or multipliers of the previous iteration.

2.3.5.2 Doubles vectors

In contrast to the singles vectors, the virtual space for the doubles vectors is restricted to pair-domains. Therefore, transformation of the occupied orbitals would lead to a mixing of these pair-specific virtual spaces, thus leading to loss of the locality of the update. Instead, the inversion of the occupied-occupied part of the Fock matrix is approximated via use of the diagonal elements of the Fock matrix in local basis.
For the virtual space we introduce pair-specific transformations to a "pseudo-canonical" pair basis as suggested by Hampel and Werner[74], i.e. we obtain transformation matrices and virtual orbital energies for each pair by diagonalizing the Fock matrix in the pair specific virtual basis. Note that elimination of redundancies is again essential.
For each pair $[ij]$, we transform the doubles residual vectors from the domain restricted PAO basis a_σ to the pseudo-canonical pair basis $\bar{a}_\sigma$ according to

$$V^{[i_\sigma j_\tau]}_{\bar{a}_\sigma \bar{b}_\tau} = W^{[i_\sigma j_\tau]}_{c_\sigma \bar{a}_\sigma} V^{[i_\sigma j_\tau]}_{c_\sigma d_\tau} W^{[i_\sigma j_\tau]}_{d_\tau \bar{b}_\tau}. \tag{2.184}$$

The superscript $[i_\sigma j_\tau]$ is here to be understood not as an index to be contracted over but as an indication that each pair has its own pair-specific virtual space and therefore transformation matrices. Note that the left and right transformation matrices are only identical for same spin pairs, whereas the case $\sigma \neq \tau$ requires two independent matrices.[55] The perturbative update is then given by

$$\Delta U^{[i_\sigma j_\tau]}_{\bar{a}_\sigma \bar{b}_\tau} = -\frac{V^{[i_\sigma j_\tau]}_{\bar{a}_\sigma \bar{b}_\tau}}{\epsilon^{[i_\sigma j_\tau]}_{\bar{a}_\sigma} + \epsilon^{[i_\sigma j_\tau]}_{\bar{b}_\sigma} - f_{i_\sigma i_\sigma} - f_{j_\tau j_\tau}} \tag{2.185}$$

with the virtual orbital energies $\epsilon^{[i_\sigma j_\tau]}_{\bar{a}_\sigma}$ in the pseudo-canonical pair basis and the diagonal elements $f_{i_\sigma i_\sigma}$ of the Fock matrix in the local basis.
Finally, the update is transformed back to the local basis

$$\Delta U^{[i_\sigma j_\tau]}_{a_\sigma b_\tau} = W^{[i_\sigma j_\tau]}_{a_\sigma \bar{c}_\sigma} \Delta U^{[i_\sigma j_\tau]}_{\bar{c}_\sigma \bar{d}_\tau} W^{[i_\sigma j_\tau]}_{b_\tau \bar{d}_\tau} \tag{2.186}$$

and added to the doubles amplitudes or multipliers of the previous iteration.

2.3.6 Density matrices

The density matrices are implicitly defined by the equations

$$L^{[1,0]} = h^{(1,0)}_{\mu\nu} D^{[0,0]}_{\nu\mu} \tag{2.187}$$

$$L^{[1,1]} = h^{(1,1)}_{\mu\nu} D^{[0,0]}_{\nu\mu} + h^{(0,1)}_{\mu\nu} D^{[1,0]}_{\nu\mu} \tag{2.188}$$

where μ and ν refer to AOs (see section 2.2.1.4 and 2.2.1.5). The type of integral and density matrix depends on the property under consideration. Note that the equations above only hold if all perturbation operators are purely one-electron operators, i.e. we only require the one-electron density matrices. Since we approximate the two-electron contributions to the electronic g-shift via an effective one-electron operator (see section 2.2.2.2) and the electric dipole moments and polarizabilities only depend on one-electron operators, this condition is fulfilled in our case.
In the LMO/PAO basis, each density matrix consists of two (one for α, one for β spin) times four blocks: occupied-occupied, occupied-virtual, virtual-occupied and virtual-virtual. Integrals and densities transform contravariant (see appendix B.3.2.3). Therefore, transformation of the spin-specific density matrices from LMO/PAO basis to the AO basis employs the same transformation matrices (2.19), (2.20), (2.21) and (2.22) that have been used for the transformation of the integrals from the AO to the LMO/PAO basis

$$\begin{aligned} D^{\sigma\ [m,n]}_{\nu\mu} =& {}^H\Lambda^{\text{occ}}_{\nu j_\sigma} D^{[m,n]P}_{j_\sigma i_\sigma} \Lambda^{\text{occ}}_{\mu i_\sigma} + {}^H\Lambda^{\text{occ}}_{\nu i_\sigma} D^{[m,n]P}_{i_\sigma a_\sigma} \Lambda^{\text{virt}}_{\mu a_\sigma} \\ &+ {}^H\Lambda^{\text{virt}}_{\nu a_\sigma} D^{[m,n]P}_{a_\sigma i_\sigma} \Lambda^{\text{occ}}_{\mu i_\sigma} + {}^H\Lambda^{\text{virt}}_{\nu b_\sigma} D^{[m,n]P}_{b_\sigma a_\sigma} \Lambda^{\text{virt}}_{\mu a_\sigma}. \end{aligned} \tag{2.189}$$

For spin-independent properties we require the charge density matrices

$$D^{[m,n]}_{\nu\mu} = \sum_\sigma D^{\sigma\ [m,n]}_{\nu\mu} \tag{2.190}$$

while spin dependent properties require contraction of the integrals with the normalized spin density matrices as derived via spin-field reduction (see appendix A)

$$D^{S\ [m,n]}_{\nu\mu} = \frac{1}{2S}\big(D^{\alpha\ [m,n]}_{\nu\mu} - D^{\beta\ [m,n]}_{\nu\mu}\big). \tag{2.191}$$

S is here just equal to the spin projection S_z, i.e. the difference of the numbers of α- and β-electrons times one-half, since we solve the equations for the component of the spin multiplet with maximum spin projection.

2.3.6.1 Unperturbed density matrix

The equations for the unperturbed density matrix have been derived in appendix B.3.2.3. The four blocks of the spin-specific unperturbed density matrix in LMO/PAO basis are given by

$$D^{[0,0]}_{j_\sigma i_\sigma} = -\sum_\tau (1 - \frac{\delta_{\sigma\tau}}{2}) \lambda^{c_\tau b_\sigma\,(0,0)}_{k_\tau j_\sigma} [StS]^{k_\tau i_\sigma\,(0,0)}_{c_\tau b_\sigma} \tag{2.192}$$

$$D^{[0,0]}_{i_\sigma a_\sigma} = \lambda^{a_\sigma\,(0,0)}_{i_\sigma} \tag{2.193}$$

$$D^{[0,0]}_{a_\sigma i_\sigma} = t^{i_\sigma\,(0,0)}_{a_\sigma} + \sum_\tau [S\lambda]^{b_\tau\,(0,0)}_{j_\tau} t^{b_\tau a_\sigma\,(0,0)}_{j_\tau i_\sigma} \tag{2.194}$$

$$D^{[0,0]}_{b_\sigma a_\sigma} = \sum_\tau (1 - \frac{\delta_{\sigma\tau}}{2}) \lambda^{c_\tau a_\sigma\,(0,0)}_{k_\tau j_\sigma} [St]^{k_\tau j_\sigma\,(0,0)}_{c_\tau b_\sigma}. \tag{2.195}$$

Note that $D^{[0,0]}_{j_\sigma i_\sigma}$ and $D^{[0,0]}_{b_\sigma a_\sigma}$ also appear as intermediates in the non-iterative part of the perturbed singles multiplier equations (2.160) as well as the perturbed density matrix (vide infra).
After transforming the spin-specific density matrices to the AO basis, the Hartree-Fock contribution needs to be added before building the charge or spin density matrix.

2.3.6.2 Perturbed density matrix

The derivation of the equations for the perturbed density matrices can be found in appendix B.3.2.8. At first glance the perturbed density matrices seem to be significantly more complicated than the unperturbed density matrix. However, many of the contractions come in pairs, with the only difference being interchange of the orders of amplitudes and multipliers. That, in addition to the general similarity to the unperturbed density matrix, allows for significant reuse of code.
For the occupied-occupied block we have

$$\begin{aligned} D^{[1,0]}_{j_\sigma i_\sigma} = &-[St]^{i_\sigma\,(1,0)}_{c_\sigma} \lambda^{c_\sigma\,(0,0)}_{j_\sigma} - \sum_\tau (1 - \frac{\delta_{\sigma\tau}}{2}) \lambda^{c_\tau b_\sigma\,(1,0)}_{k_\tau j_\sigma} [StS]^{k_\tau i_\sigma\,(0,0)}_{c_\tau b_\sigma} \\ &- \sum_\tau (1 - \frac{\delta_{\sigma\tau}}{2}) [S\lambda S]^{c_\tau b_\sigma\,(0,0)}_{k_\tau j_\sigma} t^{k_\tau i_\sigma\,(1,0)}_{c_\tau b_\sigma}. \end{aligned} \tag{2.196}$$

The occupied-virtual block is again just the singles-multipliers

$$D^{[1,0]}_{i_\sigma a_\sigma} = \lambda^{a_\sigma\,(1,0)}_{i_\sigma} \tag{2.197}$$

whereas the virtual-occupied block has significantly more terms

$$\begin{aligned} D^{[1,0]}_{a_\sigma i_\sigma} = &t^{i_\sigma\,(1,0)}_{a_\sigma} + \sum_\tau [S\lambda]^{b_\tau\,(1,0)}_{j_\tau} t^{b_\tau a_\sigma\,(0,0)}_{j_\tau i_\sigma} + \sum_\tau [S\lambda]^{b_\tau\,(0,0)}_{j_\tau} t^{b_\tau a_\sigma\,(1,0)}_{j_\tau i_\sigma} \\ &- [St]^{i_\sigma\,(1,0)}_{c_\sigma} D^{[0,0]}_{a_\sigma c_\sigma} + t^{k_\sigma\,(1,0)}_{a_\sigma} D^{[0,0]}_{k_\sigma i_\sigma}. \end{aligned} \tag{2.198}$$

Finally, the virtual-virtual block is just

$$\begin{aligned} D^{[1,0]}_{b_\sigma a_\sigma} = &\, t^{k_\sigma\,(1,0)}_{b_\sigma} \lambda^{a_\sigma\,(0,0)}_{k_\sigma} + \sum_\tau (1 - \frac{\delta_{\sigma\tau}}{2}) [S\lambda]^{c_\tau a_\sigma\,(0,0)}_{k_\tau j_\sigma} t^{k_\tau j_\sigma\,(1,0)}_{c_\tau b_\sigma} \\ &+ \sum_\tau (1 - \frac{\delta_{\sigma\tau}}{2}) \lambda^{c_\tau a_\sigma\,(1,0)}_{k_\tau j_\sigma} [St]^{k_\tau j_\sigma\,(0,0)}_{c_\tau b_\sigma}. \end{aligned} \tag{2.199}$$

In contrast to the unperturbed density matrix, there is no Hartree-Fock contribution to the perturbed density matrix.

2.3.7 First and second order static properties

In this thesis, only static properties have been implemented. Dynamic, i.e. frequency dependent, properties require generalization to time dependent response theory.[96] Time dependent CC2 response methods for the calculation of first order properties of extended systems have been implemented for singlet[46,48] and triplet[49–51] states. They are generally of the same complexity as time independent second order properties, so their implementation for unrestricted CC2 goes beyond the scope of this work.

2.3.7.1 Permanent electric dipole moments

The three components of the electric dipole moment μ_{el} are obtained by contracting the unperturbed charge density matrix with the dipole integrals

$$h^{x}_{\mu\nu}{}^{(1,0)} =< \mu|x|\nu > \tag{2.200}$$

and subtracting the result from the nuclear contribution, i.e.

$$\mu^{x}_{\mathrm{el}} = \sum_{K}^{N_{\mathrm{nuc}}} Z_K R^{x}_K - < \mu|x|\nu > D^{[0,0]}_{\nu\mu} \tag{2.201}$$

with x being any of the three Cartesian coordinates, Z_K the charge and R^x_K the position of the K-th nucleus.

2.3.7.2 Static electric dipole polarizabilities

The Cartesian components $D^{y}_{\nu\mu}{}^{[1,0]}$ of the perturbed charge density matrices required for the electric dipole polarizability are obtained by using

$$h^{y}_{\mu\nu}{}^{(1,0)} =< \mu|y|\nu > \tag{2.202}$$

in the perturbed amplitude and multiplier equations. Note that the superscript y has been suppressed in the earlier sections for readability and the perturbed equations derived above are valid for each Cartesian component individually.
Contracting these density matrices with the dipole moment integrals and multiplying by -1 yields the polarizability tensor

$$\alpha^{xy} = - < \mu|x|\nu > D^{y}_{\nu\mu}{}^{[1,0]} \tag{2.203}$$

with xy being any combination of Cartesian coordinates.

2.3.7.3 Electronic g-tensor shift

As shown in appendix A, the g-shift as defined in (2.84) is obtained via the contraction of spatial integrals derived from the spin dependent perturbation operators (2.85) and (2.94) with the normalized spin density matrices (2.191)

$$\Delta g_{xy} = [h^{(1,1)}_{\mu\nu}]_{xy} D^{S}_{\nu\mu}{}^{(0,0)} + [h^{(0,1)}_{\mu\nu}]_{x} [D^{S}_{\nu\mu}{}^{[1,0]}]_{y}. \tag{2.204}$$

The perturbation integrals for the non-iterative part of the perturbed equations are derived from the orbital Zeeman term (2.100) and are taken as

$$h_{\mu\nu}^{y\ (1,0)} = \langle\mu|(\mathbf{r}_0 \times \nabla)_y|\nu\rangle \tag{2.205}$$

with

$$\mathbf{r}_0 = \mathbf{r} - \mathbf{R}_0^{\mathrm{SDC}} \tag{2.206}$$

being the distance from the center $\mathbf{R}_0^{\mathrm{SDC}}$ of the unperturbed spin density as defined in (2.132). The prefactor of $\alpha/2$ has been dropped in order to be able to use the same convergence threshold as for the unperturbed equations. Since it corresponds to the Bohr magneton in (2.77), it will not be reintroduced later. Accounting for the factor of $-i$ from the expansion of the momentum operator however will be handled on contraction of the perturbed density matrix with the paramagnetic spin-orbit integrals.
The g-shift due to the kinetic energy correction (2.87) to the electronic Zeeman term is

$$\Delta g_{xy}^{\mathrm{ZKE}} = \delta_{xy} h_{\mu\nu}^{\mathrm{ZKE}} D_{\nu\mu}^{S\ (0,0)} \tag{2.207}$$

$$h_{\mu\nu}^{\mathrm{ZKE}} = -\alpha^2 g_e \langle\mu|\nabla^2|\nu\rangle. \tag{2.208}$$

For the effective one-electron diamagnetic spin-orbit coupling derived from (2.101) we have

$$\Delta g_{xy}^{\mathrm{DSO}} = [h_{\mu\nu}^{\mathrm{DSO}}]_{xy} D_{\nu\mu}^{S\ (0,0)} \tag{2.209}$$

$$[h_{\mu\nu}^{\mathrm{DSO}}]_{xy} = \frac{\alpha^2 g_e}{4} \sum_K Z_K^{\mathrm{eff}} \left\langle \mu \left| \frac{\delta_{xy} \mathbf{r}_K \cdot \mathbf{r}_0 - x_K y_0}{r_K^3} \right| \nu \right\rangle \tag{2.210}$$

with the distance to the K-th nucleus

$$\mathbf{r}_K = \mathbf{r} - \mathbf{R}_K. \tag{2.211}$$

Separate shifts for the one-electron and two-electron contributions can be obtained by simply evaluating the one-electron term with the actual nuclear charges as

$$\Delta g_{xy}^{\text{1el-DSO}} = [h_{\mu\nu}^{\text{1el-DSO}}]_{xy} D_{\nu\mu}^{S\ (0,0)} \tag{2.212}$$

$$[h_{\mu\nu}^{\text{1el-DSO}}]_{xy} = \frac{\alpha^2 g_e}{4} \sum_K Z_K \left\langle \mu \left| \frac{\delta_{xy} \mathbf{r}_K \cdot \mathbf{r}_0 - x_K y_0}{r_K^3} \right| \nu \right\rangle \tag{2.213}$$

and defining the two-electron contribution via

$$\Delta g_{xy}^{2el-DSO} = \Delta g_{xy}^{DSO} - \Delta g_{xy}^{1el-DSO}. \tag{2.214}$$

Finally, the contribution from the effective one-electron paramagnetic spin-orbit operator (2.102) is

$$\Delta g_{xy}^{\mathrm{PSO}} = [h_{\mu\nu}^{\mathrm{PSO}}]_x [D_{\nu\mu}^{S\ [1,0]}]_y \tag{2.215}$$

$$[h_{\mu\nu}^{\mathrm{PSO}}]_x = -\frac{\alpha^2 g_e}{4} \sum_K Z_K^{\mathrm{eff}} \left\langle \mu \left| \frac{(\mathbf{r}_K \times \nabla)_x}{r_K^3} \right| \nu \right\rangle. \tag{2.216}$$

We can again split this into the actual one-electron

$$\Delta g_{xy}^{\text{1el-PSO}} = [h_{\mu\nu}^{\text{1el-PSO}}]_x [D_{\nu\mu}^{S\,[1,0]}]_y \tag{2.217}$$

$$[h_{\mu\nu}^{\text{1el-PSO}}]_x = -\frac{\alpha^2 g_e}{4} \sum_K Z_K \left\langle \mu \left| \frac{(\mathbf{r}_K \times \nabla)_x}{r_K^3} \right| \nu \right\rangle. \tag{2.218}$$

and an approximate two-electron contribution

$$\Delta g_{xy}^{\text{2el-PSO}} = \Delta g_{xy}^{\text{PSO}} - \Delta g_{xy}^{\text{1el-PSO}}. \tag{2.219}$$

The complete g-shift is then simply

$$\Delta g_{xy} = \Delta g_{xy}^{\text{ZKE}} + \Delta g_{xy}^{\text{DSO}} + \Delta g_{xy}^{\text{PSO}} \tag{2.220}$$

$$= \Delta g_{xy}^{\text{ZKE}} + \Delta g_{xy}^{\text{1el-DSO}} + \Delta g_{xy}^{\text{2el-DSO}} + \Delta g_{xy}^{\text{1el-PSO}} + \Delta g_{xy}^{\text{2el-PSO}}. \tag{2.221}$$

All the required integrals are essentially identical to those used by Loibl in his implementation of nuclear magnetic shielding tensors.[52,53,93] Aside from slight modification, his code has been reused for the integral evaluation.

Chapter 3

Results

3.1 Computational details

In the following, the method developed in this thesis will be referred to as Z_{eff}-SDC-DF-LUCC2. It has been implemented as part of the Molpro[97,98] quantum chemistry package. Due to the sheer number of investigated g-shifts and degrees of freedom in the approximations, we will only compare the isotropic g-shifts

$$\Delta g_{iso} = \frac{1}{3}(\Delta g_{xx} + \Delta g_{yy} + \Delta g_{zz}). \tag{3.1}$$

This also removes the dependence on the orientation of the molecules. To improve convergence of the reference method to the correct state, the actual DF-HF[99] reference calculations have been preceded by DF-MCSCF[100] calculations. The calculations did not make use of parallelization, which is an option to increase the efficiency of the code to be explored in future work. The plots in this thesis have been generated with Matplotlib.[101]

3.1.1 Benchmark sets

To test the accuracy of the method developed in this thesis as well as the effect of varying the extent of the local correlation and density fitting approximations, we will employ five benchmark sets of molecules.

3.1.1.1 Perera set

The first is the benchmark set of small molecules used by Perera *et al.*[34] in their study of GIAO-CCSD at the aug-cc-pVTZ[102–107] level with exact two-electron spin-orbit operators. Their data, which includes results and geometries, have kindly been provided by Perera and Morales.[108] This allows for comparison of the individual contributions to the g-tensor for the entire set in addition to the net g-shifts. In their calculations, Perera *et al.*[34] used UHF reference functions. To ensure comparability of the results, we will do so as well.

3.1.1.2 Gauss set

A subset of the Perera benchmark molecules had been used in a previous study by Gauss *et al.*[33] for their investigation of Z_{eff}-GIAO-CCSD. It has also been used by Glasbrenner *et al.*[36] for the comparison of their Z_{eff}-GIAO-B3LYP and SOMF-GIAO-B3LYP results with CCSD.

3.1.1.3 Glasbrenner small molecule set

The third set of molecules we are going to examine is the set of small molecules used by Glasbrenner *et al.*[35] in their investigation of the effects of gauge shifts on the g-tensors obtained with SOMF-B3LYP. There is a significant overlap of the set with the molecules of the Perera benchmark set, but direct comparison is not meaningful, since they used different basis sets and some of the optimized geometries are different. Since it has previously been established that coupled-cluster g-tensor calculations require at least triple-zeta basis sets to be meaningful,[33] we will only examine their results obtained with the def2-TZVP[109] basis set.

3.1.1.4 Glasbrenner single spin-center set

In the same study, Glasbrenner *et al.*[35] used two additional sets of molecules to estimate the applicability of the SDC approximation when compared to GIAOs. The first of those is a set of molecules with a single spin-center.

3.1.1.5 Glasbrenner multiple spin-center set

The final test set employed by Glasbrenner *et al.*[35] consists of molecules with multiple spin-centers. Choosing the SDC as a common gauge origin is likely to yield unsatisfactory results for these molecules compared to a truly gauge invariant solution like GIAOs, but investigating the severity of the error is nevertheless worthwhile.

3.1.2 Error measures

Two error estimates will be given in each case for the results with and without outliers, the mean absolute deviation (MAD)

$$\text{MAD [ppm]} = \frac{1}{N_{\text{molecules}}} \sum_{i}^{N_{\text{molecules}}} |\Delta g(i) - \Delta g^{ref}(i)| \tag{3.2}$$

and the mean relative deviation (MRD)

$$\text{MRD [\%]} = \frac{1}{N_{\text{molecules}}} \sum_{i}^{N_{\text{molecules}}} \frac{|\Delta g(i) - \Delta g^{ref}(i)|}{|\Delta g^{ref}(i)|}. \tag{3.3}$$

As has been previously remarked by Perera *et al.*,[34] the uncertainties in experimental g-shifts are on the order of 500 to 1000 ppm. Therefore, an agreement with the reference values within this interval can be deemed sufficient.

3.1.3 General problems and outliers

3.1.3.1 Error sources

We are in the unfortunate position that the vast majority of the reference results use not just different methods (GIAO-CCSD or GIAO-B3LYP), but also different approximations for the two-electron spin-orbit part (exact two-electron spin-orbit operators or the SOMF operator for the PSO contribution and effective charges for the DSO contribution). This makes isolating the source of the errors in the method presented here rather difficult.

However, as Perera *et al.*[34] pointed out, B3LYP yields results very close to CCSD. And the work of Neese[89] showed that g-tensors obtained using the SOMF operator are generally within 10 % of those obtained with effective charges. This together with an analysis of the individual contributions to the g-tensor as compared to GIAO-CCSD should allow for at least a qualitative judgment of the accuracy of Z_{eff}-SDC-DF-LUCC2 g-tensors.

3.1.3.2 Relative versus absolute errors

A further problem arises for very large g-shifts of the order of approximately 10^5 ppm. Even a small relative error of only 1 % would lead to an absolute error of 1000 ppm or more in these cases, which is already larger than the experimental uncertainty. Since we can expect errors far larger than that from use of effective charges alone, it is unlikely that the Z_{eff}-SDC-DF-LUCC2 method will yield satisfactory results for these molecules. Mean deviations will be provided for inclusion and exclusion of these molecules, and explicit values for their g-shifts will be provided in the respective subsections. Furthermore, to increase the readability we will exclude their shifts from the majority of the plots. Examples for molecules with isotropic g-shifts predicted by Z_{eff}-SDC-DF-LUCC2 of more than 70000 ppm are $C_{19}H_{39}O$, NaF^+ and Cys-Gly$_4$ of the Glasbrenner single spin-center set.
On the other end of the magnitude of g-shifts we have LiH^+ with an isotropic g-shift of 37 ppm. It is very insensitive to the method used due to only having a single valence electron and has therefore been excluded from the Glasbrenner single spin-center set.

3.1.3.3 Near-degeneracies and convergence issues

A final problem arises in the case of near-degeneracies, which may prevent the convergence of the DF-HF reference calculation to the correct ground state. For AlO and C_6H_5 the DF-UHF reference calculation failed to converge, and the two molecules have been excluded from our analysis.
For comparison to the GIAO-CCSD results, we can actually investigate this by comparing the reference energies included in the data provided by Perera and Morales. Due to density fitting, we expect an error in the energy on the order of 10^{-5} Hartree per atom.[99] For the molecules ClO_2 and NO_3^{2-} however we find a deviation of $9 \cdot 10^{-3}$ and $19 \cdot 10^{-3}$ Hartree, respectively. This clearly indicates convergence to different states, making comparison of the g-shifts obtained with GIAO-CCSD and Z_{eff}-SDC-DF-LUCC2 meaningless for these two molecules. Therefore, they have been removed from the test set for the comparison to the reference method but have been kept for the investigation of internal degrees of freedom. For the SOMF-B3LYP calculations, convergence to different states can unfortunately not be determined so easily. The molecule $C_{19}FH_{26}N$ had to be removed from the Glasbrenner multiple spin-center set, since the DF-LUCC2 ground state calculation did not converge.
Furthermore, near-degeneracies and multi-reference situations can pose a significant challenge to single-reference methods like Hartree-Fock, Møller-Plesset perturbation, coupled-cluster and even density functional theory.
The outliers will be discussed in the relevant sections.

3.2 Comparison to other methods and experiment

3.2.1 Perera and Gauss sets

3.2.1.1 GIAO-CCSD

For the comparison to the isotropic g-shifts obtained with GIAO-CCSD at the aug-cc-pVTZ level with a UHF reference extracted from the data of Perera *et al.*[108], we use g-shifts obtained with Z_{eff}-SDC-DF-LUCC2 at the aug-cc-pVTZ level with aug-cc-pVQZ fitting basis[110,111], inclusion of all LMO pairs, Boughton-Pulay domains extended by one bond (in the following referred to as "extended domains") and a DF-UHF reference. The former are collected in table C.5, the latter in table C.6.
Comparing the total isotropic g-shifts (fig. 3.1) we find on average good agreement between the methods (MAD = 300 ppm, MRD = 11.4 %), especially considering that GIAO-CCSD uses the exact two-electron integrals whereas the method developed in this thesis only uses the effective charge approximation, which can already be expected to yield relative errors of approximately 10 %.
The ZKE contribution to the g-shift (fig. 3.2) is always negative and has a rather small ($<$ 400 ppm) absolute value for the entire test set. Its method error is virtually zero (MAD = 6.0 ppm, MRD = 2.3 %).
A similarly good agreement (MAD = 10 ppm, MRD = 5.5 %) is found for the 1el-DSO contribution (fig. 3.3), which is always positive and has also a very small absolute value ($<$ 300 ppm).
Given the nearly identical 1el-DSO contributions, we would expect the 2el-DSO contributions to be of similar quality, assuming the effective charge approximation is valid. However, that is clearly not the case (fig. 3.4) if we consider the relative errors (MRD = 70.7 %). This should not come as a surprise, since the effective charges were obtained empirically for the matrix elements of the PSO operator between different states.[85,86] While the absolute values of the 2el-DSO contribution are systematically underestimated (MAD = 153 ppm) by the effective charge approximation, it is still qualitatively correct, i.e. all the contributions are negative, but that is a rather poor consolation. For the systems under investigation, simply neglecting the 2el-DSO component actually constitutes a barely noticeable improvement of the absolute errors in the total g-shift (MAD = 293 ppm) although the relative errors are slightly larger (MRD = 13.0 %).
The errors (MAD = 593 ppm, MRD = 11.9 %) in the 1el-PSO contribution (fig. 3.5) are on average larger than the errors in the total g-shift and are approaching the experimental inaccuracies of 500 to 1000 ppm. Since the one-electron integrals are identical for both methods, this is purely a method error.
The average errors (MAD = 406 ppm, MRD = 28.7 %) for the 2el-PSO contribution (fig. 3.6) are again larger than those for the total g-shift. However, since the one-electron and two-electron terms are of opposite sign and the absolute values are underestimated in both cases, these errors compensate each other at least to some degree, leading to the overall improvement observed in the total g-shifts.
In general, we conclude that the Z_{eff}-SDC-DF-LUCC2 method is able to approximate the CCSD results within the experimental uncertainties for the vast majority of the molecules in the Perera benchmark set. Nevertheless, an improvement of the two-electron spin-orbit approximation is desirable. Using effective charges fails utterly to accurately approximate the 2el-DSO contributions and even for the 2el-PSO terms it is in some cases, e.g. CF_3Cl^-, not even qualitatively correct.

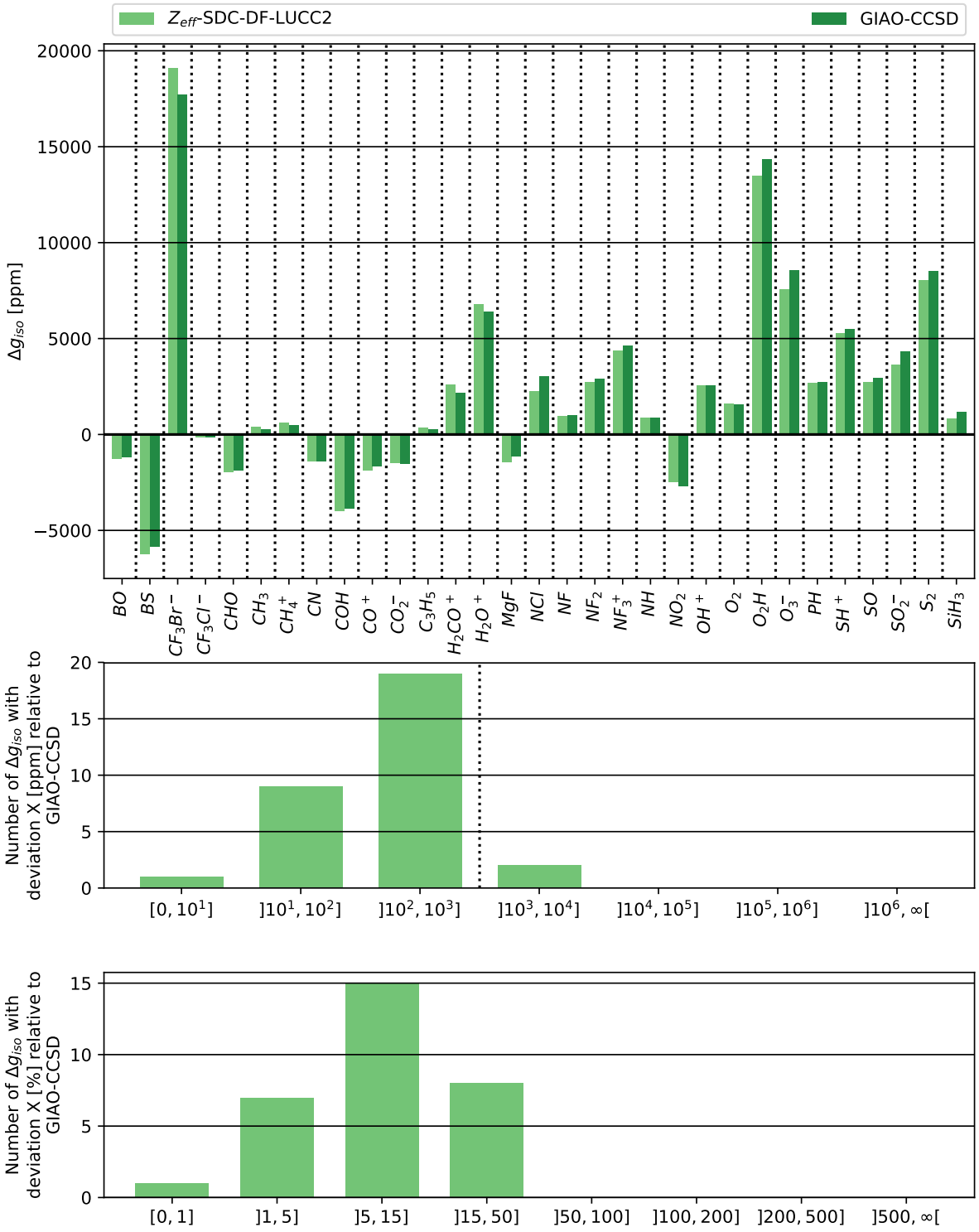

Figure 3.1: Comparison of the isotropic g-shift Δg_{iso} calculated with Z_{eff}-SDC-DF-LUCC2 at the aug-cc-pVTZ/aug-cc-pVQZ level with DF-UHF reference, extended Boughton-Pulay domains and full pair lists for a subset of the benchmark set of Perera *et al.* to GIAO-CCSD using exact two-electron spin-orbit operators at the aug-cc-pVTZ level.[108]

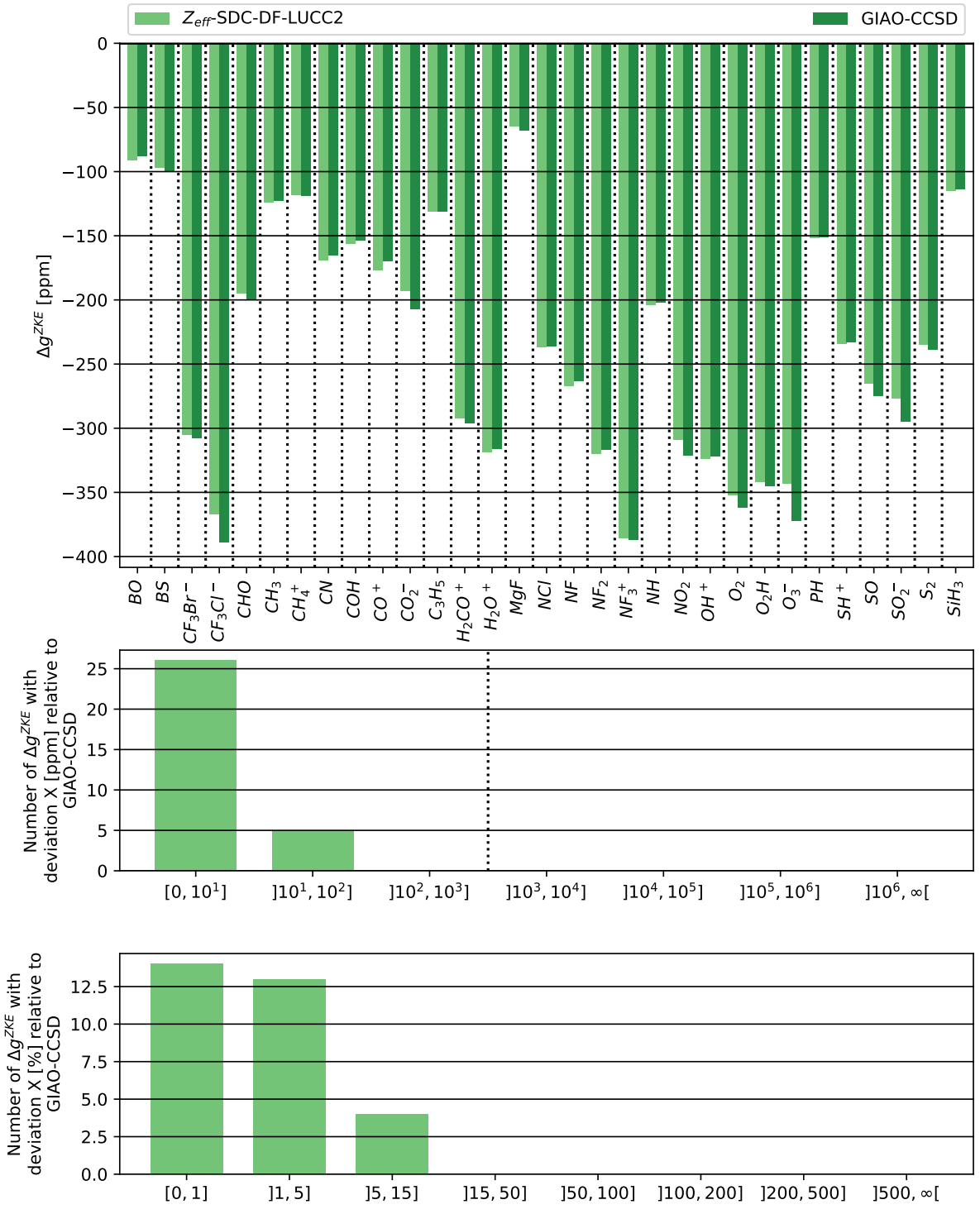

Figure 3.2: Comparison of the Zeeman kinetic energy correction contribution Δg^{ZKE} to the diagonal elements of the g-shift Δg calculated with Z_{eff}-SDC-DF-LUCC2 at the aug-cc-pVTZ/aug-cc-pVQZ level with DF-UHF reference, extended Boughton-Pulay domains and full pair lists for a subset of the benchmark set of Perera *et al.* to GIAO-CCSD using exact two-electron spin-orbit operators at the aug-cc-pVTZ level.[108]

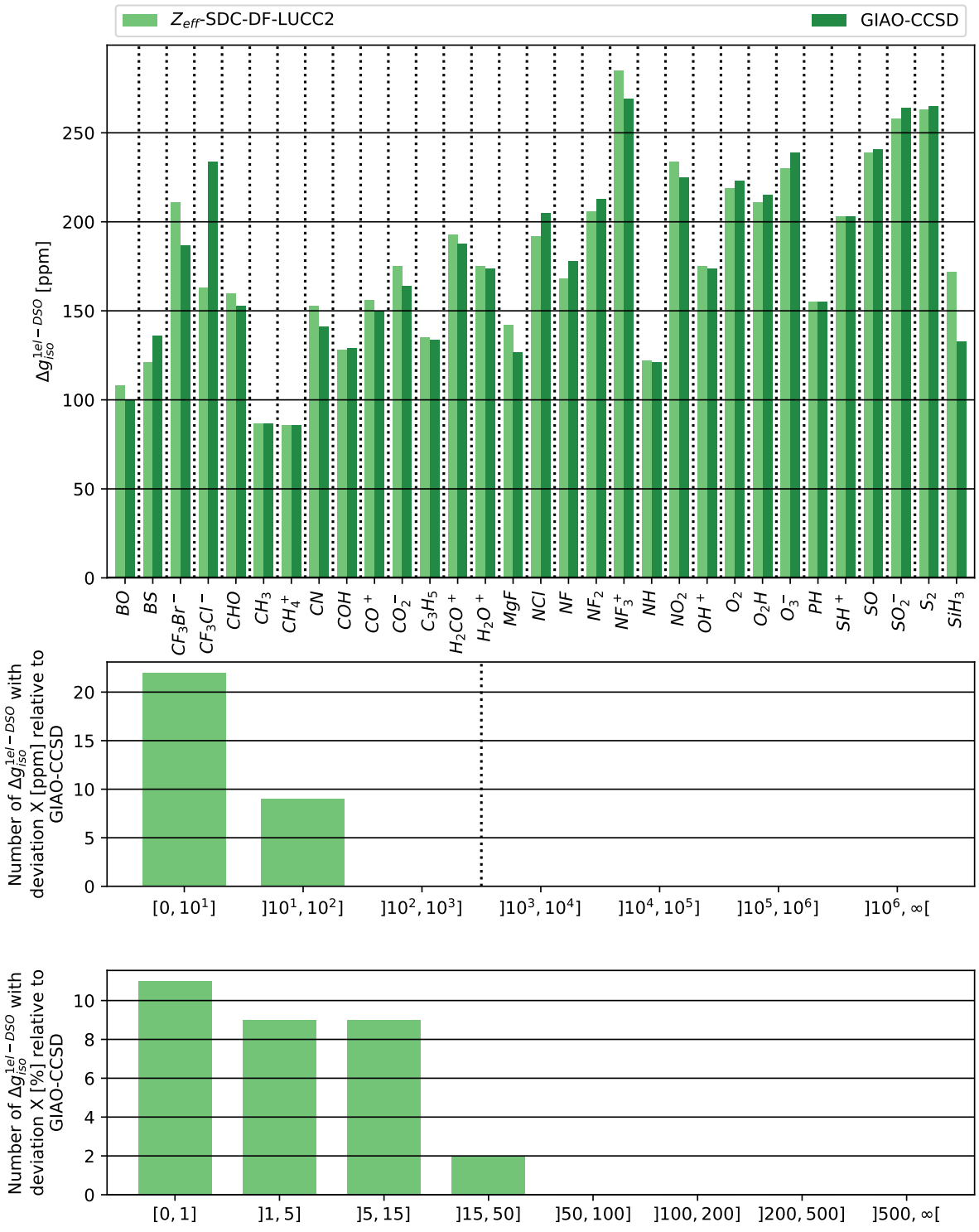

Figure 3.3: Comparison of the one-electron diamagnetic spin-orbit contribution $\Delta g_{iso}^{1el-DSO}$ to the isotropic g-shift Δg_{iso} calculated with Z_{eff}-SDC-DF-LUCC2 at the aug-cc-pVTZ/aug-cc-pVQZ level with DF-UHF reference, extended Boughton-Pulay domains and full pair lists for a subset of the benchmark set of Perera *et al.* to GIAO-CCSD using exact two-electron spin-orbit operators at the aug-cc-pVTZ level.[108]

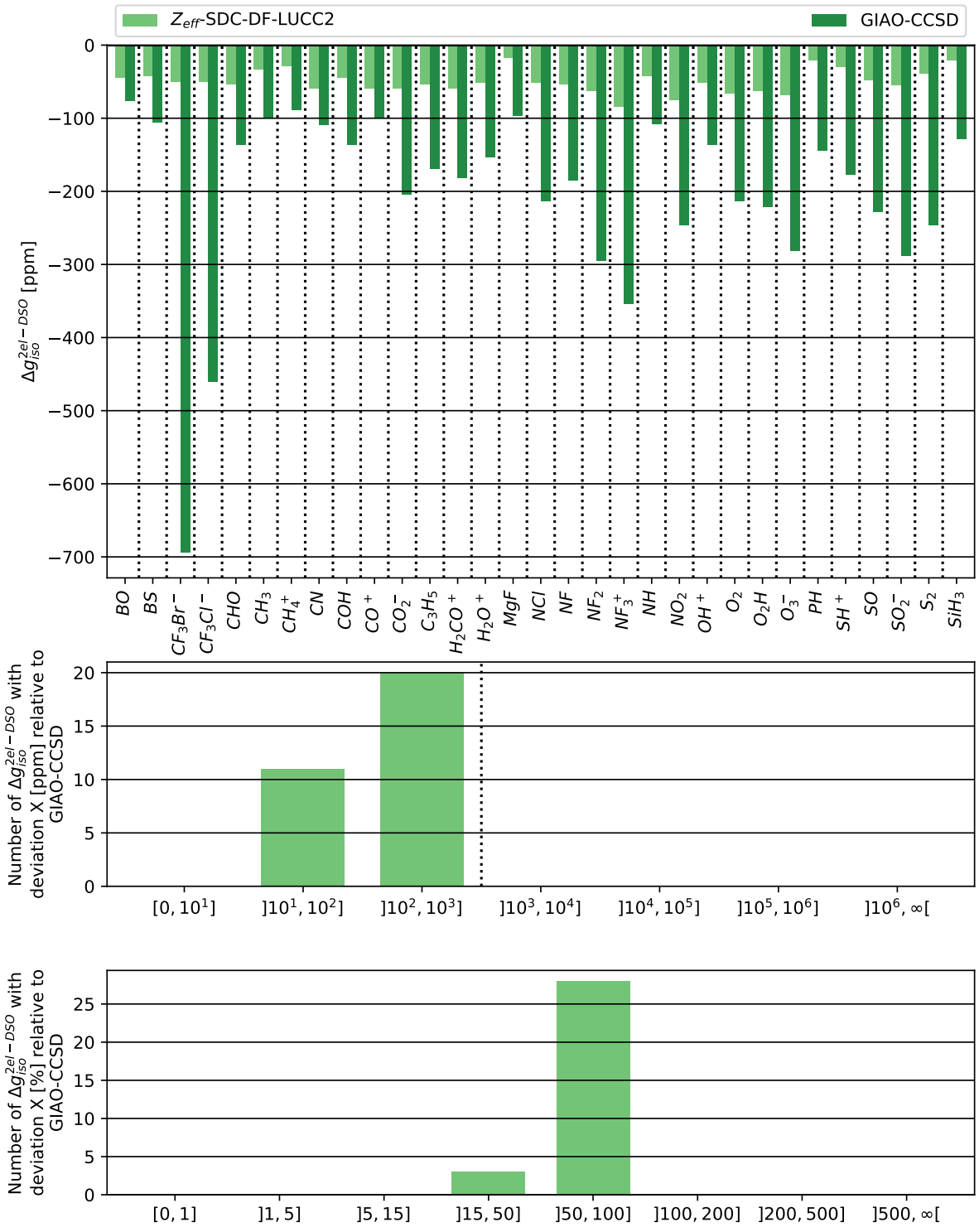

Figure 3.4: Comparison of the two-electron diamagnetic spin-orbit contribution $\Delta g_{iso}^{2el-DSO}$ to the isotropic g-shift Δg_{iso} calculated with Z_{eff}-SDC-DF-LUCC2 at the aug-cc-pVTZ/aug-cc-pVQZ level with DF-UHF reference, extended Boughton-Pulay domains and full pair lists for a subset of the benchmark set of Perera *et al.* to GIAO-CCSD using exact two-electron spin-orbit operators at the aug-cc-pVTZ level.[108]

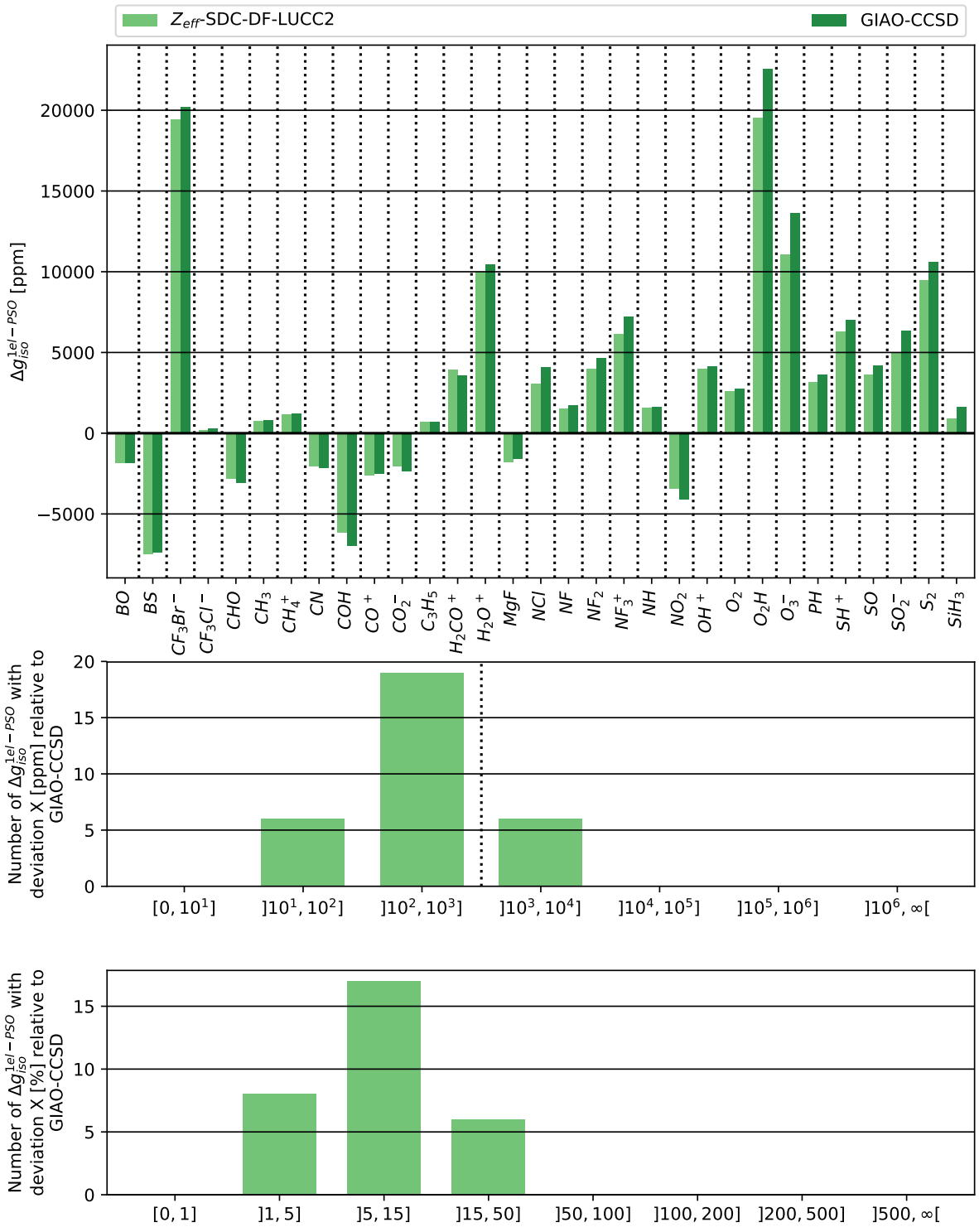

Figure 3.5: Comparison of the one-electron paramagnetic spin-orbit contribution $\Delta g_{iso}^{1el-PSO}$ to the isotropic g-shift Δg_{iso} calculated with Z_{eff}-SDC-DF-LUCC2 at the aug-cc-pVTZ/aug-cc-pVQZ level with DF-UHF reference, extended Boughton-Pulay domains and full pair lists for a subset of the benchmark set of Perera *et al.* to GIAO-CCSD using exact two-electron spin-orbit operators at the aug-cc-pVTZ level.[108]

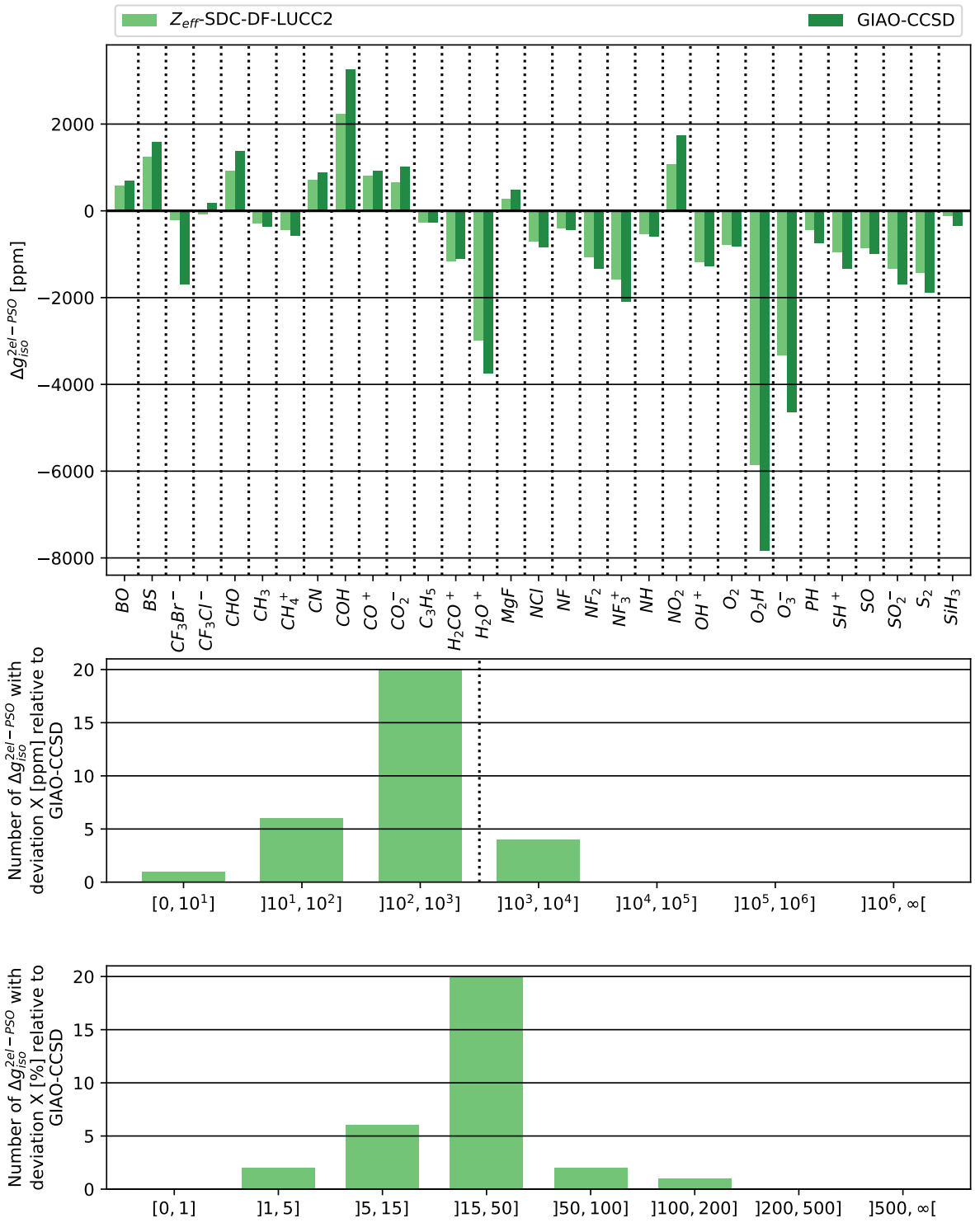

Figure 3.6: Comparison of the two-electron paramagnetic spin-orbit contribution $\Delta g_{iso}^{2el-PSO}$ to the isotropic g-shift Δg_{iso} calculated with Z_{eff}-SDC-DF-LUCC2 at the aug-cc-pVTZ/aug-cc-pVQZ level with DF-UHF reference, extended Boughton-Pulay domains and full pair lists for a subset of the benchmark set of Perera *et al.* to GIAO-CCSD using exact two-electron spin-orbit operators at the aug-cc-pVTZ level.[108]

3.2.1.2 Experiment

The experimental g-shifts assembled by Perera *et al.*[34] are collected in table C.4. Since the molecules under investigation are only a subset of the Perera benchmark set, we can simply reuse the previously employed Z_{eff}-SDC-DF-LUCC2 and GIAO-CCSD results. At first glance, the agreement of experiment with either of the methods is rather disappointing. The GIAO-CCSD results are only in slightly better agreement (MAD = 1423 ppm, MRD = 43.0 %) with the experiment than the Z_{eff}-SDC-DF-LUCC2 results (MAD = 1549 ppm, MRD = 51.3 %). For the two molecules ClO_2 and NO_3^{2-} with disagreement of the reference energies, it is noteworthy that the calculation with the lower reference energy produces results in significantly better agreement with the experiment in both cases (see table 3.1). This provides additional support for the claim that the calculations did indeed converge to different states.

Table 3.1: Data for the subset of problematic molecules

	Method	ClO_2	NO_3^{2-}	CF_3Cl^-	CF_3Br^-
E_{HF}[Hartree]	Z_{eff}-SDC-DF-LUCC2	-609.064	-278.762	-795.699	-2908.796
	GIAO-CCSD[108]	-609.055	-278.779	-795.699	-2908.796
Δg_{iso}[ppm]	Z_{eff}-SDC-DF-LUCC2	7323	-80	-146	19091
	GIAO-CCSD[108]	10594	1855	-132	17705
	Experiment[34]	7933 (I), 8433 (II)	2000	7167	3067

Removing these two molecules and the additional outliers CF_3Cl^- and CF_3Br^- brings both CCSD (MAD = 480 ppm, MRD = 22.5 %) and CC2 (MAD = 626 ppm, MRD = 27.9 %) within the desired area of a deviation of less than 1000 ppm. The still quite significant relative deviations however point towards a deeper problem in the comparison to experimental values. Even experiments for the same molecule can vary by several hundred ppm, as can be seen for every molecule that is listed with two entries in table C.4. In order to get true agreement with experiment, it may be necessary to account for the existence of multiple minima, the environmental effects of the specific experiment and vibrational averaging of the calculated g-shifts.

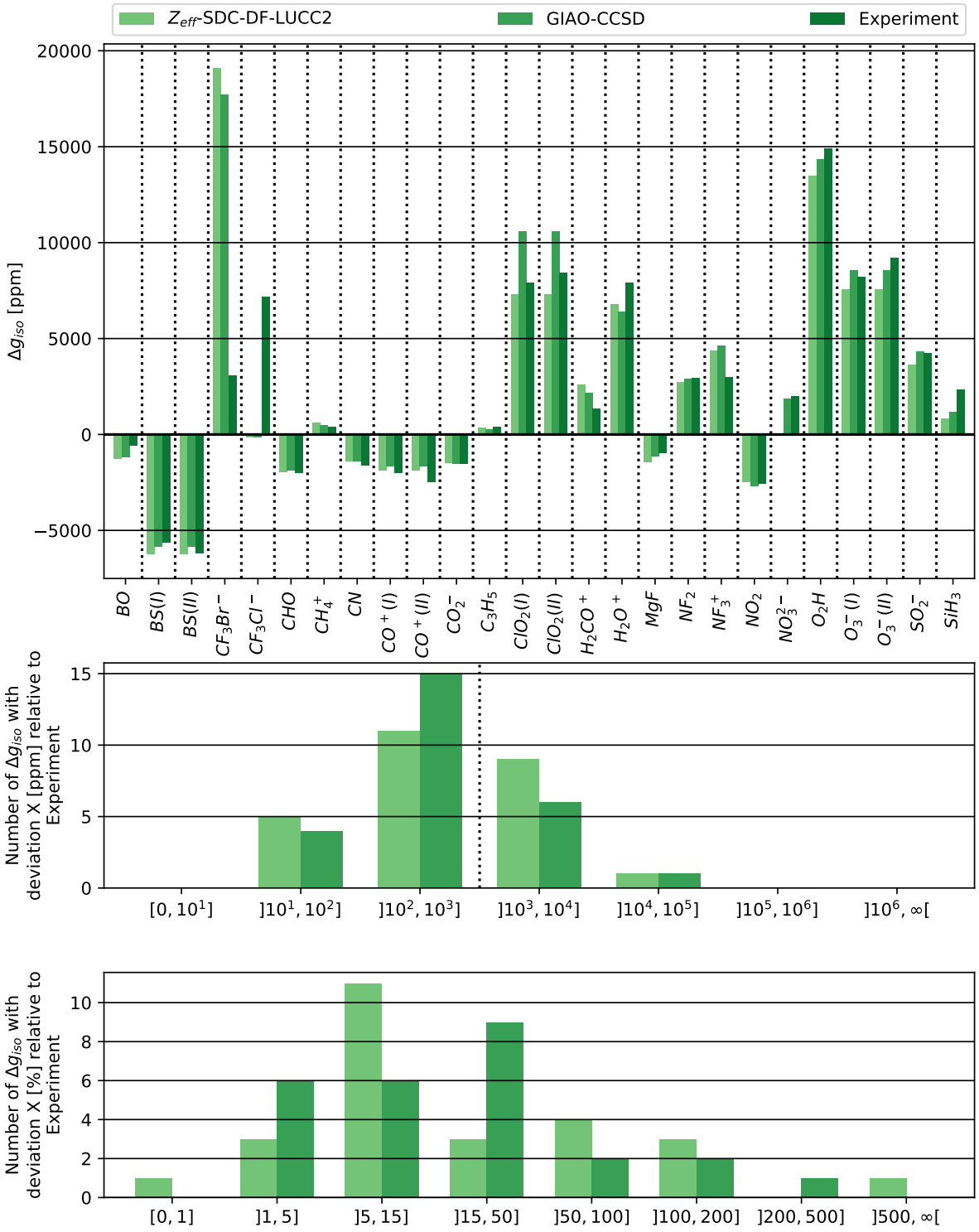

Figure 3.7: Comparison of the isotropic g-shift Δg_{iso} calculated with Z_{eff}-SDC-DF-LUCC2 at the aug-cc-pVTZ/aug-cc-pVTZ level with DF-UHF reference, extended Boughton-Pulay domains, and full pair lists to GIAO-CCSD using exact two-electron spin-orbit operators at the aug-cc-pVTZ level[108] and a subset of the experimental data assembled by Perera *et al.*[34]

3.2.1.3 Effective one-electron approximations

In order to justify the use of SOMF-GIAO-B3LYP as a reference for large molecules, we first need to establish that it provides results in good agreement with GIAO-CCSD. Since in addition to the method error we also have an error due to the approximation of the two-electron spin-orbit contribution, that is not entirely trivial.
Fortunately, Glasbrenner *et al.*[36] compared their GIAO-B3LYP method with the effective charge and SOMF approximations to the results obtained by Perera *et al.*[34] for the benchmark set employed by Gauss *et al.*[33] for their Z_{eff}-GIAO-CCSD method using the aug-cc-pVTZ basis set. Although the test set is very small, this allows us to isolate the method error.
As has been mentioned previously, the Gauss benchmark set is just a subset of the Perera set and we can reuse the previous values for Z_{eff}-SDC-DF-LUCC2 and GIAO-CCSD. The additional values for Z_{eff}-GIAO-CCSD, Z_{eff}-GIAO-B3LYP and SOMF-GIAO-B3LYP are collected in tables C.1, C.2 and C.3, respectively.
The average errors are remarkably similar for all methods under investigation (fig. 3.8). For GIAO-B3LYP, we note that use of effective charges (MAD = 244 ppm, MRD = 10.6 %) produces slightly worse agreement with GIAO-CCSD than the results obtained with the SOMF operator (MAD = 191 ppm, MRD = 6.9 %). Aside from justifying the use of SOMF-GIAO-B3LYP as a reference, this supports the need for a better spin-orbit approximation than has been used for the CC2 method developed in this thesis.
The molecule NF_3^+ is not included in the reported GIAO-B3LYP results. Excluding it from the analysis of the Z_{eff}-CC methods, we find that both Z_{eff}-GIAO-CCSD (MAD = 238 ppm, MRD = 10.9 %) and Z_{eff}-SDC-DF-LUCC2 (MAD = 214 ppm, MRD = 9.3 %) are in good agreement with the GIAO-CCSD results using the exact two-electron spin-orbit integrals. Curiously, the Z_{eff}-SDC-DF-LUCC2 results are actually in slightly better agreement with GIAO-CCSD compared to Z_{eff}-GIAO-CCSD, which points to error compensation of the method error and the error due to the effective charge approximation. This trend becomes even stronger if we include NF_3^+, since the Z_{eff}-GIAO-CCSD (MAD = 388 ppm, MRD = 13.7 %) result of Gauss *et al.*[33] differs by approximately a factor of two from the actual GIAO-CCSD value, whereas the Z_{eff}-SDC-DF-LUCC2 (MAD = 217 ppm, MRD = 9.1 %) method reproduces this value almost perfectly.
Even though the test set is neither large nor diverse enough to make general statements, we see nevertheless that at least for this small test set, SOMF-GIAO-B3LYP yields agreement with GIAO-CCSD significantly below the experimental errors. This mirrors the observation by Perera *et al.*[34] that B3LYP provides good agreement with their GIAO-CCSD results.[34] Lacking any more satisfying alternatives, we can therefore justify use of the SOMF-GIAO-B3LYP method as a preliminary reference for the quality of the g-shifts obtained with Z_{eff}-SDC-DF-LUCC2 for large molecules.

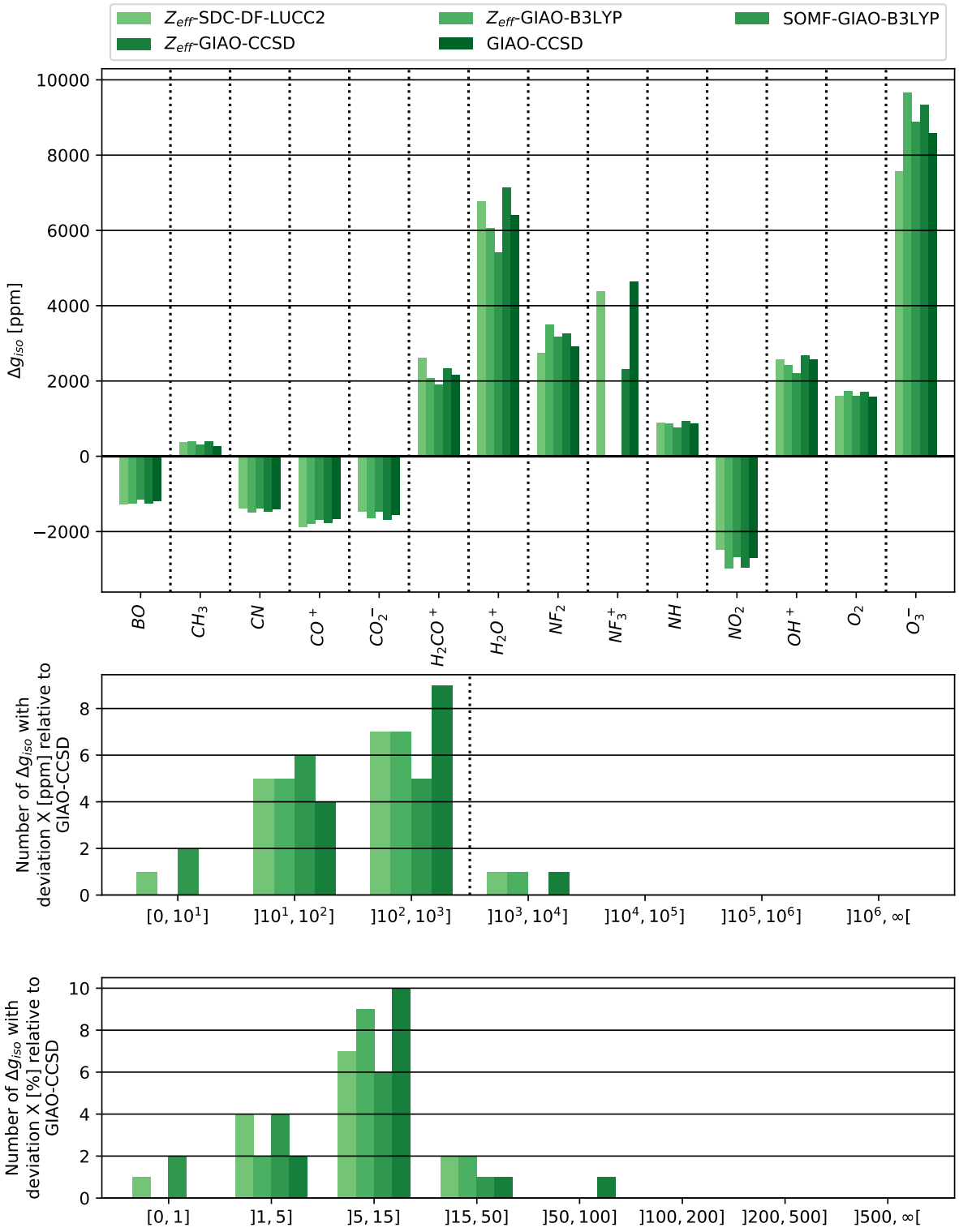

Figure 3.8: Comparison of the isotropic g-shift Δg_{iso} calculated with Z_{eff}-SDC-DF-LUCC2 at the aug-cc-pVTZ/aug-cc-pVQZ level with DF-UHF reference, extended Boughton-Pulay domains and full pair lists for the benchmark set of Gauss *et al.*[33] to Z_{eff}-GIAO-B3LYP,[36] SOMF-GIAO-B3LYP,[36] Z_{eff}-GIAO-CCSD[33] and GIAO-CCSD[108] using exact two-electron spin-orbit operators at the aug-cc-pVTZ level.

3.2.2 Glasbrenner sets

3.2.2.1 Glasbrenner small molecule set

As previously mentioned, the small molecule benchmark set of Glasbrenner *et al.*[35] has a significant overlap with the Perera benchmark set. However, some of the geometries differ quite significantly (an extreme example is CF_3Cl^-, where the *C-Cl* bond has been broken during optimization) and instead of aug-cc-pVTZ the def2-TZVP basis set was employed. A direct comparison with the GIAO-CCSD results of Perera *et al.* is therefore not meaningful, and the Z_{eff}-SDC-DF-LUCC2 results can vary quite significantly for the "same" molecule between the two sets.
We have again used all pairs, extended domains and a DF-UHF reference for the Z_{eff}-SDC-DF-LUCC2 calculations. The AO basis was def2-TZVP and the fitting basis was def2-QZVPP.[112,113] The results for Z_{eff}-SDC-DF-LUCC2 and SOMF-GIAO-B3LYP have been reported in tables C.23 and C.22, respectively.
Investigating the isotropic g-shifts (fig. 3.9, table 3.2), we find a very disappointing agreement between SOMF-GIAO-B3LYP and Z_{eff}-SDC-DF-LUCC2 (MAD = 7061 ppm, MRD = 58.5 %). The average error is more than seven times the experimental uncertainty of up to 1000 ppm. The deviations appear to be particularly large for molecules with g-shifts predicted by SOMF-GIAO-B3LYP of more than 7500 ppm, which have been excluded from fig. 3.9 and are reported in table 3.2 instead, together with GIAO-CCSD[108] – despite the different basis set – and experimental[34] values if available.

Table 3.2: Data for molecules with Δg_{iso}(SOMF-GIAO-B3LYP) > 7500 ppm. Note that GIAO-CCSD results are at the aug-cc-pVTZ level and may use different geometries.

Molecule	SOMF-GIAO-B3LYP[35]	Z_{eff}-SDC-DF-LUCC2	GIAO-CCSD[108]	Experiment[34]
AsO_3^{2-}	8208	853	-	-
CF_3Br^-	33924	18009	17705	3067
CF_3Cl^-	7934	3376	-132	7167
CH	-4683	-35966	-	-
CH_4^+	8872	8617	494	400
CO_3^-	8791	7551		-
ClO_2	9526	7461	10594	7933 (I), 8433 (II)
GeH_3	10962	6906	-	-
KrF	24325	42852	-	-
NO	-36509	-121602	-	-
NO_3	10071	7819	-	-
OCH_3	17812	45360	-	-
OH	20585	118265	-	-
O_2H	10793	13326	-	-
O_3^-	9287	8133	8576	8200 (I), 9233 (II)

Analysis of these molecules yields an inconclusive picture. For CF_3Br^-, Z_{eff}-SDC-DF-LUCC2 is in very good agreement with GIAO-CCSD while SOMF-GIAO-B3LYP predicts a value of roughly twice the GIAO-CCSD result, but all of them disagree with the experimental value by an order of magnitude. For CF_3Cl^-, SOMF-GIAO-B3LYP has the best agreement with experiment, but the abovementioned dissociated geometry employed for this calculation makes it rather likely that this is just a coincidence. For CH_4^+ we have close agreement between Z_{eff}-SDC-DF-LUCC2 and SOMF-GIAO-B3LYP, but they differ from the GIAO-CCSD and experimental values by more than an order of magni-

tude. Since the Z_{eff}-SDC-DF-LUCC2 value of 627 ppm for the Perera test set is much closer to the GIAO-CCSD value, this is most likely a result of the different geometries employed. For ClO_2, Z_{eff}-SDC-DF-LUCC2 yields the best agreement with experiment. As has been previously noted, convergence to the correct ground state can be problematic for this molecule, which could explain the deviant SOMF-GIAO-B3LYP value. For KrF, the Z_{eff}-SDC-DF-LUCC2 calculation runs into the problem of Kr not having an effective charge, which implies neglect of a part of the two-electron contribution. Finally, O_3^- shows rather curious behavior. Both SOMF-GIAO-B3LYP and Z_{eff}-SDC-DF-LUCC2 are in near perfect agreement with experiment, but not with the same one. Furthermore, state-averaged CASPT2/aug-cc-pVDZ two-state calculations showed (near-)degeneracy of the ground and excited state ($\Delta E < 3$ mH) for CH, CH_4^+, NO and OH, which makes the CC2 method itself unreliable for these systems. The origins of the discrepancies for the remaining molecules are unclear, although multi-reference character cannot be conclusively ruled out.

Removing all molecules listed in table 3.2 from the error estimation yields an average deviation within the experimental uncertainties (MAD = 316 ppm, MRD = 22.1 %), but with still quite significant relative deviations.

The observations made for these small molecules cast doubt on the validity of the SOMF-GIAO-B3LYP method as a reliable reference for extended molecules, at least if they possess large g-shifts. Furthermore, unlike for the GIAO-CCSD calculations, convergence to different states cannot be identified. However, since many of the g-shifts for the single and multiple spin-center benchmark sets are very small, we will still use the SOMF-GIAO-B3LYP method as a preliminary reference. Future work should focus on implementing a more suitable reference, like SOMF-GIAO-DF-LUCCSD.

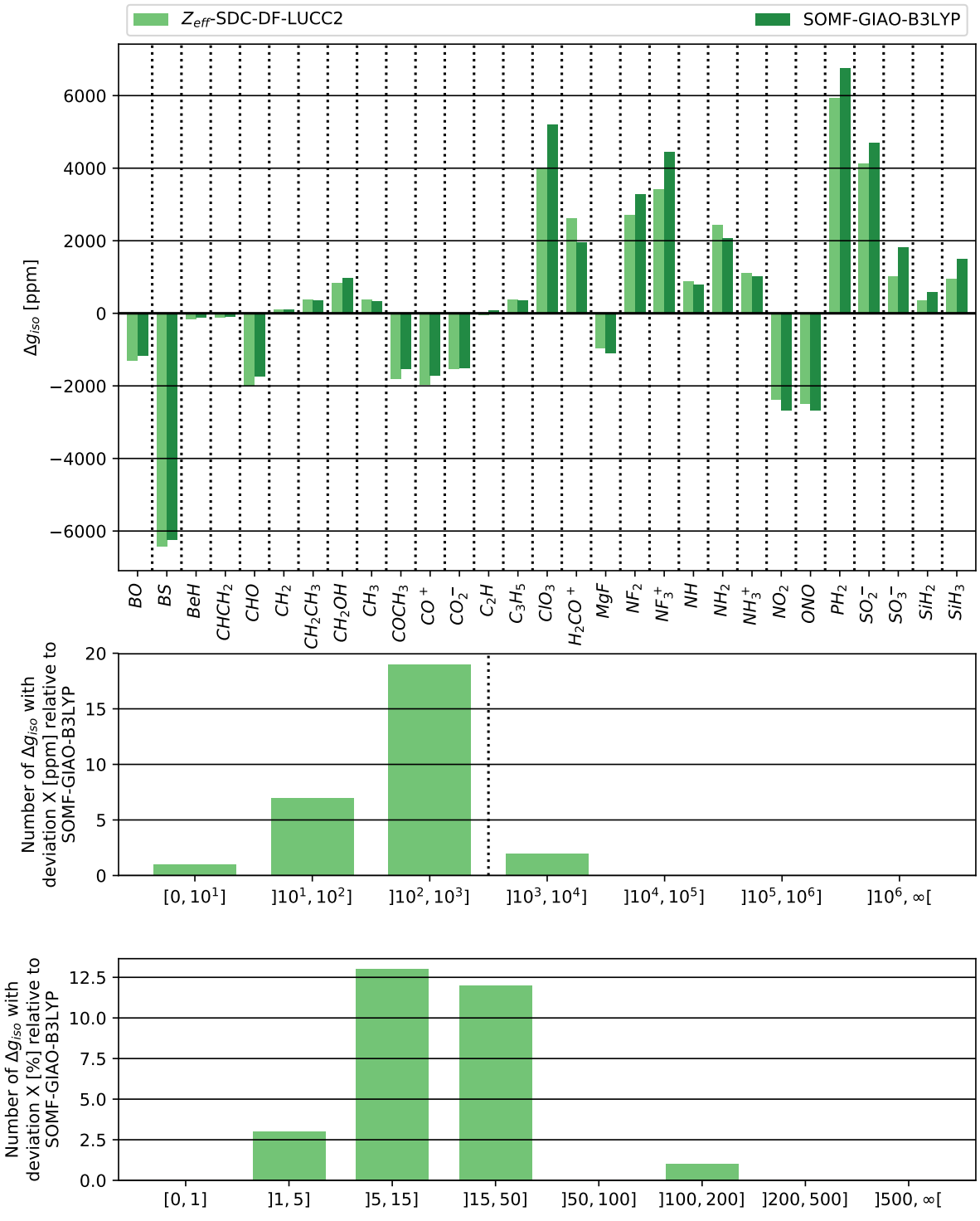

Figure 3.9: Comparison of the isotropic g-shift Δg_{iso} calculated with Z_{eff}-SDC-DF-LUCC2 at the def2-TZVP/def2-QZVPP level with DF-UHF reference, extended Boughton-Pulay domains and full pair lists for a subset of the small molecule benchmark set of Glasbrenner *et al.* to SOMF-GIAO-B3LYP at the def2-TZVP level.[35]

3.2.2.2 Glasbrenner single spin-center set

For the single spin-center benchmark set, we use the same local restrictions and basis sets as for the small molecule set (table C.27). In addition to using SOMF-GIAO-B3LYP as a reference (table C.25), we also compare SOMF-SDC-B3LYP (table C.26) with it to obtain a rough estimate of the significance of the gauge error.
As indicated in a previous section, the molecules NaF^+, Cys-Gly_4 and $C_{19}H_{39}O$ have been excluded from the plot in fig. 3.10 and are instead listed in table 3.2.

Table 3.3: Data for the subset of molecules with very large g-shifts

	Method	$C_{19}H_{39}O$	NaF^+	Cys-Gly_4
Δg_{iso}[ppm]	Z_{eff}-SDC-DF-LUCC2	71363	178129	84784
	SOMF-SDC-B3LYP[35]	24095	55635	79284
	SOMF-GIAO-B3LYP[35]	24096	55654	79256

Since none of these molecules show significant agreement between Z_{eff}-SDC-DF-LUCC2 and SOMF-B3LYP, including them would lead to a distortion of the error estimation (MAD = 11008 ppm, MRD = 34.1 %). The agreement between SOMF-SDC-B3LYP and SOMF-GIAO-B3LYP however is virtually perfect (MAD = 24 ppm, MRD = 5.3 %), proving that the SDC approximation is indeed a valid approach to solving the gauge dependence issue for this class of molecule.
Removing the offending molecules from the benchmark set, we obtain significantly better agreement between Z_{eff}-SDC-DF-LUCC2 and SOMG-GIAO-B3LYP (MAD = 66 ppm, MRD = 9.4 %) while the error in SOMF-SDC-B3LYP stays essentially the same (MAD = 26 ppm, MRD = 6.5 %). Nevertheless, the high relative error indicates that the agreement of the absolute values is indeed to blame on their comparatively small scale.

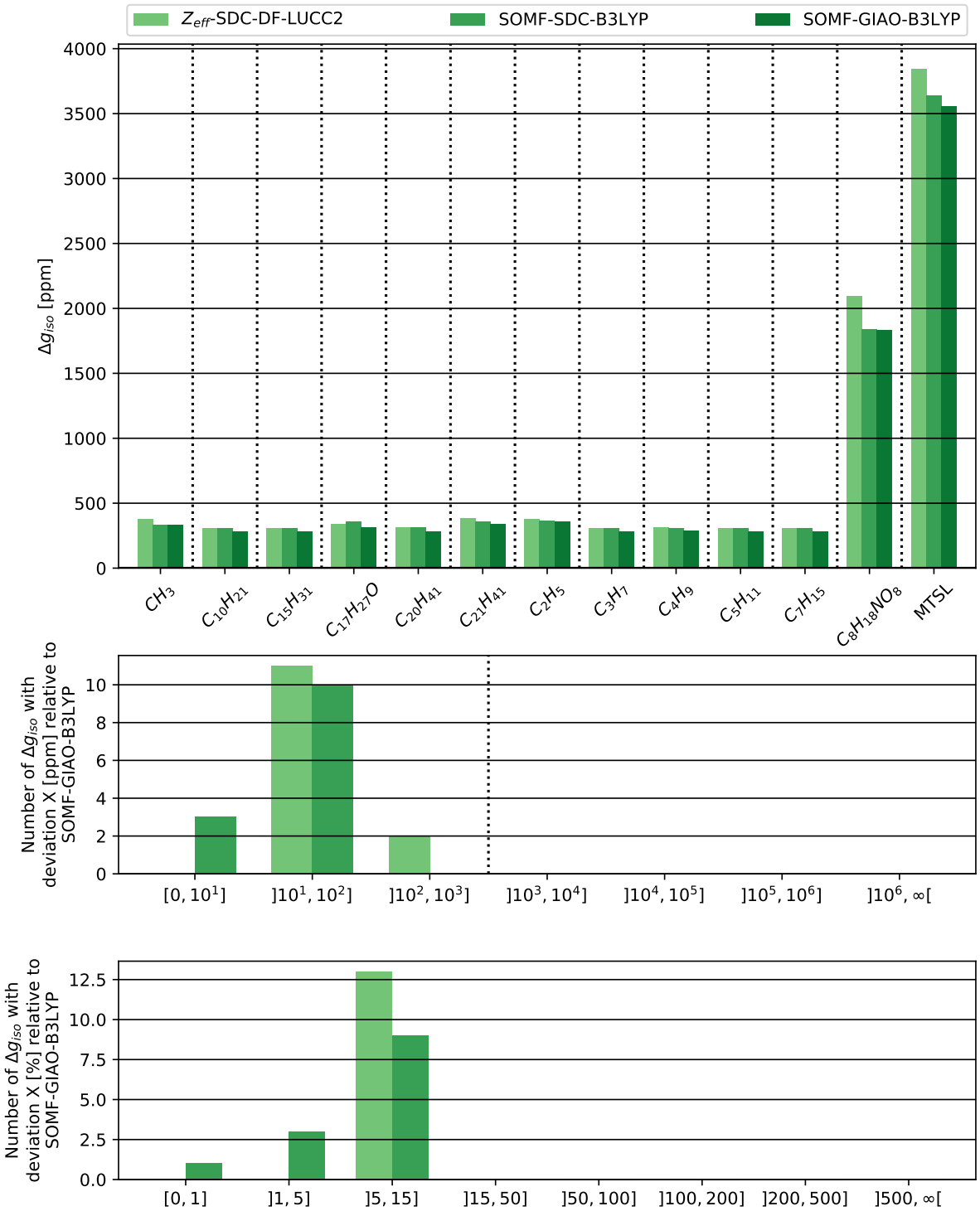

Figure 3.10: Comparison of the isotropic g-shift Δg_{iso} calculated with Z_{eff}-SDC-DF-LUCC2 at the def2-TZVP/def2-QZVPP level with extended Boughton-Pulay domains and full pair lists for a subset of the molecules with a single spin-center used by Glasbrenner *et al.* to SOMF-SDC-B3LYP and SOMF-GIAO-B3LYP at the def2-TZVP level.[35]

3.2.2.3 Glasbrenner multiple spin-center set

Finally, the results for the multiple spin-center benchmark set have been accumulated in tables C.41, C.42, and C.43. The Z_{eff}-SDC-DF-LUCC2 calculations used the same local restrictions and basis sets as for the previous Glasbrenner sets.
Since the DF-LUCC2 ground state calculation did not converge, $C_{19}FH_{26}N$ has been removed from the benchmark set of molecules with multiple spin-centers (fig. 3.11). Generally, we observe the expected deterioration of the performance of both the SOMF-SDC-B3LYP (MAD = 178 ppm, MRD = 10.9 %) and the Z_{eff}-SDC-DF-LUCC2 (MAD = 3860 ppm, MRD = 33.9 %) methods due to gauge errors.
Removing the outliers $C_7H_{14}NOS$ and $O[CH_2]_{18}NH$ from the analysis, the error in the Z_{eff}-SDC-DF-LUCC2 results drops into the acceptable range (MAD = 387 ppm, MRD = 18.8 %) while the error in SOMF-SDC-B3LYP remains largely unaffected (MAD = 142 ppm, MRD = 10.9 %). But for both methods, especially the relative but also the absolute errors remain significantly larger than for the single spin-center benchmark set, underlining the need for a truly gauge invariant method for many extended molecules in triplet and higher spin states.
In conclusion, we find that even for molecules with multiple spin-centers, i.e. systems for which choosing the SDC as a common gauge origin leads to significant gauge errors, Z_{eff}-SDC-DF-LUCC2 is still in surprisingly good agreement with the SOMF-GIAO-B3LYP method as long as the absolute value of the g-shift is not of the order of several tens of thousands ppm. However, a real estimation of the method error will only be possible after implementation of the SOMF-GIAO-DF-LUCC2 method.

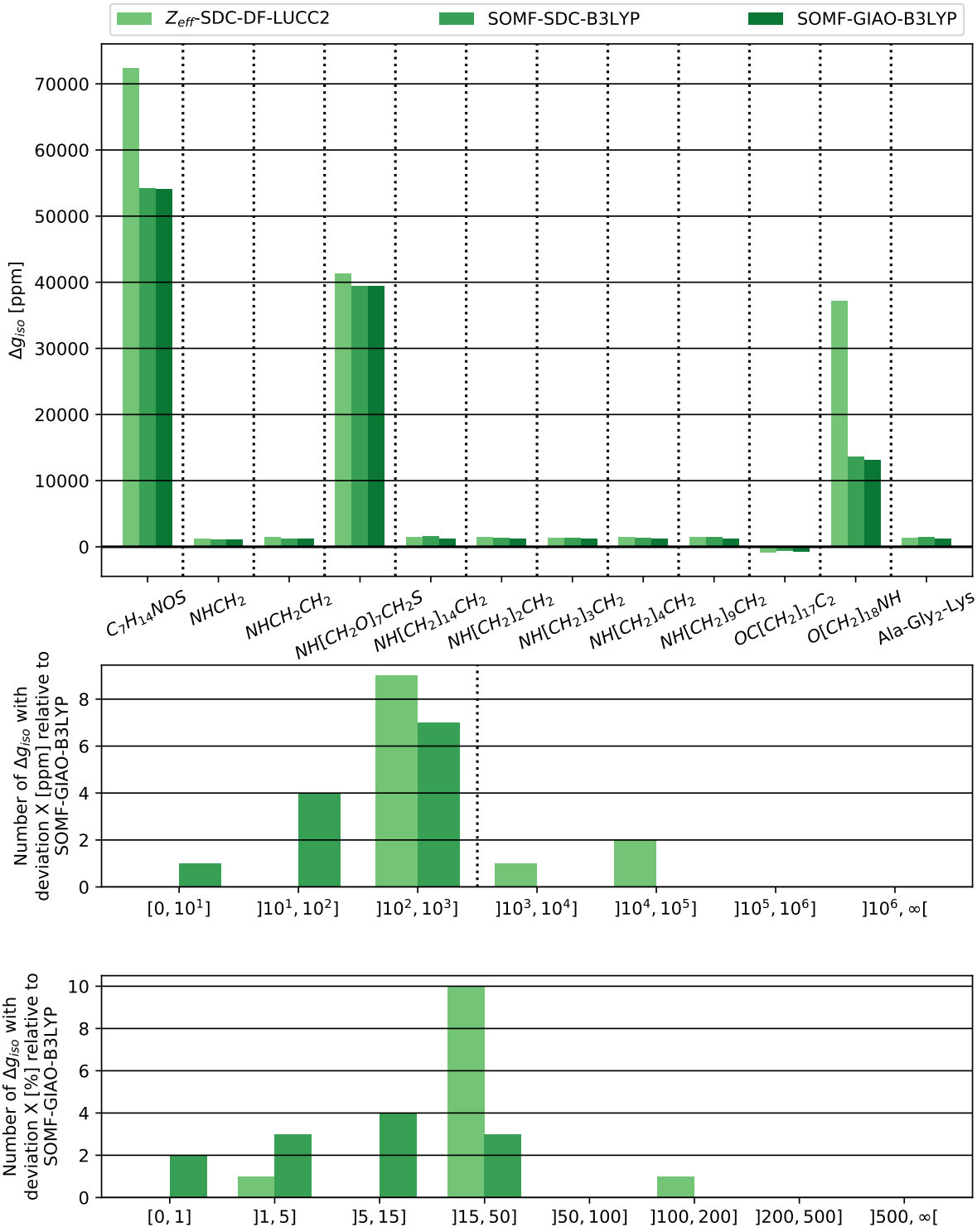

Figure 3.11: Comparison of the isotropic g-shift Δg_{iso} calculated with Z_{eff}-SDC-DF-LUCC2 at the def2-TZVP/def2-QZVPP level with extended Boughton-Pulay domains and full pair lists for a subset of the molecules with multiple spin-centers used by Glasbrenner *et al.* to SOMF-SDC-B3LYP and SOMF-GIAO-B3LYP at the def2-TZVP level.[35]

3.3 Internal parameters

Having established that the Z_{eff}-SDC-DF-LUCC2 is able to provide reasonable results for many small and extended molecules, we will now examine the effect of several degrees of freedom – type of reference determinant, fitting basis size, domain and pair list restrictions – on its efficiency and the quality of the obtained g-shifts.
To this purpose, we will compare the isotropic g-shifts obtained for the Perera set at the aug-cc-pVTZ level with a DF-UHF reference, aug-cc-pVQZ fitting basis, extended domains and full pair lists (see table C.6) to results that vary in one or more of these categories.
To investigate the effect on larger molecules, we will do the same for the single spin-center benchmark set of Glasbrenner *et al.* at the def2-TZVP level with a def2-QZVPP fitting basis (see table C.27).
A subset of the molecules of the latter set constitute a progression of alkyl radicals, which are ideal for the investigation of the CPU time t_{CPU} required for the g-tensor calculation and the effect of the intensity of the local and density fitting approximation on them. The scaling of the method with the systems size, quantified by the number of atomic orbitals N_{AO}, has been approximately determined for the different levels of approximations via linear regression of the natural logarithm of t_{CPU} against the natural logarithm of N_{AO} for the three largest alkyl radicals.

3.3.1 Reference function

The results for the calculations with a DF-ROHF reference function are listed in tables C.8 and C.29. Miscellaneous data for the previously specified problematic molecules has been collected in table 3.4 for convenience.

Table 3.4: Data for the set of problematic molecules

	Reference	$C_{19}H_{39}O$	NaF^+	Cys-Gly$_4$
E [Hartree]	DF-UHF	-820.733	-261.250	-1550.809
	DF-ROHF	-820.733	-261.249	-1550.809
Δg_{iso}[ppm]	DF-UHF	71363	178129	84784
	DF-ROHF	85377	546167	102249
Δg^{ZKE}[ppm]	DF-UHF	-299	-412	-229
	DF-ROHF	-303	-406	-217
$\Delta g_{iso}^{1el-DSO}$[ppm]	DF-UHF	202	222	226
	DF-ROHF	203	220	223
$\Delta g_{iso}^{1el-PSO}$[ppm]	DF-UHF	102262	237777	99849
	DF-ROHF	122300	728265	120392

The absolute deviations (MAD = 157 ppm) for the Perera test set (fig. 3.12) lie generally well below the experimental uncertainty of upwards of 500 ppm, but the relative deviations (MRD = 10.2 %) are of a comparable level as the error to be expected from use of the effective charge approximation.
For the single spin-center test set (fig. 3.13) we observe a very large dependence on the reference function if we include the problematic molecules (MAD = 24980 ppm, MRD = 16.9%). Removing these molecules yields a significant improvement of the average errors (MAD = 13 ppm, MRD = 1.9 %), making the choice of reference determinant virtually irrelevant for the remaining molecules.
It is not immediately obvious why these three molecules are so sensitive to the reference determinant employed. The ground state energies for the different types of reference determinant are nearly identical in these cases, which makes it unlikely that they converged to different states unless there is a (near-)degeneracy for each of these molecules. This appears to be the case for NaF^+, for which ground and excited state have been found to be degenerate in a CASPT2/aug-cc-pVDZ calculation. The other two molecules are unfortunately too large to be easily accessible via standard CASPT2.
An investigation of the determinant weights in the DF-MCSCF calculations yields no clarification either. $C_{19}H_{39}O$ shows slightly stronger multi-reference character, with the highest contribution to the norm from a single determinant being approximately 96.3 %, which can still be considered well within the region that should be unproblematic for single-reference methods. The highest contribution for a single determinant in Cys-Gly$_4$ is only 93.1 %, indicating a possible multi-reference case, although the next most important determinant contributes only about 2.7 % to the norm.
In general, the choice of reference determinant does not matter to a significant degree in the vast majority of cases. But as discussed, there are notable exceptions.

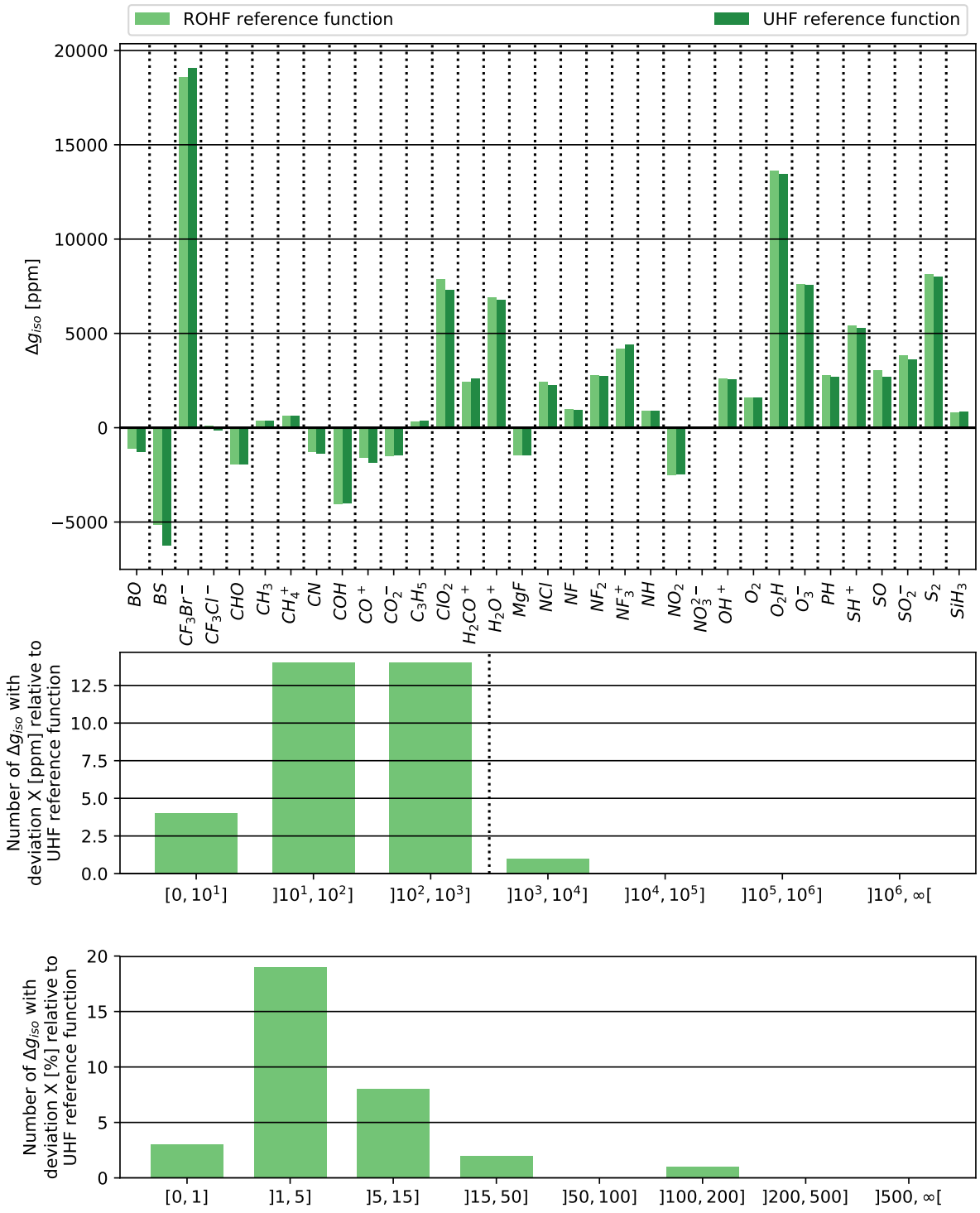

Figure 3.12: Dependence on the reference function of the isotropic g-shift Δg_{iso} calculated with Z_{eff}-SDC-DF-LUCC2 at the aug-cc-pVTZ/aug-cc-pVQZ level with extended Boughton-Pulay domains and full pair lists for a subset of the benchmark set of Perera *et al.*[34]

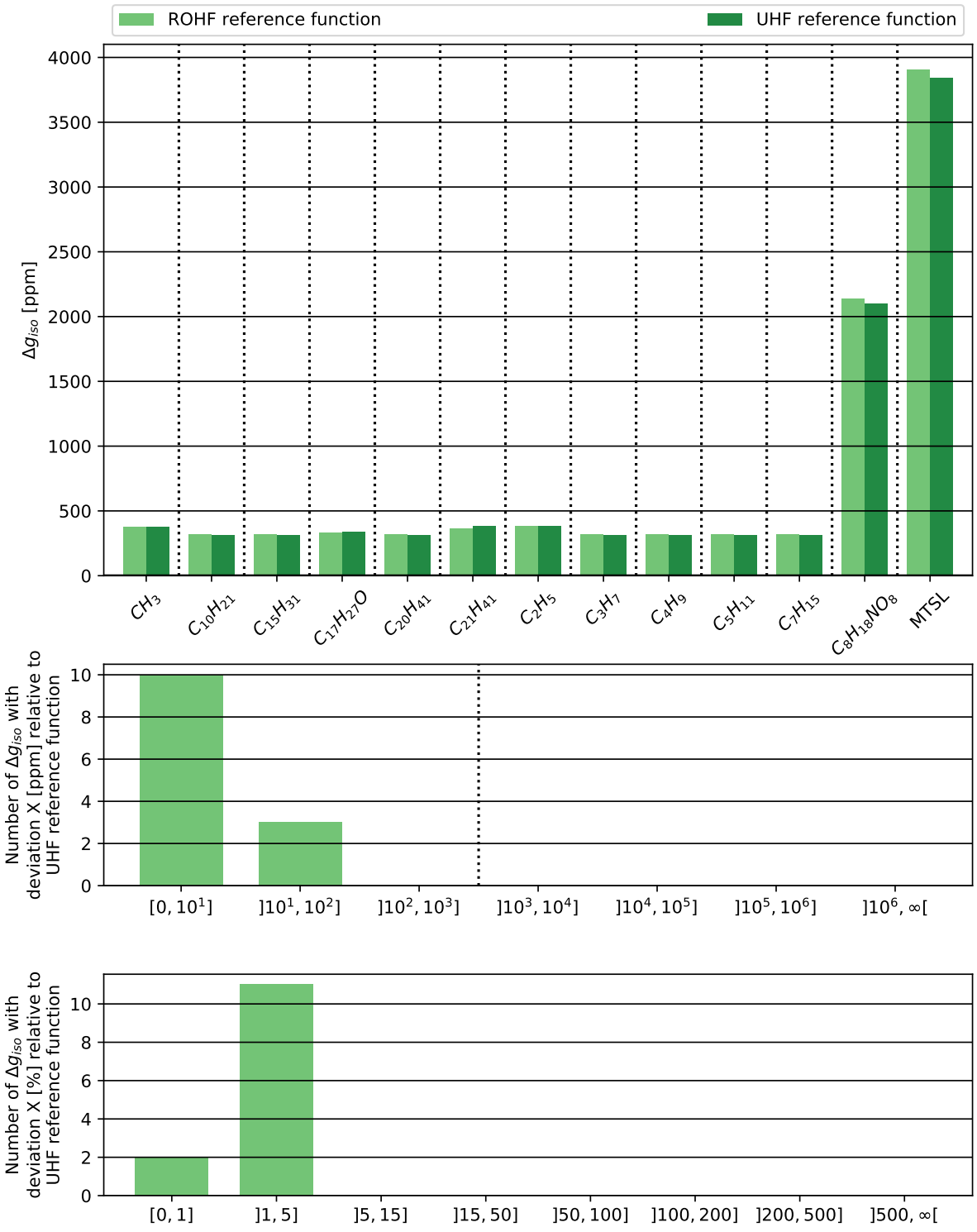

Figure 3.13: Dependence on the reference function of the isotropic g-shift Δg_{iso} calculated with Z_{eff}-SDC-DF-LUCC2 at the def2-TZVP/def2-QZVPP level with extended Boughton-Pulay domains and full pair lists for a subset of the molecules with a single spin-center used by Glasbrenner *et al.*[35]

3.3.2 Fitting basis size

The calculations for the Perera test set with aug-cc-pVTZ AO basis and aug-cc-pVDZ or aug-cc-pVTZ fitting basis can be found in C.10 and C.12, respectively. For the Glasbrenner single spin-center set, the calculations with def2-TZVP AO basis and def2-TZVPP fitting basis[113–115] are reported in C.31.
Taking the quadruple zeta fitting basis sets as a reference, we observe rapid convergence of the g-shifts with the size of the fitting basis for both test sets.
For the Perera test set (fig. 3.15), we have only very small absolute deviations for reducing the quality of the fitting basis set to triple zeta (MAD = 1 ppm, MRD < 0.1 %) or even double zeta (MAD = 11 ppm, MRD = 0.2 %). Note that the relative deviations are virtually non-existent.
We make an equivalent observation for the single spin-center benchmark set (fig. 3.16). Going from the quadruple zeta fitting basis to the triple zeta fitting basis leads to comparatively small absolute errors (MAD = 71 ppm) even if we include the molecules NaF^+, Cys-Gly_4 and $C_{19}H_{39}O$. Removing them from the test set essentially eliminates this error (MAD < 1 ppm). In either case, the relative deviations are negligible (MRD < 0.1 %).
Investigating the effect on the timings (fig. 3.14), we see that, as expected, the reduction of the fitting basis size does not affect the scaling of the method. The asymptotic scaling is $\mathcal{O}(\mathcal{N}^4)$, although the actual scaling for the molecules under investigation is still closer to $\mathcal{O}(\mathcal{N}^3)$. It does however reduce the prefactor, lowering the CPU time for the largest alkyl radical, $C_{20}H_{41}$, by about a third from 34 h to 23 h when going from the quadruple zeta to the triple zeta fitting basis.
In conclusion, we find the error due to reduction of size of the fitting basis to be negligible, even for g-shifts of more than 100000 ppm. Even a reduction to or below the quality of the AO basis set can still provide very good results, but with significant savings in computational effort.

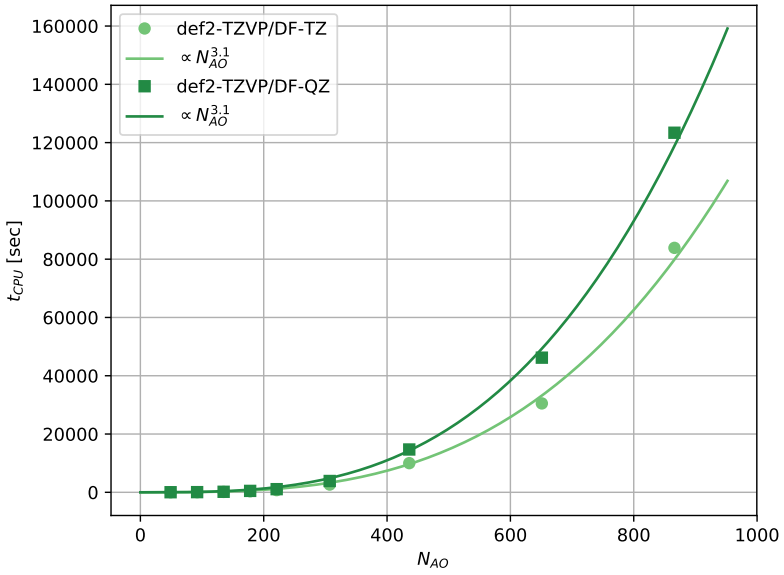

Figure 3.14: Dependence on the fitting basis size of the CPU time required for the Z_{eff}-SDC-DF-LUCC2 part of the g-tensor calculation at the def2-TZVP/def2-XZVPP (X = T, Q) level with DF-UHF reference, extended Boughton-Pulay domains and full pair lists for the alkyl radicals used by Glasbrenner *et al.*[35]

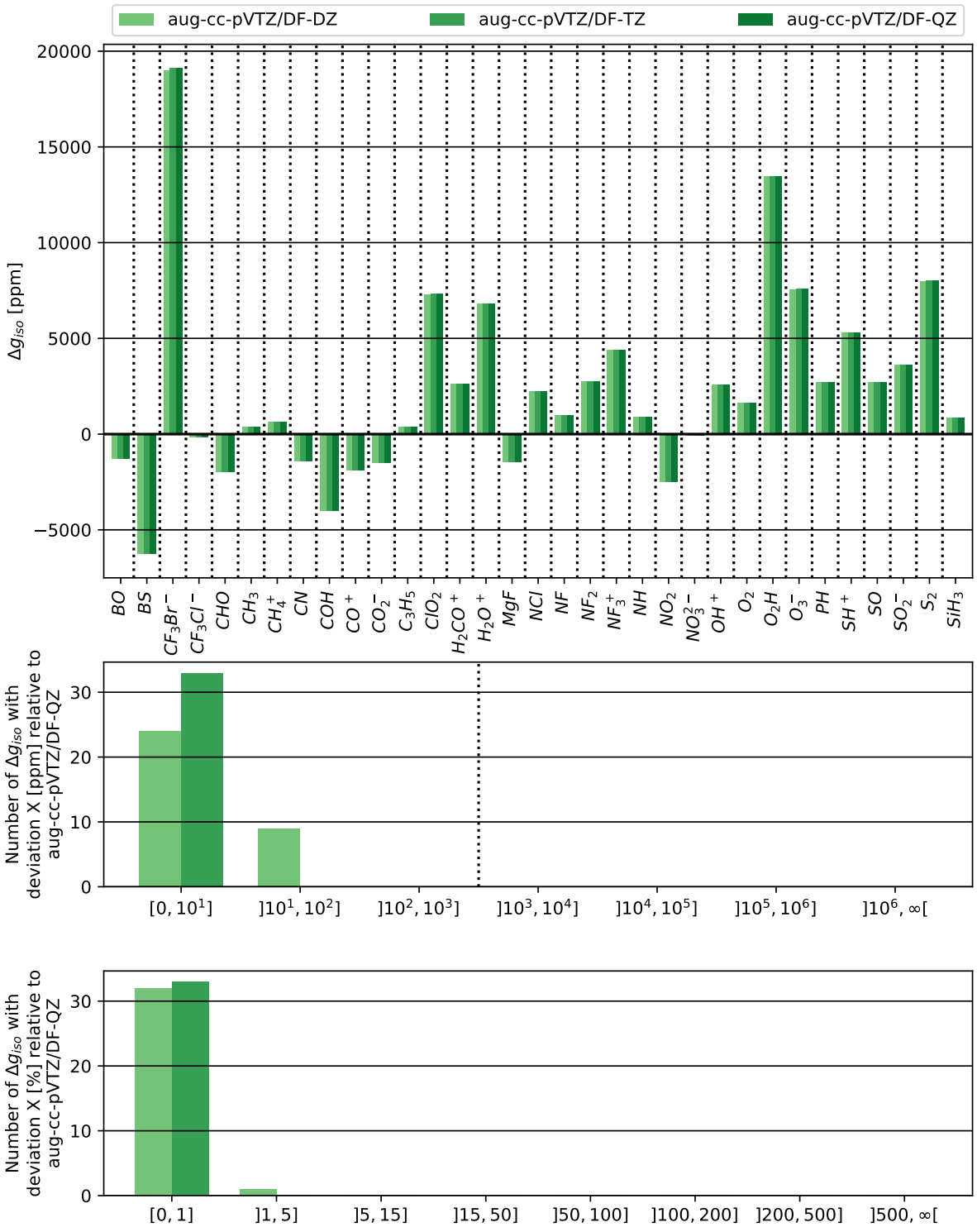

Figure 3.15: Dependence on the fitting basis size of the isotropic g-shift Δg_{iso} calculated with Z_{eff}-SDC-DF-LUCC2 at the aug-cc-pVTZ/aug-cc-pVXZ (X = D, T, Q) level with DF-UHF reference, extended Boughton-Pulay domains and full pair lists for a subset of the benchmark set of Perera *et al.*[34]

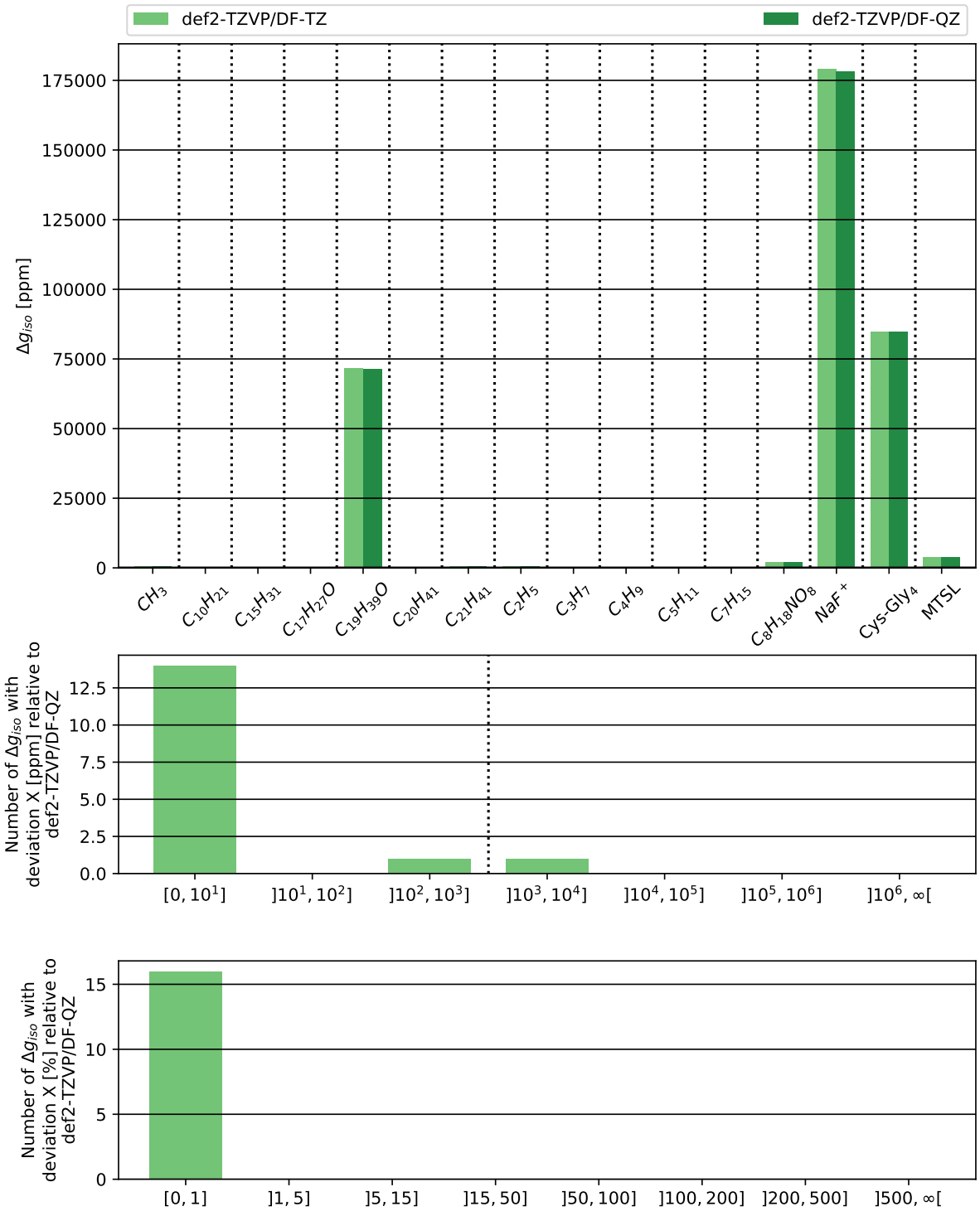

Figure 3.16: Dependence on the fitting basis size of the isotropic g-shift Δg_{iso} calculated with Z_{eff}-SDC-DF-LUCC2 at the def2-TZVP/def2-XZVPP (X = T, Q) level with DF-UHF reference, extended Boughton-Pulay domains and full pair lists for a subset of the molecules with a single spin-center used by Glasbrenner *et al.*[35]

3.3.3 Domain size

The results for standard Boughton-Pulay domains are reported in tables C.14, and C.33. The values for the problematic molecules are listed in table 3.5.

Table 3.5: Data for the set of problematic molecules

	Domain size	$C_{19}H_{39}O$	NaF^+	Cys-Gly$_4$
Δg_{iso}[ppm]	Extended	71363	178129	84784
	Standard	59202	176935	77361
Δg^{ZKE}[ppm]	Extended	-299	-412	-229
	Standard	-299	-412	-229
$\Delta g_{iso}^{1el-DSO}$[ppm]	Extended	202	222	226
	Standard	197	222	224
$\Delta g_{iso}^{1el-PSO}$[ppm]	Extended	102262	237777	99849
	Standard	84882	236185	91112

For the Perera test set (fig. 3.18), reducing the domain size yields only negligible errors (MAD = 34 ppm, MRD = 2.3 %). Nevertheless, for very large g-shifts even a small relative error can matter, but in that case the errors due the effective charge approximation are expected to be significantly larger.
For the single spin-center benchmark set (fig. 3.19), we obtain an average absolute deviation higher than the experimental uncertainty (MAD = 1305 ppm) if we include the previously problematic molecules NaF^+, Cys-Gly$_4$ and $C_{19}H_{39}O$. However, the average relative error (MRD = 2.1 %) is nearly identical to the Perera test set. Removing these molecules from the set again essentially eliminates the average absolute error (MAD = 8 ppm) while also reducing the already small average relative error (MRD = 0.5 %), thus confirming the observations made for the Perera test set.
Examining the effect on the timings for the alkyl radicals (fig. 3.17), we observe again the same asymptotic scaling of $\mathcal{O}(\mathcal{N}^4)$ in both cases, but for the molecules under investigation we are still closer to $\mathcal{O}(\mathcal{N}^3)$ scaling. However, using standard Boughton-Pulay domains instead of extended domains is significantly cheaper for large molecules, reducing the time required for the calculation of the g-shift of $C_{20}H_{41}$ by a factor of approximately two from 34 h to 18 h.
In conclusion, extending the domains by the adjacent atoms has only a very small effect on the calculated g-shifts, except when they are already of the order of several tens of thousands ppm. In this case however, the results are of questionable quality already due to the rather crude approximation of the two-electron spin-orbit contributions via effective charges. Therefore, we can achieve a significant reduction of the computational effort without losing much accuracy by using the standard Boughton-Pulay domains instead.

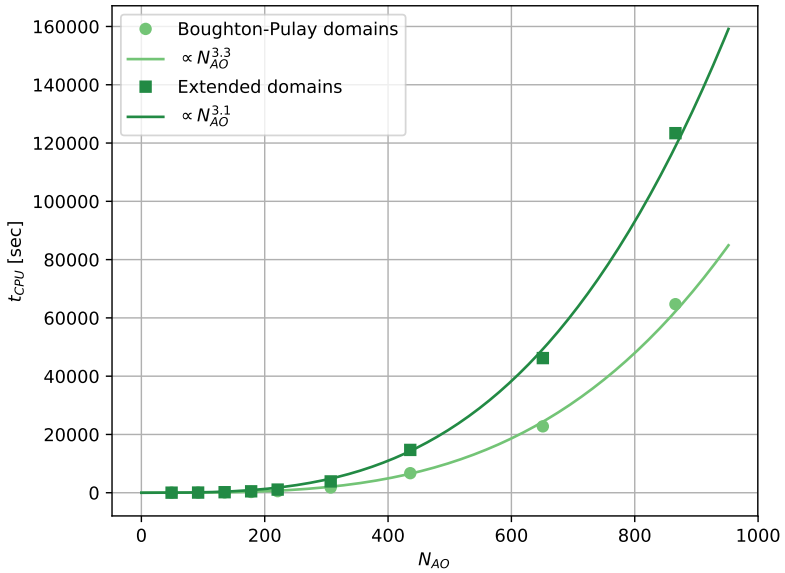

Figure 3.17: Dependence on the domain size of the CPU time required for the Z_{eff}-SDC-DF-LUCC2 part of the g-tensor calculation at the def2-TZVP/def2-QZVPP level with DF-UHF reference and full pair lists for the alkyl radicals used by Glasbrenner *et al.*[35]

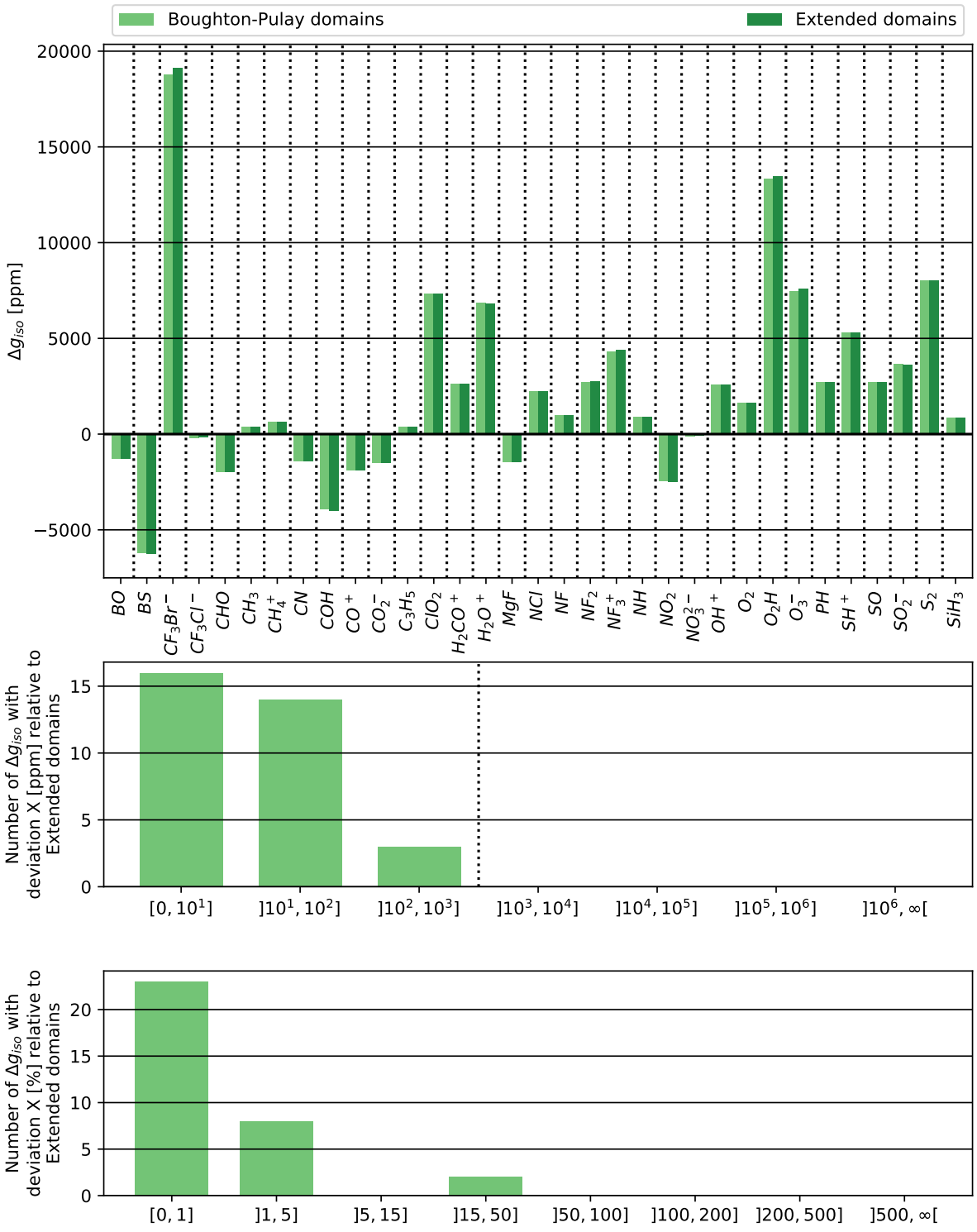

Figure 3.18: Dependence on the domain size of the isotropic g-shift Δg_{iso} calculated with Z_{eff}-SDC-DF-LUCC2 at the aug-cc-pVTZ/aug-cc-pVQZ level with DF-UHF reference and full pair lists for a subset of the benchmark set of Perera *et al.*[34]

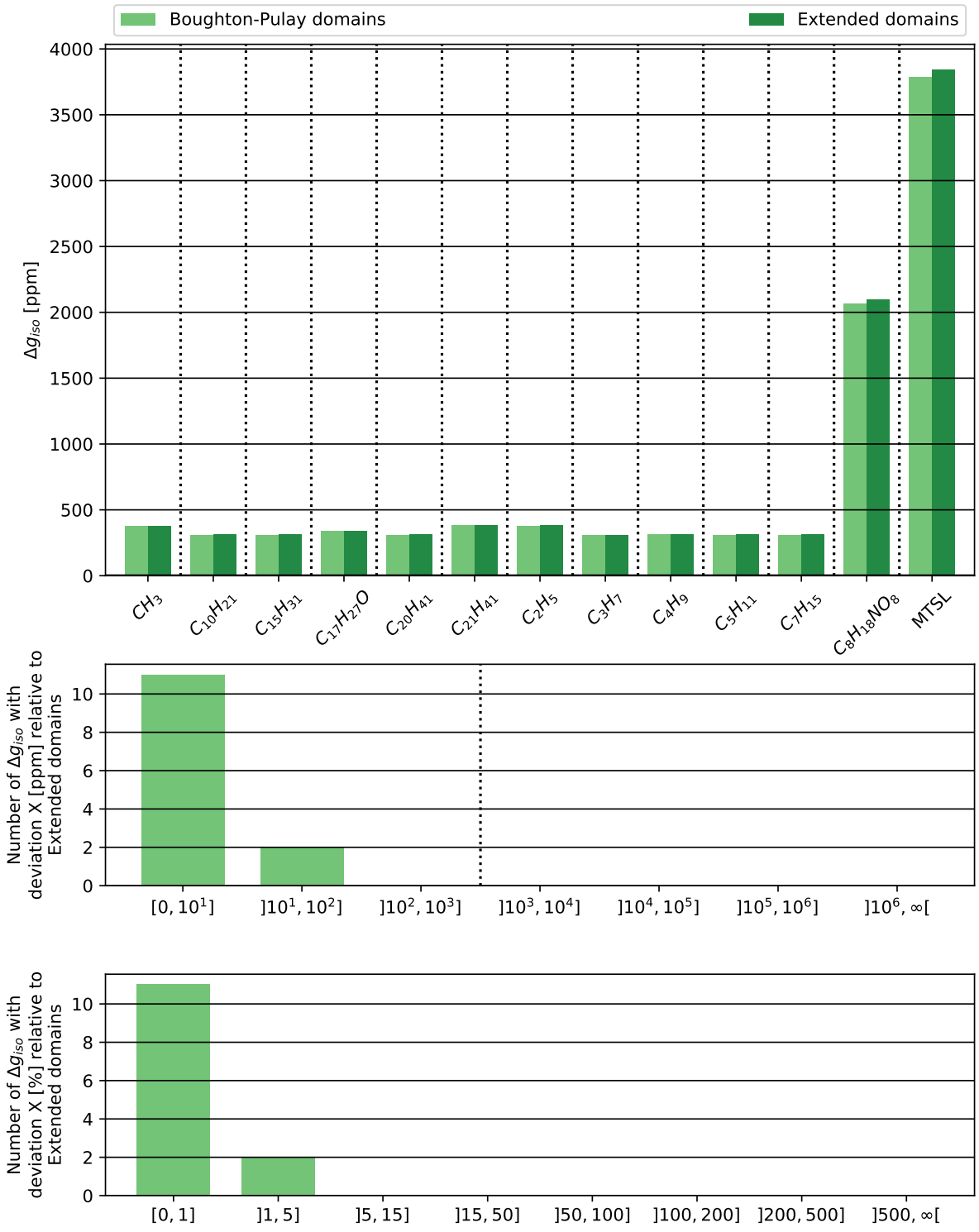

Figure 3.19: Dependence on the domain size of the isotropic g-shift Δg_{iso} calculated with Z_{eff}-SDC-DF-LUCC2 at the def2-TZVP/def2-QZVPP level with DF-UHF reference and full pair lists for a subset of the molecules with a single spin-center used by Glasbrenner *et al.*[35]

3.3.4 Pair list restriction

In this section, we investigate inclusion of all pairs, weak and strong pairs ($|E^{[IJ]}| > 0.03 \cdot 10^{-3}$ Hartree) or only strong pairs ($|E^{[IJ]}| > 3.0 \cdot 10^{-3}$ Hartree), with the thresholds having been chosen as suggested by Saebø and Pulay.[43] Restricting the pair lists based on the UMP2 pair energies $E^{[IJ]}$ for spin-independent calculations is unlikely to be optimal for spin density dependent properties. Nevertheless, it can enable us to judge the possible savings in computational effort we can expect from local restrictions based on the unperturbed spin density as suggested by Glasbrenner *et al.*[36]
The results for the calculations with pair lists restricted to strong and weak pairs ($|E_{IJ}| > 3.0 \cdot 10^{-5}$ Hartree) are reported in tables C.16 and C.35. For calculations including only strong ($|E_{IJ}| > 3.0 \cdot 10^{-3}$ Hartree) pairs, the results have been reported in tables C.18 and C.37. Relevant data for the previously problematic molecules has been collected in table 3.6.

Table 3.6: Data for the set of problematic molecules

	Pair restriction	$C_{19}H_{39}O$	NaF^+	Cys-Gly$_4$
$\frac{N_{pairs}^{included}}{N_{pairs}^{all}}$ [%]	strong + weak	25.7	100.0	27.1
	strong	5.4	72.7	5.3
Δg_{iso}[ppm]	all pairs	71363	178129	84784
	strong + weak	66031		83761
	strong	47256	177760	72417
Δg^{ZKE}[ppm]	all pairs	-299	-412	-229
	strong + weak	-299		-229
	strong	-300	-412	-230
$\Delta g_{iso}^{1el-DSO}$[ppm]	all pairs	202	222	226
	strong + weak	202		225
	strong	197	222	223
$\Delta g_{iso}^{1el-PSO}$[ppm]	all pairs	102262	237777	99849
	strong + weak	94639		98545
	strong	67794	237282	85291

Restricting the pair lists of the Perera test set consisting entirely of very small molecules to strong and weak pairs (fig. 3.21) has a predictably small effect on the results (MAD = 80 ppm, MRD = 2.1 %), since in many cases all pairs still contribute. The only molecule performing badly under restriction to weak pairs is CF_3Br^-, where a neglect of 23 % of pairs leads to an error in the isotropic g-shift of almost 2500 ppm.
When restricting further to strong pairs only, the quality of the results deteriorates significantly (MAD = 645 ppm, MRD = 25.8 %). While the deviations are still in the acceptable range of below 1000 ppm, the relative errors are quite significant. Therefore, the suitability of the strong pair approximation for investigation of the Perera benchmark set is questionable.
For the single spin-center benchmark set (fig. 3.22) restriction of the pair lists to strong and weak pairs yields an average error slightly below the experimental uncertainty (MAD = 401 ppm), which almost vanishes (MAD = 5 ppm) on exclusion of the molecules NaF^+, Cys-Gly$_4$ and $C_{19}H_{39}O$. In both cases, the relative errors (MRD = 1.0 %, MRD = 0.6 %)

are insignificant. Nevertheless, the error of more than 5000 ppm in $C_{19}H_{39}O$ is concerning. Enforcing the restriction of the pair lists to strong pairs only yields significantly larger absolute and relative errors (MAD = 2363 ppm, MRD = 9.7 %). Excluding the molecules NaF^+, Cys-Gly$_4$ and $C_{19}H_{39}O$ greatly improves the absolute errors (MAD = 74 ppm), but has only a minor effect on the relative errors (MRD = 8.2 %). While MTSL has an uncharacteristically large deviation of 620 ppm, we have still excellent agreement of the strong pair with the full pair calculations - despite neglecting up to almost 95 % of pairs in very large molecules - for the majority of molecules, at least as far as the absolute values are concerned.
The timings for the set of alkyl radicals are plotted in fig 3.20. The scaling is again still very close to $\mathcal{O}(\mathcal{N}^3)$ for the molecules under investigation. But the computational effort is reduced significantly compared to the all pair calculations when excluding very distant pairs. These savings improve only moderately when removing weak pairs as well, which coupled with the unreliability of the strong pair approximation makes it rather undesirable. For the largest molecule, removing very distant pairs from the calculation approximately halves the CPU time from 34 h to 17 h. Going to only strong pairs reduces the CPU time by only a few more hours to 13 h.
In conclusion we observe that a restriction to weak and strong pairs can be carried out without a significant loss in accuracy for the vast majority of molecules of the studied benchmark sets. A further restriction to strong pairs however is problematic in many of the small molecules already, but yields satisfactory results for large alkyl radicals, most likely due to very small absolute values (< 500 ppm) of their g-shifts.

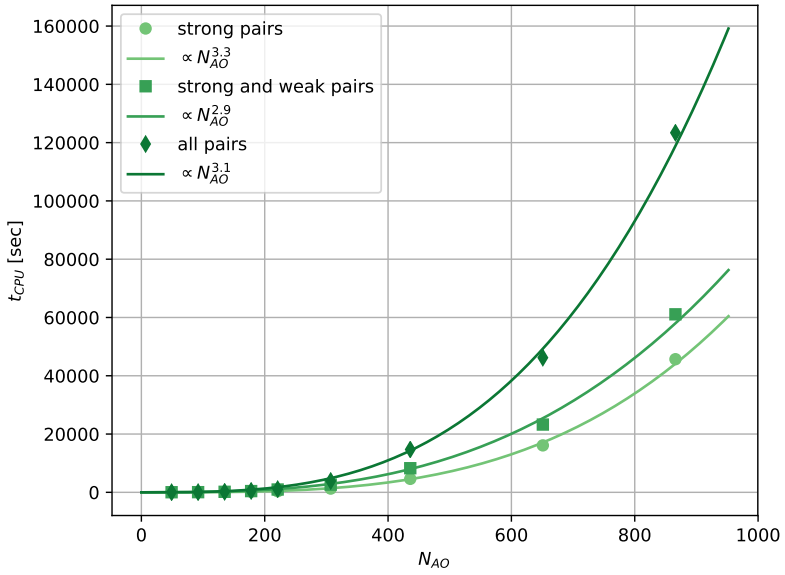

Figure 3.20: Dependence on restriction of the pair lists based on the UMP2 pair energies $E^{[IJ]}$ of the CPU time required for the Z_{eff}-SDC-DF-LUCC2 part of the g-tensor calculation at the def2-TZVP/def2-QZVPP level with DF-UHF reference extended Boughton-Pulay domains for the alkyl radicals used by Glasbrenner *et al.*[35]

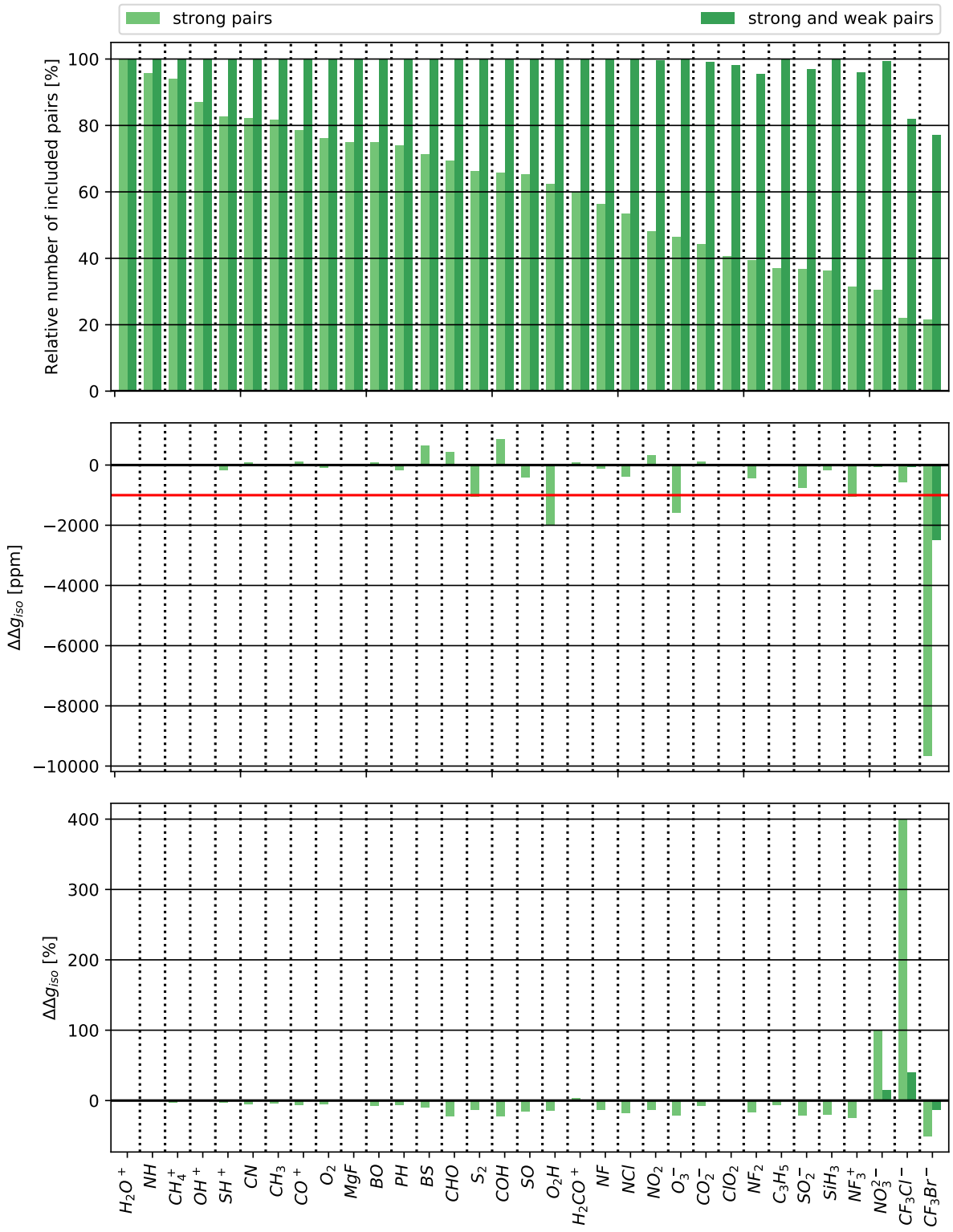

Figure 3.21: Dependence on the restriction of the pair lists based on the UMP2 pair energies $E^{[IJ]}$ of the isotropic g-shift Δg_{iso} calculated with Z_{eff}-SDC-DF-LUCC2 at the aug-cc-pVTZ/aug-cc-pVQZ level with DF-UHF reference extended Boughton-Pulay domains for a subset of the benchmark set of Perera *et al.*[34]

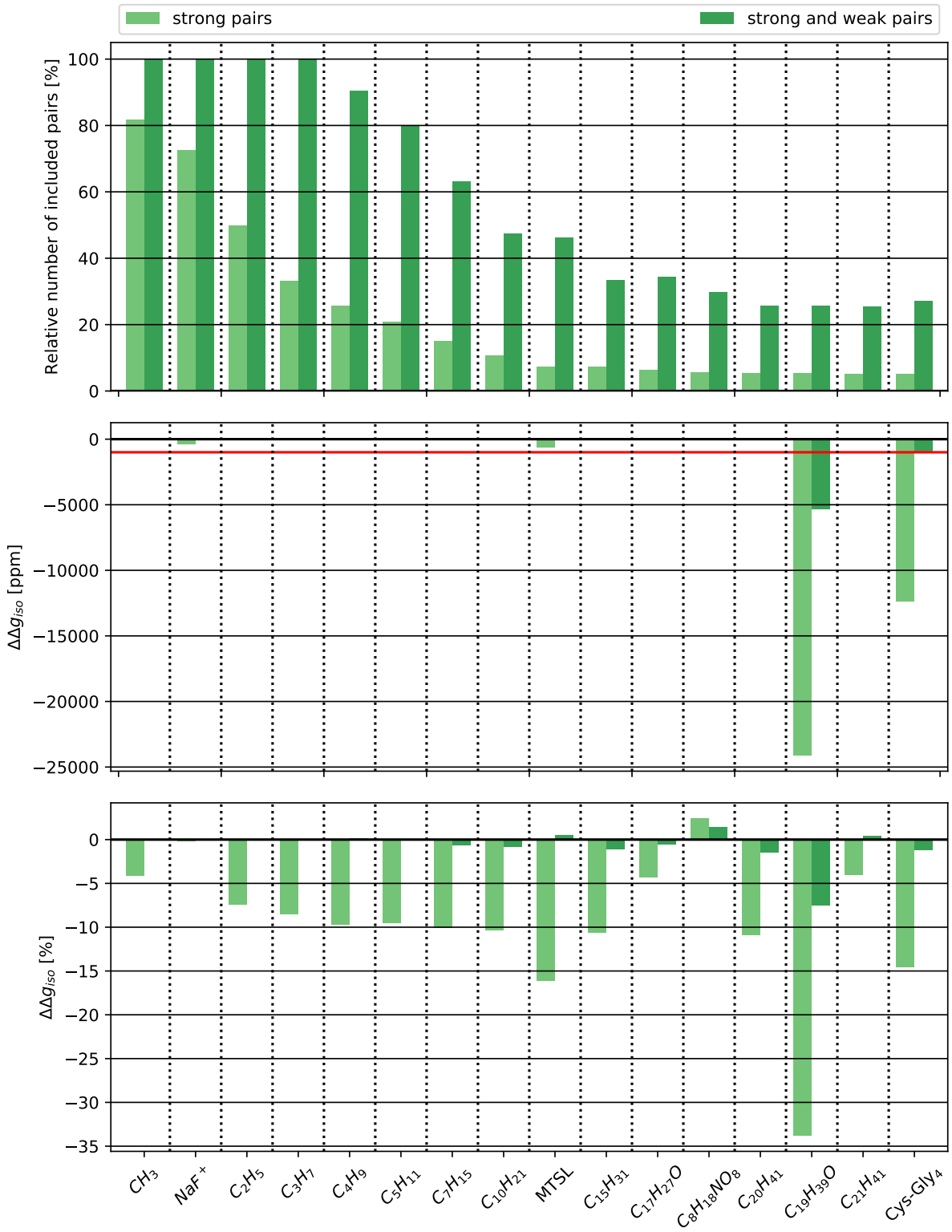

Figure 3.22: Dependence on the restriction of the pair lists based on the UMP2 pair energies $E^{[IJ]}$ of the isotropic g-shift Δg_{iso} calculated with Z_{eff}-SDC-DF-LUCC2 at the def2-TZVP/def2-QZVPP level with DF-UHF reference extended Boughton-Pulay domains for a subset of the molecules with a single spin-center used by Glasbrenner *et al.*[35]

3.3.5 Combined approximations

Having investigated the individual effects of the quality of the fitting basis, the size of the domains and the restriction of the pair lists on the quality of the calculated g-shifts and the computational effort, we now investigate the effect of applying the best compromise for each of these.
The results for the Perera benchmark set with aug-cc-pVTZ/aug-cc-pVDZ basis, standard Boughton-Pulay domains and strong and weak pairs ($|E_{IJ}| > 3.0 \cdot 10^{-5}$ Hartree) can be found in table C.20 and are represented in fig 3.24. The errors are still well within acceptable limits (MAD = 114 ppm, MRD = 4.1 %) for the vast majority of molecules and are only slightly larger than for reduction of domain size or neglect of very distant pairs alone.
The results for the calculations on the Glasbrenner single spin-center benchmark set with def2-TZVP/def2-TZVPP basis, standard Boughton-Pulay domains and pair lists restricted to strong and weak pairs ($|E_{IJ}| > 3.0 \cdot 10^{-5}$ Hartree) are listed in table C.39. We already know that we cannot expect good results if we include the molecules Cys-Gly_4, $C_{19}H_{39}O$ and to a lesser degree NaF^+ (see table 3.7), and this is what we observe (MAD = 1442 ppm, MRD = 2.5 %). However, if we restrict ourselves to the molecules included in fig. 3.25, we observe errors (MAD = 6 ppm, MRD = 0.8 %) that are essentially zero.

Table 3.7: Data for the set of problematic molecules

	approximations	$C_{19}H_{39}O$	NaF^+	Cys-Gly_4
Δg_{iso}[ppm]	extended domains, def2-TZVP/def2-QZVPP, all pairs	71363	178129	84784
	standard domains, def2-TZVP/def2-TZVPP, strong and weak pairs	56760	177920	76603
Δg^{ZKE}[ppm]	extended domains, def2-TZVP/def2-QZVPP, all pairs	-299	-412	-229
	standard domains, def2-TZVP/def2-TZVPP, strong and weak pairs	-299	-412	-229
$\Delta g_{iso}^{1el-DSO}$[ppm]	extended domains, def2-TZVP/def2-QZVPP, all pairs	202	222	226
	standard domains, def2-TZVP/def2-TZVPP, strong and weak pairs	197	222	223
$\Delta g_{iso}^{1el-PSO}$[ppm]	extended domains, def2-TZVP/def2-QZVPP, all pairs	102262	237777	99849
	standard domains, def2-TZVP/def2-TZVPP, strong and weak pairs	81390	237498	90219

For the timings of the alkyl radicals (fig 3.23) we observe again an asymptotic scaling of $\mathcal{O}(\mathcal{N}^4)$, which we are almost reaching this time. The prefactor however is significantly smaller, reducing the time required for $C_{20}H_{41}$ by a factor of approximately 4.5 from 34 h to 7 h.
Therefore, we conclude that the local correlation and density fitting approximations are well suited to the study of the electronic g-shift, at least if the spin density is highly localized and the PSO contributions are relatively small.

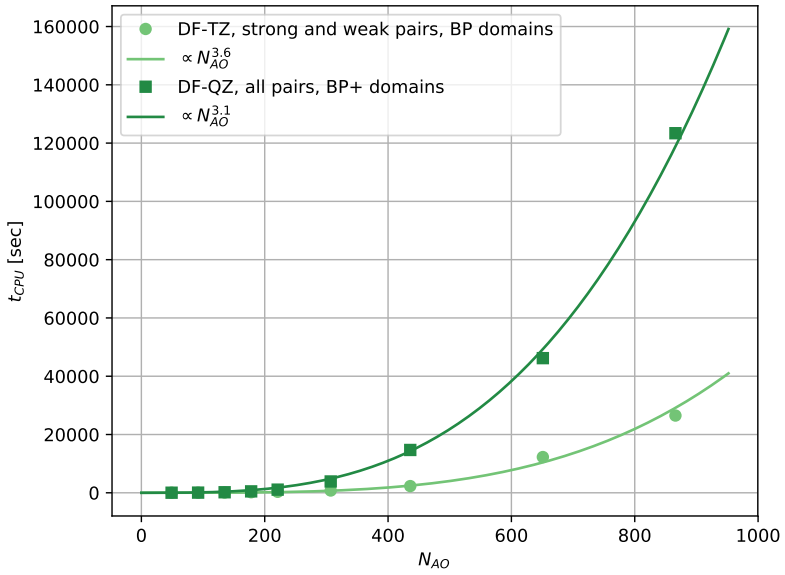

Figure 3.23: CPU times at the def2-TZVP/def2-TZVPP level with Boughton-Pulay domains and neglect of very distant pairs ($|E_{IJ}| > 3.0 \cdot 10^{-5}$ Hartree) versus those at the def2-TZVP/def2-QZVPP level with extended domains and full pair lists required for the Z_{eff}-SDC-DF-LUCC2 part of the g-tensor calculation with DF-UHF reference for the alkyl radicals used by Glasbrenner *et al.*[35]

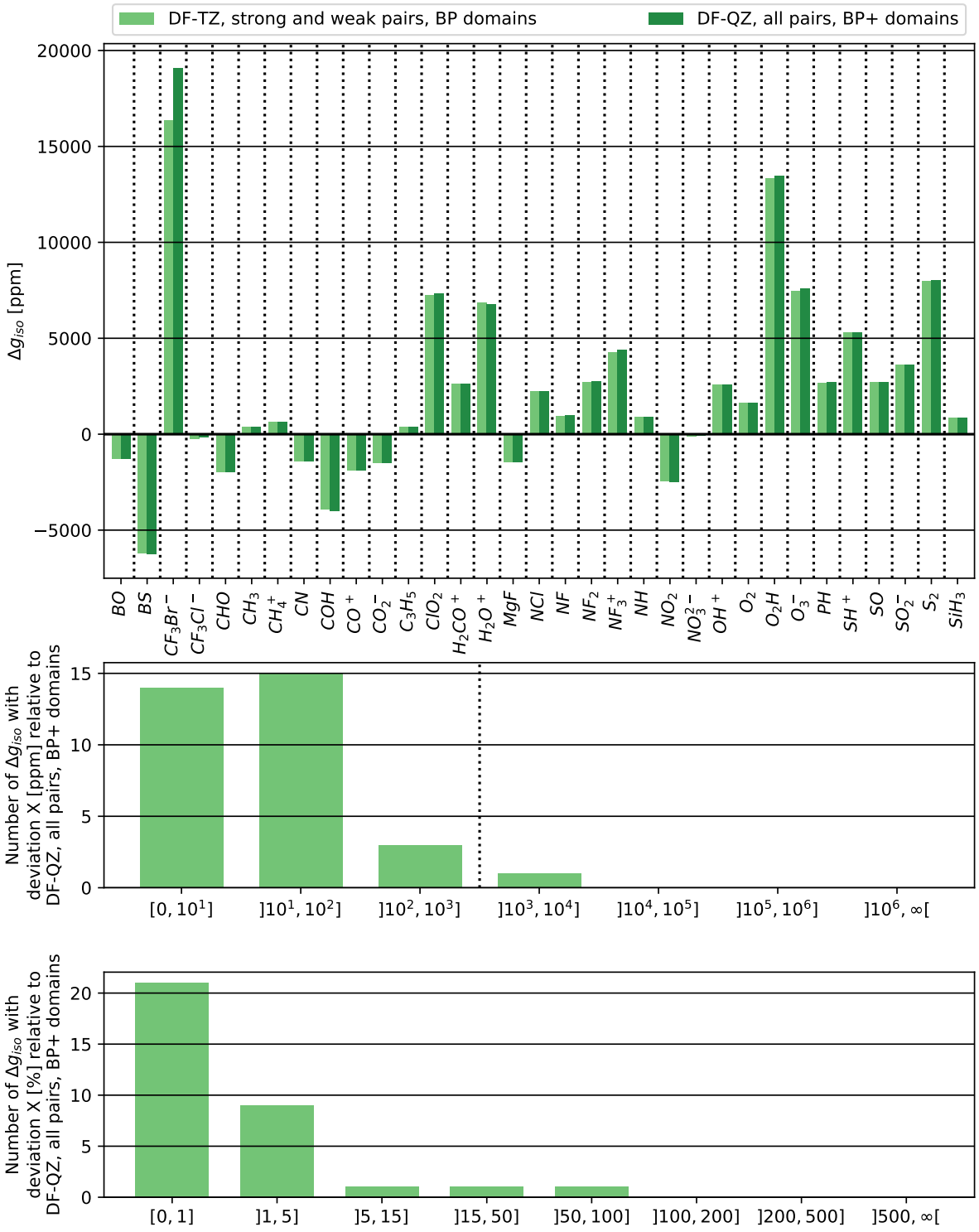

Figure 3.24: Isotropic g-shift Δg_{iso} calculated with Z_{eff}-SDC-DF-LUCC2 with DF-UHF reference at the aug-cc-pVTZ/aug-cc-pVDZ level with Boughton-Pulay domains and neglect of very distant pairs ($|E_{IJ}| > 3.0 \cdot 10^{-5}$ Hartree) versus those at the aug-cc-pVTZ/aug-cc-pVQZ level with extended domains and full pair lists for a subset of the benchmark set of Perera *et al.*[34]

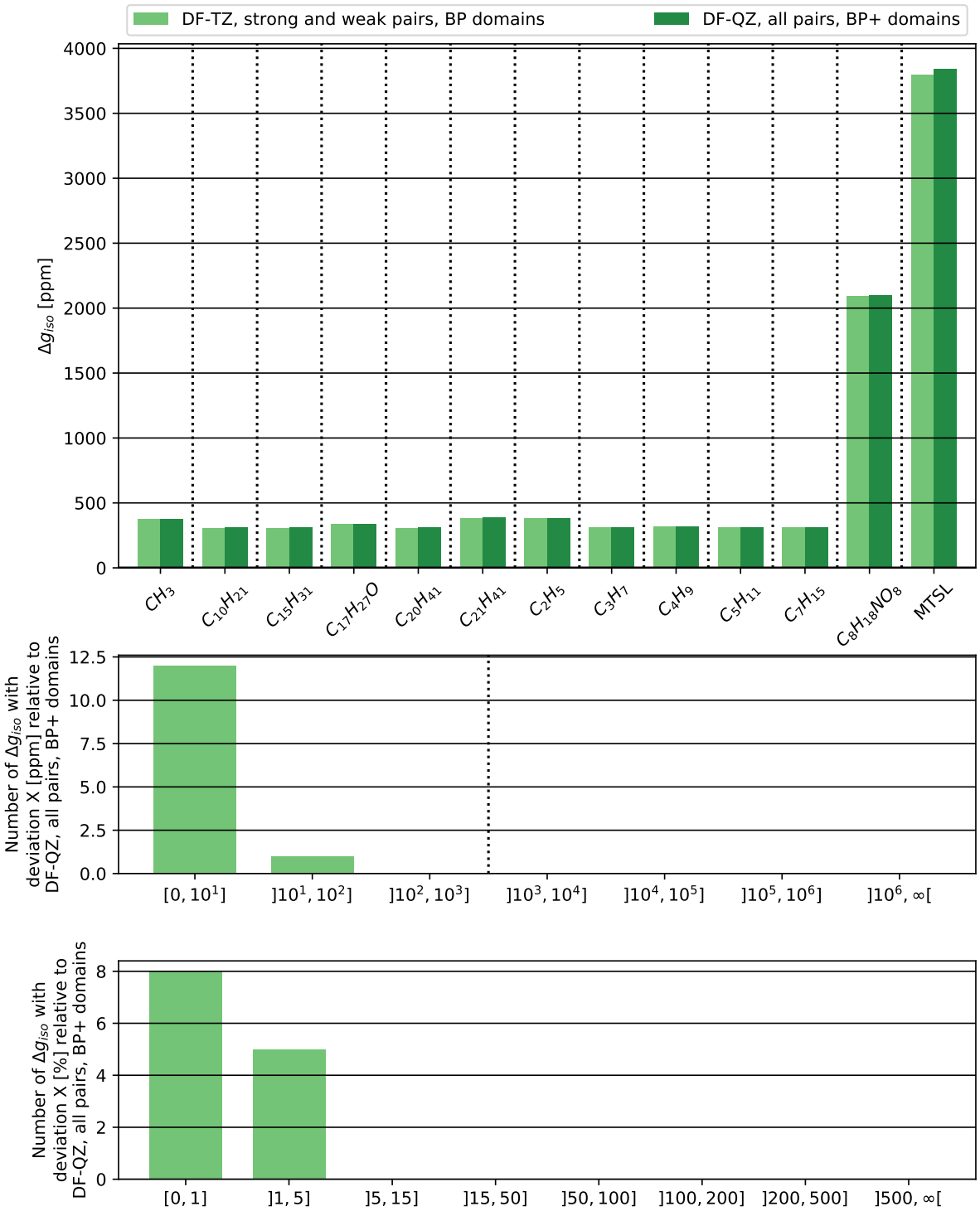

Figure 3.25: Isotropic g-shift Δg_{iso} calculated with Z_{eff}-SDC-DF-LUCC2 with DF-UHF reference at the def2-TZVP/def2-TZVPP level with Boughton-Pulay domains and neglect of very distant pairs ($|E_{IJ}| > 3.0 \cdot 10^{-5}$ Hartree) versus those at the def2-TZVP/def2-QZVPP level with extended domains and full pair lists for a subset of the molecules with a single spin-center used by Glasbrenner *et al.*[35]

Chapter 4

Summary and outlook

An unrestricted coupled-cluster method (DF-LUCC2) using local correlation and density fitting approximations for the calculation of first and second order properties based on response theory has been developed and implemented. It scales asymptotically as $\mathcal{O}(\mathcal{N}^4)$ with the molecular size $\mathcal{N}$ and has been applied to systems with up to 62 atoms and 897 atomic orbital basis functions. Parallelization has not been used, but further computational savings can be expected from doing so.
Focus of this work has been the electronic g-tensor. The two-electron spin-orbit contributions have been approximated via effective charges. This approximation has been found to be reasonable for the paramagnetic spin-orbit contribution, partially due to favorable error compensation of one- and two-electron terms, but provides only qualitatively correct results for the usually significantly smaller diamagnetic spin-orbit coupling. An improvement can be achieved via use of a spin-orbit mean-field (SOMF) operator with the appropriate local approximations and potentially density fitting of the required two-electron integrals. The gauge problem has been addressed via use of the spin density center (SDC) as a common gauge origin. Due to the locality of the spin density, this virtually eliminates the gauge error for systems with only a single well-defined spin-center. For the systems with multiple spin-centers investigated in this work, the SDC approximation still yields reasonable results, although with significantly higher deviations as for the systems with only a single spin-center. Therefore, a truly gauge invariant solution, like gauge including atomic orbitals (GIAOs) with use of explicit orbital relaxation, is desirable.
The errors introduced due to density fitting of the electron repulsion integrals have been found to be negligible, even when using fitting basis sets at or below the quality of the atomic orbital basis. The local correlation approximation introduces slightly larger errors, but they remain well below those due to use of effective charges. Use of standard Boughton-Pulay domains and neglect of very distant pairs have been observed to be sufficient to maintain the quality of the results and ensure that the prefactor of the computational effort remains small. However, there are some notable exceptions, but for these systems the CC2 method itself appears to be unreliable, possibly due to their multi-reference nature or near-degeneracies.
The restriction of the pair lists based on a pair energy criterion has yielded satisfactory results and savings, but is unlikely to be optimal. An improved approximation may be possible by enforcing an additional restriction of the domains based on the contribution of the atoms to the spin density and applying this restriction also to the singles vectors. This in turn would lead to a natural restriction of the pair list, since many pair domains

would disappear. An extension of this restriction could then be achieved via a distance criterion to prevent evaluating (presumably negligible) interactions between pairs on very distant spin-centers. This approach follows naturally from the observation that the spin density is zero over vast areas of the system. Furthermore, this reason has been used to justify choosing the spin density center as a common gauge origin, and a similar idea has already been employed by Glasbrenner *et al.*[36] to achieve sub-linear scaling of their SOMF-GIAO-B3LYP method via their locally projected perturbation (LPP) approach with no significant loss of accuracy. An analogy in our case would be the restriction of subsequent calculations based on either the MP2 or unperturbed CC2 spin density, or possibly even the HF spin density.

The results of the method presented here (Z_{eff}-SDC-DF-LUCC2) are in good agreement with the GIAO-CCSD results of Perera *et al.*[34] and with many of the results for small and extended systems obtained by Glasbrenner *et al.*[36] with their SOMF-GIAO-B3LYP method. A conclusive statement about the quality of the calculations on extended systems will require further study, since some ambiguity exists regarding the reliability of the comparison with SOMF-GIAO-B3LYP even for small molecules. However, it has been observed that systems with g-shifts of up to a few thousand ppm are in good agreement between Z_{eff}-SDC-DF-LUCC2 and SOMF-GIAO-B3LYP. Comparison to experiment shows only slightly worse agreement than GIAO-CCSD and shows results still within the rather large experimental uncertainties. Inclusion of vibrational averaging and environmental effects for the specific experimental conditions may be worth investigating.

The method presented in this work has demonstrated that g-tensor calculations for extended molecules are accessible to coupled-cluster methods with acceptable computational effort. The next logical step is the implementation of higher order coupled-cluster methods under exploitation of the locality of the spin density. This should also include use of GIAOs as well as SOMF operators. The development time required for implementation of this LPP-SOMF-GIAO-DF-UCC hierarchy can be significantly reduced via use of the local integrated tensor framework (LITF).[116]

Appendix A

Spin-field reduction

Using response theory, the electronic g-tensor is the second derivative of the energy with respect to the external magnetic field $\mathbf{B}$ and the magnetic moment $\mu_S = \mu_B \mathbf{S}$ due to the (effective) electronic net spin $\mathbf{S}$ of the system

$$g_{xy} = \left. \frac{d^2 E}{dB_x d(\mu_S)_y} \right|_{\mathbf{B},\mu_S=0}. \tag{A.1}$$

While the derivative with respect to the magnetic field is straightforward, the derivative with respect to spin is not for several reasons.
Firstly, unlike the magnetic field the net spin of the electrons is a non-multiplicative operator. What it means to take the derivative with respect to such an operator is not immediately obvious.
Secondly, the net spin $\mathbf{S}$ is the sum of the spin operators for the individual electrons $\mathbf{s}(i)$

$$\mathbf{S} = \sum_{i}^{N_{\text{elec}}} \mathbf{s}(i). \tag{A.2}$$

However, many of the terms relevant to electronic g-tensor calculations arising from the reduction of the Dirac-Coulomb-Breit Hamiltonian to the non-relativistic limit, i.e. the Zeeman kinetic energy correction and the diamagnetic and paramagnetic spin-orbit operators (see sections 2.2.2.1.1 and 2.2.2.1.2), do not explicitly depend on the net spin. Instead each electron or electron pair contributes a product of spin and spatial operators

$$H_1 = \sum_{i} \mathbf{h}_1(\mathbf{r}_i) \cdot \mathbf{s}(s_i) \tag{A.3}$$

$$H_2 = \sum_{ij}{}' \mathbf{h}_2(\mathbf{r}_i, \mathbf{r}_j) \cdot \mathbf{s}(s_i). \tag{A.4}$$

The first of these issues will be circumvented via the introduction of a phenomenological spin Hamiltonian and comparison of matrix elements of this operator between pure spin eigenfunctions with the expressions using the true Hamiltonian obtained via degenerate perturbation theory. The second problem will be solved via application of the Wigner-Eckart-Theorem for irreducible tensor operators. Using these considerations, we will see that the g-tensor can be evaluated by simple contraction of normalized spin- and spin-orbit density matrices with purely spatial integrals.
This appendix leans very heavily on the treatments by Harriman[12] and McWeeny[84] presented in their respective books.

A.1 Irreducible tensor operators

The following is only a very rough and incomplete description of what an irreducible tensor operator is and how to work with them that is restricted to the bare minimum of what is required in order to derive the working equations in this thesis. More detailed accounts can be found in the literature if desired.[12,84]

In general any quantity associated with one or more indices is often called a tensor. There is however also a stricter definition of what constitutes a tensor which is very useful for dealing with angular momentum and therefore spin.

An irreducible tensor operator $\mathbf{T}^{(k)}$ of rank k can be defined as a set of $2k+1$ operators that transform under rotation of axes among each other like angular momentum eigenfunctions. Such an operator can be represented in Cartesian coordinates or in spherical coordinates. Since the electronic spin operators for individual electrons and for the entire system are irreducible tensor operators of rank $k = 1$, we do not have to consider any other cases here.

The spin operator $\mathbf{s}^{(1)}(s_j)$ for the j-th electron in spherical coordinates has the three components

$$s_{+1}(j) = -\frac{s_x(j) + is_y(j)}{\sqrt{2}} = -\frac{s_+(j)}{\sqrt{2}} \tag{A.5}$$

$$s_0(j) = s_z(j) \tag{A.6}$$

$$s_{-1}(j) = \frac{s_x(j) - is_y(j)}{\sqrt{2}} = \frac{s_-(j)}{\sqrt{2}}, \tag{A.7}$$

where i is the imaginary unit and s_+ and s_- are the familiar ladder operators. An equivalent definition holds for any other tensor operator of the same rank including the net spin operator $\mathbf{S}^{(1)}$.

The operators derived from relativistics generally employ Cartesian coordinates. A switch from Cartesian to spherical coordinates is easily accomplished via the invariance of the scalar product

$$\mathbf{h}^{(1)} \cdot \mathbf{s}^{(1)} = \sum_{x \in x,y,z} h_x s_x = \sum_{\kappa \in -1,0,1} (-1)^\kappa h_\kappa s_{-\kappa}. \tag{A.8}$$

Having introduced the concept of irreducible tensor operators we are now able to state the Wigner-Eckart-Theorem[117,118] for matrix elements of such operators between angular momentum eigenfunctions

$$\langle ajm|T^{(k)}_\mu|a'j'm'\rangle = (-1)^{j-m} \begin{pmatrix} j & k & j' \\ -m & \mu & m' \end{pmatrix} \langle aj||\mathbf{T}^{(k)}||a'j'\rangle \tag{A.9}$$

where we have included the rank of the operator $\mathbf{T}^{(k)}$ on its individual elements for clarity. Before explaining the meaning of this theorem, we first need to define the terms appearing in this equation. The quantum numbers j and m are associated with an angular momentum operator $\mathbf{J}$ and its eigenfunctions $|ajm\rangle$ according to

$$J^2|ajm\rangle = j(j+1)|ajm\rangle \qquad\qquad J_z|ajm\rangle = m|ajm\rangle. \tag{A.10}$$

The additional index a is used to signify further differences in the functions independent of angular momentum. The Wigner-3j symbol

$$\begin{pmatrix} j & k & j' \\ -m & \mu & m' \end{pmatrix} \tag{A.11}$$

is just a group theoretical coupling coefficient and is aside from a constant factor identical to a Clebsch-Gordan coefficient. It has several properties and is defined via a rather complicated product of the quantum numbers. As we shall see later, we do not have to care about their actual values and the only property we need is that the m-type indices must fulfill the equation

$$\mu = m - m' \tag{A.12}$$

for it to have a non-zero value. The reduced matrix element

$$\langle aj||\mathbf{T}^{(k)}||a'j'\rangle \tag{A.13}$$

is independent of any m-type indices. The double bars indicate here that it is not actually an integral, but just a constant.
Thus, the Wigner-Eckart-Theorem states that the matrix elements of an irreducible tensor operator between angular momentum eigenfunctions for a given set of a- and j-type indices are proportional to the same reduced matrix element and the only difference is in the multiplication by a number. This means that from knowledge of the matrix element for any component μ we can derive the reduced matrix element and therefore the matrix elements for all other components, provided the initial matrix element is non-zero.
Since the Wigner-Eckart-Theorem is valid for all irreducible tensor operators we arrive at the following equality for non-vanishing reduced matrix elements

$$(-1)^{j-m}\begin{pmatrix} j & k & j' \\ -m & \mu & m' \end{pmatrix} = \frac{\langle ajm|T^{(k)}_{\mu}|a'j'm'\rangle}{\langle aj||\mathbf{T}^{(k)}||a'j'\rangle} = \frac{\langle ajm|S^{(k)}_{\mu}|a'j'm'\rangle}{\langle aj||\mathbf{S}^{(k)}||a'j'\rangle}. \tag{A.14}$$

This so-called replacement theorem can be used to replace the irreducible tensor operator $\mathbf{T}^{(k)}$ with any other irreducible tensor operator of the same rank, in this case $\mathbf{S}^{(k)}$. This insight will be vital in deriving expressions that depend on the net spin operator of the electrons $\mathbf{S}^{(1)}$ instead of the spin operators $\mathbf{s}^{(1)}(s_j)$ for the individual electrons.

A.2 Spin Hamiltonian

A spin Hamiltonian is an operator which only depends on the external magnetic field $\mathbf{B}$, nuclear spins $\mathbf{I}_K$, the (effective) net spin of the electrons $\mathbf{S}$ and observable coupling constants. However, there is no dependence on electronic or nuclear positions. This information has instead been absorbed in the coupling constants. When acting on pure spin eigenfunctions the spin Hamiltonian reproduces the observed energy levels. Thus, it serves as an interface between experiment and theory.
For electron spin resonance (ESR) spectroscopy, only terms that depend on $\mathbf{S}$ are of interest. Note that $\mathbf{S}$ may, but does not have to, coincide with the actual electronic net spin of the system. The spin Hamiltonian for ESR spectroscopy is therefore

$$H^{\mathrm{ESR}}_{\mathrm{Spin}} = \mu_B \mathbf{B}^T \mathbf{g} \mathbf{S} + \sum_K \mathbf{I}_K^T \mathbf{A}_K \mathbf{S} + \mathbf{S}^T \mathbf{D} \mathbf{S}. \tag{A.15}$$

Note that there is no term depending on only $\mathbf{S}$ since all the spin-orbit operators are Hermitian imaginary operators, i.e. their expectation values are zero.
The coupling constants in our spin Hamiltonian are generally anisotropic 3×3 matrices. The first term of the spin Hamiltonian represents the Zeeman interaction of the external

magnetic field with the electronic net spin and depends on the so-called "electronic g-tensor" $\mathbf{g}$. It is responsible for the initial splitting of the energy levels observed in ESR spectroscopy. The second term corresponds to an additional hyperfine splitting $\mathbf{A}_K$ of the energy levels due to interaction of the nuclear spins with the electronic spin. Finally, there is a zero-field splitting tensor $\mathbf{D}$ for triplet and higher spin states due to the electronic net spin.
In this thesis, we are only interested in the electronic g-tensor. Aside from determining these coupling constants experimentally, they can also be derived using ab initio calculations. To do so, we will employ degenerate perturbation theory.

A.3 Degenerate perturbation theory

We want to obtain an analytical expression for the energy shift due to application of an external magnetic field to a degenerate set of ground states belonging to the same spin multiplet, i.e. they only differ in their spin projection. To this purpose, we first partition our electronic Hamiltonian into

$$H = H^{(0,0)} + H^{(1,0)} + H^{(0,1)} + H^{(1,1)}. \tag{A.16}$$

The unperturbed operator is just the non-relativistic Born-Oppenheimer Hamiltonian

$$H^{(0,0)} = T^{\mathrm{e}} + V^{\mathrm{ee}} + V^{\mathrm{en}} + V^{\mathrm{nn}} \tag{A.17}$$

with the kinetic energy T^{e} of the electrons, the Coulomb repulsions V^{ee} between the electrons and V^{nn} between the nuclei and the Coulomb attraction V^{en} between electrons and nuclei. Note that neglect of nuclear motion may require averaging over vibrational modes in order to get agreement with the experiment, but this option is not further pursued in this work.
The perturbation is separated into three parts. First we have a set of operators that depend both on the spin of the electrons $\mathbf{s}(s_i)$ and the magnetic field $\mathbf{B}$

$$\begin{aligned} H^{(1,1)} =& H^{\mathrm{SB}}(\mathbf{B}, \mathbf{s}(s_i)) + H^{\mathrm{ZKE}}(\mathbf{B}, \mathbf{s}(s_i)) \\ &+ H^{\text{1el-DSO}}(\mathbf{B}, \mathbf{s}(s_i)) + H^{\text{2el-DSO}}(\mathbf{B}, \mathbf{s}(s_i)), \end{aligned} \tag{A.18}$$

where we have suppressed explicit dependence on the spatial coordinates for simplicity of the formalism. The individual operators are the electronic Zeeman term H^{SB}, the relativistic correction to this term usually referred to as the Zeeman kinetic energy (or relativistic mass correction) term H^{ZKE} and the one- and two-electron diamagnetic spin-orbit terms $H^{\text{1el-DSO}}$ and $H^{\text{2el-DSO}}$, respectively. The explicit expressions for the required operators can be found in section 2.2.2.1 of the main part of the thesis. At this point we only need to know that each of these operators can be written as a scalar product between a spatial and a spin operator in accordance with (A.3) and (A.4). The same goes for the purely spin-perturbed operator

$$H^{(0,1)} = H^{1el-PSO}(\mathbf{s}(s_i)) + H^{2el-PSO}(\mathbf{s}(s_i)), \tag{A.19}$$

which consists of the one- and two-electron paramagnetic spin-orbit operators. Finally, we have the purely field dependent perturbation operator

$$H^{(1,0)} = H^{LB}(\mathbf{B}) \tag{A.20}$$

with the only contribution being the orbital Zeeman term. There is also a relativistic kinetic energy correction to this Zeeman term, but since it is of higher order in the fine structure constant α we will neglect it. For the sake of simplicity we collect the perturbed operators in a single term

$$H' = H^{(1,0)} + H^{(0,1)} + H^{(1,1)}. \tag{A.21}$$

In order to (approximately) solve the eigenvalue problem

$$H|\Psi\rangle = E|\Psi\rangle, \tag{A.22}$$

we expand the wave function in an orthonormal basis of size n_K greater than the degeneracy due to spin

$$|\Psi\rangle = \sum_{K}^{n_K} |K\rangle c_K \tag{A.23}$$

leading us to

$$(\mathbf{H}_{KK} - E\mathbf{1}_{KK})\mathbf{C}_K = 0. \tag{A.24}$$

Here $\mathbf{H}_{KK}$ and $\mathbf{1}_{KK}$ are the Hamiltonian and unity matrix in the basis $|K\rangle$, respectively and $\mathbf{C}_K$ is the vector of the coefficients c_K.
It is now convenient to separate these equations into two spaces. The a-space describing the degenerate set of ground states and the b-space describing the "excited" states

$$\begin{pmatrix} \mathbf{H}_{AA} - E\mathbf{1}_{AA} & \mathbf{H}_{AB} \\ \mathbf{H}_{BA} & \mathbf{H}_{BB} - E\mathbf{1}_{BB} \end{pmatrix} \begin{pmatrix} \mathbf{C}_A \\ \mathbf{C}_B \end{pmatrix} = 0. \tag{A.25}$$

This enables us to make use of the functions of the b-space to find approximate solutions for the a-space.
Solving the second row for the coefficient vector for the b-space

$$\mathbf{C}_B = (E\mathbf{1}_{BB} - \mathbf{H}_{BB})^{-1}\mathbf{H}_{BA}\mathbf{C}_A \tag{A.26}$$

we can insert this result into the equation for the first row to obtain

$$\mathbf{H}^{\text{eff}}_{AA}\mathbf{C}_A = E\mathbf{C}_A \tag{A.27}$$

with the effective Hamiltonian

$$\mathbf{H}^{\text{eff}}_{AA} = \mathbf{H}_{AA} + \mathbf{H}_{AB}(E\mathbf{1}_{BB} - \mathbf{H}_{BB})^{-1}\mathbf{H}_{BA}. \tag{A.28}$$

In other words, the effect of the perturbation on the ground state energy can be determined by solving the significantly smaller $n_A \times n_A$ eigenvalue problem for this effective Hamiltonian instead of the complete problem for the full $n_K \times n_K$ space. This effective Hamiltonian has no intrinsic physical meaning, but can be used to derive properties up to second order.
Further simplification occurs from expanding the Hamiltonian and assuming the a-group to be eigenstates of the unperturbed Hamiltonian with the energy E_a

$$\mathbf{H}^{\text{eff}}_{AA} = E_a\mathbf{1}_{AA} + \mathbf{H}'_{AA} + \mathbf{H}'_{AB}(E\mathbf{1}_{BB} - \mathbf{H}_{BB})^{-1}\mathbf{H}'_{BA}. \tag{A.29}$$

In particular, the dependency on the unperturbed Hamiltonian drops out of the product term since we have assumed the a-group to be orthonormal to the b-group. If we now further assume that $E \approx E_a$ and only keep the lowest order of $\mathbf{H}_{BB}$, we obtain for an arbitrary matrix element between a-group functions

$$\langle a|H^{\text{eff}}|a'\rangle \approx \delta_{aa'}E_a + \langle a|H'|a'\rangle + \sum_b \frac{\langle a|H'|b\rangle\langle b|H'|a'\rangle}{E_a - E_b} \tag{A.30}$$

with

$$E_b = \langle b|H^{(0,0)}|b\rangle. \tag{A.31}$$

For the g-tensor, only terms of first order in both perturbations are of interest

$$\begin{aligned}\langle a|H^{\text{eff}}|a'\rangle^{[1,1]} = \langle a|H^{(1,1)}|a'\rangle &+ \sum_b \frac{\langle a|H^{(1,0)}|b\rangle\langle b|H^{(0,1)}|a'\rangle}{E_a - E_b} \\ &+ \sum_b \frac{\langle a|H^{(0,1)}|b\rangle\langle b|H^{(1,0)}|a'\rangle}{E_a - E_b}.\end{aligned} \tag{A.32}$$

Taking the a-group functions as zeroth order

$$|a\rangle \equiv |a^{(0,0)}\rangle \tag{A.33}$$

we can now define perturbed a-group functions of first order as

$$|a^{(1,0)}\rangle = \sum_b \frac{|b\rangle\langle b|H^{(1,0)}|a'^{(0,0)}\rangle}{E_a - E_b}. \tag{A.34}$$

The relevant second order matrix elements of the effective Hamiltonian are then

$$\langle a|H^{\text{eff}}|a'\rangle^{[1,1]} = \langle a^{(0,0)}|H^{(1,1)}|a'^{(0,0)}\rangle + \langle a^{(0,0)}|H^{(1,0)}|a'^{(0,1)}\rangle + \langle a^{(0,0)}|H^{(0,1)}|a'^{(1,0)}\rangle \tag{A.35}$$

$$= \langle a^{(0,0)}|H^{(1,1)}|a'^{(0,0)}\rangle + \langle a^{(1,0)}|H^{(0,1)}|a'^{(0,0)}\rangle + \langle a^{(0,0)}|H^{(0,1)}|a'^{(1,0)}\rangle. \tag{A.36}$$

The second equality implies that it is sufficient to obtain the perturbed wave function for only one of the perturbations, but for non-Hermitian theories (like non-variational coupled-cluster) the bra-functions must be obtained separately.
Having derived a representation of the energy shift due to an external perturbation as a matrix element of proper quantum mechanical operators, the next step will be finding an analogous expression using a spin Hamiltonian.

A.4 Spin density matrices

We are now able to derive expressions for the matrix elements (A.36) of the effective Hamiltonian. We assume the only degeneracy in the functions to be due to spin. This implies that the a-group consists of functions $\Psi_{aSM}^{(n,m)}$ with the same spin quantum number S and the same index a for all functions with the only difference being the M quantum number. The superscripts n and m determine the rank of functions in a perturbative sense as has been already used in previous sections.

For the matrix elements of the doubly perturbed operator (A.18) we first examine the case of a sum of one-electron operators, e.g. the one-electron diamagnetic spin-orbit operator

$$H^{\text{1el-DSO}}(\mathbf{B}, \mathbf{r}_i, \mathbf{s}(s_i)) = \sum_i^{N_{\text{el}}} \mathbf{h}^{\text{1el-DSO}}(\mathbf{r}_i, \mathbf{B}) \cdot \mathbf{s}(s_i) \tag{A.37}$$

The one-electron operator $\mathbf{h}^{\text{1el-DSO}}(\mathbf{r}_i, \mathbf{B})$ contains the dependence on the spatial coordinate of the i-th electron, the magnetic field as well as constant scaling factors. Thus, we obtain for the matrix element

$$\begin{aligned}&\langle a^{(0,0)} SM | H^{\text{1el-DSO}}(\mathbf{B}, \mathbf{s}(s_i)) | a^{(0,0)} SM' \rangle \\ &\qquad = \sum_i^{N_{\text{el}}} \langle a^{(0,0)} SM | \mathbf{h}^{\text{1el-DSO}}(\mathbf{r}_i, \mathbf{B}) \cdot \mathbf{s}(s_i) | a^{(0,0)} SM' \rangle.\end{aligned} \tag{A.38}$$

In order to simplify this expression we make use of the indistinguishability of the electrons to introduce the unperturbed one-electron density matrix

$$\rho_1^{(0,0)}(aSMM'|\mathbf{x}_1'; \mathbf{x}_1) = N_{\text{el}} \int \Psi_{aSM}^{(0,0)\,*}(\mathbf{x}_1', \mathbf{x}_2, ...) \Psi_{aSM'}^{(0,0)}(\mathbf{x}_1, \mathbf{x}_2, ..) d\mathbf{x}_2 d\mathbf{x}_3 ... \tag{A.39}$$

with $\mathbf{x}_i$ being the combined spatial- and spin-coordinate of the i-th electron. Inserting this into the definition of the matrix element and expanding the scalar product into a sum over the spherical components of the vectors we arrive at

$$\begin{aligned}&\langle a^{(0,0)} SM | H^{\text{1el-DSO}}(\mathbf{B}, \mathbf{s}(s_i)) | a^{(0,0)} SM' \rangle \\ &\qquad = \sum_\kappa (-1)^\kappa \int_{\mathbf{x}_1' = \mathbf{x}_1} h_{-\kappa}^{\text{1el-DSO}}(\mathbf{r}_1, \mathbf{B}) s_\kappa(s_1) \rho_1^{(0,0)}(aSMM'|\mathbf{x}_1'; \mathbf{x}_1) d\mathbf{x}_1,\end{aligned} \tag{A.40}$$

where the subscript on the integration sign implies renaming of $\mathbf{x}_1'$ to $\mathbf{x}_1$ after application of all operators but before integration. It is convenient to remove the explicit dependence on spin by integrating over it and introducing the spin density matrices

$$Q_\kappa^{(0,0)}(aSMM'|\mathbf{r}_1'; \mathbf{r}_1) = \int_{s_1' = s_1} \mathbf{s}_\kappa(s_1) \rho_1^{(0,0)}(aSMM'|\mathbf{x}_1'; \mathbf{x}_1) ds_1, \tag{A.41}$$

leading to the spin-independent expression

$$\begin{aligned}&\langle a^{(0,0)} SM | H^{\text{1el-DSO}}(\mathbf{B}, \mathbf{s}(s_i)) | a^{(0,0)} SM' \rangle \\ &\qquad = \sum_\kappa (-1)^\kappa \int_{\mathbf{r}_1' = \mathbf{r}_1} h_{-\kappa}^{\text{1el-DSO}}(\mathbf{r}_1, \mathbf{B}) Q_\kappa^{(0,0)}(aSMM'|\mathbf{r}_1'; \mathbf{r}_1) d\mathbf{r}_1.\end{aligned} \tag{A.42}$$

Since the spin density matrices are essentially a matrix element of an irreducible tensor operator between spin eigenfunctions, we can now use the Wigner-Eckart-Theorem (A.9) to express them in terms of a reduced spin density matrix $Q^{(0,0)}(aS||\mathbf{r}_1'; \mathbf{r}_1)$ via

$$Q_\kappa^{(0,0)}(aSMM'|\mathbf{r}_1'; \mathbf{r}_1) = (-1)^{S-M} \begin{pmatrix} S & 1 & S \\ -M & \kappa & M' \end{pmatrix} Q^{(0,0)}(aS||\mathbf{r}_1'; \mathbf{r}_1). \tag{A.43}$$

Since the reduced spin density matrix is independent of the m-type indices κ, M and M', we can obtain it from any convenient choice of these indices. The generally most

advantageous choice is $M = M' = S$, which also implies $\kappa = 0$ due to the condition (A.12) for m-type indices of non-zero Wigner-3j symbols

$$Q^{(0,0)}(aS||\mathbf{r}'_1;\mathbf{r}_1) = \begin{pmatrix} S & 1 & S \\ -S & 0 & S \end{pmatrix}^{-1} Q_0^{(0,0)}(aSSS|\mathbf{r}'_1;\mathbf{r}_1). \tag{A.44}$$

Note that in accordance with (A.6), the spin density matrix $Q_0^{(0,0)}(aSSS|\mathbf{r}'_1;\mathbf{r}_1)$ is obtained via the expectation value of the $s_z(1)$ operator between the a-group function for the state with maximum spin projection

$$Q_0^{(0,0)}(aSSS|\mathbf{r}'_1;\mathbf{r}_1) = \int_{s'_1=s_1} s_z(s_1)\rho_1^{(0,0)}(aSSS|\mathbf{x}'_1;\mathbf{x}_1)ds_1 \tag{A.45}$$

$$= \frac{1}{2}\left(P_1^{\alpha(0,0)}(aS|\mathbf{r}'_1;\mathbf{r}_1) - P_1^{\beta(0,0)}(aS|\mathbf{r}'_1;\mathbf{r}_1)\right) \tag{A.46}$$

and is just equal to one half times the difference of the spin-specific spatial density matrices $P_1^{\alpha(0,0)}(aS|\mathbf{r}'_1;\mathbf{r}_1)$ and $P_1^{\beta(0,0)}(aS|\mathbf{r}'_1;\mathbf{r}_1)$ for this state.
Using the definition (A.44) we can reframe the general spin density matrix (A.43) in terms of the spin density matrix for the state of maximal spin projection as

$$\begin{aligned} Q_\kappa^{(0,0)}(aSMM'|\mathbf{r}'_1;\mathbf{r}_1) =& (-1)^{S-M} \begin{pmatrix} S & 1 & S \\ -M & \kappa & M' \end{pmatrix} \begin{pmatrix} S & 1 & S \\ -S & 0 & S \end{pmatrix}^{-1} \\ & \times Q_0^{(0,0)}(aSSS|\mathbf{r}'_1;\mathbf{r}_1). \end{aligned} \tag{A.47}$$

The same equation is also valid for the matrix elements of the net spin operator $\mathbf{S}$ between pure spin eigenfunctions $|SM\rangle$

$$\langle SM|S_\kappa|SM'\rangle = (-1)^{S-M} \begin{pmatrix} S & 1 & S \\ -M & \kappa & M' \end{pmatrix} \begin{pmatrix} S & 1 & S \\ -S & 0 & S \end{pmatrix}^{-1} \langle SS|S_z|SS\rangle. \tag{A.48}$$

As already implied previously when we inferred the replacement theorem (A.14), we can use this insight to introduce the net spin into the definition of the spin density matrix

$$Q_\kappa^{(0,0)}(aSMM'|\mathbf{r}'_1;\mathbf{r}_1) = \frac{\langle SM|S_\kappa|SM'\rangle}{\langle SS|S_z|SS\rangle} Q_0^{(0,0)}(aSSS|\mathbf{r}'_1;\mathbf{r}_1). \tag{A.49}$$

provided the expectation value

$$\langle SS|S_z|SS\rangle = S \tag{A.50}$$

does not vanish. Since there is no splitting due to spin for singlet states ($S = 0$) and therefore no g-tensor, this does not cause any problems for us.
Before returning to the original matrix element, it is convenient to define a normalized spin density matrix

$$D^{(0,0)}(aS|\mathbf{r}'_1;\mathbf{r}_1) = \frac{1}{S} Q_0^{(0,0)}(aSSS|\mathbf{r}'_1;\mathbf{r}_1). \tag{A.51}$$

Note that for the state with maximum spin projection, S is identical to the difference between the number of α- and the number of β-electrons multiplied by one half

$$S = \frac{1}{2}(n_\alpha - n_\beta). \tag{A.52}$$

We are now able to achieve our original goal of finding an equivalent expression to (A.38) as a matrix element of a spin Hamiltonian between spin eigenfunctions. Inserting (A.51) into (A.49) and the result into (A.42) and switching to Cartesian coordinates, we obtain

$$\begin{aligned}&\langle a^{(0,0)}SM|H^{\text{1el-DSO}}(\mathbf{B},\mathbf{s}(s_i))|a^{(0,0)}SM'\rangle\\&\quad=\sum_x\langle SM|S_x|SM'\rangle\int_{\mathbf{r}_1'=\mathbf{r}_1}h_x^{\text{1el-DSO}}(\mathbf{r}_1,\mathbf{B})D^{(0,0)}(aS|\mathbf{r}_1';\mathbf{r}_1)d\mathbf{r}_1.\end{aligned}\tag{A.53}$$

Since the diamagnetic spin-orbit operator (as well as all other field dependent operators we have to deal with) depends only linearly on the magnetic field, we can rewrite this as

$$\begin{aligned}&\langle a^{(0,0)}SM|H^{\text{1el-DSO}}(\mathbf{B},\mathbf{s}(s_i))|a^{(0,0)}SM'\rangle\\&\quad=\sum_{xy}\langle SM|S_x|SM'\rangle\int_{\mathbf{r}_1'=\mathbf{r}_1}\left.\frac{\partial h_x^{\text{1el-DSO}}(\mathbf{r}_1,\mathbf{B})}{\partial B_y}\right|_{\mathbf{B}=0}B_yD^{(0,0)}(aS|\mathbf{r}_1';\mathbf{r}_1)d\mathbf{r}_1\end{aligned}\tag{A.54}$$

It is easy to see that this conforms to the definition of the spin Hamiltonian (A.15), and we obtain for this contribution

$$H_{\text{Spin}}^{\text{1el-DSO}}=\mu_B\mathbf{B}\cdot\boldsymbol{\Delta}g^{\text{1el-DSO}}\cdot\mathbf{S}\tag{A.55}$$

with the g-shift due to the one-electron diamagnetic spin-orbit coupling being defined via

$$\mu_B\Delta g_{yx}^{\text{1el-DSO}}=\int_{\mathbf{r}_1'=\mathbf{r}_1}\left.\frac{\partial h_x^{\text{1el-DSO}}(\mathbf{r}_1,\mathbf{B})}{\partial B_y}\right|_{\mathbf{B}=0}D^{(0,0)}(aS|\mathbf{r}_1';\mathbf{r}_1)d\mathbf{r}_1.\tag{A.56}$$

For the remaining doubly perturbed one-electron operators we arrive at equivalent expressions. For the two-electron diamagnetic spin-orbit term however we have to make a slight change to the equation, since the spatial operator depends on the coordinates of two electrons. This can be easily taken into account via introduction of a normalized spin-orbit density matrix

$$\mu_B\Delta g_{yx}^{\text{2el-DSO}}=\int_{\substack{\mathbf{r}_1'=\mathbf{r}_1\\\mathbf{r}_2'=\mathbf{r}_2}}\left.\frac{\partial h_x^{\text{2el-DSO}}(\mathbf{r}_1,\mathbf{r}_2,\mathbf{B})}{\partial B_y}\right|_{\mathbf{B}=0}D^{(0,0)}(aS|\mathbf{r}_1',\mathbf{r}_2';\mathbf{r}_1,\mathbf{r}_2)d\mathbf{r}_1d\mathbf{r}_2.\tag{A.57}$$

Since we are accounting for this term via an effective one-electron operator, we will not go into any more detail here.

The derivation for the spin Hamiltonian reproducing the sum of products of singly perturbed quantities in (A.36) is essentially identical. For the one-electron paramagnetic spin-orbit coupling contribution we obtain for instance

$$\mu_B\Delta g_{yx}^{\text{1el-PSO}}=\int_{\mathbf{r}_1'=\mathbf{r}_1}h_x^{\text{1el-PSO}}(\mathbf{r}_1)D_y^{(1,0)}(aS|\mathbf{r}_1';\mathbf{r}_1)d\mathbf{r}_1,\tag{A.58}$$

i.e. we have to contract the spatial spin-orbit integrals with the perturbed spin density matrices

$$D_y^{(1,0)}(aS|\mathbf{r}_1';\mathbf{r}_1)=\left.\frac{\partial D(aS|\mathbf{r}_1';\mathbf{r}_1)}{\partial B_y}\right|_{\mathbf{B}=0}.\tag{A.59}$$

Instead of appearing explicitly, the orbital Zeeman term (A.20) contributes implicitly to these density matrices, since it is used in their derivation.

We have shown, that the g-tensor is obtained via contraction of spatial integrals with the normalized spin density or spin-orbit density matrices for the state of maximum spin projection. This is a very general result that can also be applied if the density matrices have been obtained with approximate theories like the coupled-cluster method presented in this thesis (see also section 2.3.7.3).

Appendix B

Diagrammatic coupled-cluster

B.1 Second quantization

The following discussion of second quantization as applied to coupled-cluster theory follows primarily the treatments by Helgaker *et al.*[119] and Shavitt and Bartlett.[60] Only the most vital aspects required for the application of second quantization to coupled-cluster theory have been included.

B.1.1 Occupation number vector and elementary operators

Assuming a set of M orthonormal spin-orbitals $|\phi_P\rangle$, a Slater determinant in second quantization is represented by an occupation number vector

$$|k\rangle = |k_1, k_2, ..., k_M\rangle, \qquad k_P \in 0, 1 \; \forall \; P \in 1, 2, ..., M. \tag{B.1}$$

Occupied and unoccupied orbitals are assigned $k_P = 1$ and $k_P = 0$, respectively. The true vacuum state, i.e. the absence of electrons, is an occupation number vector with $k_P = 0 \; \forall P \in 1, 2, ..., M$

$$|\text{vac}\rangle = |0, 0, ..., 0\rangle. \tag{B.2}$$

Any state can be created from this vacuum state via application of appropriate creation operators

$$a_P^\dagger |k\rangle = \delta_{k_P 0} \Gamma_P^k |k_1, k_2, ..., k_{P-1}, 1, k_{P+1}, ..., k_M\rangle, \tag{B.3}$$

where the phase factor

$$\Gamma_P^k = \prod_{Q=1}^{k_P - 1} (-1)^{k_Q}, \tag{B.4}$$

has to be included to ensure identity with equations derived from first quantization. Note that attempting to create an electron in an occupied orbital destroys the state in agreement with the Pauli exclusion principle.
Annihilation operators for the removal of electrons from occupied orbitals are just the adjoint of the creation operators

$$a_P |k\rangle = \delta_{k_P 1} \Gamma_P^k |k_1, k_2, ..., k_{P-1}, 0, k_{P+1}, ..., k_M\rangle. \tag{B.5}$$

Attempting to destroy an electron in an unoccupied orbital will again destroy the state. Having introduced both creation and annihilation operators, we can now state their anti-commutation relations

$$[a_P^\dagger, a_Q^\dagger]_+ = 0 \tag{B.6}$$

$$[a_P^\dagger, a_Q]_+ = \delta_{PQ} \tag{B.7}$$

$$[a_P, a_Q]_+ = 0. \tag{B.8}$$

Repeated application of these relations allows for the reduction of matrix elements of annihilation and creation operator strings to expressions involving only integrals and coefficients.

B.1.2 Operators in second quantization

Consider the first quantization one- and two-electron operators

$$F^c = \sum_i^{N_{\text{elec}}} f^c(x_i) \tag{B.9}$$

$$G^c = \frac{1}{2} \sum_{i \neq j}^{N_{\text{elec}}} g^c(x_i, x_j) \tag{B.10}$$

The second quantization representation of these operators are

$$F = \sum_{PQ} f_{PQ} a_P^\dagger a_Q \tag{B.11}$$

$$G = \frac{1}{2} \sum_{PQRS} g_{PQRS} a_P^\dagger a_R^\dagger a_S a_Q. \tag{B.12}$$

Requiring identity of matrix elements using first and second quantization operators, the coefficients turn out to be just integrals between spin-orbitals

$$f_{PQ} = \int \phi_P^*(x) f^c(x) \phi_Q(x) dx \tag{B.13}$$

$$g_{PQRS} = \int \phi_P^*(x_1) \phi_R^*(x_2) g^c(x_1, x_2) \phi_Q(x_1) \phi_S(x_2) dx_1 dx_2. \tag{B.14}$$

The unperturbed electronic Hamiltonian in second quantization is therefore

$$H = \sum_{PQ} h_{PQ} a_P^\dagger a_Q + \frac{1}{2} \sum_{PQRS} g_{PQRS} a_P^\dagger a_R^\dagger a_S a_Q + h_{\text{nuc}} \tag{B.15}$$

with the coefficients

$$h_{PQ} = -\frac{1}{2} \langle \phi_P | \nabla^2 | \phi_Q \rangle - \sum_I^{N_{\text{nuc}}} Z_I \langle \phi_P | r_I^{-1} | \phi_Q \rangle \tag{B.16}$$

$$g_{PQRS} = \langle \phi_P \phi_R | r_{12}^{-1} | \phi_Q \phi_S \rangle \tag{B.17}$$

$$h_{\text{nuc}} = \frac{1}{2} \sum_{I \neq J}^{N_{\text{nuc}}} Z_I Z_J R_{IJ}^{-1}. \tag{B.18}$$

Here $\mathbf{r}_I$ and Z_I are distance to and charge of the I-th nucleus, $\mathbf{r}_{12}$ the inter-electronic distance and $\mathbf{R}_{IJ}$ the distance between nuclei I and J.

B.1.3 Normal order

A string of elementary annihilation and creation operators is said to have normal order if all annihilators are to the right of the creators. It follows trivially that any normal ordered operator containing at least one annihilator will destroy the vacuum state

$$\{...a_Q...\}|\text{vac}\rangle = 0 \tag{B.19}$$

with the curly brackets indicating normal order. Consequently, the vacuum expectation value of all normal ordered operators vanishes

$$\langle\text{vac}|\{O\}|\text{vac}\rangle = 0 \tag{B.20}$$

since we have either an annihilator acting to the right on $|\text{vac}\rangle$ or a creator acting to the left on $\langle\text{vac}|$.
To obtain the normal ordered form of an arbitrary operator string, the operators are permuted until they fulfill the abovementioned criterion and the string is multiplied by $(-1)^p$, where p is the number of required permutations. For operator strings of length two the normal ordered operators are therefore

$$\{a_P^\dagger a_Q\} = a_P^\dagger a_Q \tag{B.21}$$

$$\{a_Q a_P^\dagger\} = -\, a_P^\dagger a_Q. \tag{B.22}$$

Note that strings consisting of only creation or annihilation operators always have normal order.
The difference of an unordered string of two operators and its normal ordered form defines the so-called contraction

$$\overbrace{a_P^\dagger a_Q} = a_P^\dagger a_Q - \{a_P^\dagger a_Q\} \tag{B.23}$$

$$\overbrace{a_Q a_P^\dagger} = a_Q a_P^\dagger - \{a_Q a_P^\dagger\} \tag{B.24}$$

It immediately follows that the only non-vanishing contraction for a pair of elementary operators is of the type

$$\overbrace{a_Q a_P^\dagger} = a_Q a_P^\dagger + a_P^\dagger a_Q = \delta_{PQ}, \tag{B.25}$$

where the second equality follows from the elementary anti-commutation relation (B.7).

B.1.4 Wick's theorem

According to Wick's theorem, an arbitrary string of creation and annihilation operators can be expressed as the sum of normal ordered strings with all possible contractions including no contraction, i.e.

$$ABC... = \{ABC...\} + \sum_{\text{single contractions}} \{\overbrace{ABC...}\} + \sum_{\text{double contractions}} \{\overbrace{A\overbrace{BC...}}\} + ... \tag{B.26}$$

Note that before contraction, two operators must be next to each other in the respective string, which is achieved by permutation and multiplication with $(-1)^p$.
The generalized Wick's theorem states that a product of two normal ordered operators can be expressed as a similar sum, but all non-vanishing contractions occur only between the normal ordered operators, since all contractions within the operators are zero. This is an essential insight enabling the use of diagrammatic methods in the derivation of working equations.

B.1.5 Non-orthonormal orbitals

Since the virtual space used in this work is spanned by non-orthonormal orbitals $|\bar{P}\rangle$ with overlap

$$\bar{S}_{PQ} = \langle \bar{\phi}_P | \bar{\phi}_Q \rangle, \tag{B.27}$$

the effect of this choice on the second quantization formalism has to be investigated.
It is convenient to introduce an auxiliary set of orbitals

$$|\tilde{\phi}_P\rangle = \sum_Q |\bar{\phi}_Q\rangle [\bar{S}^{-\frac{1}{2}}]_{QP} \tag{B.28}$$

which are orthonormal to each other

$$\tilde{S}_{PQ} = [\bar{S}^{-\frac{1}{2}} \bar{S} \bar{S}^{-\frac{1}{2}}]_{PQ} = \delta_{PQ}. \tag{B.29}$$

This allows for analogous definition of creation and annihilation operators for the auxiliary orbital set that fulfill the previously introduced anti-commutator relations

$$\tilde{a}_P^\dagger = \sum_Q \bar{a}_Q [\bar{S}^{-\frac{1}{2}}]_{QP} \tag{B.30}$$

$$\tilde{a}_P = \sum_Q [\bar{S}^{-\frac{1}{2}}]_{PQ} \bar{a}_Q. \tag{B.31}$$

Inverting the transformation

$$\bar{a}_P^\dagger = \sum_Q \tilde{a}_Q^\dagger [\bar{S}^{\frac{1}{2}}]_{QP} \tag{B.32}$$

$$\bar{a}_P = \sum_Q [\bar{S}^{\frac{1}{2}}]_{PQ} \tilde{a}_Q. \tag{B.33}$$

and plugging these definitions into the anti-commutator relations (B.6), (B.7) and (B.8), we arrive at

$$[\bar{a}_P^\dagger, \bar{a}_Q^\dagger]_+ = 0 \tag{B.34}$$

$$[\bar{a}_P^\dagger, \bar{a}_Q]_+ = \bar{S}_{PQ} \tag{B.35}$$

$$[\bar{a}_P, \bar{a}_Q]_+ = 0. \tag{B.36}$$

Additionally, the coefficients in the operator definitions need to be altered. The correct integrals can be obtained by using the procedure employed for orthonormal orbitals with the auxiliary orbitals. For a one-electron operator we have

$$F = \sum_{PQ} \tilde{f}_{PQ} \tilde{a}_P^\dagger \tilde{a}_Q = \sum_{RS} [\bar{S}^{-\frac{1}{2}} \tilde{f} \bar{S}^{-\frac{1}{2}}]_{RS} \bar{a}_R^\dagger \bar{a}_S \tag{B.37}$$

and with

$$\tilde{f}_{RS} = \sum_{TV} [\bar{S}^{-\frac{1}{2}}]_{RT} \int \bar{\phi}_T^*(x) f^c(x) \bar{\phi}_V(x) dx [\bar{S}^{-\frac{1}{2}}]_{VS} \tag{B.38}$$

we obtain

$$F = \sum_{PQ} [\bar{S}^{-1} \bar{f} \bar{S}^{-1}]_{PQ} \bar{a}_P^\dagger \bar{a}_Q. \tag{B.39}$$

For a two-electron operator we obtain analogously

$$G = \frac{1}{2} \sum_{PQRS} \sum_{TUVW} [S^{-1}]_{PT} [S^{-1}]_{RV} g_{PQRS} [S^{-1}]_{UQ} [S^{-1}]_{WS} \bar{a}_P^\dagger \bar{a}_R^\dagger \bar{a}_S \bar{a}_Q. \tag{B.40}$$

The inverse overlap can be included when transforming from the atomic orbital (AO) basis $|\mu\rangle$ (here not the space of excited determinants) to the molecular orbital (MO) basis

$$|\bar{P}\rangle = \sum_{\mu} \sum_{Q} |\mu\rangle C_{\mu Q} [S^{-1}]_{QP} = \sum_{\mu} |\mu\rangle \bar{C}_{\mu P}. \tag{B.41}$$

In the rest of this thesis the bar for non-othonormal operators is dropped and it is to be implicitly understood that virtual orbitals are non-orthonormal if not otherwise specified. Furthermore, it should be noted that the overlap and its inverse for occupied orbitals remain of course the unit matrix.

B.2 Coupled-cluster diagrams

B.2.1 Fermi-vacuum

In chemistry one rarely deals with true vacuums. Instead it is more convenient to start the discussion from a reference state where the lowest N_{elec} orbitals are already occupied, the so-called Fermi-vacuum

$$|0\rangle = \prod_{I=1}^{N_{\text{elec}}} a_I^\dagger |\text{vac}\rangle. \tag{B.42}$$

We have adopted here the convention used in the main part of this thesis that orbitals which are occupied in the Fermi-vacuum are designated with $I, J, K, ...$ whereas unoccupied (or virtual) orbitals use $A, B, C, ...$ For general orbitals we will continue to use $P, Q, R, ...$ Recall that the virtual orbitals used in this work are non-orthonormal, in contrast to the occupied orbitals. Furthermore, initial and maximum values of sums over these index spaces will be dropped and implicit summation over the entire corresponding spaces is to be assumed.

We can now define quasi-creators as operators which either create a particle in a virtual orbital (e.g. $a_A^\dagger$) or a hole in an occupied orbital (e.g. a_I). Quasi-annihilators on the other hand annihilate the Fermi-vacuum by attempting to either create a particle in an occupied orbital (e.g. $a_I^\dagger$) or to create a hole in an empty orbital (e.g. a_A).

It is useful to explicitly consider the anti-commutator relations for quasi-creators and -annihilators

$$[a_A^\dagger, a_I]_+ = \delta_{AI} = 0 \tag{B.43}$$

$$[a_I^\dagger, a_A]_+ = \delta_{IA} = 0 \tag{B.44}$$

$$[a_A^\dagger, a_B]_+ = S_{AB} \tag{B.45}$$

$$[a_I^\dagger, a_J]_+ = \delta_{IJ}. \tag{B.46}$$

We see that in addition to anti-commutation of true creation and annihilation operators, quasi-creators and quasi-annihilators also anti-commute with operators of their own class.

B.2.2 Quasi-normal order

We define quasi-normal ordered operators as operator strings with all quasi-creators being to the left of all quasi-annihilators. Using the same rules as for normal order with respect to the true vacuum (see section B.1.3), we get

$$\{a_A^\dagger a_B\} = a_A^\dagger a_B \tag{B.47}$$
$$\{a_B a_A^\dagger\} = -\, a_A^\dagger a_B \tag{B.48}$$
$$\{a_I^\dagger a_J\} = -\, a_J a_I^\dagger \tag{B.49}$$
$$\{a_J a_I^\dagger\} = a_J a_I^\dagger. \tag{B.50}$$

The only non-vanishing contractions are then

$$\overbrace{a_I^\dagger a_J} = \delta_{IJ} \tag{B.51}$$
$$\overbrace{a_A a_B^\dagger} = S_{AB}. \tag{B.52}$$

Contractions between operators acting on occupied orbitals and operators acting on virtual orbitals are always zero due to their vanishing anti-commutator and do not need to be explicitly considered. Having defined quasi-normal order, we are now able to apply Wick's theorem to products in the same way we did for normal ordered operators.

B.2.3 Quasi-normal ordered Hamiltonian

In order to find the quasi-normal ordered Hamiltonian, we expand the unordered operator in a sum of normal ordered operators including all possible contractions in accordance with Wick's theorem.
For a one-electron operator we have

$$a_P^\dagger a_Q = \overbrace{a_P^\dagger a_Q} + \{a_P^\dagger a_Q\} = \delta_{PI}\delta_{QJ}\delta_{IJ} \;+\; \{a_P^\dagger a_Q\}, \tag{B.53}$$

where we have used (B.51). Analogously, a two-electron operator expands to

$$\begin{aligned} a_P^\dagger a_R^\dagger a_S a_Q =& \delta_{PI}\delta_{QJ}\delta_{IJ}\delta_{RK}\delta_{SL}\delta_{KL} - \delta_{PI}\delta_{SL}\delta_{IL}\delta_{RK}\delta_{QJ}\delta_{KJ} && \text{(B.54)}\\ &+ \delta_{PI}\delta_{QJ}\delta_{IJ}\{a_R^\dagger a_S\} - \delta_{PI}\delta_{SJ}\delta_{IJ}\{a_R^\dagger a_Q\} && \text{(B.55)}\\ &+ \delta_{RI}\delta_{SJ}\delta_{IJ}\{a_P^\dagger a_Q\} - \delta_{RI}\delta_{QJ}\delta_{IJ}\{a_P^\dagger a_S\} && \text{(B.56)}\\ &+ \{a_P^\dagger a_R^\dagger a_S a_Q\} && \text{(B.57)} \end{aligned}$$

where the minus signs are due to use of the anti-commutator relations to bring the operators next to each other before applying (B.51).
Inserting this into the Hamiltonian (B.15) yields

$$\begin{aligned} H =& \sum_I h_{II} + \frac{1}{2}\sum_{IJ}\left(g_{IIJJ} - g_{IJJI}\right) + h_{\text{nuc}} && \text{(B.58)}\\ &+ \sum_{PQ}\left(h_{PQ} + \sum_I \left(g_{PQII} - g_{PIIQ}\right)\right)\{a_P^\dagger a_Q\} && \text{(B.59)}\\ &+ \frac{1}{2}\sum_{PQRS} g_{PQRS}\{a_P^\dagger a_R^\dagger a_S a_Q\}, && \text{(B.60)} \end{aligned}$$

where we have used that the contributions arising from (B.55) and (B.56) are identical after renaming of the summation indices due to the symmetry of the two-electron integrals. It is convenient to introduce here the antisymmetrized two-electron integrals

$$\langle PR||QS\rangle = g_{PQRS} - g_{PSRQ}. \tag{B.61}$$

When taking the expectation value with respect to the Fermi-vacuum only the first line (B.58) survives, since by definition quasi-normal ordered operators destroy this state

$$\langle 0|H|0\rangle = \sum_I h_{II} + \frac{1}{2}\sum_{IJ}\langle IJ||IJ\rangle + h_{\text{nuc}}. \tag{B.62}$$

If we take for the Fermi-vacuum the converged Hartree-Fock determinant, this is just the Hartree-Fock energy.
Examining the second line (B.59) of the Hamiltonian

$$F_N = \sum_{PQ}\left(h_{PQ} + \sum_I \langle PI||QI\rangle\right)\{a_P^\dagger a_Q\} = \sum_{PQ} f_{PQ}\{a_P^\dagger a_Q\}, \tag{B.63}$$

we see that this is just the normal ordered Fock operator. Here and in subsequent sections the index N indicates normal order with respect to the Fermi-vacuum.
The final line (B.60) yields the normal ordered fluctuation potential

$$V_N = \frac{1}{4}\sum_{PQRS}\langle PR||QS\rangle\{a_P^\dagger a_R^\dagger a_S a_Q\}, \tag{B.64}$$

where we have added the two-electron term a second time, introduced an additional factor of one half to compensate, swapped the creation operators by using their anti-commutation relation and renamed the summation indices in order to make use of the antisymmetrized two-electron integrals.
Note that any quasi-normal ordered operator can be obtained by subtracting its Fermi-vacuum expectation value from the unordered operator

$$H_N = H - \langle 0|H|0\rangle. \tag{B.65}$$

B.2.4 Cluster operator

The substitution operators creating "excited" determinants from the Fermi-vacuum can be expressed in terms of quasi-creation operators

$$T_1 = \sum_{IA} t_A^I \tau_I^A = \sum_{IA} t_A^I a_A^\dagger a_I \tag{B.66}$$

$$T_2 = \frac{1}{4}\sum_{\substack{IJ\\AB}} t_{AB}^{IJ}\tau_{IJ}^{AB} = \frac{1}{4}\sum_{\substack{IJ\\AB}} t_{AB}^{IJ} a_A^\dagger a_I a_B^\dagger a_J. \tag{B.67}$$

Note that the cluster operator consists of only quasi-creators and is therefore always in quasi-normal order.

B.2.5 Baker-Campbell-Hausdorff expansion

Having introduced second quantization expressions for Hamiltonian and cluster operators, we are now able to investigate the Baker-Campbell-Hausdorff (BCH) expansion of the similarity transformed Hamiltonian

$$\exp(-T)H\exp(T) = \sum_{n=0}\frac{1}{n!}\big([]\big)^n H\big(,T]\big)^n \tag{B.68}$$

$$= \langle 0|H|0\rangle + H_N + \sum_{n=1}\frac{1}{n!}\big([]\big)^n H_N\big(,T]\big)^n. \tag{B.69}$$

Note that the expectation value with respect to the Fermi-vacuum is just a number and therefore immediately drops out of all commutators.
In order to further simplify this expression we investigate the example of the commutator

$$[F_N, T_1] = \sum_{PQ}\sum_{AI} f_{PQ}t_A^I[\{a_P^\dagger a_Q\}, \{a_A^\dagger a_I\}]. \tag{B.70}$$

Using Wick's theorem to obtain the quasi-normal ordered form of the operator string

$$[\{a_P^\dagger a_Q\}, \{a_A^\dagger a_I\}] = \{a_P^\dagger a_Q a_A^\dagger a_I\} + \{a_P^\dagger a_I\}\delta_{QB}S_{AB} + \{a_Q a_A^\dagger\}\delta_{PI} + \delta_{PI}\delta_{QB}S_{AB} - \{a_A^\dagger a_I a_P^\dagger a_Q\} \tag{B.71}$$

$$= \{a_P^\dagger a_I\}\delta_{QB}S_{AB} + \{a_Q a_A^\dagger\}\delta_{PI} + \delta_{PI}\delta_{QB}S_{AB}, \tag{B.72}$$

we see that only terms with at least one contraction between the operators F_N and T_1 yield a non-zero contribution. Using this insight we can greatly reduce the complexity of the BCH expansion

$$\exp(-T)H\exp(T) = \langle 0|H|0\rangle + H_N + (H_N T)_C + \frac{1}{2}(H_N T^2)_C + \frac{1}{3!}(V_N T^3)_C + \frac{1}{4!}(V_N T^4)_C. \tag{B.73}$$

Here the subscript C implies that every cluster operator must have at least one contraction with the quasi-normal ordered Hamiltonian, i.e. only "linked" terms are non-zero. Since H_N has at most four elementary operators, this requirement cannot be fulfilled for more than four cluster operators and the expansion terminates.
Also of note is that the expectation value of the Hamiltonian with respect to the Fermi-vacuum does not contribute to the amplitude equations since

$$\langle\mu|H|0\rangle = \langle 0|H|0\rangle\langle\mu|0\rangle + \langle\mu|H_N|0\rangle = \langle\mu|H_N|0\rangle \tag{B.74}$$

due to orthogonality of the occupied and virtual spaces.

B.2.6 T_1-transformation

The singles substitution operator T_1 creates a vast number of contributions to matrix elements of the similarity transformed Hamiltonian. A convenient way to include all of them is the use of transformed operators. Since we can insert between any two elementary operators the unity

$$1 = \exp(T_1)\exp(-T_1) \tag{B.75}$$

it is sufficient to consider the transformation of the elementary operators

$$\hat{a}_P^\dagger = \exp(-T_1) a_P^\dagger \exp(T_1) = a_P^\dagger + (a_P^\dagger T_1)_C \tag{B.76}$$

$$\hat{a}_P = \exp(-T_1) a_P \exp(T_1) = a_P + (a_P T_1)_C \tag{B.77}$$

Here $\hat{}$ indicates T_1-transformed ("dressed") operators (and later integrals) and the BCH expansion terminates after the first commutator due to the connectivity requirement. Using the usual rules for contraction, we have for dressed creation operators

$$\hat{a}_P^\dagger = a_P^\dagger - \sum_{IA} t_A^I \delta_{PI} a_A^\dagger = \sum_R x_{RP} a_R^\dagger, \tag{B.78}$$

where we have introduced the transformation matrix

$$x_{RP} = \delta_{RP} - \sum_{IA} t_A^I \delta_{RA} \delta_{PI}. \tag{B.79}$$

Likewise, for annihilation operators we arrive at

$$\hat{a}_Q = a_Q + \sum_{IAB} t_A^I S_{AB} \delta_{QB} a_I = \sum_S y_{QS} a_S, \tag{B.80}$$

with the transformation matrix

$$y_{QS} = \delta_{QS} + \sum_{IAB} t_A^I S_{AB} \delta_{QB} \delta_{SI}. \tag{B.81}$$

We can now transfer the transformation of the operators to a transformation of the integrals

$$\sum_{PQ} h_{PQ} \hat{a}_P^\dagger \hat{a}_Q^\dagger = \sum_{RS} \hat{h}_{RS} a_R^\dagger a_S \tag{B.82}$$

with the dressed integrals

$$\hat{h}_{RS} = \sum_{PQ} x_{RP} h_{PQ} y_{QS}. \tag{B.83}$$

For the sake of simplicity, we will only investigate two cases explicitly. For occupied orbitals in both bra and ket the transformation yields

$$\begin{aligned}
\hat{h}_{KL} =& \sum_{PQ} x_{KP} h_{PQ} y_{QL} \\
=& \sum_{PQ} (\delta_{KP} - \sum_{IA} t_A^I \delta_{KA} \delta_{PI}) h_{PQ} (\delta_{QL} + \sum_{IAB} t_A^I S_{AB} \delta_{QB} \delta_{LI}) \\
=& h_{KL} + \sum_{AB} h_{KB} S_{AB} t_A^L,
\end{aligned} \tag{B.84}$$

whereas for virtual orbitals we have

$$\begin{aligned}
\hat{h}_{CD} =& \sum_{PQ} x_{CP} h_{PQ} y_{QD} \\
=& \sum_{PQ} (\delta_{CP} - \sum_{IA} t_A^I \delta_{CA} \delta_{PI}) h_{PQ} (\delta_{QD} + \sum_{IAB} t_A^I S_{AB} \delta_{QB} \delta_{DI}) \\
=& h_{CD} - \sum_I h_{ID} t_C^I.
\end{aligned} \tag{B.85}$$

It is convenient to combine the T_1-transformation of the integrals in MO basis with the transformation (B.41) from the AO basis $|\mu\rangle$ to the MO basis (also see section 2.1.3.1)

$$|I\rangle = \sum_{\mu} |\mu\rangle L_{\mu I} \tag{B.86}$$

$$|A\rangle = \sum_{B\mu} |\mu\rangle P_{\mu B} [S^{-1}]_{BA}. \tag{B.87}$$

Note that the transformations for occupied and virtual orbitals differ and the latter includes multiplication with the inverse of the overlap matrix due to the non-orthonormality of the virtual space.
Combining the transformations (B.86) and (B.87) with the T_1-transformation (B.84) of the integrals over occupied orbitals we arrive at

$${}^{P}\Lambda^{\mathrm{occ}}_{\mu K} = L_{\mu K} \tag{B.88}$$

$${}^{H}\Lambda^{\mathrm{occ}}_{\mu L} = L_{\mu L} + \sum_{A} P_{\mu A} t^{L}_{A}. \tag{B.89}$$

The superscripts P and H refer to transformation of a "particle"-index (i.e. ket) or a "hole"-index (i.e. bra), respectively.
Analogously, combining (B.86) and (B.87) with the T_1-transformation (B.85) for the virtual indices yields

$${}^{P}\bar{\Lambda}^{\mathrm{virt}}_{\mu C} = \sum_{D} P_{\mu D} [S^{-1}]_{DC} - \sum_{I} t^{I}_{C} L_{\mu I} \tag{B.90}$$

$${}^{H}\bar{\Lambda}^{\mathrm{virt}}_{\mu D} = \sum_{C} P_{\mu C} [S^{-1}]_{CD}. \tag{B.91}$$

Using these transformations, we can transform any integral from the AO basis directly to the dressed MO basis.
Note that integrals with only occupied indices in the bra and only virtual indices in the ket are in general identical to their undressed counterparts

$$\hat{h}_{IA} = h_{IA} \tag{B.92}$$

$$\langle IJ\hat{|}|AB\rangle = \langle IJ||AB\rangle. \tag{B.93}$$

However, care has to be taken when transforming effective one-electron operators like the Fock operator, which have an internal dependence on two-electron integrals that must be appropriately transformed as well. This also implies that dressed Fock integrals are in general never equal to undressed Fock integrals, since we always have internal dressing of the two-electron integrals

$$\hat{f}_{IA} = h_{IA} + \sum_{J} \langle IJ\hat{|}|AJ\rangle \neq f_{IA}. \tag{B.94}$$

B.2.7 Contraction of Hamiltonian fragments with non-orthonormal operators

Fully contracting the term

$$\sum_{PQ} \hat{h}_{PQ} a_A \{a^{\dagger}_P a_Q\} a^{\dagger}_B = \sum_{CD} S_{AC} \hat{h}_{CD} S_{DB} + S_{AB} \sum_{PQ} \hat{h}_{PQ} \{a^{\dagger}_P a_Q\} \tag{B.95}$$

we see that contractions with the Hamiltonian fragment yield overlap integrals. These overlap integrals compensate the inverse overlap integrals in (B.39) and (B.40). It is thus convenient to include these overlap integrals in the integrals and to modify the contraction rule (B.52) for the case that one of the involved operators belongs to a Hamiltonian fragment to

$$\overbrace{a_A a_B^\dagger} = \delta_{AB}. \tag{B.96}$$

Note that contractions between other operators, i.e. contractions of operators creating "excited" determinants to the left with the cluster operator, still follow

$$\overbrace{a_A a_B^\dagger} = S_{AB}. \tag{B.97}$$

Despite this added complexity, this convention is greatly advantageous since it enables us to use the original integrals instead of having to multiply them with the inverse overlap matrix. It also removes a majority of explicit references to the overlap matrix.
In order to remain consistent, we have to include the overlap arising from the contraction in the transformation matrices (B.90) and (B.91) for the virtual space

$${}^P\Lambda_{\mu A}^{\text{virt}} = \sum_C {}^P\bar{\Lambda}_{\mu C}^{\text{virt}} S_{CA} = P_{\mu A} - \sum_{IC} t_C^I S_{CA} L_{\mu I} \tag{B.98}$$

$${}^H\Lambda_{\mu A}^{\text{virt}} = \sum_D {}^H\bar{\Lambda}_{\mu D}^{\text{virt}} S_{DA} = P_{\mu A}. \tag{B.99}$$

Note that this has removed all explicit refererences to the inverse of the overlap matrix. The virtual space used in this work is spanned by projected atomic orbitals (PAOs) (see section 2.1.3.1), which form a redundant set of orbitals. Therefore, some eigenvalues of their overlap matrix are (numerically) zero and it cannot be inverted. Although this can be circumvented by using of a pseudo-inverse overlap matrix (see section 2.3.5), the disappearance of dependence on the inverse overlap means that we do not have to consider this problem any further here.

B.2.8 Rules for drawing and interpreting diagrams

We are now able to exploit the systematic nature of the contraction of quasi-normal ordered operators to replace the tedious task of repeatedly applying the contraction rules with a diagrammatic scheme. The following rules hold for drawing and interpreting diagrams. Examples for their use have not been given, since a multitude of diagrams and their interpretations can be found in appendix B.3.

1. Integrals, amplitudes and multipliers are represented by horizontal lines ("interaction lines").

2. Contractions are represented by "vertical" lines. These lines do not need to be strictly "vertical", i.e. they may be curved or non-orthogonal to the interaction lines.

3. Each interaction line has a number of so-called "vertices" equal to the number of creator/annihilator pairs of the associated operator.

4. Each vertex of an interaction line has an outgoing and incoming line corresponding to the associated creator and annihilator, respectively.

5. Each vertical line is associated with an index. Upwards pointing lines ("particle lines") and downwards pointing lines ("hole lines") correspond to virtual and occupied indices, respectively.

6. Lines above the interaction line correspond to quasi-creators ($a_A^\dagger$, a_I), lines below the interaction line correspond to quasi-annihilators ($a_I^\dagger$, a_A). Note that amplitudes can only have quasi-creators, while multipliers are always associated with quasi-annihilators (i.e. quasi-creators acting on the bra function). Therefore, amplitudes are at the bottom of a diagram with vertical lines above the interaction line while multipliers are at the top of the diagram with vertical lines below the interaction line.

7. Each interaction line contributes an integral, amplitude or multiplier. For integrals, outgoing indices are associated with bra indices and incoming indices with ket indices, i.e. $\langle P_{\text{out}}|f|Q_{\text{in}}\rangle$ for one-electron integrals and $\langle P_{\text{out}_1}R_{\text{out}_2}||Q_{\text{in}_1}S_{\text{in}_2}\rangle$ for two-electron integrals. Note that the two-electron integrals are antisymmetrized. Due to the restriction of possible indices for amplitudes and multipliers, they always follow the schemes $t_{AB..}^{IJ..}$ and $\lambda_{IJ...}^{AB...}$, respectively. Furthermore, the order of the index pairs in two-electron integrals, amplitudes and multipliers is arbitrary since they are symmetric with respect to interchange of electrons.

8. The excitation level of an interaction line is defined as the number of its quasi-creators minus the number of its quasi-annihilators divided by two. Amplitudes always have positive excitation level, multipliers always negative. The total excitation level of the diagram must correspond to zero for energy contributions or the excitation level of the corresponding amplitude or multiplier equation.

9. Contraction lines can be divided into internal lines, i.e. lines connecting two interaction lines, and external lines, i.e. lines that are connected with only one interaction line. When interpreting the diagram, summation over all internal indices is carried out.

10. Each particle line that is not linked to the Hamiltonian fragment leads to introduction of an overlap integral between the line index and a dummy index, replacement of the line index with the dummy index in the amplitude (or multiplier), and summation over the dummy index. This applies to external lines and internal lines between amplitudes and multipliers. In the latter case the dummy index replaces the line index only in the amplitude or the multiplier, not in both.

11. A loop is defined as an unbroken sequence of lines either starting and ending at the same vertex (internal loop) or an unbroken sequence of lines beginning with a particle/hole line and ending with a hole/particle line (external loop).

12. The sign of a diagram is -1 to the power of the sum of the number of loops and the number of hole lines.

13. A set of n internal particle or n internal hole lines are equivalent if they begin and end at the same two interaction lines. Each n-tuple of equivalent lines contributes a factor of $\frac{1}{n!}$ to the diagram.

14. A set of n amplitudes of the same order and excitation level are equivalent if they are connected to an (n+1)-th operator via the same number of particle and the same number of hole lines. Each n-tuple of equivalent amplitudes contributes a factor of $\frac{1}{n!}$ to the diagram. No such rule is necessary for multipliers since we will only ever have a single multiplier in a given diagram.

15. An n-tuple of external lines is unique if they are not linked to the same operator (but may be linked to equivalent operators). For each n-tuple of unique external lines an antisymmetrizing permutation operator has to be introduced.

$$\begin{aligned} P(A,B,C,...)f(A,B,C,...) &= \sum_{P_i}(-1)^{p_i}P_i f(A,B,C,...) \\ &= f(A,B,C,...) - f(B,A,C,...) + ... \end{aligned} \tag{B.100}$$

16. Due to the connectivity requirement in the BCH expansion, all amplitudes that occur in a diagram must each share at least one internal line with the Hamiltonian fragment. Multipliers however can appear disconnected from the interaction line of the integral.

17. All possible connectivities must be exhausted in order to obtain the correct contribution. In the case of multiple amplitudes in a diagram, the unique diagrams can be determined using the method described by Shaviit and Bartlett.[60]

B.3 Derivation of working equations

B.3.1 Derivation and interpretation of diagrams

For the unrestricted coupled-cluster model, α and β orbitals are not the same. Therefore, we will be working with explicitly spin dependent indices in the following

$$|P\rangle \rightarrow |p_\sigma\rangle \qquad\qquad \sigma \in \alpha, \beta. \tag{B.101}$$

This will increase the complexity of the initial diagram interpretation, but allows for subsequent elimination of many terms via analytical spin-integration.
We will be using the Einstein convention for summation over repeated spatial indices. However, sums over spin will be included explicitly for the sake of clarity since repeated occurrence of the same spin index does not necessarily imply summation over this index.
In this work, we are using the CC2 model with additional one-electron perturbations $H^{(1,0)}$, $H^{(0,1)}$ and $H^{(1,1)}$ (see section 2.2.1.1). The Lagrangian is then

$$\begin{aligned} L =& \langle 0|\hat{H} + [\hat{H}, T_2]|0\rangle + \lambda_{\mu_1}\langle \mu_1|\hat{H} + [\hat{H}, T_2]|0\rangle \\ &+ \lambda_{\mu_2}\langle \mu_2|\hat{H} + [F + \alpha\hat{H}^{(1,0)} + \beta\hat{H}^{(0,1)} + \alpha\beta\hat{H}^{(1,1)}, T_2]|0\rangle \end{aligned} \tag{B.102}$$

with

$$\hat{H} = \hat{F} + \hat{V} + \alpha\hat{H}^{(1,0)} + \beta\hat{H}^{(0,1)} + \alpha\beta\hat{H}^{(1,1)}. \tag{B.103}$$

Here, α and β are the perturbation strengths, not the spin eigenfunctions.

Furthermore, we will assume that the first perturbation $H^{(1,0)}$, and therefore all operators appearing in amplitude and multiplier equations, to be spin-independent. This implies that the only non-zero amplitudes are $t_{a_\sigma}^{i_\sigma}$ and

$$t_{a_\sigma b_\tau}^{i_\sigma j_\tau} = -t_{a_\sigma b_\tau}^{j_\tau i_\sigma} = -t_{b_\tau a_\sigma}^{i_\sigma j_\tau} = t_{b_\tau a_\sigma}^{j_\tau i_\sigma}. \tag{B.104}$$

The equivalent holds for multipliers.
The use of dressed operators allows us to avoid having to explicitly consider unperturbed singles amplitudes when drawing diagrams (with some exceptions for energy and density matrix diagrams). Using

$$\frac{\partial}{\partial t_\mu} \exp(-T) H \exp(T) = \exp(-T)[H, \tau_\mu] \exp(T). \tag{B.105}$$

for the derivative of a similarity transformed operator we see that

$$\begin{aligned}\left[\frac{d}{d\alpha} \exp(-T) H \exp(T)\right]_{\alpha=0} =& \exp(-T^{(0,0)}) H^{(1,0)} \exp(T^{(0,0)}) \\ &+ \exp(-T^{(0,0)})[H^{(0,0)}, T^{(1,0)}] \exp(T^{(0,0)})\end{aligned} \tag{B.106}$$

with

$$H^{(1,0)} = \left.\frac{\partial H}{\partial \alpha}\right|_{\alpha=0} \tag{B.107}$$

$$T^{(1,0)} = \left.\frac{\partial T}{\partial \alpha}\right|_{\alpha=0} = \sum_\mu \left.\frac{\partial t_\mu}{\partial \alpha}\right|_{\alpha=0} \tau_\mu = \sum_\mu t_\mu^{(1,0)} \tau_\mu \tag{B.108}$$

Therefore, only the unperturbed singles contribute to the transformations (B.89) and (B.98).
We will have cause to simplify terms with three contractions between doubles amplitudes and multipliers

$$(\lambda_{\mu_2} t_{\mu_2})_{i_\sigma j_\sigma} = \sum_{\rho\zeta\tau} \lambda_{i_\sigma l_\rho}^{c_\tau d_\zeta} t_{c_\tau d_\zeta}^{j_\sigma l_\rho} \tag{B.109}$$

$$(\lambda_{\mu_2} t_{\mu_2})_{a_\sigma b_\sigma} = \sum_{\rho\zeta\tau} \lambda_{k_\tau l_\rho}^{a_\sigma d_\zeta} t_{b_\sigma d_\zeta}^{k_\tau l_\rho}. \tag{B.110}$$

Examining the first of these terms for the case of the α-spin, we have

$$(\lambda_{\mu_2} t_{\mu_2})_{i_\alpha j_\alpha} = \left(\lambda_{i_\alpha l_\alpha}^{c_\alpha d_\alpha} t_{c_\alpha d_\alpha}^{j_\alpha l_\alpha} + \lambda_{i_\alpha l_\beta}^{c_\alpha d_\beta} t_{c_\alpha d_\beta}^{j_\alpha l_\beta} + \lambda_{i_\alpha l_\beta}^{c_\beta d_\alpha} t_{c_\beta d_\alpha}^{j_\alpha l_\beta}\right) \tag{B.111}$$

$$= \left(\lambda_{i_\alpha l_\alpha}^{c_\alpha d_\alpha} t_{c_\alpha d_\alpha}^{j_\alpha l_\alpha} + 2\lambda_{i_\alpha l_\beta}^{c_\alpha d_\beta} t_{c_\alpha d_\beta}^{j_\alpha l_\beta}\right) \tag{B.112}$$

$$= \sum_\tau (2 - \delta_{\alpha\tau}) \lambda_{i_\alpha l_\tau}^{c_\alpha d_\tau} t_{c_\alpha d_\tau}^{j_\alpha l_\tau}. \tag{B.113}$$

We have used here the assumption that all operators are spin-independent to eliminate amplitudes that do not conserve the spin projection to arrive at (B.111) and have subsequently exploited the antisymmetry of the amplitudes and multipliers to simplify further

to (B.112). Generalizing this result, we arrive at

$$(\lambda_{\mu_2} t_{\mu_2})_{i_\sigma j_\sigma} = \sum_{\rho\zeta\tau} \lambda^{c_\tau d_\zeta}_{i_\sigma l_\rho} t^{j_\sigma l_\rho}_{c_\tau d_\zeta} = \sum_{\tau} (2 - \delta_{\sigma\tau}) \lambda^{c_\sigma d_\tau}_{i_\sigma l_\tau} t^{j_\sigma l_\tau}_{c_\sigma d_\tau} \tag{B.114}$$

$$(\lambda_{\mu_2} t_{\mu_2})_{a_\sigma b_\sigma} = \sum_{\rho\zeta\tau} \lambda^{a_\sigma d_\zeta}_{k_\tau l_\rho} t^{k_\tau l_\rho}_{b_\sigma d_\zeta} = \sum_{\tau} (2 - \delta_{\sigma\tau}) \lambda^{a_\sigma d_\tau}_{k_\sigma l_\tau} t^{k_\sigma l_\tau}_{b_\sigma d_\tau}. \tag{B.115}$$

A note on simplification of the subsequent diagram interpretations or lack thereof: the mathematically most simple representation of the equations is not necessarily the most efficient from an implementation perspective. Therefore, the "final" equations in this section will be given in a form convenient for reduction to the working equations, which will happen in the next section.
Finally, a warning to the interested reader: what follows is best described as "tedious but straightforward manipulation" and is included primarily as a resource for future work.

B.3.1.1 $E^{(0,0)}$

For the zeroth order CC2 energy equation, we have the contributions

$$E = \langle 0|\hat{H}^{(0,0)}|0\rangle \tag{B.116}$$

$$+ \langle 0|(\hat{H}^{(0,0)}_N T^{(0,0)}_2)_C|0\rangle. \tag{B.117}$$

Note that the operator in (B.116) is not normal ordered, meaning we include here the Hartree-Fock energy. However, the actual Hartree-Fock energy is obtained from undressed operators. Therefore, we rewrite the energy as

$$E = \langle 0|H^{(0,0)}|0\rangle \tag{B.118}$$

$$+ \langle 0|(F_N T^{(0,0)}_1)_C|0\rangle \tag{B.119}$$

$$+ \frac{1}{2}\langle 0|(V_N T^{(0,0)}_1 T^{(0,0)}_1)_C|0\rangle \tag{B.120}$$

$$+ \langle 0|(\hat{V}_N T^{(0,0)}_2)_C|0\rangle \tag{B.121}$$

where we have expanded the dressing of (B.116) and eliminated from (B.116) and (B.117) all terms that vanish due to impossibility of achieving a total excitation level of zero.
The first term (B.118) is just the unperturbed Hartree-Fock energy

$$E^{(0,0)}_{\mathrm{HF}} = \langle 0|H^{(0,0)}|0\rangle \tag{B.122}$$

and does not need to be considered further.
The second term (B.119) contributes the diagram

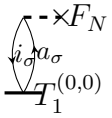

It evaluates to

$$\langle 0|(F_N T^{(0,0)}_1)_C|0\rangle = \sum_{\sigma} t^{i_\sigma\,(0,0)}_{a_\sigma} f_{i_\sigma a_\sigma}. \tag{B.123}$$

The third term (B.120) contributes the diagram

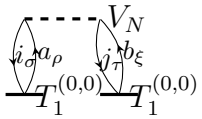

It evaluates to

$$\frac{1}{2}\langle 0|(V_N T_1^{(0,0)} T_1^{(0,0)})_C|0\rangle = \frac{1}{2}\sum_{\sigma\tau\rho\xi} t_{a_\rho}^{i_\sigma\,(0,0)} t_{b_\xi}^{j_\tau\,(0,0)} \Big(\delta_{\sigma\rho}\delta_{\tau\xi}\langle i_\sigma j_\tau|a_\rho b_\xi\rangle - \delta_{\sigma\rho}\delta_{\tau\xi}\langle i_\sigma j_\tau|b_\xi a_\rho\rangle \Big) \tag{B.124}$$

$$= \frac{1}{2}\sum_{\sigma\tau} \Big(t_{a_\sigma}^{i_\sigma\,(0,0)} t_{b_\tau}^{j_\tau\,(0,0)} \langle i_\sigma j_\tau|a_\sigma b_\tau\rangle - t_{a_\tau}^{i_\sigma\,(0,0)} t_{b_\sigma}^{j_\tau\,(0,0)} \langle i_\sigma j_\tau|b_\sigma a_\tau\rangle \Big) \tag{B.125}$$

$$= \frac{1}{2}\sum_{\sigma\tau} t_{a_\sigma}^{i_\sigma\,(0,0)} t_{b_\tau}^{j_\tau\,(0,0)} \langle i_\sigma j_\tau|a_\sigma b_\tau\rangle - \frac{1}{2}\sum_{\sigma} t_{a_\sigma}^{i_\sigma\,(0,0)} t_{b_\sigma}^{j_\sigma\,(0,0)} \langle i_\sigma j_\sigma|b_\sigma a_\sigma\rangle \tag{B.126}$$

where (B.125) follows from spin-integration of the two-electron integrals and (B.126) from spin-restriction of the amplitudes.
Finally, the last term (B.121) contributes the diagram

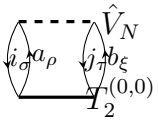

It evaluates to

$$\frac{1}{2}\langle 0|(V_N T_1^{(0,0)} T_1^{(0,0)})_C|0\rangle = \frac{1}{4}\sum_{\sigma\tau\rho\xi} t_{a_\rho b_\xi}^{i_\sigma j_\tau\,(0,0)} \Big(\delta_{\sigma\rho}\delta_{\tau\xi}\langle i_\sigma j_\tau|a_\rho b_\xi\rangle - \delta_{\sigma\rho}\delta_{\tau\xi}\langle i_\sigma j_\tau|b_\xi a_\rho\rangle \Big) \tag{B.127}$$

$$= \frac{1}{4}\sum_{\sigma\tau} t_{a_\rho b_\xi}^{i_\sigma j_\tau\,(0,0)} \Big(t_{a_\sigma b_\tau}^{i_\sigma j_\tau\,(0,0)} \langle i_\sigma j_\tau|a_\sigma b_\tau\rangle - t_{a_\tau b_\sigma}^{i_\sigma j_\tau\,(0,0)} \langle i_\sigma j_\tau|b_\sigma a_\tau\rangle \Big) \tag{B.128}$$

$$= \frac{1}{4}\sum_{\sigma\tau} \Big(t_{a_\sigma b_\tau}^{i_\sigma j_\tau\,(0,0)} \langle i_\sigma j_\tau|a_\sigma b_\tau\rangle - t_{b_\tau a_\sigma}^{i_\sigma j_\tau\,(0,0)} \langle i_\sigma j_\tau|a_\sigma b_\tau\rangle \Big) \tag{B.129}$$

$$= \frac{1}{2}\sum_{\sigma\tau} t_{a_\sigma b_\tau}^{i_\sigma j_\tau\,(0,0)} \langle i_\sigma j_\tau|a_\sigma b_\tau\rangle \tag{B.130}$$

where (B.128) follows from spin-integration of the two-electron integrals, (B.129) from renaming of indices and (B.130) from antisymmetry of the amplitudes.
Therefore, the zeroth order CC2 energy is

$$E_{\mathrm{CC2}}^{(0,0)} = E_{\mathrm{HF}}^{(0,0)} + \sum_{\sigma} t_{a_\sigma}^{i_\sigma\,(0,0)} f_{i_\sigma a_\sigma} + \frac{1}{2}\sum_{\sigma\tau} t_{a_\sigma}^{i_\sigma\,(0,0)} t_{b_\tau}^{j_\tau\,(0,0)} \langle i_\sigma j_\tau|a_\sigma b_\tau\rangle - \frac{1}{2}\sum_{\sigma} t_{a_\sigma}^{i_\sigma\,(0,0)} t_{b_\sigma}^{j_\sigma\,(0,0)} \langle i_\sigma j_\sigma|b_\sigma a_\sigma\rangle + \frac{1}{2}\sum_{\sigma\tau} t_{a_\sigma b_\tau}^{i_\sigma j_\tau\,(0,0)} \langle i_\sigma j_\tau|a_\sigma b_\tau\rangle. \tag{B.131}$$

Note that unlike for the dressed Fock matrix, the occupied-virtual block $f_{i_\sigma a_\sigma}$ of the undressed Fock matrix is zero if we are using a UHF reference function. Besides its importance for a semi-canonical ROHF reference function, the term also illustrates the similarity with higher order contributions.

B.3.1.2 $E^{(1,0)}$ and $E^{(1,1)}$

For the partial derivatives of the energy

$$E^{(1,0)} = \left.\frac{\partial E}{\partial \alpha}\right|_{\alpha,\beta=0} \tag{B.132}$$

$$E^{(1,1)} = \left.\frac{\partial^2 E}{\partial \alpha \partial \beta}\right|_{\alpha,\beta=0} \tag{B.133}$$

we have, except for interchange of the zeroth order Hamiltonian with the perturbed operators, the same terms as in (B.131). Since we assume a lack of two-electron perturbations, we have

$$E_{\mathrm{CC2}}^{(m,n)} = E_{\mathrm{HF}}^{(m,n)} + \sum_{\sigma} t_{a_\sigma}^{i_\sigma\,(0,0)} h_{i_\sigma a_\sigma}^{(m,n)}, \qquad (m,n) \in (1,0),(1,1) \tag{B.134}$$

where the Hartree-Fock contribution is simply

$$E_{\mathrm{HF}}^{(m,n)} = \langle 0|H^{(m,n)}|0\rangle. \tag{B.135}$$

B.3.1.3 $\eta_\nu^{(0,0)}$

The partial derivative of the energy with respect to the amplitudes is

$$\begin{aligned}\eta_\nu^{(0,0)} = \left.\frac{\partial E}{\partial t_\nu}\right|_{\alpha,\beta=0} = \begin{pmatrix}\eta_{\nu_1}^{(0,0)}\\ \eta_{\nu_2}^{(0,0)}\end{pmatrix} &= \begin{pmatrix}\langle 0|(\hat{H}_N^{(0,0)}\tau_{\nu_1})_C + (\hat{H}_N^{(0,0)}\tau_{\nu_1}T_2^{(0,0)})_C|0\rangle \\ \langle 0|(\hat{H}_N^{(0,0)}\tau_{\nu_2})_C|0\rangle\end{pmatrix} \\ &= \begin{pmatrix}\langle 0|(\hat{F}_N\tau_{\nu_1})_C|0\rangle \\ \langle 0|(\hat{V}_N\tau_{\nu_2})_C|0\rangle\end{pmatrix}\end{aligned} \tag{B.136}$$

Where the final equality follows from eliminating all terms that cannot be fully contracted. For the singles block, we get the diagram

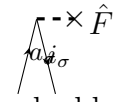

$$\eta_{i_\sigma}^{a_\sigma\,(0,0)} = \langle 0|(\hat{F}_N\tau_{i_\sigma}^{a_\sigma})_C||0\rangle = \hat{f}_{i_\sigma a_\sigma} \tag{B.137}$$

while the doubles block is

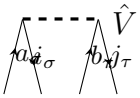

$$\begin{aligned}\eta_{i_\sigma j_\tau}^{a_\sigma b_\tau\,(0,0)} &= \langle 0|(\hat{V}_N\tau_{i_\sigma j_\tau}^{a_\sigma b_\tau})_C|0\rangle \\ &= \langle i_\sigma j_\tau|a_\sigma b_\tau\rangle - \delta_{\sigma\tau}\langle i_\sigma j_\tau|b_\tau a_\sigma\rangle.\end{aligned} \tag{B.138}$$

Note that the two-electron integrals are undressed in accordance with (B.93). Therefore, (B.136) reduces to

$$\eta_\nu^{(0,0)} = \begin{pmatrix}\eta_{i_\sigma}^{a_\sigma\,(0,0)} \\ \eta_{i_\sigma j_\tau}^{a_\sigma b_\tau\,(0,0)}\end{pmatrix} = \begin{pmatrix}\hat{f}_{i_\sigma a_\sigma} \\ \langle i_\sigma j_\tau|a_\sigma b_\tau\rangle - \delta_{\sigma\tau}\langle i_\sigma j_\sigma|b_\sigma a_\sigma\rangle\end{pmatrix}. \tag{B.139}$$

B.3.1.4 $\eta_\nu^{(1,0)}$

Since we assume all our perturbations to be one-electron perturbations, it is sufficient to examine the zeroth order diagrams. Higher order terms follow trivially by replacing the Fock integrals with the respective perturbation integrals and omitting all terms involving the two-electron integrals.

Therefore, the perturbed energy derivative is

$$\eta_\nu^{(1,0)} = \frac{\partial^2 E}{\partial\alpha\partial t_\nu}\bigg|_{\alpha,\beta=0} = \begin{pmatrix} \eta_{i_\sigma}^{a_\sigma\,(1,0)} \\ \eta_{i_\sigma j_\tau}^{a_\sigma b_\tau\,(1,0)} \end{pmatrix} = \begin{pmatrix} h_{i_\sigma a_\sigma}^{(1,0)} \\ 0 \end{pmatrix}. \tag{B.140}$$

Unlike the Fock integrals in the unperturbed case, the one-electron integrals are undressed here due to (B.92).

B.3.1.5 $\eta_\nu^{(0,1)} t_\nu^{(1,0)}$

The only contribution to the contraction of the perturbed energy derivative $\eta_\nu^{(0,1)}$ and the perturbed amplitudes $t_\nu^{(1,0)}$ for the case of exclusively one-electron perturbations is

$$\eta_{\nu_1}^{(0,1)} t_{\nu_1}^{(1,0)} = \langle 0|(\hat{H}_N^{(0,1)} T_1^{(1,0)})_C|0\rangle. \tag{B.141}$$

Except for the order of the amplitudes and operator as well as the dressing, this is identical to (B.123) and we have

$$\eta_{\nu_1}^{(0,1)} t_{\nu_1}^{(1,0)} = \sum_\sigma t_{a_\sigma}^{i_\sigma\,(1,0)} h_{i_\sigma a_\sigma}^{(0,1)}. \tag{B.142}$$

B.3.1.6 $\xi_{\nu\mu}^{(0,0)} t_\mu^{(1,0)}$

The second derivative of the energy with respect to the amplitudes is

$$\begin{aligned} \xi_{\nu\rho}^{(0,0)} =& \frac{\partial^2 E}{\partial t_\nu \partial t_\rho}\bigg|_{\alpha,\beta=0} = \frac{\partial \eta_\nu}{\partial t_\rho}\bigg|_{\alpha,\beta=0} \\ =& \begin{pmatrix} \langle 0|(\hat{H}_N^{(0,0)} \tau_{\nu_1}\tau_{\rho_1})_C|0\rangle & \langle 0|(\hat{H}_N^{(0,0)} \tau_{\nu_1}\tau_{\rho_2})_C|0\rangle \\ \langle 0|(\hat{H}_N^{(0,0)} \tau_{\nu_2}\tau_{\rho_1})_C|0\rangle & 0 \end{pmatrix} \\ =& \begin{pmatrix} \langle 0|(\hat{V}_N^{(0,0)} \tau_{\nu_1}\tau_{\rho_1})_C|0\rangle & 0 \\ 0 & 0 \end{pmatrix} \end{aligned} \tag{B.143}$$

with the last equality following from elimination of all terms that cannot be fully contracted. The only non-vanishing contribution is therefore the singles-singles block.
Since $\xi_{\nu\mu}$ only appears contracted with the amplitudes, we have to evaluate only the single diagram

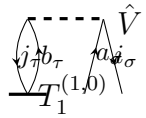

$$\begin{aligned} \left(\xi_{\nu_1\mu_1}{}^{(0,0)} t_{\mu_1}^{(1,0)}\right)_{i_\sigma}^{a_\sigma} &= \langle 0|(\hat{V}_N \tau_{i_\sigma}^{a_\sigma} T_1^{(1,0)})_C|0\rangle \\ &= \sum_\tau t_{b_\tau}^{j_\tau\,(1,0)} \langle i_\sigma j_\tau|a_\sigma b_\tau\rangle - t_{b_\sigma}^{j_\sigma\,(1,0)} \langle i_\sigma j_\sigma|b_\sigma a_\sigma\rangle \end{aligned} \tag{B.144}$$

B.3.1.7 $\Omega_\mu^{(0,0)}$

The zeroth order CC2 amplitude equations are

$$\begin{aligned} \Omega_\mu^{(0,0)} = \frac{\partial L}{\partial \lambda_\mu}\bigg|_{\alpha,\beta=0} = \begin{pmatrix} \Omega_{\mu_1}^{(0,0)} \\ \Omega_{\mu_2}^{(0,0)} \end{pmatrix} &= \begin{pmatrix} \langle \mu_1|\hat{H}_N^{(0,0)} + (\hat{H}_N^{(0,0)} T_2^{(0,0)})_C|0\rangle \\ \langle \mu_2|\hat{H}_N^{(0,0)} + (F_N T_2^{(0,0)})_C + |0\rangle \end{pmatrix} \\ &= \begin{pmatrix} \langle \mu_1|\hat{F}_N + (\hat{H}_N^{(0,0)} T_2^{(0,0)})_C|0\rangle \\ \langle \mu_2|\hat{V}_N + (F_N T_2^{(0,0)})_C|0\rangle \end{pmatrix}, \end{aligned} \tag{B.145}$$

where the second equality follows from eliminating terms that cannot yield the correct excitation level.

B.3.1.7.1 $\Omega_{\mu_1}^{(0,0)}$

The zeroth order singles block can be divided into three terms according to

$$\Omega_{i_\sigma}^{a_\sigma\,(0,0)} = \langle \phi_{i_\sigma}^{a_\sigma} | \hat{F}_N + (\hat{F}_N T_2^{(0,0)}) + (\hat{V}_N T_2^{(0,0)}) | 0 \rangle. \tag{B.146}$$

The first of these terms contributes the diagram

$$\langle \phi_{i_\sigma}^{a_\sigma} | \hat{F}_N | 0 \rangle = \hat{f}_{a_\sigma i_\sigma} \tag{B.147}$$

while the second term corresponds to

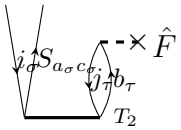

$$\langle \phi_{i_\sigma}^{a_\sigma} | (\hat{F}_N T_2^{(0,0)})_C | 0 \rangle = \sum_\tau S_{a_\sigma c_\sigma} t_{c_\sigma b_\tau}^{i_\sigma j_\tau\,(0,0)} \hat{f}_{j_\tau b_\tau}. \tag{B.148}$$

Finally, the third term contributes the two diagrams

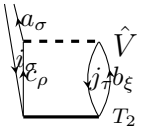

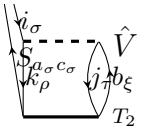

The first of these diagrams evaluates to

$$D1_{i_\sigma}^{a_\sigma} = \frac{1}{2} \sum_{\rho\tau\xi} t_{c_\rho b_\xi}^{i_\sigma j_\tau\,(0,0)} \Big(\delta_{\sigma\rho}\delta_{\tau\xi} \langle a_\sigma j_\tau | c_\rho b_\xi \rangle - \delta_{\sigma\xi}\delta_{\tau\rho} \langle a_\sigma j_\tau | b_\xi c_\rho \rangle \Big) \tag{B.149}$$

$$= \frac{1}{2} \sum_{\tau} \Big(t_{c_\sigma b_\tau}^{i_\sigma j_\tau\,(0,0)} \langle a_\sigma j_\tau | c_\sigma b_\tau \rangle - t_{c_\tau b_\sigma}^{i_\sigma j_\tau\,(0,0)} \langle a_\sigma j_\tau | b_\sigma c_\tau \rangle \Big) \tag{B.150}$$

$$= \frac{1}{2} \sum_{\tau} \Big(t_{c_\sigma b_\tau}^{i_\sigma j_\tau\,(0,0)} \langle a_\sigma j_\tau | c_\sigma b_\tau \rangle - t_{b_\tau c_\sigma}^{i_\sigma j_\tau\,(0,0)} \langle a_\sigma j_\tau | c_\sigma b_\tau \rangle \Big) \tag{B.151}$$

$$= \sum_{\tau} t_{c_\sigma b_\tau}^{i_\sigma j_\tau\,(0,0)} \langle a_\sigma j_\tau | c_\sigma b_\tau \rangle, \tag{B.152}$$

where (B.150) follows from spin-integration, (B.151) from renaming of the summation indices in the second term and (B.152) from antisymmetry of the amplitudes.
The second diagram evaluates to

$$D2_{i_\sigma}^{a_\sigma} = -\frac{1}{2} \sum_{\rho\tau\xi} S_{a_\sigma c_\sigma} t_{c_\sigma b_\tau}^{k_\rho j_\xi\,(0,0)} \Big(\delta_{\rho\sigma}\delta_{\tau\xi} \langle k_\rho j_\xi | i_\sigma b_\tau \rangle - \delta_{\rho\tau}\delta_{\sigma\xi} \langle k_\rho j_\xi | b_\tau i_\sigma \rangle \Big) \tag{B.153}$$

$$= -\frac{1}{2} \sum_{\tau} S_{a_\sigma c_\sigma} \Big(t_{c_\sigma b_\tau}^{k_\sigma j_\tau\,(0,0)} \langle k_\sigma j_\tau | i_\sigma b_\tau \rangle - t_{c_\sigma b_\tau}^{k_\tau j_\sigma\,(0,0)} \langle k_\tau j_\sigma | b_\tau i_\sigma \rangle \Big) \tag{B.154}$$

$$= -\frac{1}{2} \sum_{\tau} S_{a_\sigma c_\sigma} \Big(t_{c_\sigma b_\tau}^{k_\sigma j_\tau\,(0,0)} \langle k_\sigma j_\tau | i_\sigma b_\tau \rangle - t_{c_\sigma b_\tau}^{j_\tau k_\sigma\,(0,0)} \langle j_\tau k_\sigma | b_\tau i_\sigma \rangle \Big) \tag{B.155}$$

$$= -S_{a_\sigma c_\sigma} \sum_{\tau} t_{c_\sigma b_\tau}^{k_\sigma j_\tau\,(0,0)} \langle k_\sigma j_\tau | i_\sigma b_\tau \rangle \tag{B.156}$$

where (B.154) follows from spin-integration, (B.155) from renaming of the summation indices in the second term and (B.156) from antisymmetry of the amplitudes and the symmetry of the two-electron integrals.

Combining (B.152) and (B.156), we arrive at

$$\langle\phi_{i_\sigma}^{a_\sigma}|(\hat{V}_N T_2^{(0,0)})|0\rangle. = \sum_\tau t_{c_\sigma b_\tau}^{i_\sigma j_\tau\,(0,0)} \langle a_\sigma j_\tau \hat{|} c_\sigma b_\tau\rangle - S_{a_\sigma c_\sigma} \sum_\tau t_{c_\sigma b_\tau}^{k_\sigma j_\tau\,(0,0)} \langle k_\sigma j_\tau \hat{|} i_\sigma b_\tau\rangle. \tag{B.157}$$

Finally, the zeroth order singles amplitude equations (B.146) are therefore

$$\begin{aligned}\Omega_{i_\sigma}^{a_\sigma\,(0,0)} &= \hat{f}_{a_\sigma i_\sigma} + \sum_\tau S_{a_\sigma c_\sigma} t_{c_\sigma b_\tau}^{i_\sigma j_\tau\,(0,0)} \hat{f}_{j_\tau b_\tau} \\ &+ \sum_\tau t_{c_\sigma b_\tau}^{i_\sigma j_\tau\,(0,0)} \langle a_\sigma j_\tau \hat{|} c_\sigma b_\tau\rangle - S_{a_\sigma c_\sigma} \sum_\tau t_{c_\sigma b_\tau}^{k_\sigma j_\tau\,(0,0)} \langle k_\sigma j_\tau \hat{|} i_\sigma b_\tau\rangle.\end{aligned} \tag{B.158}$$

B.3.1.7.2 $\Omega_{\mu_2}^{(0,0)}$

The first term of the doubles block of (B.145) is represented by the diagram

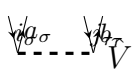

$$\langle\phi_{i_\sigma j_\tau}^{a_\sigma b_\tau}|\hat{V}_N|0\rangle = \langle a_\sigma b_\tau \hat{|} i_\sigma j_\tau\rangle - \delta_{\sigma\tau}\langle a_\sigma b_\sigma \hat{|} j_\sigma i_\sigma\rangle \tag{B.159}$$

while the second term contributes the two diagrams

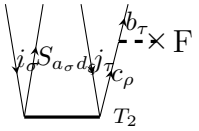

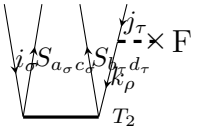

The first of these diagrams evaluates to

$$\begin{aligned}D1_{i_\sigma j_\tau}^{a_\sigma b_\tau} =& \sum_{\xi\rho} P(a_\sigma, b_\tau) S_{a_\sigma d_\xi} t_{d_\xi c_\rho}^{i_\sigma j_\tau\,(0,0)} f_{b_\tau c_\rho} && \text{(B.160)}\\ =& \sum_{\xi\rho} \left(S_{a_\sigma d_\xi} t_{d_\xi c_\rho}^{i_\sigma j_\tau\,(0,0)} f_{b_\tau c_\rho} - f_{a_\sigma c_\rho} t_{d_\xi c_\rho}^{i_\sigma j_\tau\,(0,0)} S_{b_\tau d_\xi} \right) && \text{(B.161)}\\ =& S_{a_\sigma d_\sigma} t_{d_\sigma c_\tau}^{i_\sigma j_\tau\,(0,0)} f_{b_\tau c_\tau} - f_{a_\sigma c_\sigma} t_{d_\tau c_\sigma}^{i_\sigma j_\tau\,(0,0)} S_{b_\tau d_\tau} && \text{(B.162)}\\ =& S_{a_\sigma d_\sigma} t_{d_\sigma c_\tau}^{i_\sigma j_\tau\,(0,0)} f_{b_\tau c_\tau} - f_{a_\sigma d_\sigma} t_{c_\tau d_\sigma}^{i_\sigma j_\tau\,(0,0)} S_{b_\tau c_\tau} && \text{(B.163)}\\ =& S_{a_\sigma d_\sigma} t_{d_\sigma c_\tau}^{i_\sigma j_\tau\,(0,0)} f_{b_\tau c_\tau} + f_{a_\sigma d_\sigma} t_{d_\sigma c_\tau}^{i_\sigma j_\tau\,(0,0)} S_{b_\tau c_\tau} && \text{(B.164)}\end{aligned}$$

where (B.161) follows from resolution of the permutation operator, (B.162) from spin-integration, (B.163) from renaming of summation indices and (B.164) from antisymmetry of the amplitudes.
The second diagram evaluates to

$$\begin{aligned}D2_{i_\sigma j_\tau}^{a_\sigma b_\tau} =& -\sum_\rho P(i_\sigma, j_\tau) S_{a_\sigma c_\sigma} S_{b_\tau d_\tau} t_{i_\sigma k_\rho}^{c_\sigma d_\tau\,(0,0)} f_{k_\rho j_\tau} && \text{(B.165)}\\ =& -\sum_\rho S_{a_\sigma c_\sigma} S_{b_\tau d_\tau} \left(t_{i_\sigma k_\rho}^{c_\sigma d_\tau\,(0,0)} f_{k_\rho j_\tau} - f_{k_\rho i_\sigma} t_{j_\tau k_\rho}^{c_\sigma d_\tau\,(0,0)} \right) && \text{(B.166)}\\ =& -S_{a_\sigma c_\sigma} S_{b_\tau d_\tau} \left(t_{i_\sigma k_\tau}^{c_\sigma d_\tau\,(0,0)} f_{k_\tau j_\tau} - f_{k_\sigma i_\sigma} t_{j_\tau k_\sigma}^{c_\sigma d_\tau\,(0,0)} \right) && \text{(B.167)}\\ =& -S_{a_\sigma c_\sigma} S_{b_\tau d_\tau} \left(t_{i_\sigma k_\tau}^{c_\sigma d_\tau\,(0,0)} f_{k_\tau j_\tau} + f_{k_\sigma i_\sigma} t_{k_\sigma j_\tau}^{c_\sigma d_\tau\,(0,0)} \right) && \text{(B.168)}\end{aligned}$$

where (B.166) follows from resolution of the permutation operator, (B.167) from spin-integration and (B.168) from antisymmetry of the amplitudes.
Combining (B.164) and (B.168) we get the contribution

$$\begin{aligned}\langle \phi^{a_\sigma b_\tau}_{i_\sigma j_\tau} | (F_N T_2^{(0,0)})_C | 0 \rangle =& S_{a_\sigma d_\sigma} t^{i_\sigma j_\tau\,(0,0)}_{d_\sigma c_\tau} f_{b_\tau c_\tau} + f_{a_\sigma d_\sigma} t^{i_\sigma j_\tau\,(0,0)}_{d_\sigma c_\tau} S_{b_\tau c_\tau} \\ & - S_{a_\sigma c_\sigma} t^{c_\sigma d_\tau\,(0,0)}_{i_\sigma k_\tau} S_{b_\tau d_\tau} f_{k_\tau j_\tau} - f_{k_\sigma i_\sigma} S_{a_\sigma c_\sigma} t^{c_\sigma d_\tau\,(0,0)}_{k_\sigma j_\tau} S_{b_\tau d_\tau}. \end{aligned} \tag{B.169}$$

The unperturbed doubles amplitude equations are therefore

$$\begin{aligned}\Omega^{a_\sigma b_\tau\,(0,0)}_{i_\sigma j_\tau} =& \langle a_\sigma b_\tau | \hat{i}_\sigma j_\tau \rangle - \delta_{\sigma\tau} \langle a_\sigma b_\sigma | \hat{j}_\sigma i_\sigma \rangle \\ & + S_{a_\sigma d_\sigma} t^{i_\sigma j_\tau\,(0,0)}_{d_\sigma c_\tau} f_{b_\tau c_\tau} + f_{a_\sigma d_\sigma} t^{i_\sigma j_\tau\,(0,0)}_{d_\sigma c_\tau} S_{b_\tau c_\tau} \\ & - S_{a_\sigma c_\sigma} t^{c_\sigma d_\tau\,(0,0)}_{i_\sigma k_\tau} S_{b_\tau d_\tau} f_{k_\tau j_\tau} - f_{k_\sigma i_\sigma} S_{a_\sigma c_\sigma} t^{c_\sigma d_\tau\,(0,0)}_{k_\sigma j_\tau} S_{b_\tau d_\tau}. \end{aligned} \tag{B.170}$$

B.3.1.8 $\Omega^{(1,0)}_\mu$

The partial derivative of the CC2 amplitude equations with respect to the first perturbation is

$$\begin{aligned}\Omega^{(1,0)}_\mu =& \left.\frac{\partial^2 L}{\partial\alpha \partial\lambda_\mu}\right|_{\alpha,\beta=0} = \left.\frac{\partial \Omega_\mu}{\partial\alpha}\right|_{\alpha,\beta=0} = \begin{pmatrix} \Omega^{(1,0)}_{\mu_1} \\ \Omega^{(1,0)}_{\mu_2} \end{pmatrix} \\ =& \begin{pmatrix} \langle \mu_1 | \hat{H}^{(1,0)}_N + (\hat{H}^{(1,0)}_N T_2^{(0,0)})_C | 0 \rangle \\ \langle \mu_2 | \hat{H}^{(1,0)}_N + (\hat{H}^{(1,0)}_N T_2^{(0,0)})_C + |0\rangle \end{pmatrix} \\ =& \begin{pmatrix} \langle \mu_1 | \hat{H}^{(1,0)}_N + (\hat{H}^{(1,0)}_N T_2^{(0,0)})_C | 0 \rangle \\ \langle \mu_2 | (\hat{H}^{(1,0)}_N T_2^{(0,0)})_C | 0 \rangle \end{pmatrix}, \end{aligned} \tag{B.171}$$

where we have again eliminated all terms that cannot yield the correct excitation level. Recall that we assume the perturbation to consist of one-electron operators only. Aside from dressing of the operator in the doubles amplitude equations we can again reuse the diagrams for the unperturbed case. We simply have to discard terms containing two-electron integrals in (B.158) and (B.170) and replace the dressed and undressed Fock integrals with the dressed perturbation integrals.
The partial derivative of the singles equations is therefore

$$\Omega^{a_\sigma\,(1,0)}_{i_\sigma} = \hat{h}^{(1,0)}_{a_\sigma i_\sigma} + \sum_\tau S_{a_\sigma c_\sigma} t^{i_\sigma j_\tau\,(0,0)}_{c_\sigma b_\tau} h^{(1,0)}_{j_\tau b_\tau} \tag{B.172}$$

whereas for the doubles equations we have

$$\begin{aligned}\Omega^{a_\sigma b_\tau\,(1,0)}_{i_\sigma j_\tau} =& S_{a_\sigma d_\sigma} t^{i_\sigma j_\tau\,(0,0)}_{d_\sigma c_\tau} \hat{h}^{(1,0)}_{b_\tau c_\tau} + \hat{h}^{(1,0)}_{a_\sigma d_\sigma} t^{i_\sigma j_\tau\,(0,0)}_{d_\sigma c_\tau} S_{b_\tau c_\tau} \\ & - S_{a_\sigma c_\sigma} t^{c_\sigma d_\tau\,(0,0)}_{i_\sigma k_\tau} S_{b_\tau d_\tau} \hat{h}^{(1,0)}_{k_\tau j_\tau} - \hat{h}^{(1,0)}_{k_\sigma i_\sigma} S_{a_\sigma c_\sigma} t^{c_\sigma d_\tau\,(0,0)}_{k_\sigma j_\tau} S_{b_\tau d_\tau}. \end{aligned} \tag{B.173}$$

Note that these are not the complete perturbed amplitude equations, but only the part independent of the perturbed amplitudes $t^{(1,0)}_\mu$.

B.3.1.9 $\lambda^{(0,0)}_\mu \Omega^{(1,0)}_\mu$, $\lambda^{(0,0)}_\mu \Omega^{(1,1)}_\mu$ and $\lambda^{(1,0)}_\mu \Omega^{(0,1)}_\mu$

Since we assume that singly perturbed as well as doubly perturbed operators are one-electron operators and conserve the spin-projection, it is sufficient to only examine one

case for the contraction of the multipliers with the Ω-equations (e.g. $\lambda_\mu^{(0,0)}\Omega_\mu^{(1,0)}$). The remaining cases follow from changing the orders of the multipliers and integrals.
The contraction of the partial derivative of the perturbed singles and doubles amplitude equations with the multipliers consists of three contributions

$$\lambda_\mu^{(0,0)}\Omega_\mu^{(1,0)} = \lambda_{\mu_1}\langle\mu_1|\hat{H}^{(1,0)}|0\rangle \tag{B.174}$$
$$+ \lambda_{\mu_1}\langle\mu_1|(\hat{H}^{(1,0)}T_2^{(0,0)})_C|0\rangle \tag{B.175}$$
$$+ \lambda_{\mu_2}\langle\mu_2|(\hat{H}^{(1,0)}T_2^{(0,0)})_C|0\rangle. \tag{B.176}$$

The first term (B.174) corresponds to the diagram

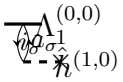

and evaluates to

$$\lambda_{\mu_1}\langle\mu_1|\hat{H}^{(1,0)}|0\rangle = \sum_\sigma \lambda_{i_\sigma}^{a_\sigma\,(0,0)}\hat{h}_{a_\sigma i_\sigma}. \tag{B.177}$$

The second term (B.175) yields the diagram

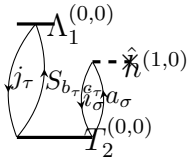

and evaluates to

$$\lambda_{\mu_1}\langle\mu_1|(\hat{H}^{(1,0)}T_2^{(0,0)})_C|0\rangle = \sum_{\sigma\tau}\lambda_{j_\tau}^{b_\tau\,(0,0)}S_{b_\tau c_\tau}t_{j_\tau i_\sigma}^{c_\tau a_\sigma\,(0,0)}h_{i_\sigma a_\sigma}^{(1,0)}. \tag{B.178}$$

The last term (B.176) yields the two diagrams

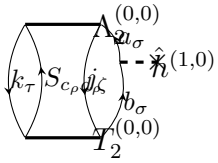

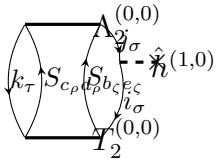

The first of these evaluates to

$$D1 = \frac{1}{2}\sum_{\substack{\sigma\tau\\ \rho\zeta}}\lambda_{k_\tau j_\zeta}^{c_\rho a_\sigma\,(0,0)}S_{c_\rho d_\rho}t_{d_\rho b_\sigma}^{k_\tau j_\zeta\,(0,0)}\hat{h}_{a_\sigma b_\sigma}^{(1,0)} \tag{B.179}$$
$$= \frac{1}{2}\sum_{\sigma\tau}(2-\delta_{\sigma\tau})\lambda_{k_\tau j_\sigma}^{c_\tau a_\sigma\,(0,0)}S_{c_\tau d_\tau}t_{d_\tau b_\sigma}^{k_\tau j_\sigma\,(0,0)}\hat{h}_{a_\sigma b_\sigma}^{(1,0)}. \tag{B.180}$$

where (B.180) follows from (B.115).
The second diagram evaluates to

$$D2 = -\frac{1}{2}\sum_{\substack{\sigma\tau\\ \rho\zeta}}\lambda_{k_\tau j_\sigma}^{c_\rho b_\zeta\,(0,0)}S_{c_\rho d_\rho}S_{b_\zeta e_\zeta}t_{d_\rho e_\zeta}^{k_\tau i_\sigma\,(0,0)}\hat{h}_{i_\sigma j_\sigma}^{(1,0)} \tag{B.181}$$
$$= -\frac{1}{2}\sum_{\sigma\tau}(2-\delta_{\sigma\tau})\lambda_{k_\tau j_\sigma}^{c_\tau b_\sigma\,(0,0)}S_{c_\tau d_\tau}S_{b_\sigma e_\sigma}t_{d_\tau e_\sigma}^{k_\tau i_\sigma\,(0,0)}\hat{h}_{i_\sigma j_\sigma}^{(1,0)} \tag{B.182}$$

where (B.182) follows from (B.114).
The complete contraction is therefore

$$\begin{aligned}\lambda_{\mu}^{(0,0)}\Omega_{\mu}^{(1,0)} =& \sum_{\sigma} \lambda_{i_\sigma}^{a_\sigma\,(0,0)} \hat{h}_{a_\sigma i_\sigma} + \sum_{\sigma\tau} \lambda_{j_\tau}^{b_\tau\,(0,0)} S_{b_\tau c_\tau} t_{j_\tau i_\sigma}^{c_\tau a_\sigma\,(0,0)} h_{i_\sigma a_\sigma}^{(1,0)} \\ &+ \sum_{\sigma\tau} (1 - \frac{\delta_{\sigma\tau}}{2}) \Bigg(\lambda_{k_\tau j_\sigma}^{c_\tau a_\sigma\,(0,0)} S_{c_\tau d_\tau} t_{d_\tau b_\sigma}^{k_\tau j_\sigma\,(0,0)} \hat{h}_{a_\sigma b_\sigma}^{(1,0)} \\ &- \lambda_{k_\tau j_\sigma}^{c_\tau b_\sigma\,(0,0)} S_{c_\tau d_\tau} S_{b_\sigma e_\sigma} t_{d_\tau e_\sigma}^{k_\tau i_\sigma\,(0,0)} \hat{h}_{i_\sigma j_\sigma}^{(1,0)} \Bigg). \end{aligned} \tag{B.183}$$

B.3.1.10 $A_{\mu\nu}^{(0,0)}$

The zeroth order Jacobian is the derivative of the amplitude equations with respect to the amplitudes

$$A_{\mu\nu}^{(0,0)} = \frac{\partial^2 L}{\partial\lambda_\mu \partial t_\nu}\bigg|_{\alpha,\beta=0} = \frac{\partial \Omega_\mu}{\partial t_\nu}\bigg|_{\alpha,\beta=0} = \begin{pmatrix} A_{\mu_1\nu_1}^{(0,0)} & A_{\mu_1\nu_2}^{(0,0)} \\ A_{\mu_2\nu_1}^{(0,0)} & A_{\mu_2\nu_2}^{(0,0)} \end{pmatrix}. \tag{B.184}$$

The four blocks of the Jacobian are

$$\begin{aligned} A_{\mu_1\nu_1}^{(0,0)} = \frac{\partial \Omega_{\mu_1}}{\partial t_{\nu_1}}\bigg|_{\alpha,\beta=0} =& \langle\mu_1|(\hat{H}_N^{(0,0)}\tau_{\nu_1})_C + (\hat{H}_N^{(0,0)}\tau_{\nu_1}T_2^{(0,0)})_C|0\rangle \\ =& \langle\mu_1|(\hat{H}_N^{(0,0)}\tau_{\nu_1})_C + (\hat{V}_N\tau_{\nu_1}T_2^{(0,0)})_C|0\rangle \end{aligned} \tag{B.185}$$

$$A_{\mu_2\nu_1}^{(0,0)} = \frac{\partial \Omega_{\mu_2}}{\partial t_{\nu_1}}\bigg|_{\alpha,\beta=0} = \langle\mu_2|(\hat{H}_N^{(0,0)}\tau_{\nu_1})_C|0\rangle = \langle\mu_2|(\hat{V}_N\tau_{\nu_1})_C|0\rangle \tag{B.186}$$

$$A_{\mu_1\nu_2}^{(0,0)} = \frac{\partial \Omega_{\mu_1}}{\partial t_{\nu_2}}\bigg|_{\alpha,\beta=0} = \langle\mu_1|(\hat{H}_N^{(0,0)}\tau_{\nu_2})_C|0\rangle \tag{B.187}$$

$$A_{\mu_2\nu_2}^{(0,0)} = \frac{\partial \Omega_{\mu_2}}{\partial t_{\nu_2}}\bigg|_{\alpha,\beta=0} = \langle\mu_2|(F_N\tau_{\nu_2})_C|0\rangle. \tag{B.188}$$

The second equality in (B.185) is due to the impossibility of compensating the excitation level of the substitution operators with the Fock operator. Elimination of the Fock operator in (B.186) follows from the connectivity requirement.

B.3.1.11 $\lambda_{\mu}^{(0,0)} A_{\mu\nu}^{(0,0)}$

B.3.1.11.1 $\lambda_{\mu_1}^{(0,0)} A_{\mu_1\nu_1}^{(0,0)}$

Contraction of the singles-singles block (B.185) of the Jacobian with the zeroth order singles multipliers contributes three terms

$$\left(\lambda_{\mu_1}^{(0,0)} A_{\mu_1\nu_1}^{(0,0)}\right)_{i_\sigma}^{a_\sigma} = \lambda_{\mu_1}^{(0,0)} \langle\mu_1|(\hat{F}_N^{(0,0)}\tau_{i_\sigma}^{a_\sigma})_C|0\rangle \tag{B.189}$$

$$+ \lambda_{\mu_1}^{(0,0)} \langle\mu_1|(\hat{V}_N^{(0,0)}\tau_{i_\sigma}^{a_\sigma})_C|0\rangle \tag{B.190}$$

$$+ \lambda_{\mu_1}^{(0,0)} \langle\mu_1|(\hat{V}_N\tau_{i_\sigma}^{a_\sigma}T_2^{(0,0)})_C|0\rangle \tag{B.191}$$

The first of these is represented by the two diagrams

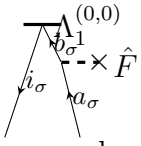

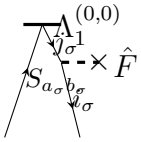

The first diagram evaluates to

$$D1_{i_\sigma}^{a_\sigma} = \lambda_{i_\sigma}^{b_\sigma (0,0)} \hat{f}_{b_\sigma a_\sigma} \tag{B.192}$$

whereas the second results in

$$D2_{i_\sigma}^{a_\sigma} = -\hat{f}_{i_\sigma j_\sigma} \lambda_{j_\sigma}^{b_\sigma (0,0)} S_{b_\sigma a_\sigma} \tag{B.193}$$

giving for the entire term

$$\lambda_{\mu_1}^{(0,0)} \langle \mu_1 | (\hat{F}_N^{(0,0)} \tau_{i_\sigma}^{a_\sigma})_C | 0 \rangle = \lambda_{i_\sigma}^{b_\sigma (0,0)} \hat{f}_{b_\sigma a_\sigma} - \hat{f}_{i_\sigma j_\sigma} \lambda_{j_\sigma}^{b_\sigma (0,0)} S_{b_\sigma a_\sigma}. \tag{B.194}$$

The second term (B.190) contributes the diagram

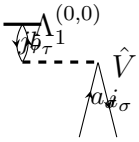

$$\lambda_{\mu_1}^{(0,0)} \langle \mu_1 | (\hat{V}_N^{(0,0)} \tau_{i_\sigma}^{a_\sigma})_C = \sum_\tau \lambda_{j_\tau}^{b_\tau (0,0)} \langle b_\tau i_\sigma | \hat{j_\tau a_\sigma} \rangle - \lambda_{j_\sigma}^{b_\sigma (0,0)} \langle b_\sigma i_\sigma | \hat{a_\sigma j_\sigma} \rangle. \tag{B.195}$$

Finally, (B.191) yields the three diagrams

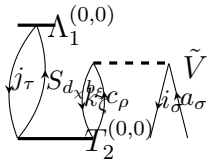

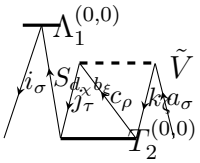

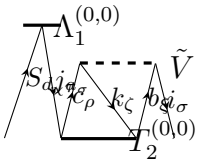

The first of these evaluates to

$$\begin{aligned} D1_{i_\sigma}^{a_\sigma} &= \sum_{\tau\xi\chi} S_{d_\chi b_\xi} \lambda_{j_\tau}^{d_\chi (0,0)} \Bigg(\sum_{\zeta\rho} t_{b_\xi c_\rho}^{j_\tau k_\zeta (0,0)} \delta_{\zeta\rho} \langle k_\zeta i_\sigma | c_\rho a_\sigma \rangle \\ &\quad - \sum_{\zeta\rho} t_{b_\xi c_\rho}^{j_\tau k_\zeta (0,0)} \delta_{\zeta\sigma} \delta_{\sigma\rho} \langle k_\zeta i_\sigma | a_\sigma c_\rho \rangle \Bigg) \qquad \text{(B.196)} \\ &= \sum_{\tau\xi\chi} S_{d_\chi b_\xi} \lambda_{j_\tau}^{d_\chi (0,0)} \Bigg(\sum_{\rho} t_{b_\xi c_\rho}^{j_\tau k_\rho (0,0)} \langle k_\rho i_\sigma | c_\rho a_\sigma \rangle - t_{b_\xi c_\sigma}^{j_\tau k_\sigma (0,0)} \langle k_\sigma i_\sigma | a_\sigma c_\sigma \rangle \Bigg) \qquad \text{(B.197)} \\ &= \sum_{\tau} S_{d_\tau b_\tau} \lambda_{j_\tau}^{d_\tau (0,0)} \Bigg(\sum_{\rho} t_{b_\tau c_\rho}^{j_\tau k_\rho (0,0)} \langle k_\rho i_\sigma | c_\rho a_\sigma \rangle - t_{b_\tau c_\sigma}^{j_\tau k_\sigma (0,0)} \langle k_\sigma i_\sigma | a_\sigma c_\sigma \rangle \Bigg) \qquad \text{(B.198)} \end{aligned}$$

where (B.197) follows from spin-integration of the two-electron integrals and (B.198) from spin-integration of overlap and multipliers.

The second diagram yields

$$D2_{i_\sigma}^{a_\sigma} = \frac{1}{2}\sum_{\xi\chi} S_{d_\chi b_\xi} \lambda_{i_\sigma}^{d_\chi(0,0)} \sum_{\rho\tau\zeta} \Big(t_{b_\xi c_\rho}^{j_\tau k_\zeta(0,0)} \delta_{\tau\rho}\delta_{\zeta\sigma} \langle j_\tau k_\zeta | c_\rho a_\sigma\rangle$$
$$- t_{b_\xi c_\rho}^{j_\tau k_\zeta(0,0)} \delta_{\tau\sigma}\delta_{\zeta\rho} \langle j_\tau k_\zeta | a_\sigma c_\rho\rangle \Big) \tag{B.199}$$
$$= \frac{1}{2}\sum_{\xi\chi} S_{d_\chi b_\xi} \lambda_{i_\sigma}^{d_\chi(0,0)} \sum_{\rho} \left(t_{b_\xi c_\rho}^{j_\rho k_\sigma(0,0)} \langle j_\rho k_\sigma | c_\rho a_\sigma\rangle - t_{b_\xi c_\rho}^{j_\sigma k_\rho(0,0)} \langle j_\sigma k_\rho | a_\sigma c_\rho\rangle \right) \tag{B.200}$$
$$= \frac{1}{2} S_{d_\sigma b_\sigma} \lambda_{i_\sigma}^{d_\sigma(0,0)} \sum_{\rho} \left(t_{b_\sigma c_\rho}^{j_\rho k_\sigma(0,0)} \langle j_\rho k_\sigma | c_\rho a_\sigma\rangle - t_{b_\sigma c_\rho}^{j_\sigma k_\rho(0,0)} \langle j_\sigma k_\rho | a_\sigma c_\rho\rangle \right) \tag{B.201}$$
$$= \frac{1}{2} S_{d_\sigma b_\sigma} \lambda_{i_\sigma}^{d_\sigma(0,0)} \sum_{\rho} \left(t_{b_\sigma c_\rho}^{k_\rho j_\sigma(0,0)} \langle k_\rho j_\sigma | c_\rho a_\sigma\rangle - t_{b_\sigma c_\rho}^{j_\sigma k_\rho(0,0)} \langle j_\sigma k_\rho | a_\sigma c_\rho\rangle \right) \tag{B.202}$$
$$= - S_{d_\sigma b_\sigma} \lambda_{i_\sigma}^{d_\sigma(0,0)} \sum_{\rho} t_{b_\sigma c_\rho}^{j_\sigma k_\rho(0,0)} \langle j_\sigma k_\rho | a_\sigma c_\rho\rangle \tag{B.203}$$

where (B.200) follows from spin-integration of the two-electron integrals, (B.201) from spin-integration of overlap and multipliers, (B.202) from renaming of indices and (B.203) from antisymmetry of the amplitudes and symmetry of the two-electron integrals.
The last diagram evaluates to

$$D3_{i_\sigma}^{a_\sigma} = \frac{1}{2}\sum_{\tau\chi} S_{d_\chi a_\sigma} \lambda_{j_\tau}^{d_\chi(0,0)} \sum_{\xi\zeta\rho} \Big(t_{c_\rho b_\xi}^{j_\tau k_\zeta(0,0)} \delta_{\zeta\rho}\delta_{\sigma\xi} \langle k_\zeta i_\sigma | c_\rho b_\xi\rangle$$
$$- t_{c_\rho b_\xi}^{j_\tau k_\zeta(0,0)} \delta_{\zeta\xi}\delta_{\sigma\rho} \langle k_\zeta i_\sigma | b_\xi c_\rho\rangle \Big) \tag{B.204}$$
$$= \frac{1}{2}\sum_{\tau\chi} S_{d_\chi a_\sigma} \lambda_{j_\tau}^{d_\chi(0,0)} \sum_{\zeta} \left(t_{c_\zeta b_\sigma}^{j_\tau k_\zeta(0,0)} \langle k_\zeta i_\sigma | c_\zeta b_\sigma\rangle - t_{c_\sigma b_\zeta}^{j_\tau k_\zeta(0,0)} \langle k_\zeta i_\sigma | b_\zeta c_\sigma\rangle \right) \tag{B.205}$$
$$= \frac{1}{2} S_{d_\sigma a_\sigma} \lambda_{j_\sigma}^{d_\sigma(0,0)} \sum_{\zeta} \left(t_{c_\zeta b_\sigma}^{j_\sigma k_\zeta(0,0)} \langle k_\zeta i_\sigma | c_\zeta b_\sigma\rangle - t_{c_\sigma b_\zeta}^{j_\sigma k_\zeta(0,0)} \langle k_\zeta i_\sigma | b_\zeta c_\sigma\rangle \right) \tag{B.206}$$
$$= \frac{1}{2} S_{d_\sigma a_\sigma} \lambda_{j_\sigma}^{d_\sigma(0,0)} \sum_{\zeta} \left(t_{c_\zeta b_\sigma}^{j_\sigma k_\zeta(0,0)} \langle k_\zeta i_\sigma | c_\zeta b_\sigma\rangle - t_{b_\sigma c_\zeta}^{j_\sigma k_\zeta(0,0)} \langle k_\zeta i_\sigma | c_\zeta b_\sigma\rangle \right) \tag{B.207}$$
$$= - S_{d_\sigma a_\sigma} \lambda_{j_\sigma}^{d_\sigma(0,0)} \sum_{\zeta} t_{b_\sigma c_\zeta}^{j_\sigma k_\zeta(0,0)} \langle k_\zeta i_\sigma | c_\zeta b_\sigma\rangle \tag{B.208}$$

where (B.205) follows from spin-integration of the two-electron integrals, (B.206) from spin-integration of overlap and multipliers, (B.207) from renaming of indices and (B.208) from antisymmetry of the amplitudes.
Combining the three diagrams (B.198), (B.203) and (B.208) gives us for (B.191)

$$\lambda_{\mu_1}^{(0,0)} \langle \mu_1 | (\hat{V}_N \tau_{i_\sigma}^{a_\sigma} T_2^{(0,0)})_C | 0\rangle = \sum_{\tau} S_{d_\tau b_\tau} \lambda_{j_\tau}^{d_\tau(0,0)} \Big(\sum_{\rho} t_{b_\tau c_\rho}^{j_\tau k_\rho(0,0)} \langle k_\rho i_\sigma | c_\rho a_\sigma\rangle$$
$$- t_{b_\tau c_\sigma}^{j_\tau k_\sigma(0,0)} \langle k_\sigma i_\sigma | a_\sigma c_\sigma\rangle \Big) - S_{d_\sigma b_\sigma} \lambda_{i_\sigma}^{d_\sigma(0,0)} \sum_{\tau} t_{b_\sigma c_\tau}^{j_\sigma k_\tau(0,0)} \langle j_\sigma k_\tau | a_\sigma c_\tau\rangle$$
$$- S_{d_\sigma a_\sigma} \lambda_{j_\sigma}^{d_\sigma(0,0)} \sum_{\tau} t_{b_\sigma c_\tau}^{j_\sigma k_\tau(0,0)} \langle k_\tau i_\sigma | c_\tau b_\sigma\rangle \tag{B.209}$$

where we have standardized all sums over spin to use the same index when possible. Therefore, the complete singles-singles block contracted with the singles multipliers is

$$\begin{aligned}\left(\lambda^{(0,0)}_{\mu_1} A^{(0,0)}_{\mu_1\nu_1}\right)^{a_\sigma}_{i_\sigma} &= \lambda^{b_\sigma\,(0,0)}_{i_\sigma}\hat{f}_{b_\sigma a_\sigma} - \hat{f}_{i_\sigma j_\sigma}\lambda^{b_\sigma\,(0,0)}_{j_\sigma} S_{b_\sigma a_\sigma} \\ &+ \sum_\tau \lambda^{b_\tau\,(0,0)}_{j_\tau}\langle b_\tau i_\sigma|\hat{}|j_\tau a_\sigma\rangle - \lambda^{b_\sigma\,(0,0)}_{j_\sigma}\langle b_\sigma i_\sigma|\hat{}|a_\sigma j_\sigma\rangle \\ &+ \sum_\tau S_{d_\tau b_\tau}\lambda^{d_\tau\,(0,0)}_{j_\tau}\left(\sum_\rho t^{j_\tau k_\rho\,(0,0)}_{b_\tau c_\rho}\langle k_\rho i_\sigma|c_\rho a_\sigma\rangle - t^{j_\tau k_\sigma\,(0,0)}_{b_\tau c_\sigma}\langle k_\sigma i_\sigma|a_\sigma c_\sigma\rangle\right) \\ &- S_{d_\sigma b_\sigma}\lambda^{d_\sigma\,(0,0)}_{i_\sigma}\sum_\tau t^{j_\sigma k_\tau\,(0,0)}_{b_\sigma c_\tau}\langle j_\sigma k_\tau|a_\sigma c_\tau\rangle \\ &- S_{d_\sigma a_\sigma}\lambda^{d_\sigma\,(0,0)}_{j_\sigma}\sum_\tau t^{j_\sigma k_\tau\,(0,0)}_{b_\sigma c_\tau}\langle k_\tau i_\sigma|c_\tau b_\sigma\rangle. \end{aligned} \tag{B.210}$$

B.3.1.11.2 $\lambda^{(0,0)}_{\mu_2} A^{(0,0)}_{\mu_2\nu_1}$

Contraction of the doubles-singles block (B.186) of the zeroth order Jacobian with the zeroth order singles multipliers contributes only a single set of diagrams

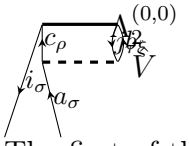

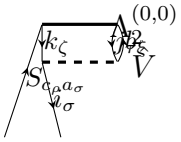

The first of these evaluates to

$$D1^{a_\sigma}_{i_\sigma} = \frac{1}{2}\sum_{\tau\xi\rho}\left(\delta_{\sigma\rho}\delta_{\tau\xi}\lambda^{c_\rho b_\xi\,(0,0)}_{i_\sigma j_\tau}\langle c_\rho b_\xi|\hat{}|a_\sigma j_\tau\rangle - \delta_{\sigma\xi}\delta_{\tau\rho}\lambda^{c_\rho b_\xi\,(0,0)}_{i_\sigma j_\tau}\langle c_\rho b_\xi|\hat{}|j_\tau a_\sigma\rangle\right) \tag{B.211}$$

$$= \frac{1}{2}\sum_{\tau}\left(\lambda^{c_\sigma b_\tau\,(0,0)}_{i_\sigma j_\tau}\langle c_\sigma b_\tau|\hat{}|a_\sigma j_\tau\rangle - \lambda^{c_\tau b_\sigma\,(0,0)}_{i_\sigma j_\tau}\langle c_\tau b_\sigma|\hat{}|j_\tau a_\sigma\rangle\right) \tag{B.212}$$

$$= \frac{1}{2}\sum_{\tau}\left(\lambda^{c_\sigma b_\tau\,(0,0)}_{i_\sigma j_\tau}\langle c_\sigma b_\tau|\hat{}|a_\sigma j_\tau\rangle - \lambda^{b_\tau c_\sigma\,(0,0)}_{i_\sigma j_\tau}\langle b_\tau c_\sigma|\hat{}|j_\tau a_\sigma\rangle\right) \tag{B.213}$$

$$= \sum_{\tau}\lambda^{c_\sigma b_\tau\,(0,0)}_{i_\sigma j_\tau}\langle c_\sigma b_\tau|\hat{}|a_\sigma j_\tau\rangle \tag{B.214}$$

where (B.212) follows from spin-integration of the two-electron integrals, (B.213) from renaming of indices and (B.214) from antisymmetry of the multipliers and symmetry of the two-electron integrals.
The second diagram yields

$$D2^{a_\sigma}_{i_\sigma} = -\frac{1}{2}\sum_{\tau\xi\rho\zeta} S_{c_\rho a_\sigma}\left(\delta_{\sigma\zeta}\delta_{\tau\xi}\lambda^{c_\rho b_\xi\,(0,0)}_{k_\zeta j_\tau}\langle i_\sigma b_\xi|\hat{}|k_\zeta j_\tau\rangle - \delta_{\sigma\tau}\delta_{\xi\zeta}\lambda^{c_\rho b_\xi\,(0,0)}_{k_\zeta j_\tau}\langle i_\sigma b_\xi|\hat{}|j_\tau k_\zeta\rangle\right) \tag{B.215}$$

$$= -\frac{1}{2}S_{c_\sigma a_\sigma}\left(\sum_\tau \lambda^{c_\sigma b_\tau\,(0,0)}_{k_\sigma j_\tau}\langle i_\sigma b_\tau|\hat{}|k_\sigma j_\tau\rangle - \sum_\zeta \lambda^{c_\sigma b_\zeta\,(0,0)}_{k_\zeta j_\sigma}\langle i_\sigma b_\zeta|\hat{}|j_\sigma k_\zeta\rangle\right) \tag{B.216}$$

$$= -\frac{1}{2}S_{c_\sigma a_\sigma}\sum_\tau\left(\lambda^{c_\sigma b_\tau\,(0,0)}_{k_\sigma j_\tau}\langle i_\sigma b_\tau|\hat{}|k_\sigma j_\tau\rangle - \lambda^{c_\sigma b_\tau\,(0,0)}_{j_\tau k_\sigma}\langle i_\sigma b_\tau|\hat{}|k_\sigma j_\tau\rangle\right) \tag{B.217}$$

$$= -S_{c_\sigma a_\sigma}\sum_\tau \lambda^{c_\sigma b_\tau\,(0,0)}_{k_\sigma j_\tau}\langle i_\sigma b_\tau|\hat{}|k_\sigma j_\tau\rangle \tag{B.218}$$

where (B.216) follows from spin-integration of the two-electron integrals and the overlap, (B.217) from renaming of indices and (B.218) from antisymmetry of the multipliers. Therefore, the contraction of the zeroth order doubles multipliers with the zeroth order doubles-singles block of the Jacobian is simply

$$\left(\lambda^{(0,0)}_{\mu_2} A^{(0,0)}_{\mu_2\nu_1}\right)^{a_\sigma}_{i_\sigma} = \sum_\tau \lambda^{c_\sigma b_\tau\,(0,0)}_{i_\sigma j_\tau} \hat{\langle} c_\sigma b_\tau | a_\sigma j_\tau \rangle - S_{c_\sigma a_\sigma} \sum_\tau \lambda^{c_\sigma b_\tau\,(0,0)}_{k_\sigma j_\tau} \hat{\langle} i_\sigma b_\tau | k_\sigma j_\tau \rangle. \tag{B.219}$$

B.3.1.11.3 $\lambda^{(0,0)}_{\mu_1} A^{(0,0)}_{\mu_1\nu_2}$

For contraction of the zeroth order singles multipliers with the singles-doubles block (B.187) of the zeroth order Jacobian we have to consider two contributions

$$\left(\lambda^{(0,0)}_{\mu_1} A^{(0,0)}_{\mu_1\nu_2}\right)^{a_\sigma b_\tau}_{i_\sigma j_\tau} = \lambda^{(0,0)}_{\mu_1} \langle \mu_1 | (\hat{F}^{(0,0)}_N \tau^{a_\sigma b_\tau}_{i_\sigma j_\tau})_C | 0 \rangle \tag{B.220}$$

$$+ \lambda^{(0,0)}_{\mu_1} \langle \mu_1 | (\hat{V}^{(0,0)}_N \tau^{a_\sigma b_\tau}_{i_\sigma j_\tau})_C | 0 \rangle. \tag{B.221}$$

Recall that the connectivity requirement only holds for amplitudes. Therefore, the first of these terms yields the disconnected diagram

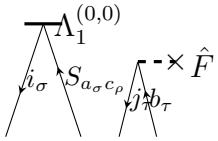

It evaluates to

$$\lambda_{\mu_1} \langle \mu_1 | (\hat{F}_N \tau^{a_\sigma b_\tau}_{i_\sigma j_\tau})_C | 0 \rangle = P(i_\sigma, j_\tau) P(a_\sigma, b_\tau) \tilde{f}_{j_\tau b_\tau} \sum_\rho S_{c_\rho a_\sigma} \lambda^{c_\rho\,(0,0)}_{i_\sigma} \tag{B.222}$$

$$= \hat{f}_{j_\tau b_\tau} \sum_\rho S_{c_\rho a_\sigma} \lambda^{c_\rho\,(0,0)}_{i_\sigma} + \hat{f}_{i_\sigma a_\sigma} \sum_\rho S_{c_\rho b_\tau} \lambda^{c_\rho\,(0,0)}_{j_\tau}$$

$$- \hat{f}_{j_\tau a_\sigma} \sum_\rho S_{c_\rho b_\tau} \lambda^{c_\rho\,(0,0)}_{i_\sigma} - \hat{f}_{i_\sigma b_\tau} \sum_\rho S_{c_\rho a_\sigma} \lambda^{c_\rho\,(0,0)}_{j_\tau} \tag{B.223}$$

$$= \hat{f}_{j_\tau b_\tau} S_{c_\sigma a_\sigma} \lambda^{c_\sigma\,(0,0)}_{i_\sigma} + \hat{f}_{i_\sigma a_\sigma} S_{c_\tau b_\tau} \lambda^{c_\tau\,(0,0)}_{j_\tau}$$

$$- \delta_{\sigma\tau} \hat{f}_{j_\sigma a_\sigma} S_{c_\sigma b_\sigma} \lambda^{c_\sigma\,(0,0)}_{i_\sigma} - \delta_{\sigma\tau} \hat{f}_{i_\sigma b_\sigma} S_{c_\sigma a_\sigma} \lambda^{c_\sigma\,(0,0)}_{j_\sigma} \tag{B.224}$$

where (B.223) follows from application of the permutation operators and (B.224) from spin-integration.
The second term (B.221) yields the diagrams

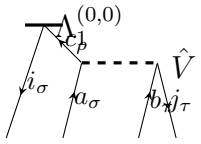

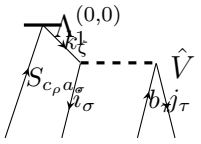

The first diagram evaluates to

$$D1^{a_\sigma b_\tau}_{i_\sigma j_\tau} = P(i_\sigma, j_\tau) \sum_\rho \lambda^{c_\rho\,(0,0)}_{i_\sigma} \Big(\langle c_\rho j_\tau \hat{|} a_\sigma b_\tau \rangle - \langle c_\rho j_\tau \hat{|} b_\tau a_\sigma \rangle \Big) \tag{B.225}$$

$$= \sum_\rho \lambda^{c_\rho\,(0,0)}_{i_\sigma} \Big(\delta_{\rho\sigma} \langle c_\rho j_\tau \hat{|} a_\sigma b_\tau \rangle - \delta_{\rho\tau}\delta_{\tau\sigma} \langle c_\rho j_\tau \hat{|} b_\tau a_\sigma \rangle \Big)$$

$$- \sum_\rho \lambda^{c_\rho\,(0,0)}_{j_\tau} \Big(\delta_{\rho\sigma}\delta_{\sigma\tau} \langle c_\rho i_\sigma \hat{|} a_\sigma b_\tau \rangle - \delta_{\rho\tau} \langle c_\rho i_\sigma \hat{|} b_\tau a_\sigma \rangle \Big) \tag{B.226}$$

$$= \lambda^{c_\sigma\,(0,0)}_{i_\sigma} \langle c_\sigma j_\tau \hat{|} a_\sigma b_\tau \rangle - \delta_{\sigma\tau} \lambda^{c_\sigma\,(0,0)}_{i_\sigma} \langle c_\sigma j_\sigma \hat{|} b_\sigma a_\sigma \rangle$$

$$- \delta_{\sigma\tau} \lambda^{c_\sigma\,(0,0)}_{j_\sigma} \langle c_\sigma i_\sigma \hat{|} a_\sigma b_\sigma \rangle + \lambda^{c_\tau\,(0,0)}_{j_\tau} \langle c_\tau i_\sigma \hat{|} b_\tau a_\sigma \rangle \tag{B.227}$$

where (B.226) follows from application of the permutation operator and (B.227) from spin-integration.
The second diagram evaluates to

$$D2^{a_\sigma b_\tau}_{i_\sigma j_\tau} = - P(a_\sigma, b_\tau) \sum_{\rho\zeta} S_{c_\rho a_\sigma} \lambda^{c_\rho\,(0,0)}_{k_\zeta} \Big(\langle i_\sigma j_\tau \hat{|} k_\zeta b_\tau \rangle - \langle i_\sigma j_\tau \hat{|} b_\tau k_\zeta \rangle \Big) \tag{B.228}$$

$$= - \sum_{\rho\zeta} S_{c_\rho a_\sigma} \lambda^{c_\rho\,(0,0)}_{k_\zeta} \Big(\delta_{\sigma\zeta} \langle i_\sigma j_\tau \hat{|} k_\zeta b_\tau \rangle - \delta_{\sigma\tau}\delta_{\tau\zeta} \langle i_\sigma j_\tau \hat{|} b_\tau k_\zeta \rangle \Big)$$

$$+ \sum_{\rho\zeta} S_{c_\rho b_\tau} \lambda^{c_\rho\,(0,0)}_{k_\zeta} \Big(\delta_{\sigma\zeta}\delta_{\tau\sigma} \langle i_\sigma j_\tau \hat{|} k_\zeta a_\sigma \rangle - \delta_{\tau\zeta} \langle i_\sigma j_\tau \hat{|} a_\sigma k_\zeta \rangle \Big) \tag{B.229}$$

$$= - S_{c_\sigma a_\sigma} \lambda^{c_\sigma\,(0,0)}_{k_\sigma} \langle i_\sigma j_\tau \hat{|} k_\sigma b_\tau \rangle + \delta_{\sigma\tau} S_{c_\sigma a_\sigma} \lambda^{c_\sigma\,(0,0)}_{k_\sigma} \langle i_\sigma j_\sigma \hat{|} b_\sigma k_\sigma \rangle$$

$$+ \delta_{\sigma\tau} S_{c_\sigma b_\sigma} \lambda^{c_\sigma\,(0,0)}_{k_\sigma} \langle i_\sigma j_\sigma \hat{|} k_\sigma a_\sigma \rangle - S_{c_\tau b_\tau} \lambda^{c_\tau\,(0,0)}_{k_\tau} \langle i_\sigma j_\tau \hat{|} a_\sigma k_\tau \rangle \tag{B.230}$$

where (B.229) follows from application of the permutation operator and (B.230) from spin-integration.
Combining these diagrams, we get for (B.221)

$$\begin{aligned} \lambda^{(0,0)}_{\mu_1} \langle \mu_1 | (\hat{V}^{(0,0)}_N \tau^{a_\sigma b_\tau}_{i_\sigma j_\tau})_C | 0 \rangle = {} & \lambda^{c_\sigma\,(0,0)}_{i_\sigma} \langle c_\sigma j_\tau \hat{|} a_\sigma b_\tau \rangle - \delta_{\sigma\tau} \lambda^{c_\sigma\,(0,0)}_{i_\sigma} \langle c_\sigma j_\sigma \hat{|} b_\sigma a_\sigma \rangle \\ & - \delta_{\sigma\tau} \lambda^{c_\sigma\,(0,0)}_{j_\sigma} \langle c_\sigma i_\sigma \hat{|} a_\sigma b_\sigma \rangle + \lambda^{c_\tau\,(0,0)}_{j_\tau} \langle c_\tau i_\sigma \hat{|} b_\tau a_\sigma \rangle \\ & - S_{c_\sigma a_\sigma} \lambda^{c_\sigma\,(0,0)}_{k_\sigma} \langle i_\sigma j_\tau \hat{|} k_\sigma b_\tau \rangle + \delta_{\sigma\tau} S_{c_\sigma a_\sigma} \lambda^{c_\sigma\,(0,0)}_{k_\sigma} \langle i_\sigma j_\sigma \hat{|} b_\sigma k_\sigma \rangle \\ & + \delta_{\sigma\tau} S_{c_\sigma b_\sigma} \lambda^{c_\sigma\,(0,0)}_{k_\sigma} \langle i_\sigma j_\sigma \hat{|} k_\sigma a_\sigma \rangle - S_{c_\tau b_\tau} \lambda^{c_\tau\,(0,0)}_{k_\tau} \langle i_\sigma j_\tau \hat{|} a_\sigma k_\tau \rangle \end{aligned} \tag{B.231}$$

The complete contraction of singles multipliers with the singles-doubles block of the zeroth order Jacobian is therefore

$$\begin{aligned} \Big(\lambda^{(0,0)}_{\mu_1} A^{(0,0)}_{\mu_1 \nu_2} \Big)^{a_\sigma b_\tau}_{i_\sigma j_\tau} = {} & \hat{f}_{j_\tau b_\tau} S_{c_\sigma a_\sigma} \lambda^{c_\sigma\,(0,0)}_{i_\sigma} + \hat{f}_{i_\sigma a_\sigma} S_{c_\tau b_\tau} \lambda^{c_\tau\,(0,0)}_{j_\tau} \\ & - \delta_{\sigma\tau} \hat{f}_{j_\sigma a_\sigma} S_{c_\sigma b_\sigma} \lambda^{c_\sigma\,(0,0)}_{i_\sigma} - \delta_{\sigma\tau} \hat{f}_{i_\sigma b_\sigma} S_{c_\sigma a_\sigma} \lambda^{c_\sigma\,(0,0)}_{j_\sigma} \\ & + \lambda^{c_\sigma\,(0,0)}_{i_\sigma} \langle c_\sigma j_\tau \hat{|} a_\sigma b_\tau \rangle - \delta_{\sigma\tau} \lambda^{c_\sigma\,(0,0)}_{i_\sigma} \langle c_\sigma j_\sigma \hat{|} b_\sigma a_\sigma \rangle \\ & - \delta_{\sigma\tau} \lambda^{c_\sigma\,(0,0)}_{j_\sigma} \langle c_\sigma i_\sigma \hat{|} a_\sigma b_\sigma \rangle + \lambda^{c_\tau\,(0,0)}_{j_\tau} \langle c_\tau i_\sigma \hat{|} b_\tau a_\sigma \rangle \\ & - S_{c_\sigma a_\sigma} \lambda^{c_\sigma\,(0,0)}_{k_\sigma} \langle i_\sigma j_\tau \hat{|} k_\sigma b_\tau \rangle + \delta_{\sigma\tau} S_{c_\sigma a_\sigma} \lambda^{c_\sigma\,(0,0)}_{k_\sigma} \langle i_\sigma j_\sigma \hat{|} b_\sigma k_\sigma \rangle \\ & + \delta_{\sigma\tau} S_{c_\sigma b_\sigma} \lambda^{c_\sigma\,(0,0)}_{k_\sigma} \langle i_\sigma j_\sigma \hat{|} k_\sigma a_\sigma \rangle - S_{c_\tau b_\tau} \lambda^{c_\tau\,(0,0)}_{k_\tau} \langle i_\sigma j_\tau \hat{|} a_\sigma k_\tau \rangle. \end{aligned} \tag{B.232}$$

B.3.1.11.4 $\lambda^{(0,0)}_{\mu_2} A^{(0,0)}_{\mu_2\nu_2}$

Contraction of the doubles-doubles block (B.188) of the zeroth order Jacobian with the zeroth order doubles multipliers contributes only a single set of diagrams

The first diagram evaluates to

$$
\begin{aligned}
D1^{a_\sigma b_\tau}_{i_\sigma j_\tau} =& P(a_\sigma, b_\tau) \sum_{\rho\xi} S_{c_\rho a_\sigma} \lambda^{c_\rho d_\xi\,(0,0)}_{i_\sigma j_\tau} f_{d_\xi b_\tau} && \text{(B.233)}\\
=& \sum_{\rho\xi} S_{c_\rho a_\sigma} \lambda^{c_\rho d_\xi\,(0,0)}_{i_\sigma j_\tau} f_{d_\xi b_\tau} - \sum_{\rho\xi} S_{c_\rho b_\tau} \lambda^{c_\rho d_\xi\,(0,0)}_{i_\sigma j_\tau} f_{d_\xi a_\sigma} && \text{(B.234)}\\
=& S_{c_\sigma a_\sigma} \lambda^{c_\sigma d_\tau\,(0,0)}_{i_\sigma j_\tau} f_{d_\tau b_\tau} - S_{c_\tau b_\tau} \lambda^{c_\tau d_\sigma\,(0,0)}_{i_\sigma j_\tau} f_{d_\sigma a_\sigma} && \text{(B.235)}\\
=& S_{c_\sigma a_\sigma} \lambda^{c_\sigma d_\tau\,(0,0)}_{i_\sigma j_\tau} f_{d_\tau b_\tau} + S_{c_\tau b_\tau} \lambda^{d_\sigma c_\tau\,(0,0)}_{i_\sigma j_\tau} f_{d_\sigma a_\sigma} && \text{(B.236)}\\
=& S_{c_\sigma a_\sigma} \lambda^{c_\sigma d_\tau\,(0,0)}_{i_\sigma j_\tau} f_{d_\tau b_\tau} + f_{c_\sigma a_\sigma} \lambda^{c_\sigma d_\tau\,(0,0)}_{i_\sigma j_\tau} S_{d_\tau b_\tau} && \text{(B.237)}
\end{aligned}
$$

where (B.234) follows from application of the permutation operator, (B.235) from spin-integration, (B.236) from antisymmetry of the multipliers and (B.237) from renaming of indices.

The second diagram evaluates to

$$
\begin{aligned}
D2^{a_\sigma b_\tau}_{i_\sigma j_\tau} =& - P(i_\sigma, j_\tau) \sum_{\rho\xi\zeta} S_{c_\rho a_\sigma} \lambda^{c_\rho d_\xi\,(0,0)}_{i_\sigma k_\zeta} S_{d_\xi b_\tau} f_{j_\tau k_\zeta} && \text{(B.238)}\\
=& \sum_{\rho\xi\zeta} -S_{c_\rho a_\sigma} \lambda^{c_\rho d_\xi\,(0,0)}_{i_\sigma k_\zeta} S_{d_\xi b_\tau} f_{j_\tau k_\zeta} + \sum_{\rho\xi\zeta} S_{c_\rho a_\sigma} \lambda^{c_\rho d_\xi\,(0,0)}_{j_\tau k_\zeta} S_{d_\xi b_\tau} f_{i_\sigma k_\zeta} && \text{(B.239)}\\
=& - S_{c_\sigma a_\sigma} \lambda^{c_\sigma d_\tau\,(0,0)}_{i_\sigma k_\tau} S_{d_\tau b_\tau} f_{j_\tau k_\tau} + S_{c_\sigma a_\sigma} \lambda^{c_\sigma d_\tau\,(0,0)}_{j_\tau k_\sigma} S_{d_\tau b_\tau} f_{i_\sigma k_\sigma} && \text{(B.240)}\\
=& - S_{c_\sigma a_\sigma} \lambda^{c_\sigma d_\tau\,(0,0)}_{i_\sigma k_\tau} S_{d_\tau b_\tau} f_{j_\tau k_\tau} - S_{c_\sigma a_\sigma} \lambda^{c_\sigma d_\tau\,(0,0)}_{k_\sigma j_\tau} S_{d_\tau b_\tau} f_{i_\sigma k_\sigma} && \text{(B.241)}
\end{aligned}
$$

where (B.239) follows from application of the permutation operator, (B.240) from spin-integration and (B.241) from antisymmetry of the multipliers.

Thus, the complete contraction of the zeroth order doubles multipliers with the zeroth order doubles-doubles block of the Jacobian is

$$
\begin{aligned}
\left(\lambda^{(0,0)}_{\mu_2} A^{(0,0)}_{\mu_2\nu_2}\right)^{a_\sigma b_\tau}_{i_\sigma j_\tau} =& S_{c_\sigma a_\sigma} \lambda^{c_\sigma d_\tau\,(0,0)}_{i_\sigma j_\tau} f_{d_\tau b_\tau} + f_{c_\sigma a_\sigma} \lambda^{c_\sigma d_\tau\,(0,0)}_{i_\sigma j_\tau} S_{d_\tau b_\tau}\\
& - S_{c_\sigma a_\sigma} \lambda^{c_\sigma d_\tau\,(0,0)}_{i_\sigma k_\tau} S_{d_\tau b_\tau} f_{j_\tau k_\tau} - S_{c_\sigma a_\sigma} \lambda^{c_\sigma d_\tau\,(0,0)}_{k_\sigma j_\tau} S_{d_\tau b_\tau} f_{i_\sigma k_\sigma}. && \text{(B.242)}
\end{aligned}
$$

B.3.1.12 $\lambda^{(1,0)}_{\mu} A^{(0,0)}_{\mu\nu}$

Contraction of the zeroth order Jacobian with perturbed multipliers is trivially obtained by simply substituting all zeroth order multipliers $\lambda^{(0,0)}_{\mu}$ in (B.210), (B.219), (B.232) and (B.242) with the first order multipliers $\lambda^{(1,0)}_{\mu}$.

B.3.1.13 $A^{(0,0)}_{\mu\nu} t^{(1,0)}_{\nu}$

B.3.1.13.1 $A^{(0,0)}_{\mu_1\nu_1} t^{(1,0)}_{\nu_1}$

Contraction of the singles-singles block (B.185) of the Jacobian with the perturbed singles

amplitudes contributes three terms

$$\left(A^{(0,0)}_{\mu_1\nu_1}t^{(1,0)}_{\nu_1}\right)^{a_\sigma}_{i_\sigma} = \langle\phi^{a_\sigma}_{i_\sigma}|(\hat{F}^{(0,0)}_N T^{(1,0)}_1)_C|0\rangle \tag{B.243}$$

$$+ \langle\phi^{a_\sigma}_{i_\sigma}|(\hat{V}^{(0,0)}_N T^{(1,0)}_1)_C|0\rangle \tag{B.244}$$

$$+ \langle\phi^{a_\sigma}_{i_\sigma}|(\hat{V}_N T^{(1,0)}_1 T^{(0,0)}_2)_C|0\rangle. \tag{B.245}$$

The first of these is represented by the two diagrams

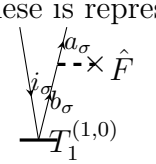

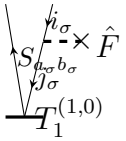

The first diagram evaluates to

$$D1^{a_\sigma}_{i_\sigma} = t^{i_\sigma\,(1,0)}_{b_\sigma}\hat{f}_{a_\sigma b_\sigma} \tag{B.246}$$

whereas the second results in

$$D2^{a_\sigma}_{i_\sigma} = -\,S_{a_\sigma b_\sigma}t^{j_\sigma\,(1,0)}_{b_\sigma}\hat{f}_{j_\sigma i_\sigma} \tag{B.247}$$

giving for the entire term

$$\langle\phi^{a_\sigma}_{i_\sigma}|(\hat{F}^{(0,0)}_N T^{(1,0)}_1)_C|0\rangle = t^{i_\sigma\,(1,0)}_{b_\sigma}\hat{f}_{a_\sigma b_\sigma} - S_{a_\sigma b_\sigma}t^{j_\sigma\,(1,0)}_{b_\sigma}\hat{f}_{j_\sigma i_\sigma}. \tag{B.248}$$

The second term (B.244) contributes the diagram

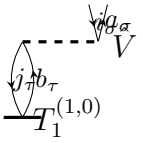

$$\langle\phi^{a_\sigma}_{i_\sigma}|(\hat{V}^{(0,0)}_N T^{(1,0)}_1)_C|0\rangle = \sum_\tau t^{j_\tau\,(1,0)}_{b_\tau}\langle j_\tau a_\sigma|\hat{b_\tau i_\sigma}\rangle - t^{j_\sigma\,(1,0)}_{b_\sigma}\langle j_\sigma a_\sigma|\hat{i_\sigma b_\sigma}\rangle. \tag{B.249}$$

Finally, (B.245) yields the three diagrams

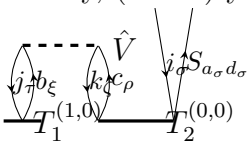

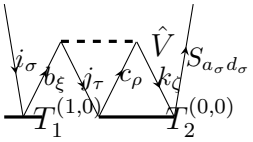

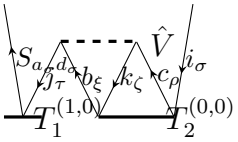

The first of these evaluates to

$$D1^{a_\sigma}_{i_\sigma} = S_{a_\sigma d_\sigma}\sum_{\tau\xi\zeta\rho}\Big(t^{j_\tau\,(1,0)}_{b_\xi}t^{k_\zeta i_\sigma\,(0,0)}_{c_\rho d_\sigma}\delta_{\tau\xi}\delta_{\zeta\rho}\langle j_\tau k_\zeta|b_\xi c_\rho\rangle$$

$$- t^{j_\tau\,(1,0)}_{b_\xi}t^{k_\zeta i_\sigma\,(0,0)}_{c_\rho d_\sigma}\delta_{\tau\rho}\delta_{\zeta\xi}\langle j_\tau k_\zeta|c_\rho b_\xi\rangle\Big) \tag{B.250}$$

$$= S_{a_\sigma d_\sigma}\sum_{\tau\zeta}\left(t^{j_\tau\,(1,0)}_{b_\tau}t^{k_\zeta i_\sigma\,(0,0)}_{c_\zeta d_\sigma}\langle j_\tau k_\zeta|b_\tau c_\zeta\rangle - t^{j_\tau\,(1,0)}_{b_\zeta}t^{k_\zeta i_\sigma\,(0,0)}_{c_\tau d_\sigma}\langle j_\tau k_\zeta|c_\tau b_\zeta\rangle\right) \tag{B.251}$$

$$= S_{a_\sigma d_\sigma}\sum_{\tau} t^{j_\tau\,(1,0)}_{b_\tau}\left(\sum_\zeta t^{k_\zeta i_\sigma\,(0,0)}_{c_\zeta d_\sigma}\langle j_\tau k_\zeta|b_\tau c_\zeta\rangle - t^{k_\tau i_\sigma\,(0,0)}_{c_\tau d_\sigma}\langle j_\tau k_\tau|c_\tau b_\tau\rangle\right) \tag{B.252}$$

where (B.251) follows from spin-integration of the two-electron integrals and (B.252) from spin-integration of the singles amplitudes.

The second diagram yields

$$
\begin{aligned}
D2_{i_\sigma}^{a_\sigma} =& \frac{1}{2} S_{a_\sigma d_\sigma} \sum_{\tau\xi\zeta\rho} (t_{b_\xi}^{i_\sigma\,(1,0)} t_{c_\rho d_\sigma}^{j_\tau k_\zeta\,(0,0)} \delta_{\tau\xi}\delta_{\zeta\rho} \langle j_\tau k_\zeta | b_\xi c_\rho\rangle \\
& - t_{b_\xi}^{i_\sigma\,(1,0)} t_{c_\rho d_\sigma}^{j_\tau k_\zeta\,(0,0)} \delta_{\tau\rho}\delta_{\zeta\xi} \langle j_\tau k_\zeta | c_\rho b_\xi\rangle) && \text{(B.253)} \\
=& \frac{1}{2} S_{a_\sigma d_\sigma} \sum_{\tau\zeta} \left(t_{b_\tau}^{i_\sigma\,(1,0)} t_{c_\zeta d_\sigma}^{j_\tau k_\zeta\,(0,0)} \langle j_\tau k_\zeta | b_\tau c_\zeta\rangle - t_{b_\zeta}^{i_\sigma\,(1,0)} t_{c_\tau d_\sigma}^{j_\tau k_\zeta\,(0,0)} \langle j_\tau k_\zeta | c_\tau b_\zeta\rangle \right) && \text{(B.254)} \\
=& \frac{1}{2} S_{a_\sigma d_\sigma} t_{b_\sigma}^{i_\sigma\,(1,0)} \left(\sum_{\zeta} t_{c_\zeta d_\sigma}^{j_\sigma k_\zeta\,(0,0)} \langle j_\sigma k_\zeta | b_\sigma c_\zeta\rangle - \sum_{\tau} t_{c_\tau d_\sigma}^{j_\tau k_\sigma\,(0,0)} \langle j_\tau k_\sigma | c_\tau b_\sigma\rangle \right) && \text{(B.255)} \\
=& \frac{1}{2} S_{a_\sigma d_\sigma} \sum_{\tau} t_{b_\sigma}^{i_\sigma\,(1,0)} \left(t_{c_\tau d_\sigma}^{j_\sigma k_\tau\,(0,0)} \langle j_\sigma k_\tau | b_\sigma c_\tau\rangle - t_{c_\tau d_\sigma}^{j_\tau k_\sigma\,(0,0)} \langle j_\tau k_\sigma | c_\tau b_\sigma\rangle \right) && \text{(B.256)} \\
=& \frac{1}{2} S_{a_\sigma d_\sigma} \sum_{\tau} t_{b_\sigma}^{i_\sigma\,(1,0)} \left(t_{c_\tau d_\sigma}^{j_\sigma k_\tau\,(0,0)} \langle j_\sigma k_\tau | b_\sigma c_\tau\rangle - t_{c_\tau d_\sigma}^{k_\tau j_\sigma\,(0,0)} \langle k_\tau j_\sigma | c_\tau b_\sigma\rangle \right) && \text{(B.257)} \\
=& - S_{a_\sigma d_\sigma} \sum_{\tau} t_{b_\sigma}^{i_\sigma\,(1,0)} t_{d_\sigma c_\tau}^{j_\sigma k_\tau\,(0,0)} \langle j_\sigma k_\tau | b_\sigma c_\tau\rangle && \text{(B.258)}
\end{aligned}
$$

where (B.254) follows from spin-integration of the two-electron integrals, (B.255) follows from spin-integration of the singles amplitudes, (B.256) from renaming of spin summation indices, (B.257) from renaming of spatial summation indices and (B.258) from symmetry of the two-electron integrals and antisymmetry of the doubles amplitudes.
The last diagram evalutes to

$$
\begin{aligned}
D3_{i_\sigma}^{a_\sigma} =& \frac{1}{2} S_{a_\sigma d_\sigma} \sum_{\tau\xi\zeta\rho} t_{d_\sigma}^{j_\tau\,(1,0)} (t_{b_\xi c_\rho}^{k_\zeta i_\sigma\,(0,0)} \delta_{\tau\xi}\delta_{\zeta\rho} \langle j_\tau k_\zeta | b_\xi c_\rho\rangle \\
& - t_{b_\xi c_\rho}^{k_\zeta i_\sigma\,(0,0)} \delta_{\tau\rho}\delta_{\zeta\xi} \langle j_\tau k_\zeta | c_\rho b_\xi\rangle) && \text{(B.259)} \\
=& \frac{1}{2} S_{a_\sigma d_\sigma} \sum_{\tau\zeta} t_{d_\sigma}^{j_\tau\,(1,0)} (t_{b_\tau c_\zeta}^{k_\zeta i_\sigma\,(0,0)} \langle j_\tau k_\zeta | b_\tau c_\zeta\rangle - t_{b_\zeta c_\tau}^{k_\zeta i_\sigma\,(0,0)} \langle j_\tau k_\zeta | c_\tau b_\zeta\rangle) && \text{(B.260)} \\
=& \frac{1}{2} S_{a_\sigma d_\sigma} t_{d_\sigma}^{j_\sigma\,(1,0)} \sum_{\zeta} (t_{b_\sigma c_\zeta}^{k_\zeta i_\sigma\,(0,0)} \langle j_\sigma k_\zeta | b_\sigma c_\zeta\rangle - t_{b_\zeta c_\sigma}^{k_\zeta i_\sigma\,(0,0)} \langle j_\sigma k_\zeta | c_\sigma b_\zeta\rangle) && \text{(B.261)} \\
=& \frac{1}{2} S_{a_\sigma d_\sigma} t_{d_\sigma}^{j_\sigma\,(1,0)} \sum_{\zeta} (t_{b_\sigma c_\zeta}^{k_\zeta i_\sigma\,(0,0)} \langle j_\sigma k_\zeta | b_\sigma c_\zeta\rangle - t_{c_\zeta b_\sigma}^{k_\zeta i_\sigma\,(0,0)} \langle j_\sigma k_\zeta | b_\sigma c_\zeta\rangle) && \text{(B.262)} \\
=& - S_{a_\sigma d_\sigma} t_{d_\sigma}^{j_\sigma\,(1,0)} \sum_{\zeta} t_{c_\zeta b_\sigma}^{k_\zeta i_\sigma\,(0,0)} \langle j_\sigma k_\zeta | b_\sigma c_\zeta\rangle && \text{(B.263)}
\end{aligned}
$$

where (B.260) follows from spin-integration of the two-electron integrals, (B.261) follows from spin-integration of the singles amplitudes, (B.262) from renaming of spatial summation indices and (B.263) from antisymmetry of the doubles amplitudes.

Combining the three diagrams (B.252), (B.258) and (B.263) gives us for (B.245)

$$\begin{aligned}\langle\phi_{i_\sigma}^{a_\sigma}|(\hat{V}_N T_1^{(1,0)} T_2^{(0,0)})_C|0\rangle =& S_{a_\sigma d_\sigma}\sum_\tau t_{b_\tau}^{j_\tau\,(1,0)}\Bigg(\sum_\rho t_{c_\rho d_\sigma}^{k_\rho i_\sigma\,(0,0)}\langle j_\tau k_\rho|b_\tau c_\rho\rangle \\ &- t_{c_\tau d_\sigma}^{k_\tau i_\sigma\,(0,0)}\langle j_\tau k_\tau|c_\tau b_\tau\rangle\Bigg) \\ &- S_{a_\sigma d_\sigma}\sum_\tau t_{b_\sigma}^{i_\sigma\,(1,0)} t_{d_\sigma c_\tau}^{j_\sigma k_\tau\,(0,0)}\langle j_\sigma k_\tau|b_\sigma c_\tau\rangle \\ &- S_{a_\sigma d_\sigma} t_{d_\sigma}^{j_\sigma\,(1,0)}\sum_\tau t_{c_\tau b_\sigma}^{k_\tau i_\sigma\,(0,0)}\langle j_\sigma k_\tau|b_\sigma c_\tau\rangle \end{aligned} \tag{B.264}$$

where we have standardized all sums over spin to use the same index when possible. Therefore, the complete singles-singles block contracted with the perturbed singles amplitudes is

$$\begin{aligned}\left(A_{\mu_1\nu_1}^{(0,0)} t_{\nu_1}^{(1,0)}\right)_{i_\sigma}^{a_\sigma} =& t_{b_\sigma}^{i_\sigma\,(1,0)}\hat{f}_{a_\sigma b_\sigma} - S_{a_\sigma b_\sigma} t_{b_\sigma}^{j_\sigma\,(1,0)}\hat{f}_{j_\sigma i_\sigma} \\ &+ \sum_\tau t_{b_\tau}^{j_\tau\,(1,0)}\langle j_\tau a_\sigma|\hat{b}_\tau i_\sigma\rangle - t_{b_\sigma}^{j_\sigma\,(1,0)}\langle j_\sigma a_\sigma|\hat{i}_\sigma b_\sigma\rangle \\ &+ S_{a_\sigma d_\sigma}\sum_\tau t_{b_\tau}^{j_\tau\,(1,0)}\left(\sum_\rho t_{c_\rho d_\sigma}^{k_\rho i_\sigma\,(0,0)}\langle j_\tau k_\rho|b_\tau c_\rho\rangle - t_{c_\tau d_\sigma}^{k_\tau i_\sigma\,(0,0)}\langle j_\tau k_\tau|c_\tau b_\tau\rangle\right) \\ &- S_{a_\sigma d_\sigma}\sum_\tau t_{b_\sigma}^{i_\sigma\,(1,0)} t_{d_\sigma c_\tau}^{j_\sigma k_\tau\,(0,0)}\langle j_\sigma k_\tau|b_\sigma c_\tau\rangle \\ &- S_{a_\sigma d_\sigma} t_{d_\sigma}^{j_\sigma\,(1,0)}\sum_\tau t_{c_\tau b_\sigma}^{k_\tau i_\sigma\,(0,0)}\langle j_\sigma k_\tau|b_\sigma c_\tau\rangle. \end{aligned} \tag{B.265}$$

B.3.1.13.2 $A_{\mu_1\nu_2}^{(0,0)} t_{\nu_2}^{(1,0)}$

For contraction of the perturbed doubles amplitudes with the singles-doubles block (B.187) of the zeroth order Jacobian we have to consider two contributions

$$\left(A_{\mu_1\nu_2}^{(0,0)} t_{\nu_2}^{(1,0)}\right)_{i_\sigma}^{a_\sigma} = \langle\phi_{i_\sigma}^{a_\sigma}|(\hat{F}_N^{(0,0)} T_2^{(1,0)})_C|0\rangle \tag{B.266}$$

$$+ \langle\phi_{i_\sigma}^{a_\sigma}|(\hat{V}_N^{(0,0)} T_2^{(1,0)})_C|0\rangle. \tag{B.267}$$

The first of these terms yields the diagram

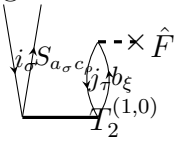

It evaluates to

$$\langle\phi_{i_\sigma}^{a_\sigma}|(\hat{F}_N^{(0,0)} T_2^{(1,0)})_C|0\rangle = \sum_{\tau\xi\rho} S_{a_\sigma c_\rho} t_{c_\rho b_\xi}^{i_\sigma j_\tau\,(1,0)}\hat{f}_{j_\tau b_\xi} \tag{B.268}$$

$$= \sum_\tau S_{a_\sigma c_\sigma} t_{c_\sigma b_\tau}^{i_\sigma j_\tau\,(1,0)}\hat{f}_{j_\tau b_\tau} \tag{B.269}$$

where (B.269) follows from spin-integration of overlap and Fock integrals.
The second term (B.267) yields the diagrams

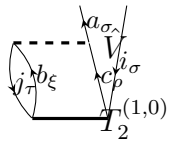

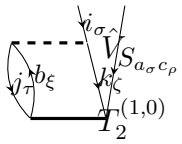

The first diagram evalutes to

$$D1_{i_\sigma}^{a_\sigma} = \frac{1}{2}\sum_{\tau\xi\rho}\left(\delta_{\tau\xi}\delta_{\sigma\rho}t_{b_\xi c_\rho}^{j_\tau i_\sigma\,(1,0)}\langle j_\tau a_\sigma\hat{|}b_\xi c_\rho\rangle - \delta_{\tau\rho}\delta_{\sigma\xi}t_{b_\xi c_\rho}^{j_\tau i_\sigma\,(1,0)}\langle j_\tau a_\sigma\hat{|}c_\rho b_\xi\rangle\right) \tag{B.270}$$

$$= \frac{1}{2}\sum_{\tau}\left(t_{b_\tau c_\sigma}^{j_\tau i_\sigma\,(1,0)}\langle j_\tau a_\sigma\hat{|}b_\tau c_\sigma\rangle - t_{b_\sigma c_\tau}^{j_\tau i_\sigma\,(1,0)}\langle j_\tau a_\sigma\hat{|}c_\tau b_\sigma\rangle\right) \tag{B.271}$$

$$= \frac{1}{2}\sum_{\tau}\left(t_{b_\tau c_\sigma}^{j_\tau i_\sigma\,(1,0)} - t_{c_\sigma b_\tau}^{j_\tau i_\sigma\,(1,0)}\right)\langle j_\tau a_\sigma\hat{|}b_\tau c_\sigma\rangle \tag{B.272}$$

$$= \sum_{\tau} t_{b_\tau c_\sigma}^{j_\tau i_\sigma\,(1,0)}\langle j_\tau a_\sigma\hat{|}b_\tau c_\sigma\rangle \tag{B.273}$$

where (B.271) follows from spin-integration of the two-electron integrals, (B.272) from renaming of indices and (B.273) from antisymmetry of the amplitudes.
The second diagram evalutes to

$$D2_{i_\sigma}^{a_\sigma} = -\frac{1}{2}\sum_{\tau\xi\rho\zeta} S_{a_\sigma c_\rho}\left(\delta_{\tau\xi}\delta_{\sigma\zeta}t_{b_\xi c_\rho}^{j_\tau k_\zeta\,(1,0)}\langle j_\tau k_\zeta\hat{|}b_\xi i_\sigma\rangle - \delta_{\sigma\tau}\delta_{\zeta\xi}t_{b_\xi c_\rho}^{j_\tau k_\zeta\,(1,0)}\langle j_\tau k_\zeta\hat{|}i_\sigma b_\xi\rangle\right) \tag{B.274}$$

$$= -\frac{1}{2}\sum_{\xi} S_{a_\sigma c_\sigma}\left(t_{b_\xi c_\sigma}^{j_\xi k_\sigma\,(1,0)}\langle j_\xi k_\sigma\hat{|}b_\xi i_\sigma\rangle - t_{b_\xi c_\sigma}^{j_\sigma k_\xi\,(1,0)}\langle j_\sigma k_\xi\hat{|}i_\sigma b_\xi\rangle\right) \tag{B.275}$$

$$= -\frac{1}{2}\sum_{\xi} S_{a_\sigma c_\sigma}\left(t_{b_\xi c_\sigma}^{j_\xi k_\sigma\,(1,0)}\langle j_\xi k_\sigma\hat{|}b_\xi i_\sigma\rangle - t_{b_\xi c_\sigma}^{k_\sigma j_\xi\,(1,0)}\langle k_\sigma j_\xi\hat{|}i_\sigma b_\xi\rangle\right) \tag{B.276}$$

$$= -\sum_{\xi} S_{a_\sigma c_\sigma} t_{b_\xi c_\sigma}^{j_\xi k_\sigma\,(1,0)}\langle j_\xi k_\sigma\hat{|}b_\xi i_\sigma\rangle \tag{B.277}$$

where (B.275) follows from spin-integration of the two-electron and overlap integrals, (B.276) from renaming of indices and (B.277) from antisymmetry of the amplitudes and symmetry of the two-electron integrals.
Combining these diagrams, we get for (B.267)

$$\begin{aligned}\langle\phi_{i_\sigma}^{a_\sigma}|(\hat{V}_N^{(0,0)}T_2^{(1,0)})_C|0\rangle = &\sum_{\tau} t_{b_\tau c_\sigma}^{j_\tau i_\sigma\,(1,0)}\langle j_\tau a_\sigma\hat{|}b_\tau c_\sigma\rangle \\ &- \sum_{\tau} S_{a_\sigma c_\sigma} t_{b_\tau c_\sigma}^{j_\tau k_\sigma\,(1,0)}\langle j_\tau k_\sigma\hat{|}b_\tau i_\sigma\rangle.\end{aligned} \tag{B.278}$$

The complete contraction of the singles multipliers with the singles-doubles block of the zeroth order Jacobian is therefore

$$\begin{aligned}\left(A_{\mu_1\nu_2}^{(0,0)}t_{\nu_2}^{(1,0)}\right)_{i_\sigma}^{a_\sigma} = &\sum_{\tau} S_{a_\sigma c_\sigma} t_{c_\sigma b_\tau}^{i_\sigma j_\tau\,(1,0)}\hat{f}_{j_\tau b_\tau} + \sum_{\tau} t_{b_\tau c_\sigma}^{j_\tau i_\sigma\,(1,0)}\langle j_\tau a_\sigma\hat{|}b_\tau c_\sigma\rangle \\ &- \sum_{\tau} S_{a_\sigma c_\sigma} t_{b_\tau c_\sigma}^{j_\tau k_\sigma\,(1,0)}\langle j_\tau k_\sigma\hat{|}b_\tau i_\sigma\rangle.\end{aligned} \tag{B.279}$$

B.3.1.13.3 $A^{(0,0)}_{\mu_2\nu_1}t^{(1,0)}_{\nu_1}$

Contraction of the doubles-singles block (B.186) of the zeroth order Jacobian with the perturbed singles amplitudes contributes only a single set of diagrams

The first of these evaluates to

$$
\begin{aligned}
D1^{a_\sigma b_\tau}_{i_\sigma j_\tau} =& P(i_\sigma, j_\tau)\sum_\rho t^{i_\sigma\,(1,0)}_{c_\rho}\Big(\langle a_\sigma b_\tau\hat{|}c_\rho j_\tau\rangle - \langle a_\sigma b_\tau\hat{|}j_\tau c_\rho\rangle\Big) && \text{(B.280)}\\
=& \sum_\rho t^{i_\sigma\,(1,0)}_{c_\rho}\Big(\delta_{\sigma\rho}\langle a_\sigma b_\tau\hat{|}c_\rho j_\tau\rangle - \delta_{\sigma\tau}\delta_{\sigma\rho}\langle a_\sigma b_\tau\hat{|}j_\tau c_\rho\rangle\Big)\\
&- \sum_\rho t^{j_\tau\,(1,0)}_{c_\rho}\Big(\delta_{\sigma\rho}\delta_{\tau\sigma}\langle a_\sigma b_\tau\hat{|}c_\rho i_\sigma\rangle - \delta_{\tau\rho}\langle a_\sigma b_\tau\hat{|}i_\sigma c_\rho\rangle\Big) && \text{(B.281)}\\
=& t^{i_\sigma\,(1,0)}_{c_\sigma}\langle a_\sigma b_\tau\hat{|}c_\sigma j_\tau\rangle - \delta_{\sigma\tau}t^{i_\sigma\,(1,0)}_{c_\sigma}\langle a_\sigma b_\sigma\hat{|}j_\sigma c_\sigma\rangle\\
&- \delta_{\sigma\tau}t^{j_\sigma\,(1,0)}_{c_\sigma}\langle a_\sigma b_\sigma\hat{|}c_\sigma i_\sigma\rangle + t^{j_\tau\,(1,0)}_{c_\tau}\langle a_\sigma b_\tau\hat{|}i_\sigma c_\tau\rangle && \text{(B.282)}
\end{aligned}
$$

where (B.281) follows from application of the permutation operator and (B.282) from spin-integration of the two-electron integrals.
The second diagram yields

$$
\begin{aligned}
D2^{a_\sigma b_\tau}_{i_\sigma j_\tau} =& -P(a_\sigma, b_\tau)\sum_{\zeta\rho} S_{a_\sigma c_\rho}t^{k_\zeta\,(1,0)}_{c_\rho}\Big(\langle k_\zeta b_\tau\hat{|}i_\sigma j_\tau\rangle - \langle k_\zeta b_\tau\hat{|}j_\tau i_\sigma\rangle\Big) && \text{(B.283)}\\
=& -\sum_{\zeta\rho} S_{a_\sigma c_\rho}t^{k_\zeta\,(1,0)}_{c_\rho}\Big(\delta_{\zeta\sigma}\langle k_\zeta b_\tau\hat{|}i_\sigma j_\tau\rangle - \delta_{\zeta\tau}\delta_{\tau\sigma}\langle k_\zeta b_\tau\hat{|}j_\tau i_\sigma\rangle\Big)\\
&+ \sum_{\zeta\rho} S_{b_\tau c_\rho}t^{k_\zeta\,(1,0)}_{c_\rho}\Big(\delta_{\zeta\sigma}\delta_{\sigma\tau}\langle k_\zeta a_\sigma\hat{|}i_\sigma j_\tau\rangle - \delta_{\zeta\tau}\langle k_\zeta a_\sigma\hat{|}j_\tau i_\sigma\rangle\Big) && \text{(B.284)}\\
=& -\sum_\rho S_{a_\sigma c_\rho}\Big(t^{k_\sigma\,(1,0)}_{c_\rho}\langle k_\sigma b_\tau\hat{|}i_\sigma j_\tau\rangle - \delta_{\tau\sigma}t^{k_\sigma\,(1,0)}_{c_\rho}\langle k_\sigma b_\sigma\hat{|}j_\sigma i_\sigma\rangle\Big)\\
&+ \sum_\rho S_{b_\tau c_\rho}\Big(\delta_{\sigma\tau}t^{k_\sigma\,(1,0)}_{c_\rho}\langle k_\sigma a_\sigma\hat{|}i_\sigma j_\sigma\rangle - t^{k_\tau\,(1,0)}_{c_\rho}\langle k_\tau a_\sigma\hat{|}j_\tau i_\sigma\rangle\Big) && \text{(B.285)}\\
=& -S_{a_\sigma c_\sigma}t^{k_\sigma\,(1,0)}_{c_\sigma}\langle k_\sigma b_\tau\hat{|}i_\sigma j_\tau\rangle + \delta_{\tau\sigma}S_{a_\sigma c_\sigma}t^{k_\sigma\,(1,0)}_{c_\sigma}\langle k_\sigma b_\sigma\hat{|}j_\sigma i_\sigma\rangle\\
&+ \delta_{\sigma\tau}S_{b_\sigma c_\sigma}t^{k_\sigma\,(1,0)}_{c_\sigma}\langle k_\sigma a_\sigma\hat{|}i_\sigma j_\sigma\rangle - S_{b_\tau c_\tau}t^{k_\tau\,(1,0)}_{c_\tau}\langle k_\tau a_\sigma\hat{|}j_\tau i_\sigma\rangle && \text{(B.286)}
\end{aligned}
$$

where (B.284) follows from application of the permutation operator, (B.285) from spin-integration of the two-electron integrals and (B.286) from spin-integration of the amplitudes.
Therefore, the contraction of perturbed singles amplitudes with the zeroth order doubles-singles block of the Jacobian is simply

$$\left(A^{(0,0)}_{\mu_2\nu_1}t^{(1,0)}_{\nu_1}\right)^{a_\sigma b_\tau}_{i_\sigma j_\tau} = t^{i_\sigma\,(1,0)}_{c_\sigma}\langle a_\sigma b_\tau\hat{|}c_\sigma j_\tau\rangle - \delta_{\sigma\tau}t^{i_\sigma\,(1,0)}_{c_\sigma}\langle a_\sigma b_\sigma\hat{|}j_\sigma c_\sigma\rangle$$
$$- \delta_{\sigma\tau}t^{j_\sigma\,(1,0)}_{c_\sigma}\langle a_\sigma b_\sigma\hat{|}c_\sigma i_\sigma\rangle + t^{j_\tau\,(1,0)}_{c_\tau}\langle a_\sigma b_\tau\hat{|}i_\sigma c_\tau\rangle$$
$$- S_{a_\sigma c_\sigma}t^{k_\sigma\,(1,0)}_{c_\sigma}\langle k_\sigma b_\tau\hat{|}i_\sigma j_\tau\rangle + \delta_{\tau\sigma}S_{a_\sigma c_\sigma}t^{k_\sigma\,(1,0)}_{c_\sigma}\langle k_\sigma b_\sigma\hat{|}j_\sigma i_\sigma\rangle$$
$$+ \delta_{\sigma\tau}S_{b_\sigma c_\sigma}t^{k_\sigma\,(1,0)}_{c_\sigma}\langle k_\sigma a_\sigma\hat{|}i_\sigma j_\sigma\rangle - S_{b_\tau c_\tau}t^{k_\tau\,(1,0)}_{c_\tau}\langle k_\tau a_\sigma\hat{|}j_\tau i_\sigma\rangle. \tag{B.287}$$

B.3.1.13.4 $A^{(0,0)}_{\mu_2\nu_2}t^{(1,0)}_{\nu_2}$

Contraction of the doubles-doubles block (B.188) of the zeroth order Jacobian with the perturbed doubles amplitudes contributes only a single set of diagrams

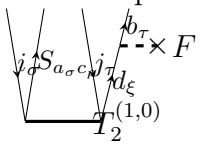

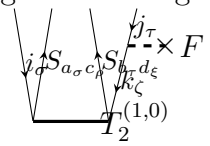

The first diagram evalutes to

$$D1^{a_\sigma b_\tau}_{i_\sigma j_\tau} = P(a_\sigma, b_\tau)\sum_{\rho\xi} S_{a_\sigma c_\rho}t^{i_\sigma j_\tau\,(1,0)}_{c_\rho d_\xi}f_{b_\tau d_\xi} \tag{B.288}$$
$$= \sum_{\rho\xi} S_{a_\sigma c_\rho}t^{i_\sigma j_\tau\,(1,0)}_{c_\rho d_\xi}f_{b_\tau d_\xi} - \sum_{\rho\xi} f_{a_\sigma d_\xi}t^{i_\sigma j_\tau\,(1,0)}_{c_\rho d_\xi}S_{b_\tau c_\rho} \tag{B.289}$$
$$= S_{a_\sigma c_\sigma}t^{i_\sigma j_\tau\,(1,0)}_{c_\sigma d_\tau}f_{b_\tau d_\tau} - f_{a_\sigma d_\sigma}t^{i_\sigma j_\tau\,(1,0)}_{c_\tau d_\sigma}S_{b_\tau c_\tau} \tag{B.290}$$
$$= S_{a_\sigma c_\sigma}t^{i_\sigma j_\tau\,(1,0)}_{c_\sigma d_\tau}f_{b_\tau d_\tau} - f_{a_\sigma c_\sigma}t^{i_\sigma j_\tau\,(1,0)}_{d_\tau c_\sigma}S_{b_\tau d_\tau} \tag{B.291}$$
$$= S_{a_\sigma c_\sigma}t^{i_\sigma j_\tau\,(1,0)}_{c_\sigma d_\tau}f_{b_\tau d_\tau} + f_{a_\sigma c_\sigma}t^{i_\sigma j_\tau\,(1,0)}_{c_\sigma d_\tau}S_{b_\tau d_\tau} \tag{B.292}$$

where (B.289) follows from application of the permutation operator, (B.290) from spin-integration of overlap and Fock integrals, (B.291) from renaming of indices and (B.292) from antisymmetry of the amplitudes.
The second diagram evaluates to

$$D2^{a_\sigma b_\tau}_{i_\sigma j_\tau} = -P(i_\sigma, j_\tau)\sum_{\rho\xi\zeta} S_{a_\sigma c_\rho}t^{i_\sigma k_\zeta\,(1,0)}_{c_\rho d_\xi}S_{b_\tau d_\xi}f_{k_\zeta j_\tau} \tag{B.293}$$
$$= -\sum_{\rho\xi\zeta} S_{a_\sigma c_\rho}t^{i_\sigma k_\zeta\,(1,0)}_{c_\rho d_\xi}S_{b_\tau d_\xi}f_{k_\zeta j_\tau} + \sum_{\rho\xi\zeta} S_{a_\sigma c_\rho}t^{j_\tau k_\zeta\,(1,0)}_{c_\rho d_\xi}S_{b_\tau d_\xi}f_{k_\zeta i_\sigma} \tag{B.294}$$
$$= -S_{a_\sigma c_\sigma}t^{i_\sigma k_\tau\,(1,0)}_{c_\sigma d_\tau}S_{b_\tau d_\tau}f_{k_\tau j_\tau} + S_{a_\sigma c_\sigma}t^{j_\tau k_\sigma\,(1,0)}_{c_\sigma d_\tau}S_{b_\tau d_\tau}f_{k_\sigma i_\sigma} \tag{B.295}$$
$$= -S_{a_\sigma c_\sigma}t^{i_\sigma k_\tau\,(1,0)}_{c_\sigma d_\tau}S_{b_\tau d_\tau}f_{k_\tau j_\tau} - S_{a_\sigma c_\sigma}t^{k_\sigma j_\tau\,(1,0)}_{c_\sigma d_\tau}S_{b_\tau d_\tau}f_{k_\sigma i_\sigma} \tag{B.296}$$

where (B.294) follows from application of the permutation operator, (B.295) from spin-integration of overlap and Fock integrals and (B.296) from antisymmetry of the amplitudes.
Thus, the complete contraction of the perturbed doubles amplitudes with the zeroth order doubles-doubles block of the Jacobian is

$$\left(A^{(0,0)}_{\mu_2\nu_2}t^{(1,0)}_{\nu_2}\right)^{a_\sigma b_\tau}_{i_\sigma j_\tau} = S_{a_\sigma c_\sigma}t^{i_\sigma j_\tau\,(1,0)}_{c_\sigma d_\tau}f_{b_\tau d_\tau} + f_{a_\sigma c_\sigma}t^{i_\sigma j_\tau\,(1,0)}_{c_\sigma d_\tau}S_{b_\tau d_\tau}$$
$$- S_{a_\sigma c_\sigma}t^{i_\sigma k_\tau\,(1,0)}_{c_\sigma d_\tau}S_{b_\tau d_\tau}f_{k_\tau j_\tau} - S_{a_\sigma c_\sigma}t^{k_\sigma j_\tau\,(1,0)}_{c_\sigma d_\tau}S_{b_\tau d_\tau}f_{k_\sigma i_\sigma}. \tag{B.297}$$

B.3.1.14 $A^{(1,0)}_{\mu\nu}$

The partial derivative of the Jacobian with respect to the perturbation α is

$$A^{(1,0)}_{\mu\nu} = \frac{\partial^3 L}{\partial\alpha\partial\lambda_\mu\partial t_\nu}\bigg|_{\alpha,\beta=0} = \frac{\partial^2\Omega_\mu}{\partial\alpha\partial t_\nu}\bigg|_{\alpha,\beta=0} = \frac{\partial A_{\mu\nu}}{\partial\alpha}\bigg|_{\alpha,\beta=0} = \begin{pmatrix} A^{(1,0)}_{\mu_1\nu_1} & A^{(1,0)}_{\mu_1\nu_2} \\ A^{(1,0)}_{\mu_2\nu_1} & A^{(1,0)}_{\mu_2\nu_2} \end{pmatrix}. \tag{B.298}$$

The expression for the four blocks are similar to equations (B.185), (B.186), (B.187) and (B.188). However, there are some differences due to the absence of two-electron operators and the dressing of the perturbed Hamiltonian in all terms of the doubles amplitude equations.

$$A^{(1,0)}_{\mu_1\nu_1} = \frac{\partial^2\Omega_{\mu_1}}{\partial\alpha\partial t_{\nu_1}}\bigg|_{\alpha,\beta=0} = \langle\mu_1|(\hat{H}^{(1,0)}_N\tau_{\nu_1})_C|0\rangle \tag{B.299}$$

$$A^{(1,0)}_{\mu_2\nu_1} = \frac{\partial^2\Omega_{\mu_2}}{\partial\alpha\partial t_{\nu_1}}\bigg|_{\alpha,\beta=0} = \langle\mu_2|(\hat{H}^{(1,0)}_N\tau_{\nu_1}T^{(0,0)}_2)_C|0\rangle \tag{B.300}$$

$$A^{(1,0)}_{\mu_1\nu_2} = \frac{\partial^2\Omega_{\mu_1}}{\partial\alpha\partial t_{\nu_2}}\bigg|_{\alpha,\beta=0} = \langle\mu_1|(\hat{H}^{(1,0)}_N\tau_{\nu_2})_C|0\rangle \tag{B.301}$$

$$A^{(1,0)}_{\mu_2\nu_2} = \frac{\partial^2\Omega_{\mu_2}}{\partial\alpha\partial t_{\nu_2}}\bigg|_{\alpha,\beta=0} = \langle\mu_2|(\hat{H}^{(1,0)}_N\tau_{\nu_2})_C|0\rangle. \tag{B.302}$$

Consequently, we can reuse the equations derived for the unperturbed case in the usual way except for the doubles-singles block (B.300). For the latter, there are no shared diagrams with the zeroth order case (B.186) and we will have to explicitly consider them in the following.

B.3.1.15 $\lambda^{(0,0)}_{\mu_1}A^{(1,0)}_{\mu\nu}$

B.3.1.15.1 $\lambda^{(0,0)}_{\mu_1}A^{(1,0)}_{\mu_1\nu_1}$

Contraction of the zeroth order singles multipliers with the singles-singles block of the perturbed Jacobian is obtained from (B.210) via the usual procedure as

$$\left(\lambda^{(0,0)}_{\mu_1}A^{(1,0)}_{\mu_1\nu_1}\right)^{a_\sigma}_{i_\sigma} = \lambda^{b_\sigma(0,0)}_{i_\sigma}\hat{h}^{(1,0)}_{b_\sigma a_\sigma} - \hat{h}^{(1,0)}_{i_\sigma j_\sigma}\lambda^{b_\sigma(0,0)}_{j_\sigma}S_{b_\sigma a_\sigma}. \tag{B.303}$$

B.3.1.15.2 $\lambda^{(0,0)}_{\mu_2}A^{(1,0)}_{\mu_2\nu_1}$

The contraction of the zeroth order doubles multipliers with the doubles-singles block of the perturbed Jacobian consists of the pair of diagrams

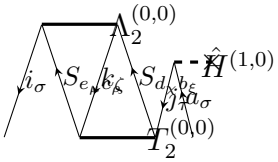

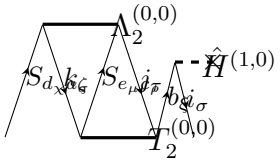

The first diagram evaluates to

$$D1_{i_\sigma}^{a_\sigma} = \frac{1}{2} \sum_{\xi\tau\zeta\rho\chi\mu} \lambda_{i_\sigma k_\zeta}^{e_\mu d_\chi (0,0)} S_{e_\mu c_\rho} S_{d_\chi b_\xi} t_{c_\rho b_\xi}^{k_\zeta j_\tau (0,0)} h_{j_\tau a_\sigma}^{(1,0)} \tag{B.304}$$

$$= \frac{1}{2} \sum_{\xi\zeta\rho} \lambda_{i_\sigma k_\zeta}^{e_\rho d_\xi (0,0)} S_{e_\rho c_\rho} S_{d_\xi b_\xi} t_{c_\rho b_\xi}^{k_\zeta j_\sigma (0,0)} h_{j_\sigma a_\sigma}^{(1,0)} \tag{B.305}$$

$$= -\frac{1}{2} \sum_{\xi\zeta\rho} \lambda_{i_\sigma k_\zeta}^{e_\rho d_\xi (0,0)} S_{e_\rho c_\rho} S_{d_\xi b_\xi} t_{c_\rho b_\xi}^{j_\sigma k_\zeta (0,0)} h_{j_\sigma a_\sigma}^{(1,0)} \tag{B.306}$$

$$= -\frac{1}{2} \sum_{\tau} (2 - \delta_{\sigma\tau}) \lambda_{i_\sigma k_\tau}^{e_\sigma d_\tau (0,0)} S_{e_\sigma c_\sigma} S_{d_\tau b_\tau} t_{c_\sigma b_\tau}^{j_\sigma k_\tau (0,0)} h_{j_\sigma a_\sigma}^{(1,0)} \tag{B.307}$$

where (B.305) follows from spin-integration of overlap and one-electron integrals, (B.306) from antisymmetry of the amplitudes and (B.307) from application of (B.114).
The second diagram evaluates to

$$D2_{i_\sigma}^{a_\sigma} = \frac{1}{2} \sum_{\xi\tau\zeta\rho\chi\mu} S_{d_\chi a_\sigma} \lambda_{k_\zeta j_\tau}^{d_\chi e_\mu (0,0)} S_{e_\mu c_\rho} t_{c_\rho b_\xi}^{k_\zeta j_\tau (0,0)} h_{i_\sigma b_\xi}^{(1,0)} \tag{B.308}$$

$$= \frac{1}{2} \sum_{\tau\zeta\rho} S_{d_\sigma a_\sigma} \lambda_{k_\zeta j_\tau}^{d_\sigma e_\rho (0,0)} S_{e_\rho c_\rho} t_{c_\rho b_\sigma}^{k_\zeta j_\tau (0,0)} h_{i_\sigma b_\sigma}^{(1,0)} \tag{B.309}$$

$$= -\frac{1}{2} \sum_{\tau\zeta\rho} S_{d_\sigma a_\sigma} \lambda_{k_\zeta j_\tau}^{d_\sigma e_\rho (0,0)} S_{e_\rho c_\rho} t_{b_\sigma c_\rho}^{k_\zeta j_\tau (0,0)} h_{i_\sigma b_\sigma}^{(1,0)} \tag{B.310}$$

$$= -\frac{1}{2} \sum_{\tau} (2 - \delta_{\sigma\tau}) S_{d_\sigma a_\sigma} \lambda_{k_\sigma j_\tau}^{d_\sigma e_\tau (0,0)} S_{e_\tau c_\tau} t_{b_\sigma c_\tau}^{k_\sigma j_\tau (0,0)} h_{i_\sigma b_\sigma}^{(1,0)} \tag{B.311}$$

where (B.309) follows from spin-integration of overlap and one-electron integrals, (B.310) from antisymmetry of the amplitudes, and (B.311) from application of (B.115).
Therefore, contraction of the unperturbed doubles multipliers with the doubles-singles block of the perturbed Jacobian is

$$\begin{aligned} \left(\lambda_{\mu_2}^{(0,0)} A_{\mu_2\nu_1}^{(1,0)} \right)_{i_\sigma}^{a_\sigma} = & \sum_{\tau} \left(\frac{\delta_{\sigma\tau}}{2} - 1 \right) \lambda_{i_\sigma k_\tau}^{e_\sigma d_\tau (0,0)} S_{e_\sigma c_\sigma} S_{d_\tau b_\tau} t_{c_\sigma b_\tau}^{j_\sigma k_\tau (0,0)} h_{j_\sigma a_\sigma}^{(1,0)} \\ & + \sum_{\tau} \left(\frac{\delta_{\sigma\tau}}{2} - 1 \right) S_{d_\sigma a_\sigma} \lambda_{k_\sigma j_\tau}^{d_\sigma e_\tau (0,0)} S_{e_\tau c_\tau} t_{b_\sigma c_\tau}^{k_\sigma j_\tau (0,0)} h_{i_\sigma b_\sigma}^{(1,0)}. \end{aligned} \tag{B.312}$$

B.3.1.15.3 $\lambda_{\mu_1}^{(0,0)} A_{\mu_1\nu_2}^{(1,0)}$

Contraction of the zeroth order singles multipliers with the singles-doubles block of the perturbed Jacobian is obtained from (B.232) via the usual procedure as

$$\begin{aligned} \left(\lambda_{\mu_1}^{(0,0)} A_{\mu_1\nu_2}^{(1,0)} \right)_{i_\sigma j_\tau}^{a_\sigma b_\tau} = & h_{j_\tau b_\tau}^{(1,0)} S_{c_\sigma a_\sigma} \lambda_{i_\sigma}^{c_\sigma (0,0)} + h_{i_\sigma a_\sigma}^{(1,0)} S_{c_\tau b_\tau} \lambda_{j_\tau}^{c_\tau (0,0)} \\ & - \delta_{\sigma\tau} h_{j_\sigma a_\sigma}^{(1,0)} S_{c_\sigma b_\sigma} \lambda_{i_\sigma}^{c_\sigma (0,0)} - \delta_{\sigma\tau} h_{i_\sigma b_\sigma}^{(1,0)} S_{c_\sigma a_\sigma} \lambda_{j_\sigma}^{c_\sigma (0,0)}. \end{aligned} \tag{B.313}$$

B.3.1.15.4 $\lambda_{\mu_2}^{(0,0)} A_{\mu_2\nu_2}^{(1,0)}$

Contraction of the zeroth order doubles multipliers with the doubles-doubles block of the

perturbed Jacobian is obtained from (B.242) via the usual procedure as

$$\left(\lambda^{(0,0)}_{\mu_2} A^{(1,0)}_{\mu_2\nu_2}\right)^{a_\sigma b_\tau}_{i_\sigma j_\tau} = S_{c_\sigma a_\sigma} \lambda^{c_\sigma d_\tau\,(0,0)}_{i_\sigma j_\tau} \hat{h}^{(1,0)}_{d_\tau b_\tau} + \hat{h}^{(1,0)}_{c_\sigma a_\sigma} \lambda^{c_\sigma d_\tau\,(0,0)}_{i_\sigma j_\tau} S_{d_\tau b_\tau} - S_{c_\sigma a_\sigma} \lambda^{c_\sigma d_\tau\,(0,0)}_{i_\sigma k_\tau} S_{d_\tau b_\tau} \hat{h}^{(1,0)}_{j_\tau k_\tau} - S_{c_\sigma a_\sigma} \lambda^{c_\sigma d_\tau\,(0,0)}_{k_\sigma j_\tau} S_{d_\tau b_\tau} \hat{h}^{(1,0)}_{i_\sigma k_\sigma}. \tag{B.314}$$

B.3.1.16 $\lambda^{(0,0)}_{\mu} A^{(1,0)}_{\mu\nu} t^{(1,0)}_{\nu}$

It is convenient to examine the contraction of zeroth order multipliers and perturbed amplitudes with the perturbed Jacobian for each block separately.
For contraction with the singles-singles block (B.299) of the perturbed Jacobian, we have the two diagrams

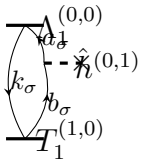

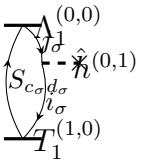

The first of these evaluates to

$$D1 = \sum_\sigma t^{k_\sigma\,(1,0)}_{b_\sigma} \lambda^{a_\sigma\,(0,0)}_{k_\sigma} \hat{h}^{(0,1)}_{a_\sigma b_\sigma} \tag{B.315}$$

whereas the second gives

$$D2 = -\sum_\sigma t^{i_\sigma\,(1,0)}_{d_\sigma} S_{c_\sigma d_\sigma} \lambda^{c_\sigma\,(0,0)}_{j_\sigma} \hat{h}^{(0,1)}_{i_\sigma j_\sigma} \tag{B.316}$$

giving in total

$$\lambda^{(0,0)}_{\mu_1} A^{(0,1)}_{\mu_1\nu_1} t^{(1,0)}_{\nu_1} = \sum_\sigma \left(t^{k_\sigma\,(1,0)}_{b_\sigma} \lambda^{a_\sigma\,(0,0)}_{k_\sigma} \hat{h}^{(0,1)}_{a_\sigma b_\sigma} - t^{i_\sigma\,(1,0)}_{d_\sigma} S_{c_\sigma d_\sigma} \lambda^{c_\sigma\,(0,0)}_{j_\sigma} \hat{h}^{(0,1)}_{i_\sigma j_\sigma} \right). \tag{B.317}$$

For contraction with the doubles-singles block (B.300) we have the diagrams

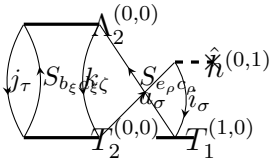

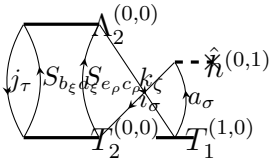

The first of these evaluates to

$$D1 = -\frac{1}{2} \sum_{\substack{\sigma\tau \\ \rho\xi\zeta}} t^{j_\tau k_\zeta\,(0,0)}_{d_\xi a_\sigma} S_{d_\xi b_\xi} \lambda^{b_\xi c_\rho\,(0,0)}_{j_\tau k_\zeta} S_{c_\rho e_\rho} t^{i_\sigma\,(1,0)}_{e_\rho} h^{(1,0)}_{i_\sigma a_\sigma} \tag{B.318}$$

$$= -\frac{1}{2} \sum_{\substack{\sigma\tau \\ \xi\zeta}} t^{j_\tau k_\zeta\,(0,0)}_{d_\xi a_\sigma} S_{d_\xi b_\xi} \lambda^{b_\xi c_\sigma\,(0,0)}_{j_\tau k_\zeta} S_{c_\sigma e_\sigma} t^{i_\sigma\,(1,0)}_{e_\sigma} h^{(1,0)}_{i_\sigma a_\sigma} \tag{B.319}$$

$$= -\frac{1}{2} \sum_{\sigma\tau} (2 - \delta_{\sigma\tau}) t^{j_\tau k_\sigma\,(0,0)}_{d_\tau a_\sigma} S_{d_\tau b_\tau} \lambda^{b_\tau c_\sigma\,(0,0)}_{j_\tau k_\sigma} S_{c_\sigma e_\sigma} t^{i_\sigma\,(1,0)}_{e_\sigma} h^{(1,0)}_{i_\sigma a_\sigma} \tag{B.320}$$

where (B.319) follows from spin-integration of the singles amplitudes and (B.320) from (B.115).

The second diagram evaluates to

$$D2 = -\frac{1}{2}\sum_{\substack{\sigma\tau\\ \rho\xi\zeta}} t^{j_\tau i_\sigma\,(0,0)}_{d_\xi e_\rho} S_{d_\xi b_\xi} S_{e_\rho d_\rho} \lambda^{b_\xi d_\rho\,(0,0)}_{j_\tau k_\zeta} t^{k_\zeta\,(1,0)}_{a_\sigma} h^{(1,0)}_{i_\sigma a_\sigma} \tag{B.321}$$

$$= -\frac{1}{2}\sum_{\substack{\sigma\tau\\ \rho\xi}} t^{j_\tau i_\sigma\,(0,0)}_{d_\xi e_\rho} S_{d_\xi b_\xi} S_{e_\rho d_\rho} \lambda^{b_\xi d_\rho\,(0,0)}_{j_\tau k_\sigma} t^{k_\sigma\,(1,0)}_{a_\sigma} h^{(1,0)}_{i_\sigma a_\sigma} \tag{B.322}$$

$$= -\frac{1}{2}\sum_{\sigma\tau} (2-\delta_{\sigma\tau}) t^{j_\tau i_\sigma\,(0,0)}_{d_\tau e_\sigma} S_{d_\tau b_\tau} S_{e_\sigma d_\sigma} \lambda^{b_\tau d_\sigma\,(0,0)}_{j_\tau k_\sigma} t^{k_\sigma\,(1,0)}_{a_\sigma} h^{(1,0)}_{i_\sigma a_\sigma} \tag{B.323}$$

where (B.322) follows from spin-integration of the singles amplitudes and (B.323) from (B.114).
Thus, the complete contraction with the doubles-singles block is

$$\begin{aligned}\lambda^{(0,0)}_{\mu_2} A^{(0,1)}_{\mu_2\nu_1} t^{(1,0)}_{\nu_1} = \sum_{\sigma\tau} (\frac{\delta_{\sigma\tau}}{2} - 1) \Bigg(& t^{j_\tau k_\sigma\,(0,0)}_{d_\tau a_\sigma} S_{d_\tau b_\tau} \lambda^{b_\tau c_\sigma\,(0,0)}_{j_\tau k_\sigma} S_{c_\sigma e_\sigma} t^{i_\sigma\,(1,0)}_{e_\sigma} \\ & + t^{j_\tau i_\sigma\,(0,0)}_{d_\tau e_\sigma} S_{d_\tau b_\tau} S_{e_\sigma d_\sigma} \lambda^{b_\tau d_\sigma\,(0,0)}_{j_\tau k_\sigma} t^{k_\sigma\,(1,0)}_{a_\sigma} \Bigg) h^{(1,0)}_{i_\sigma a_\sigma}. \end{aligned} \tag{B.324}$$

Contraction with the singles-doubles block (B.300) yields the diagram

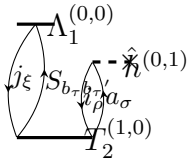

whereas the contraction with the doubles-doubles block (B.300) yields the diagrams

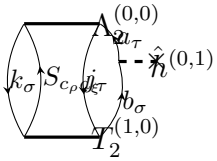

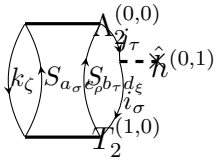

These diagrams are essentially identical to the three diagrams we obtained from (B.175) and (B.176) when contracting the multipliers with the partial derivative of the amplitude equations. We only have to change the orders of amplitudes and integrals in the relevant terms of (B.183) accordingly to arrive at

$$\lambda^{(0,0)}_{\mu_1} A^{(0,1)}_{\mu_1\nu_2} t^{(1,0)}_{\nu_2} = \sum_{\sigma\tau} \lambda^{b_\tau\,(0,0)}_{j_\tau} S_{b_\tau c_\tau} t^{c_\tau a_\sigma\,(1,0)}_{j_\tau i_\sigma} h^{(0,1)}_{i_\sigma a_\sigma} \tag{B.325}$$

$$\begin{aligned}\lambda^{(0,0)}_{\mu_2} A^{(0,1)}_{\mu_2\nu_2} t^{(1,0)}_{\nu_2} = \sum_{\sigma\tau} (1 - \frac{\delta_{\sigma\tau}}{2}) \Bigg(& \lambda^{c_\tau a_\sigma\,(0,0)}_{k_\tau j_\sigma} S_{c_\tau d_\tau} t^{k_\tau j_\sigma\,(1,0)}_{d_\tau b_\sigma} \hat{h}^{(0,1)}_{a_\sigma b_\sigma} \\ & - \lambda^{c_\tau b_\sigma\,(0,0)}_{k_\tau j_\sigma} S_{c_\tau d_\tau} S_{b_\sigma e_\sigma} t^{k_\tau i_\sigma\,(1,0)}_{d_\tau e_\sigma} \hat{h}^{(0,1)}_{i_\sigma j_\sigma} \Bigg). \end{aligned} \tag{B.326}$$

Since the doubles amplitudes appear only linearly in CC2, it is hardly surprising that taking the derivative with respect to them and then contracting with another set of doubles amplitudes does not change the diagrams significantly.

Finally, for the complete contraction we have

$$\begin{aligned}\lambda_\mu^{(0,0)} A_{\mu\nu}^{(0,1)} t_\nu^{(1,0)} =& \sum_\sigma \Bigg[t_{b_\sigma}^{k_\sigma\,(1,0)} \lambda_{k_\sigma}^{a_\sigma\,(0,0)} \hat{h}_{a_\sigma b_\sigma}^{(0,1)} - t_{d_\sigma}^{i_\sigma\,(1,0)} S_{c_\sigma d_\sigma} \lambda_{j_\sigma}^{c_\sigma\,(0,0)} \hat{h}_{i_\sigma j_\sigma}^{(0,1)} \\ & \sum_\tau (\frac{\delta_{\sigma\tau}}{2} - 1) \Bigg(t_{d_\tau a_\sigma}^{j_\tau k_\sigma\,(0,0)} S_{d_\tau b_\tau} \lambda_{j_\tau k_\sigma}^{b_\tau c_\sigma\,(0,0)} S_{c_\sigma e_\sigma} t_{e_\sigma}^{i_\sigma\,(1,0)} \\ & + t_{d_\tau e_\sigma}^{j_\tau i_\sigma\,(0,0)} S_{d_\tau b_\tau} S_{e_\sigma d_\sigma} \lambda_{j_\tau k_\sigma}^{b_\tau d_\sigma\,(0,0)} t_{a_\sigma}^{k_\sigma\,(1,0)} \Bigg) h_{i_\sigma a_\sigma}^{(1,0)} \\ & + \sum_\tau \lambda_{j_\tau}^{b_\tau\,(0,0)} S_{b_\tau c_\tau} t_{j_\tau i_\sigma}^{c_\tau a_\sigma\,(1,0)} h_{i_\sigma a_\sigma}^{(0,1)} \\ & + \sum_\tau (1 - \frac{\delta_{\sigma\tau}}{2}) \Bigg(\lambda_{k_\tau j_\sigma}^{c_\tau a_\sigma\,(0,0)} S_{c_\tau d_\tau} t_{d_\tau b_\sigma}^{k_\tau j_\sigma\,(1,0)} \hat{h}_{a_\sigma b_\sigma}^{(0,1)} \\ & - \lambda_{k_\tau j_\sigma}^{c_\tau b_\sigma\,(0,0)} S_{c_\tau d_\tau} S_{b_\sigma e_\sigma} t_{d_\tau e_\sigma}^{k_\tau i_\sigma\,(1,0)} \hat{h}_{i_\sigma j_\sigma}^{(0,1)} \Bigg) \Bigg]. \end{aligned} \tag{B.327}$$

B.3.1.17 $B_{\mu\nu\rho}^{(0,0)}$

The second derivative of the amplitude equations with respect to the amplitudes is the B-matrix

$$B_{\mu\nu\rho}^{(0,0)} = \left.\frac{\partial^3 L}{\partial\lambda_\mu \partial t_\nu \partial t_\rho}\right|_{\alpha,\beta=0} = \left.\frac{\partial^2 \Omega_\mu}{\partial t_\nu \partial t_\rho}\right|_{\alpha,\beta=0} = \left.\frac{\partial A_{\mu\nu}}{\partial t_\rho}\right|_{\alpha,\beta=0}. \tag{B.328}$$

Since the doubles amplitudes appear only linearly in the CC2 model, the singles-doubles-doubles and the doubles-doubles-doubles blocks vanish

$$B_{\mu_1\nu_2\rho_2}^{(0,0)} = \left.\frac{\partial^2 \Omega_{\mu_1}}{\partial t_{\nu_2} \partial t_{\rho_2}}\right|_{\alpha,\beta=0} = 0 \tag{B.329}$$

$$B_{\mu_2\nu_2\rho_2}^{(0,0)} = \left.\frac{\partial^2 \Omega_{\mu_2}}{\partial t_{\nu_2} \partial t_{\rho_2}}\right|_{\alpha,\beta=0} = 0. \tag{B.330}$$

Furthermore, there is no mixed derivative with respect to singles and doubles amplitudes of the doubles CC2 amplitude equations, since the Fock operator is undressed

$$B_{\mu_2\nu_1\rho_2}^{(0,0)} = \left.\frac{\partial^2 \Omega_{\mu_2}}{\partial t_{\nu_1} \partial t_{\rho_2}}\right|_{\alpha,\beta=0} = 0 \tag{B.331}$$

$$B_{\mu_2\nu_2\rho_1}^{(0,0)} = \left.\frac{\partial^2 \Omega_{\mu_2}}{\partial t_{\nu_2} \partial t_{\rho_1}}\right|_{\alpha,\beta=0} = 0. \tag{B.332}$$

Therefore, the only non-zero blocks are

$$\begin{aligned} B_{\mu_1\nu_1\rho_1}^{(0,0)} =& \langle\mu_1|(\hat{H}_N^{(0,0)} \tau_{\nu_1}\tau_{\rho_1})_C|0\rangle + \langle\mu_1|(\hat{H}_N^{(0,0)} \tau_{\nu_1}\tau_{\rho_1} T_2^{(0,0)})_C|0\rangle \\ =& \langle\mu_1|(\hat{F}_N^{(0,0)} \tau_{\nu_1}\tau_{\rho_1})_C|0\rangle + \langle\mu_1|(\hat{V}_N^{(0,0)} \tau_{\nu_1}\tau_{\rho_1})_C|0\rangle \end{aligned} \tag{B.333}$$

$$B_{\mu_1\nu_1\rho_2}^{(0,0)} = \langle\mu_1|(\hat{H}_N^{(0,0)} \tau_{\nu_1}\tau_{\rho_2})_C|0\rangle = \langle\mu_1|(\hat{V}_N^{(0,0)} \tau_{\nu_1}\tau_{\rho_2})_C|0\rangle \tag{B.334}$$

$$B_{\mu_1\nu_2\rho_1}^{(0,0)} = \langle\mu_1|(\hat{H}_N^{(0,0)} \tau_{\nu_2}\tau_{\rho_1})_C|0\rangle = \langle\mu_1|(\hat{V}_N^{(0,0)} \tau_{\nu_2}\tau_{\rho_1})_C|0\rangle \tag{B.335}$$

$$B_{\mu_2\nu_1\rho_1}^{(0,0)} = \langle\mu_2|(\hat{H}_N^{(0,0)} \tau_{\nu_1}\tau_{\rho_1})_C|0\rangle = \langle\mu_2|(\hat{V}_N^{(0,0)} \tau_{\nu_1}\tau_{\rho_1})_C|0\rangle \tag{B.336}$$

where the second equalities follow from elimination of terms due to insufficient excitation level of the Hamiltonian fragments in addition to application of the connectivity requirement for the derivative of the doubles amplitude equations.
In this work, the B-matrix only appears contracted with the zeroth order multipliers and the perturbed amplitudes. Thus, it is sufficient to only consider the corresponding diagrams. Due to symmetry of the B-matrix, the choice of contraction index (ν or ρ) for the amplitudes is arbitrary, but once a choice has been made for one term it has to be made for all terms. We will contract over the indices ρ.

B.3.1.17.1 $\lambda^{(0,0)}_{\mu_1} B^{(0,0)}_{\mu_1\nu_1\rho_1} t^{(1,0)}_{\rho_1}$

The first term of (B.333) contracted with the zeroth order multipliers and the perturbed singles amplitudes contributes the two diagrams

The first of these diagrams evaluates to

$$D1^{a_\sigma}_{i_\sigma} = -\hat{f}_{i_\sigma b_\sigma} t^{j_\sigma\,(1,0)}_{b_\sigma} \lambda^{c_\sigma\,(0,0)}_{j_\sigma} S_{a_\sigma c_\sigma}. \tag{B.337}$$

The second diagram evaluates to

$$D2^{a_\sigma}_{i_\sigma} = -\lambda^{c_\sigma\,(0,0)}_{i_\sigma} S_{c_\sigma b_\sigma} t^{j_\sigma\,(1,0)}_{b_\sigma} \hat{f}_{j_\sigma a_\sigma}. \tag{B.338}$$

Therefore, we have

$$\begin{aligned}\lambda^{(0,0)}_{\mu_1}\langle\mu_1|(\hat{F}^{(0,0)}_N \tau^{a_\sigma}_{i_\sigma} T^{(1,0)}_1)_C|0\rangle = &-\hat{f}_{i_\sigma b_\sigma} t^{j_\sigma\,(1,0)}_{b_\sigma} \lambda^{c_\sigma\,(0,0)}_{j_\sigma} S_{a_\sigma c_\sigma} \\ &- \lambda^{c_\sigma\,(0,0)}_{i_\sigma} S_{c_\sigma b_\sigma} t^{j_\sigma\,(1,0)}_{b_\sigma} \hat{f}_{j_\sigma a_\sigma}.\end{aligned} \tag{B.339}$$

The second term of (B.333) gives rise to four diagrams

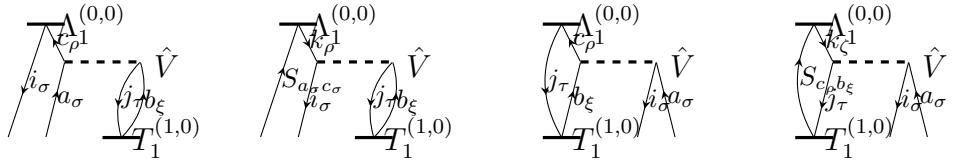

The first of these diagrams evaluates to

$$D1^{a_\sigma}_{i_\sigma} = \sum_{\tau\xi\rho} \lambda^{c_\rho\,(0,0)}_{i_\sigma} \Big(\delta_{\sigma\rho}\delta_{\tau\xi} \langle c_\rho j_\tau \hat{|} a_\sigma b_\xi\rangle - \delta_{\sigma\tau}\delta_{\rho\xi} \langle c_\rho j_\tau \hat{|} b_\xi a_\sigma\rangle \Big) t^{j_\tau\,(1,0)}_{b_\xi} \tag{B.340}$$

$$= \lambda^{c_\sigma\,(0,0)}_{i_\sigma} \sum_{\tau} \Big(\langle c_\sigma j_\tau \hat{|} a_\sigma b_\tau\rangle - \delta_{\sigma\tau} \langle c_\sigma j_\tau \hat{|} b_\tau a_\sigma\rangle \Big) t^{j_\tau\,(1,0)}_{b_\tau} \tag{B.341}$$

$$= \lambda^{c_\sigma\,(0,0)}_{i_\sigma} \sum_{\tau} \langle c_\sigma j_\tau \hat{|} a_\sigma b_\tau\rangle t^{j_\tau\,(1,0)}_{b_\tau} - \lambda^{c_\sigma\,(0,0)}_{i_\sigma} \langle c_\sigma j_\sigma \hat{|} b_\sigma a_\sigma\rangle t^{j_\sigma\,(1,0)}_{b_\sigma} \tag{B.342}$$

where (B.341) follows from spin-integration of amplitudes and multipliers and (B.342) from spin-integration of the two-electron integrals.

The second diagram evaluates to

$$D2_{i_\sigma}^{a_\sigma} = - S_{a_\sigma c_\sigma} \sum_{\tau\xi\rho} \lambda_{k_\rho}^{c_\sigma\,(0,0)} \Big(\delta_{\sigma\rho}\delta_{\tau\xi} \langle i_\sigma j_\tau \hat{|} k_\rho b_\xi \rangle - \delta_{\sigma\xi}\delta_{\tau\rho} \langle i_\sigma j_\tau \hat{|} b_\xi k_\rho \rangle \Big) t_{b_\xi}^{j_\tau\,(1,0)} \tag{B.343}$$

$$= - S_{a_\sigma c_\sigma} \lambda_{k_\sigma}^{c_\sigma\,(0,0)} \sum_{\tau} \Big(\langle i_\sigma j_\tau \hat{|} k_\sigma b_\tau \rangle - \delta_{\sigma\tau} \langle i_\sigma j_\tau \hat{|} b_\tau k_\sigma \rangle \Big) t_{b_\tau}^{j_\tau\,(1,0)} \tag{B.344}$$

$$= - S_{a_\sigma c_\sigma} \lambda_{k_\sigma}^{c_\sigma\,(0,0)} \sum_{\tau} \langle i_\sigma j_\tau \hat{|} k_\sigma b_\tau \rangle t_{b_\tau}^{j_\tau\,(1,0)}$$

$$+ S_{a_\sigma c_\sigma} \lambda_{k_\sigma}^{c_\sigma\,(0,0)} \langle i_\sigma j_\sigma \hat{|} b_\sigma k_\sigma \rangle t_{b_\sigma}^{j_\sigma\,(1,0)} \tag{B.345}$$

where (B.344) follows from spin-integration of amplitudes and multipliers and (B.345) from spin-integration of the two-electron integrals.
The third diagram evaluates to

$$D3_{i_\sigma}^{a_\sigma} = \sum_{\tau\xi} \lambda_{j_\tau}^{c_\rho\,(0,0)} \Big(\delta_{\rho\xi} \langle c_\rho i_\sigma \hat{|} b_\xi a_\sigma \rangle - \delta_{\sigma\rho}\delta_{\sigma\xi} \langle c_\rho i_\sigma \hat{|} a_\sigma b_\xi \rangle \Big) t_{b_\xi}^{j_\tau\,(1,0)} \tag{B.346}$$

$$= \sum_{\tau} \lambda_{j_\tau}^{c_\tau\,(0,0)} \Big(\langle c_\tau i_\sigma \hat{|} b_\tau a_\sigma \rangle - \delta_{\sigma\tau} \langle c_\tau i_\sigma \hat{|} a_\sigma b_\tau \rangle \Big) t_{b_\tau}^{j_\tau\,(1,0)} \tag{B.347}$$

$$= \sum_{\tau} \lambda_{j_\tau}^{c_\tau\,(0,0)} \langle c_\tau i_\sigma \hat{|} b_\tau a_\sigma \rangle t_{b_\tau}^{j_\tau\,(1,0)} - \lambda_{j_\sigma}^{c_\sigma\,(0,0)} \langle c_\sigma i_\sigma \hat{|} a_\sigma b_\sigma \rangle t_{b_\sigma}^{j_\sigma\,(1,0)} \tag{B.348}$$

where (B.347) follows from spin-integration of amplitudes and multipliers and (B.348) from spin-integration of the two-electron integrals.
The last diagram evaluates to

$$D4_{i_\sigma}^{a_\sigma} = - \sum_{\tau\xi\zeta\rho} S_{c_\rho b_\xi} \lambda_{k_\zeta}^{c_\rho\,(0,0)} \Big(\delta_{\tau\zeta} \langle j_\tau i_\sigma | k_\zeta a_\sigma \rangle - \delta_{\sigma\tau}\delta_{\sigma\zeta} \langle j_\tau i_\sigma | a_\sigma k_\zeta \rangle \Big) t_{b_\xi}^{j_\tau\,(1,0)} \tag{B.349}$$

$$= - \sum_{\tau} S_{c_\tau b_\tau} \lambda_{k_\tau}^{c_\tau\,(0,0)} \Big(\langle j_\tau i_\sigma | k_\tau a_\sigma \rangle - \delta_{\sigma\tau} \langle j_\tau i_\sigma | a_\sigma k_\tau \rangle \Big) t_{b_\tau}^{j_\tau\,(1,0)} \tag{B.350}$$

$$= - \sum_{\tau} S_{c_\tau b_\tau} \lambda_{k_\tau}^{c_\tau\,(0,0)} \langle j_\tau i_\sigma | k_\tau a_\sigma \rangle t_{b_\tau}^{j_\tau\,(1,0)} + S_{c_\sigma b_\sigma} \lambda_{k_\sigma}^{c_\sigma\,(0,0)} \langle j_\sigma i_\sigma | a_\sigma k_\sigma \rangle t_{b_\sigma}^{j_\sigma\,(1,0)} \tag{B.351}$$

where (B.350) follows from spin-integration of amplitudes, multipliers and overlap integrals and (B.351) from spin-integration of the two-electron integrals.
Finally, we get for the sum of the four diagrams

$$\begin{aligned}
\lambda_{\mu_1}^{(0,0)} \langle \mu_1 | (\hat{V}_N^{(0,0)} \tau_{i_\sigma}^{a_\sigma} T_1^{(1,0)})_C | 0 \rangle &= \lambda_{i_\sigma}^{c_\sigma\,(0,0)} \sum_{\tau} \langle c_\sigma j_\tau \hat{|} a_\sigma b_\tau \rangle t_{b_\tau}^{j_\tau\,(1,0)} \\
&- \lambda_{i_\sigma}^{c_\sigma\,(0,0)} \langle c_\sigma j_\sigma \hat{|} b_\sigma a_\sigma \rangle t_{b_\sigma}^{j_\sigma\,(1,0)} - S_{a_\sigma c_\sigma} \lambda_{k_\sigma}^{c_\sigma\,(0,0)} \sum_{\tau} \langle i_\sigma j_\tau \hat{|} k_\sigma b_\tau \rangle t_{b_\tau}^{j_\tau\,(1,0)} \\
&+ S_{a_\sigma c_\sigma} \lambda_{k_\sigma}^{c_\sigma\,(0,0)} \langle i_\sigma j_\sigma \hat{|} b_\sigma k_\sigma \rangle t_{b_\sigma}^{j_\sigma\,(1,0)} + \sum_{\tau} \lambda_{j_\tau}^{c_\tau\,(0,0)} \langle c_\tau i_\sigma \hat{|} b_\tau a_\sigma \rangle t_{b_\tau}^{j_\tau\,(1,0)} \\
&- \lambda_{j_\sigma}^{c_\sigma\,(0,0)} \langle c_\sigma i_\sigma \hat{|} a_\sigma b_\sigma \rangle t_{b_\sigma}^{j_\sigma\,(1,0)} - \sum_{\tau} S_{c_\tau b_\tau} \lambda_{k_\tau}^{c_\tau\,(0,0)} \langle j_\tau i_\sigma | k_\tau a_\sigma \rangle t_{b_\tau}^{j_\tau\,(1,0)} \\
&+ S_{c_\sigma b_\sigma} \lambda_{k_\sigma}^{c_\sigma\,(0,0)} \langle j_\sigma i_\sigma | a_\sigma k_\sigma \rangle t_{b_\sigma}^{j_\sigma\,(1,0)}
\end{aligned} \tag{B.352}$$

The complete contraction is therefore

$$\begin{aligned}\left(\lambda_{\mu_1}^{(0,0)}B_{\mu_1\nu_1\rho_1}^{(0,0)}t_{\rho_1}^{(1,0)}\right)_{i_\sigma}^{a_\sigma} &= -\hat{f}_{i_\sigma b_\sigma}t_{b_\sigma}^{j_\sigma(1,0)}\lambda_{j_\sigma}^{c_\sigma(0,0)}S_{a_\sigma c_\sigma} - \lambda_{i_\sigma}^{c_\sigma(0,0)}S_{c_\sigma b_\sigma}t_{b_\sigma}^{j_\sigma(1,0)}\hat{f}_{j_\sigma a_\sigma}\\ &+ \lambda_{i_\sigma}^{c_\sigma(0,0)}\sum_\tau\langle c_\sigma j_\tau\hat{|}a_\sigma b_\tau\rangle t_{b_\tau}^{j_\tau(1,0)} - \lambda_{i_\sigma}^{c_\sigma(0,0)}\langle c_\sigma j_\sigma\hat{|}b_\sigma a_\sigma\rangle t_{b_\sigma}^{j_\sigma(1,0)}\\ &- S_{a_\sigma c_\sigma}\lambda_{k_\sigma}^{c_\sigma(0,0)}\sum_\tau\langle i_\sigma j_\tau\hat{|}k_\sigma b_\tau\rangle t_{b_\tau}^{j_\tau(1,0)} + S_{a_\sigma c_\sigma}\lambda_{k_\sigma}^{c_\sigma(0,0)}\langle i_\sigma j_\sigma\hat{|}b_\sigma k_\sigma\rangle t_{b_\sigma}^{j_\sigma(1,0)}\\ &+ \sum_\tau\lambda_{j_\tau}^{c_\tau(0,0)}\langle c_\tau i_\sigma\hat{|}b_\tau a_\sigma\rangle t_{b_\tau}^{j_\tau(1,0)} - \lambda_{j_\sigma}^{c_\sigma(0,0)}\langle c_\sigma i_\sigma\hat{|}a_\sigma b_\sigma\rangle t_{b_\sigma}^{j_\sigma(1,0)}\\ &- \sum_\tau S_{c_\tau b_\tau}\lambda_{k_\tau}^{c_\tau(0,0)}\langle j_\tau i_\sigma|k_\tau a_\sigma\rangle t_{b_\tau}^{j_\tau(1,0)} + S_{c_\sigma b_\sigma}\lambda_{k_\sigma}^{c_\sigma(0,0)}\langle j_\sigma i_\sigma|a_\sigma k_\sigma\rangle t_{b_\sigma}^{j_\sigma(1,0)}\end{aligned} \tag{B.353}$$

B.3.1.17.2 $\lambda_{\mu_1}^{(0,0)}B_{\mu_1\nu_1\rho_2}^{(0,0)}t_{\rho_2}^{(1,0)}$

Since the contraction of the zeroth order singles multipliers and the perturbed doubles amplitudes with the singles-singles-doubles block (B.334) of the B-matrix is identical to the third contribution (B.209) to the contraction of the zeroth order singles multipliers with the the zeroth order singles-singles block of the zeroth order Jacobian except for a change in orders of the doubles multipliers, we get essentially the same diagrams

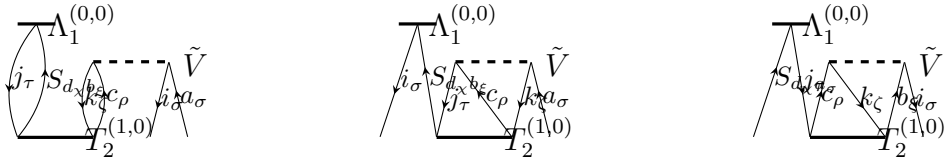

with the evaluation

$$\begin{aligned}\left(\lambda_{\mu_1}^{(0,0)}B_{\mu_1\nu_1\rho_2}^{(0,0)}t_{\rho_2}^{(1,0)}\right)_{i_\sigma}^{a_\sigma} &= \lambda_{\mu_1}^{(0,0)}\langle\mu_1|(\hat{V}_N\tau_{i_\sigma}^{a_\sigma}T_2^{(1,0)})_C|0\rangle\\ &= \sum_\tau S_{d_\tau b_\tau}\lambda_{j_\tau}^{d_\tau(0,0)}\left(\sum_\rho t_{b_\tau c_\rho}^{j_\tau k_\rho(1,0)}\langle k_\rho i_\sigma|c_\rho a_\sigma\rangle - t_{b_\tau c_\sigma}^{j_\tau k_\sigma(1,0)}\langle k_\sigma i_\sigma|a_\sigma c_\sigma\rangle\right)\\ &- S_{d_\sigma b_\sigma}\lambda_{i_\sigma}^{d_\sigma(0,0)}\sum_\tau t_{b_\sigma c_\tau}^{j_\sigma k_\tau(1,0)}\langle j_\sigma k_\tau|a_\sigma c_\tau\rangle\\ &- S_{d_\sigma a_\sigma}\lambda_{j_\sigma}^{d_\sigma(0,0)}\sum_\tau t_{b_\sigma c_\tau}^{j_\sigma k_\tau(1,0)}\langle k_\tau i_\sigma|c_\tau b_\sigma\rangle.\end{aligned} \tag{B.354}$$

B.3.1.17.3 $\lambda_{\mu_1}^{(0,0)}B_{\mu_1\nu_2\rho_1}^{(0,0)}t_{\rho_1}^{(1,0)}$

For the contraction of the zeroth order singles multipliers and the perturbed singles amplitudes with the singles-doubles-singles block (B.335) of the B-matrix we have to consider the three diagrams

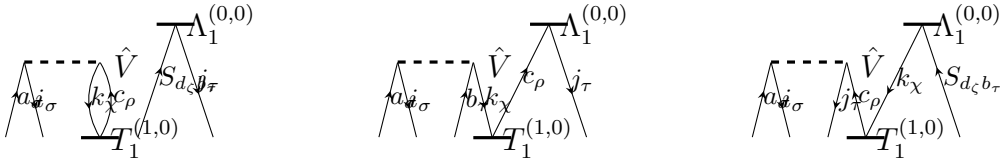

Note that the multipliers in the first diagram are disconnected from the rest.
The first of these diagrams evaluates to

$$D1_{i_\sigma j_\tau}^{a_\sigma b_\tau} = P(i_\sigma,j_\tau)P(a_\sigma,b_\tau)\sum_{\rho\chi\zeta}S_{d_\zeta b_\tau}\lambda_{j_\tau}^{d_\zeta(0,0)}t_{c_\rho}^{k_\chi(1,0)}\left(\langle i_\sigma k_\chi|a_\sigma c_\rho\rangle - \langle i_\sigma k_\chi|c_\rho a_\sigma\rangle\right) \tag{B.355}$$

$$
\begin{aligned}
=&\sum_{\rho\chi\zeta} S_{d_\zeta b_\tau} \lambda_{j_\tau}^{d_\zeta(0,0)} t_{c_\rho}^{k_\chi(1,0)} \Big(\langle i_\sigma k_\chi | a_\sigma c_\rho \rangle - \langle i_\sigma k_\chi | c_\rho a_\sigma \rangle \Big) \\
&+ \sum_{\rho\chi\zeta} S_{d_\zeta a_\sigma} \lambda_{i_\sigma}^{d_\zeta(0,0)} t_{c_\rho}^{k_\chi(1,0)} \Big(\langle j_\tau k_\chi | b_\tau c_\rho \rangle - \langle j_\tau k_\chi | c_\rho b_\tau \rangle \Big) \\
&- \sum_{\rho\chi\zeta} S_{d_\zeta b_\tau} \lambda_{i_\sigma}^{d_\zeta(0,0)} t_{c_\rho}^{k_\chi(1,0)} \Big(\langle j_\tau k_\chi | a_\sigma c_\rho \rangle - \langle j_\tau k_\chi | c_\rho a_\sigma \rangle \Big) \\
&- \sum_{\rho\chi\zeta} S_{d_\zeta a_\sigma} \lambda_{j_\tau}^{d_\zeta(0,0)} t_{c_\rho}^{k_\chi(1,0)} \Big(\langle i_\sigma k_\chi | b_\tau c_\rho \rangle - \langle i_\sigma k_\chi | c_\rho b_\tau \rangle \Big) \qquad \text{(B.356)} \\
=&S_{d_\tau b_\tau} \lambda_{j_\tau}^{d_\tau(0,0)} \sum_\rho t_{c_\rho}^{k_\rho(1,0)} \Big(\langle i_\sigma k_\rho | a_\sigma c_\rho \rangle - \delta_{\sigma\rho} \langle i_\sigma k_\rho | c_\rho a_\sigma \rangle \Big) \\
&+ S_{d_\sigma a_\sigma} \lambda_{i_\sigma}^{d_\sigma(0,0)} \sum_\rho t_{c_\rho}^{k_\rho(1,0)} \Big(\langle j_\tau k_\rho | b_\tau c_\rho \rangle - \delta_{\tau\rho} \langle j_\tau k_\rho | c_\rho b_\tau \rangle \Big) \\
&- \delta_{\sigma\tau} S_{d_\sigma b_\sigma} \lambda_{i_\sigma}^{d_\sigma(0,0)} \sum_\rho t_{c_\rho}^{k_\rho(1,0)} \Big(\langle j_\sigma k_\rho | a_\sigma c_\rho \rangle - \delta_{\sigma\rho} \langle j_\sigma k_\rho | c_\rho a_\sigma \rangle \Big) \\
&- \delta_{\sigma\tau} S_{d_\sigma a_\sigma} \lambda_{j_\sigma}^{d_\sigma(0,0)} \sum_\rho t_{c_\rho}^{k_\rho(1,0)} \Big(\langle i_\sigma k_\rho | b_\sigma c_\rho \rangle - \delta_{\sigma\rho} \langle i_\sigma k_\rho | c_\rho b_\sigma \rangle \Big) \qquad \text{(B.357)} \\
=&S_{d_\tau b_\tau} \lambda_{j_\tau}^{d_\tau(0,0)} \Big(\sum_\rho t_{c_\rho}^{k_\rho(1,0)} \langle i_\sigma k_\rho | a_\sigma c_\rho \rangle - t_{c_\sigma}^{k_\sigma(1,0)} \langle i_\sigma k_\sigma | c_\sigma a_\sigma \rangle \Big) \\
&+ S_{d_\sigma a_\sigma} \lambda_{i_\sigma}^{d_\sigma(0,0)} \Big(\sum_\rho t_{c_\rho}^{k_\rho(1,0)} \langle j_\tau k_\rho | b_\tau c_\rho \rangle - t_{c_\tau}^{k_\tau(1,0)} \langle j_\tau k_\tau | c_\tau b_\tau \rangle \Big) \\
&- \delta_{\sigma\tau} S_{d_\sigma b_\sigma} \lambda_{i_\sigma}^{d_\sigma(0,0)} \Big(\sum_\rho t_{c_\rho}^{k_\rho(1,0)} \langle j_\sigma k_\rho | a_\sigma c_\rho \rangle - t_{c_\sigma}^{k_\sigma(1,0)} \langle j_\sigma k_\sigma | c_\sigma a_\sigma \rangle \Big) \\
&- \delta_{\sigma\tau} S_{d_\sigma a_\sigma} \lambda_{j_\sigma}^{d_\sigma(0,0)} \Big(\sum_\rho t_{c_\rho}^{k_\rho(1,0)} \langle i_\sigma k_\rho | b_\sigma c_\rho \rangle - t_{c_\sigma}^{k_\sigma(1,0)} \langle i_\sigma k_\sigma | c_\sigma b_\sigma \rangle \Big) \qquad \text{(B.358)}
\end{aligned}
$$

where (B.356) follows from application of the permutation operators, (B.357) from spin-integration of overlap integrals, multipliers and amplitudes and (B.358) from spin-integration of the integrals.
The second diagram evaluates to

$$
\begin{aligned}
D2_{i_\sigma j_\tau}^{a_\sigma b_\tau} =& - P(i_\sigma, j_\tau) \sum_{\rho\chi} \lambda_{j_\tau}^{d_\rho(0,0)} S_{d_\rho c_\rho} t_{c_\rho}^{k_\chi(1,0)} \Big(\langle i_\sigma k_\chi | a_\sigma b_\tau \rangle - \langle i_\sigma k_\chi | b_\tau a_\sigma \rangle \Big) \qquad \text{(B.359)} \\
=& - \sum_{\rho\chi} \lambda_{j_\tau}^{d_\rho(0,0)} S_{d_\rho c_\rho} t_{c_\rho}^{k_\chi(1,0)} \Big(\langle i_\sigma k_\chi | a_\sigma b_\tau \rangle - \langle i_\sigma k_\chi | b_\tau a_\sigma \rangle \Big) \\
&+ \sum_{\rho\chi} \lambda_{i_\sigma}^{d_\rho(0,0)} S_{d_\rho c_\rho} t_{c_\rho}^{k_\chi(1,0)} \Big(\langle j_\tau k_\chi | a_\sigma b_\tau \rangle - \langle j_\tau k_\chi | b_\tau a_\sigma \rangle \Big) \qquad \text{(B.360)} \\
=& - \lambda_{j_\tau}^{d_\tau(0,0)} S_{d_\tau c_\tau} t_{c_\tau}^{k_\tau(1,0)} \Big(\langle i_\sigma k_\tau | a_\sigma b_\tau \rangle - \delta_{\sigma\tau} \langle i_\sigma k_\tau | b_\tau a_\sigma \rangle \Big) \\
&+ \lambda_{i_\sigma}^{d_\sigma(0,0)} S_{d_\sigma c_\sigma} t_{c_\sigma}^{k_\sigma(1,0)} \Big(\delta_{\sigma\tau} \langle j_\tau k_\sigma | a_\sigma b_\tau \rangle - \langle j_\tau k_\sigma | b_\tau a_\sigma \rangle \Big) \qquad \text{(B.361)}
\end{aligned}
$$

where (B.360) follows from application of the permutation operator and (B.361) from spin-integration of amplitudes and multipliers.
The last diagram evaluates to

$$D3^{a_\sigma b_\tau}_{i_\sigma j_\tau} = -P(a_\sigma, b_\tau) \sum_{\rho\chi\zeta} S_{d_\zeta b_\tau} \lambda^{d_\zeta\,(0,0)}_{k_\chi} t^{k_\chi(1,0)}_{c_\rho} \Big(\langle i_\sigma j_\tau | a_\sigma c_\rho \rangle - \langle i_\sigma j_\tau | c_\rho a_\sigma \rangle \Big) \tag{B.362}$$

$$= -\sum_{\rho\chi\zeta} S_{d_\zeta b_\tau} \lambda^{d_\zeta\,(0,0)}_{k_\chi} t^{k_\chi(1,0)}_{c_\rho} \Big(\langle i_\sigma j_\tau | a_\sigma c_\rho \rangle - \langle i_\sigma j_\tau | c_\rho a_\sigma \rangle \Big)$$
$$+ \sum_{\rho\chi\zeta} S_{d_\zeta a_\sigma} \lambda^{d_\zeta\,(0,0)}_{k_\chi} t^{k_\chi(1,0)}_{c_\rho} \Big(\langle i_\sigma j_\tau | b_\tau c_\rho \rangle - \langle i_\sigma j_\tau | c_\rho b_\tau \rangle \Big) \tag{B.363}$$

$$= -S_{d_\tau b_\tau} \lambda^{d_\tau\,(0,0)}_{k_\tau} t^{k_\tau(1,0)}_{c_\tau} \Big(\langle i_\sigma j_\tau | a_\sigma c_\tau \rangle - \delta_{\sigma\tau} \langle i_\sigma j_\tau | c_\tau a_\sigma \rangle \Big)$$
$$+ S_{d_\sigma a_\sigma} \lambda^{d_\sigma\,(0,0)}_{k_\sigma} t^{k_\sigma(1,0)}_{c_\sigma} \Big(\delta_{\sigma\tau} \langle i_\sigma j_\tau | b_\tau c_\sigma \rangle - \langle i_\sigma j_\tau | c_\sigma b_\tau \rangle \Big) \tag{B.364}$$

where (B.363) follows from application of the permutation operator and (B.364) from spin-integration of amplitudes and multipliers.
Thus, the complete contraction is

$$\Big(\lambda^{(0,0)}_{\mu_1} B^{(0,0)}_{\mu_1\nu_2\rho_1} t^{(1,0)}_{\rho_1} \Big)^{a_\sigma b_\tau}_{i_\sigma j_\tau} = S_{d_\tau b_\tau} \lambda^{d_\tau\,(0,0)}_{j_\tau} \Big(\sum_\rho t^{k_\rho(1,0)}_{c_\rho} \langle i_\sigma k_\rho | a_\sigma c_\rho \rangle - t^{k_\sigma(1,0)}_{c_\sigma} \langle i_\sigma k_\sigma | c_\sigma a_\sigma \rangle \Big)$$
$$+ S_{d_\sigma a_\sigma} \lambda^{d_\sigma\,(0,0)}_{i_\sigma} \Big(\sum_\rho t^{k_\rho(1,0)}_{c_\rho} \langle j_\tau k_\rho | b_\tau c_\rho \rangle - t^{k_\tau(1,0)}_{c_\tau} \langle j_\tau k_\tau | c_\tau b_\tau \rangle \Big)$$
$$- \delta_{\sigma\tau} S_{d_\sigma b_\sigma} \lambda^{d_\sigma\,(0,0)}_{i_\sigma} \Big(\sum_\rho t^{k_\rho(1,0)}_{c_\rho} \langle j_\sigma k_\rho | a_\sigma c_\rho \rangle - t^{k_\sigma(1,0)}_{c_\sigma} \langle j_\sigma k_\sigma | c_\sigma a_\sigma \rangle \Big)$$
$$- \delta_{\sigma\tau} S_{d_\sigma a_\sigma} \lambda^{d_\sigma\,(0,0)}_{j_\sigma} \Big(\sum_\rho t^{k_\rho(1,0)}_{c_\rho} \langle i_\sigma k_\rho | b_\sigma c_\rho \rangle - t^{k_\sigma(1,0)}_{c_\sigma} \langle i_\sigma k_\sigma | c_\sigma b_\sigma \rangle \Big)$$
$$- \lambda^{d_\tau\,(0,0)}_{j_\tau} S_{d_\tau c_\tau} t^{k_\tau(1,0)}_{c_\tau} \Big(\langle i_\sigma k_\tau | a_\sigma b_\tau \rangle - \delta_{\sigma\tau} \langle i_\sigma k_\tau | b_\tau a_\sigma \rangle \Big)$$
$$+ \lambda^{d_\sigma\,(0,0)}_{i_\sigma} S_{d_\sigma c_\sigma} t^{k_\sigma(1,0)}_{c_\sigma} \Big(\delta_{\sigma\tau} \langle j_\tau k_\sigma | a_\sigma b_\tau \rangle - \langle j_\tau k_\sigma | b_\tau a_\sigma \rangle \Big)$$
$$- S_{d_\tau b_\tau} \lambda^{d_\tau\,(0,0)}_{k_\tau} t^{k_\tau(1,0)}_{c_\tau} \Big(\langle i_\sigma j_\tau | a_\sigma c_\tau \rangle - \delta_{\sigma\tau} \langle i_\sigma j_\tau | c_\tau a_\sigma \rangle \Big)$$
$$+ S_{d_\sigma a_\sigma} \lambda^{d_\sigma\,(0,0)}_{k_\sigma} t^{k_\sigma(1,0)}_{c_\sigma} \Big(\delta_{\sigma\tau} \langle i_\sigma j_\tau | b_\tau c_\sigma \rangle - \langle i_\sigma j_\tau | c_\sigma b_\tau \rangle \Big) \tag{B.365}$$

B.3.1.17.4 $\lambda^{(0,0)}_{\mu_2} B^{(0,0)}_{\mu_2\nu_1\rho_1} t^{(1,0)}_{\rho_1}$

Contraction of the zeroth order doubles multipliers and perturbed singles amplitudes with the singles-singles-doubles block (B.336) of the B-matrix consists of the four diagrams

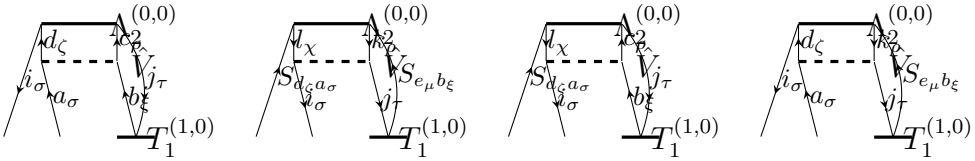

The first of these diagrams evaluates to

$$D1_{i_\sigma}^{a_\sigma} = \frac{1}{2}\sum_{\substack{\tau\xi\\ \zeta\rho}} t_{b_\xi}^{j_\tau(1,0)} \lambda_{i_\sigma j_\tau}^{d_\zeta c_\rho(0,0)} \Big(\langle d_\zeta c_\rho \hat{|} a_\sigma b_\xi\rangle - \langle d_\zeta c_\rho \hat{|} b_\xi a_\sigma\rangle \Big) \tag{B.366}$$

$$= \frac{1}{2}\sum_{\tau\zeta\rho} t_{b_\tau}^{j_\tau(1,0)} \Big(\delta_{\zeta\sigma}\delta_{\rho\tau} \lambda_{i_\sigma j_\tau}^{d_\zeta c_\rho(0,0)} \langle d_\zeta c_\rho \hat{|} a_\sigma b_\tau\rangle - \lambda_{i_\sigma j_\tau}^{d_\zeta c_\rho(0,0)} \delta_{\zeta\tau}\delta_{\rho\sigma} \langle d_\zeta c_\rho \hat{|} b_\tau a_\sigma\rangle \Big) \tag{B.367}$$

$$= \frac{1}{2}\sum_{\tau} t_{b_\tau}^{j_\tau(1,0)} \Big(\lambda_{i_\sigma j_\tau}^{d_\sigma c_\tau(0,0)} \langle d_\sigma c_\tau \hat{|} a_\sigma b_\tau\rangle - \lambda_{i_\sigma j_\tau}^{d_\tau c_\sigma(0,0)} \langle d_\tau c_\sigma \hat{|} b_\tau a_\sigma\rangle \Big) \tag{B.368}$$

$$= \frac{1}{2}\sum_{\tau} t_{b_\tau}^{j_\tau(1,0)} \Big(\lambda_{i_\sigma j_\tau}^{c_\sigma d_\tau(0,0)} \langle c_\sigma d_\tau \hat{|} a_\sigma b_\tau\rangle - \lambda_{i_\sigma j_\tau}^{d_\tau c_\sigma(0,0)} \langle d_\tau c_\sigma \hat{|} b_\tau a_\sigma\rangle \Big) \tag{B.369}$$

$$= \sum_{\tau} t_{b_\tau}^{j_\tau(1,0)} \lambda_{i_\sigma j_\tau}^{c_\sigma d_\tau(0,0)} \langle c_\sigma d_\tau \hat{|} a_\sigma b_\tau\rangle \tag{B.370}$$

where (B.367) follows from spin-integration of the amplitudes, (B.368) from spin-integration of the two-electron integrals, (B.369) from renaming of summation indices and (B.370) from symmetry of the two-electron integrals and antisymmetry of the multipliers.
The second diagram evaluates to

$$D2_{i_\sigma}^{a_\sigma} = \frac{1}{2}\sum_{\substack{\tau\xi\zeta\\ \mu\chi\rho}} t_{b_\xi}^{j_\tau(1,0)} S_{d_\zeta a_\sigma} S_{e_\mu b_\xi} \lambda_{l_\chi k_\rho}^{d_\zeta e_\mu(0,0)} \Big(\langle i_\sigma j_\tau \hat{|} l_\chi k_\rho\rangle - \langle i_\sigma j_\tau \hat{|} k_\rho l_\chi\rangle \Big) \tag{B.371}$$

$$= \frac{1}{2} S_{d_\sigma a_\sigma} \sum_{\tau\chi\rho} t_{b_\tau}^{j_\tau(1,0)} S_{e_\tau b_\tau} \Big(\lambda_{l_\chi k_\rho}^{d_\sigma e_\tau(0,0)} \delta_{\sigma\chi}\delta_{\tau\rho} \langle i_\sigma j_\tau \hat{|} l_\chi k_\rho\rangle$$

$$- \lambda_{l_\chi k_\rho}^{d_\sigma e_\tau(0,0)} \delta_{\sigma\rho}\delta_{\tau\chi} \langle i_\sigma j_\tau \hat{|} k_\rho l_\chi\rangle \Big) \tag{B.372}$$

$$= \frac{1}{2} S_{d_\sigma a_\sigma} \sum_{\tau} t_{b_\tau}^{j_\tau(1,0)} S_{e_\tau b_\tau} \Big(\lambda_{l_\sigma k_\tau}^{d_\sigma e_\tau(0,0)} \langle i_\sigma j_\tau \hat{|} l_\sigma k_\tau\rangle - \lambda_{l_\tau k_\sigma}^{d_\sigma e_\tau(0,0)} \langle i_\sigma j_\tau \hat{|} k_\sigma l_\tau\rangle \Big) \tag{B.373}$$

$$= \frac{1}{2} S_{d_\sigma a_\sigma} \sum_{\tau} t_{b_\tau}^{j_\tau(1,0)} S_{e_\tau b_\tau} \Big(\lambda_{k_\sigma l_\tau}^{d_\sigma e_\tau(0,0)} \langle i_\sigma j_\tau \hat{|} k_\sigma l_\tau\rangle - \lambda_{l_\tau k_\sigma}^{d_\sigma e_\tau(0,0)} \langle i_\sigma j_\tau \hat{|} k_\sigma l_\tau\rangle \Big) \tag{B.374}$$

$$= S_{d_\sigma a_\sigma} \sum_{\tau} t_{b_\tau}^{j_\tau(1,0)} S_{e_\tau b_\tau} \lambda_{k_\sigma l_\tau}^{d_\sigma e_\tau(0,0)} \langle i_\sigma j_\tau \hat{|} k_\sigma l_\tau\rangle \tag{B.375}$$

where (B.372) follows from spin-integration of the amplitudes and overlap integrals, (B.373) from spin-integration of the two-electron integrals, (B.374) from renaming of summation indices and (B.375) from antisymmetry of the multipliers.
The third diagram evaluates to

$$D3_{i_\sigma}^{a_\sigma} = -\sum_{\substack{\tau\xi\zeta\\ \rho\chi}} t_{b_\xi}^{j_\tau(1,0)} S_{d_\zeta a_\sigma} \lambda_{l_\chi j_\tau}^{d_\zeta c_\rho(0,0)} \Big(\langle i_\sigma c_\rho \hat{|} l_\chi b_\xi\rangle - \langle i_\sigma c_\rho \hat{|} b_\xi l_\chi\rangle \Big) \tag{B.376}$$

$$= - S_{d_\sigma a_\sigma} \sum_{\tau\rho\chi} t_{b_\tau}^{j_\tau(1,0)} \lambda_{l_\chi j_\tau}^{d_\sigma c_\rho(0,0)} \delta_{\sigma\chi}\delta_{\rho\tau} \langle i_\sigma c_\rho \hat{|} l_\chi b_\tau\rangle$$

$$+ S_{d_\sigma a_\sigma} \sum_{\tau\rho\chi} t_{b_\tau}^{j_\tau(1,0)} \lambda_{l_\chi j_\tau}^{d_\sigma c_\rho(0,0)} \delta_{\sigma\tau}\delta_{\rho\chi} \langle i_\sigma c_\rho \hat{|} b_\tau l_\chi\rangle \tag{B.377}$$

$$= - S_{d_\sigma a_\sigma} \sum_{\rho} t_{b_\rho}^{j_\rho(1,0)} \lambda_{l_\sigma j_\rho}^{d_\sigma c_\rho(0,0)} \langle i_\sigma c_\rho \hat{|} l_\sigma b_\rho\rangle$$

$$+ S_{d_\sigma a_\sigma} \sum_{\rho} t_{b_\sigma}^{j_\sigma(1,0)} \lambda_{l_\rho j_\sigma}^{d_\sigma c_\rho(0,0)} \langle i_\sigma c_\rho \hat{|} b_\sigma l_\rho \rangle \tag{B.378}$$

$$= - S_{d_\sigma a_\sigma} \sum_{\rho} t_{b_\rho}^{j_\rho(1,0)} \lambda_{l_\sigma j_\rho}^{d_\sigma c_\rho(0,0)} \langle i_\sigma c_\rho \hat{|} l_\sigma b_\rho \rangle$$

$$- S_{d_\sigma a_\sigma} t_{b_\sigma}^{j_\sigma(1,0)} \sum_{\rho} \lambda_{j_\sigma l_\rho}^{d_\sigma c_\rho(0,0)} \langle i_\sigma c_\rho \hat{|} b_\sigma l_\rho \rangle \tag{B.379}$$

where (B.377) follows from spin-integration of the amplitudes and overlap integrals, (B.378) from spin-integration of the two-electron integrals and (B.379) from antisymmetry of the multipliers.
The last diagram evaluates to

$$D4_{i_\sigma}^{a_\sigma} = - \sum_{\substack{\tau\xi\mu \\ \zeta\rho}} t_{b_\xi}^{j_\tau(1,0)} S_{e_\mu b_\xi} \lambda_{i_\sigma k_\rho}^{d_\zeta e_\mu(0,0)} \Big(\langle d_\zeta j_\tau \hat{|} a_\sigma k_\rho \rangle - \langle d_\zeta j_\tau \hat{|} k_\rho a_\sigma \rangle \Big) \tag{B.380}$$

$$= - \sum_{\tau\zeta\rho} t_{b_\tau}^{j_\tau(1,0)} S_{e_\tau b_\tau} \lambda_{i_\sigma k_\rho}^{d_\zeta e_\tau(0,0)} \delta_{\zeta\sigma} \delta_{\tau\rho} \langle d_\zeta j_\tau \hat{|} a_\sigma k_\rho \rangle$$

$$+ \sum_{\tau\zeta\rho} t_{b_\tau}^{j_\tau(1,0)} S_{e_\tau b_\tau} \lambda_{i_\sigma k_\rho}^{d_\zeta e_\tau(0,0)} \delta_{\zeta\rho} \delta_{\tau\sigma} \langle d_\zeta j_\tau \hat{|} k_\rho a_\sigma \rangle \tag{B.381}$$

$$= - \sum_{\rho} t_{b_\rho}^{j_\rho(1,0)} S_{e_\rho b_\rho} \lambda_{i_\sigma k_\rho}^{d_\sigma e_\rho(0,0)} \langle d_\sigma j_\rho \hat{|} a_\sigma k_\rho \rangle$$

$$+ S_{e_\sigma b_\sigma} t_{b_\sigma}^{j_\sigma(1,0)} \sum_{\rho} \lambda_{i_\sigma k_\rho}^{d_\rho e_\sigma(0,0)} \langle d_\rho j_\sigma \hat{|} k_\rho a_\sigma \rangle \tag{B.382}$$

$$= - \sum_{\rho} t_{b_\rho}^{j_\rho(1,0)} S_{e_\rho b_\rho} \lambda_{i_\sigma k_\rho}^{d_\sigma e_\rho(0,0)} \langle d_\sigma j_\rho \hat{|} a_\sigma k_\rho \rangle$$

$$- S_{e_\sigma b_\sigma} t_{b_\sigma}^{j_\sigma(1,0)} \sum_{\rho} \lambda_{i_\sigma k_\rho}^{e_\sigma d_\rho(0,0)} \langle d_\rho j_\sigma \hat{|} k_\rho a_\sigma \rangle \tag{B.383}$$

where (B.381) follows from spin-integration of the amplitudes and overlap integrals, (B.382) from spin-integration of the two-electron integrals, and (B.383) from antisymmetry of the multipliers.
Thus, the complete contraction is

$$\begin{aligned}
\Big(\lambda_{\mu_2}^{(0,0)} B_{\mu_2\nu_1\rho_1}^{(0,0)} t_{\rho_1}^{(1,0)} \Big)_{i_\sigma}^{a_\sigma} = & \sum_{\tau} t_{b_\tau}^{j_\tau(1,0)} \lambda_{i_\sigma j_\tau}^{c_\sigma d_\tau(0,0)} \langle c_\sigma d_\tau \hat{|} a_\sigma b_\tau \rangle \\
& + S_{d_\sigma a_\sigma} \sum_{\tau} t_{b_\tau}^{j_\tau(1,0)} S_{e_\tau b_\tau} \lambda_{k_\sigma l_\tau}^{d_\sigma e_\tau(0,0)} \langle i_\sigma j_\tau \hat{|} k_\sigma l_\tau \rangle \\
& - S_{d_\sigma a_\sigma} \sum_{\tau} t_{b_\tau}^{j_\tau(1,0)} \lambda_{l_\sigma j_\tau}^{d_\sigma c_\tau(0,0)} \langle i_\sigma c_\tau \hat{|} l_\sigma b_\tau \rangle \\
& - S_{d_\sigma a_\sigma} t_{b_\sigma}^{j_\sigma(1,0)} \sum_{\tau} \lambda_{j_\sigma l_\tau}^{d_\sigma c_\tau(0,0)} \langle i_\sigma c_\tau \hat{|} b_\sigma l_\tau \rangle \\
& - \sum_{\tau} t_{b_\tau}^{j_\tau(1,0)} S_{e_\tau b_\tau} \lambda_{i_\sigma k_\tau}^{d_\sigma e_\tau(0,0)} \langle d_\sigma j_\tau \hat{|} a_\sigma k_\tau \rangle \\
& - S_{e_\sigma b_\sigma} t_{b_\sigma}^{j_\sigma(1,0)} \sum_{\tau} \lambda_{i_\sigma k_\tau}^{e_\sigma d_\tau(0,0)} \langle d_\tau j_\sigma \hat{|} k_\tau a_\sigma \rangle
\end{aligned} \tag{B.384}$$

where we have standardized the spin summation indices.

B.3.2 Reduction to working equations

In the following sections we will introduce several intermediates into the expressions we derived so far. Note that we do not seek the mathematically most beautiful intermediates, but those that are most convenient from an implementation and efficiency perspective. Thus, priorities are reduction of the matrix sizes, avoidance of repeated reading of the same integrals and efficient multiplication of intermediates. Introduction of a four index intermediate, for example, is usually very counterproductive even if it would apparently simplify the equations.
Many of the intermediates will be similar or even identical to those used by Kats *et al.*[46] for closed-shell excited states and their first order properties. This has the advantage that a lot of existing code could be reused or at least adapted for the open-shell case implemented in this work.
The most fundamental intermediate will be the density fitting of the two-electron integrals introduced in section 2.1.4

$$\langle p_\sigma r_\tau \hat{|} q_\sigma s_\tau \rangle \approx (P \hat{|} p_\sigma q_\sigma)[J^{-1}]_{PQ}(Q \hat{|} r_\tau s_\tau) = (P \hat{|} p_\sigma q_\sigma)\hat{C}_P^{r_\tau s_\tau} = \hat{C}_P^{p_\sigma q_\sigma}(P \hat{|} r_\tau s_\tau) \tag{B.385}$$

Note that capital letters P and Q represent here and in the following an additional auxiliary basis set, not general molecular orbital indices. Furthermore, due to (B.93) we have

$$(P \hat{|} i_\sigma a_\sigma) = (P|i_\sigma a_\sigma) \tag{B.386}$$
$$\hat{C}_P^{i_\sigma a_\sigma} = C_P^{i_\sigma a_\sigma}. \tag{B.387}$$

Generally, the integrals can be obtained from transformation of the atomic orbital integrals $(P|\mu\nu)$ with the matrices (B.88), (B.89), (B.98) and (B.99).
A second set of recurring intermediates are contractions of the overlap matrix with amplitudes

$$[St]_{a_\sigma}^{i_\sigma\,(m,n)} = S_{a_\sigma b_\sigma} t_{a_\sigma}^{i_\sigma\,(m,n)} \tag{B.388}$$
$$[St]_{a_\sigma b_\tau}^{i_\sigma j_\tau\,(m,n)} = S_{a_\sigma c_\sigma} t_{c_\sigma b_\tau}^{i_\sigma j_\tau\,(m,n)} \tag{B.389}$$
$$[tS]_{a_\sigma b_\tau}^{i_\sigma j_\tau\,(m,n)} = t_{a_\sigma d_\tau}^{i_\sigma j_\tau\,(m,n)} S_{d_\tau b_\tau} \tag{B.390}$$
$$[StS]_{a_\sigma b_\tau}^{i_\sigma j_\tau\,(m,n)} = S_{a_\sigma c_\sigma} t_{c_\sigma d_\tau}^{i_\sigma j_\tau\,(m,n)} S_{d_\tau b_\tau}. \tag{B.391}$$

and multipliers

$$[S\lambda]_{i_\sigma}^{a_\sigma\,(m,n)} = S_{a_\sigma b_\sigma} \lambda_{i_\sigma}^{a_\sigma\,(m,n)} \tag{B.392}$$
$$[S\lambda]_{i_\sigma j_\tau}^{a_\sigma b_\tau\,(m,n)} = S_{a_\sigma c_\sigma} \lambda_{i_\sigma j_\tau}^{c_\sigma b_\tau\,(m,n)} \tag{B.393}$$
$$[\lambda S]_{i_\sigma j_\tau}^{a_\sigma b_\tau\,(m,n)} = \lambda_{i_\sigma j_\tau}^{a_\sigma d_\tau\,(m,n)} S_{d_\tau b_\tau} \tag{B.394}$$
$$[S\lambda S]_{i_\sigma j_\tau}^{a_\sigma b_\tau\,(m,n)} = S_{a_\sigma c_\sigma} \lambda_{i_\sigma j_\tau}^{c_\sigma d_\tau\,(m,n)} S_{d_\tau b_\tau}. \tag{B.395}$$

Note that due to antisymmetry of doubles amplitudes and multipliers we have the equalities

$$[S\lambda]_{i_\sigma j_\tau}^{a_\sigma b_\tau\,(m,n)} = -[S\lambda]_{j_\tau i_\sigma}^{a_\sigma b_\tau\,(m,n)} = [\lambda S]_{j_\tau i_\sigma}^{b_\tau a_\sigma\,(m,n)} = -[\lambda S]_{i_\sigma j_\tau}^{b_\tau a_\sigma\,(m,n)} \tag{B.396}$$
$$[St]_{i_\sigma j_\tau}^{a_\sigma b_\tau\,(m,n)} = -[St]_{j_\tau i_\sigma}^{a_\sigma b_\tau\,(m,n)} = [tS]_{j_\tau i_\sigma}^{b_\tau a_\sigma\,(m,n)} = -[tS]_{i_\sigma j_\tau}^{b_\tau a_\sigma\,(m,n)}. \tag{B.397}$$

B.3.2.1 Zeroth order singles multiplier equations

The zeroth order singles multiplier equations have the following three contributions

$$\Lambda^{(0,0)}_{\nu_1} = \eta^{(0,0)}_{\nu_1} + \lambda^{(0,0)}_{\mu_1} A^{(0,0)}_{\mu_1\nu_1} + \lambda^{(0,0)}_{\mu_2} A^{(0,0)}_{\mu_2\nu_1} \stackrel{!}{=} 0. \tag{B.398}$$

B.3.2.1.1 $\eta^{(0,0)}_{\nu_1}$

The singles block of the energy derivative (B.139) yields the intermediate

$$\eta^{a_\sigma\,(0,0)}_{i_\sigma} = \hat{f}_{i_\sigma a_\sigma}. \tag{B.399}$$

Since this does not depend on the multipliers, it is constant throughout the iterations.

B.3.2.1.2 $\lambda^{(0,0)}_{\mu_1} A^{(0,0)}_{\mu_1\nu_1}$

For the contraction (B.210) of singles multipliers with the singles-singles block of the Jacobian we have

$$\begin{aligned}
\left(\lambda^{(0,0)}_{\mu_1} A^{(0,0)}_{\mu_1\nu_1}\right)^{a_\sigma}_{i_\sigma} &= \lambda^{b_\sigma\,(0,0)}_{i_\sigma} \hat{f}_{b_\sigma a_\sigma} - \hat{f}_{i_\sigma j_\sigma} [S\lambda]^{a_\sigma\,(0,0)}_{j_\sigma} + \sum_\tau \lambda^{b_\tau\,(0,0)}_{j_\tau} C_P^{b_\tau j_\tau}(P|i_\sigma a_\sigma) \\
&- \lambda^{b_\sigma\,(0,0)}_{j_\sigma} (P\hat{|}b_\sigma a_\sigma) \hat{C}_P^{i_\sigma j_\sigma} + \sum_\tau [S\lambda]^{b_\tau\,(0,0)}_{j_\tau} \sum_\rho t^{j_\tau k_\rho\,(0,0)}_{b_\tau c_\rho} C_P^{k_\rho c_\rho}(P|i_\sigma a_\sigma) \\
&- \sum_\tau [S\lambda]^{b_\tau\,(0,0)}_{j_\tau} t^{j_\tau k_\sigma\,(0,0)}_{b_\tau c_\sigma} (P|k_\sigma a_\sigma) C_P^{i_\sigma c_\sigma} \\
&- [S\lambda]^{b_\sigma\,(0,0)}_{i_\sigma} \sum_\tau t^{j_\sigma k_\tau\,(0,0)}_{b_\sigma c_\tau} (P|j_\sigma a_\sigma) C_P^{k_\tau c_\tau} \\
&- [S\lambda]^{a_\sigma\,(0,0)}_{j_\sigma} \sum_\tau t^{j_\sigma k_\tau\,(0,0)}_{b_\sigma c_\tau} C_P^{k_\tau c_\tau}(P|i_\sigma b_\sigma).
\end{aligned} \tag{B.400}$$

where we have introduced the density fitting (B.385) of the two-electron integrals.
The first intermediates we are going to introduce are the contraction of the doubles amplitudes with the fitting coefficients

$$A_P^{i_\sigma a_\sigma\,(0,0)} = \sum_\tau t^{i_\sigma j_\tau\,(0,0)}_{a_\sigma b_\tau} C_P^{j_\tau b_\tau}, \tag{B.401}$$

the contraction of the doubles amplitudes with the singles multipliers and the overlap integrals

$$\tilde{X}^{(0,0)}_{k_\sigma c_\sigma} = \sum_\tau [S\lambda]^{b_\tau\,(0,0)}_{j_\tau} t^{j_\tau k_\sigma\,(0,0)}_{b_\tau c_\sigma} \tag{B.402}$$

and the contraction of the singles multipliers with the fitting coefficients

$$\Delta\tilde{C}_P^{(0,0)} = \sum_\tau C_P^{b_\tau j_\tau} \lambda^{b_\tau\,(0,0)}_{j_\tau}. \tag{B.403}$$

This leads us to

$$\begin{aligned}
\left(\lambda^{(0,0)}_{\mu_1} A^{(0,0)}_{\mu_1\nu_1}\right)^{a_\sigma}_{i_\sigma} &= \lambda^{b_\sigma\,(0,0)}_{i_\sigma} \hat{f}_{b_\sigma a_\sigma} - \hat{f}_{i_\sigma j_\sigma} [S\lambda]^{a_\sigma\,(0,0)}_{j_\sigma} + \Delta\tilde{C}_P^{(0,0)}(P|i_\sigma a_\sigma) \\
&- \lambda^{b_\sigma\,(0,0)}_{j_\sigma} (P\hat{|}b_\sigma a_\sigma) \hat{C}_P^{i_\sigma j_\sigma} + \sum_\tau [S\lambda]^{b_\tau\,(0,0)}_{j_\tau} A_P^{j_\tau b_\tau\,(0,0)}(P|i_\sigma a_\sigma) \\
&- \tilde{X}^{(0,0)}_{k_\sigma c_\sigma}(P|k_\sigma a_\sigma) C_P^{i_\sigma c_\sigma} - [S\lambda]^{b_\sigma\,(0,0)}_{i_\sigma} A_P^{j_\sigma b_\sigma\,(0,0)}(P|j_\sigma a_\sigma) \\
&- [S\lambda]^{a_\sigma\,(0,0)}_{j_\sigma} A_P^{j_\sigma b_\sigma\,(0,0)}(P|i_\sigma b_\sigma).
\end{aligned} \tag{B.404}$$

Introducing the additional intermediates (the minus signs are here included to get agreement with the actual code)

$$Z_{i_\sigma j_\sigma}^{(0,0)} = -(P|i_\sigma b_\sigma) A_P^{j_\sigma b_\sigma\,(0,0)} \tag{B.405}$$

$$\tilde{Y}_P^{k_\sigma i_\sigma\,(0,0)} = -\tilde{X}_{k_\sigma c_\sigma}^{(0,0)} C_P^{i_\sigma c_\sigma} \tag{B.406}$$

$$\Delta\tilde{Y}_P^{j_\sigma i_\sigma\,(0,0)} = -A_P^{j_\sigma b_\sigma\,(0,0)} [S\lambda]_{i_\sigma}^{b_\sigma\,(0,0)} \tag{B.407}$$

yields

$$\begin{aligned}\left(\lambda_{\mu_1}^{(0,0)} A_{\mu_1\nu_1}^{(0,0)}\right)_{i_\sigma}^{a_\sigma} &= \lambda_{i_\sigma}^{b_\sigma\,(0,0)} \hat{f}_{b_\sigma a_\sigma} - \hat{f}_{i_\sigma j_\sigma} [S\lambda]_{j_\sigma}^{a_\sigma\,(0,0)} + \Delta\tilde{C}_P^{(0,0)} (P|i_\sigma a_\sigma) \\ &- \lambda_{j_\sigma}^{b_\sigma\,(0,0)} (P\hat{|}b_\sigma a_\sigma) \hat{C}_P^{i_\sigma j_\sigma} - \sum_\tau \Delta\tilde{Y}_P^{j_\tau j_\tau\,(0,0)} (P|i_\sigma a_\sigma) \\ &+ \tilde{Y}_P^{k_\sigma i_\sigma\,(0,0)} (P|k_\sigma a_\sigma) + \Delta\tilde{Y}_P^{j_\sigma i_\sigma\,(0,0)} (P|j_\sigma a_\sigma) + [S\lambda]_{j_\sigma}^{a_\sigma\,(0,0)} Z_{i_\sigma j_\sigma}^{(0,0)}.\end{aligned} \tag{B.408}$$

After defining the final intermediate of this section

$$\tilde{C}_P^{(0,0)} = \Delta\tilde{C}_P^{(0,0)} - \sum_\tau \tilde{Y}_P^{j_\tau j_\tau\,(0,0)} \tag{B.409}$$

and renaming of some indices we arrive at

$$\begin{aligned}\left(\lambda_{\mu_1}^{(0,0)} A_{\mu_1\nu_1}^{(0,0)}\right)_{i_\sigma}^{a_\sigma} &= \lambda_{i_\sigma}^{c_\sigma\,(0,0)} \hat{f}_{c_\sigma a_\sigma} - \hat{f}_{i_\sigma k_\sigma} [S\lambda]_{k_\sigma}^{a_\sigma\,(0,0)} + [S\lambda]_{k_\sigma}^{a_\sigma\,(0,0)} Z_{i_\sigma k_\sigma}^{(0,0)} \\ &+ \tilde{C}_P^{(0,0)} (P|i_\sigma a_\sigma) + \left(\tilde{Y}_P^{k_\sigma i_\sigma\,(0,0)} + \Delta\tilde{Y}_P^{k_\sigma i_\sigma\,(0,0)}\right) (P|k_\sigma a_\sigma) \\ &- \lambda_{k_\sigma}^{c_\sigma\,(0,0)} (P\hat{|}c_\sigma a_\sigma) \hat{C}_P^{i_\sigma k_\sigma}\end{aligned} \tag{B.410}$$

which are the equations as documented in the actual code (including choice of indices).

B.3.2.1.3 $\lambda_{\mu_2}^{(0,0)} A_{\mu_2\nu_1}^{(0,0)}$

Using the density fitting (B.385) to decompose the two-electron integrals in the contraction (B.219) of the doubles multipliers with the doubles-singles block of the Jacobian yields

$$\left(\lambda_{\mu_2}^{(0,0)} A_{\mu_2\nu_1}^{(0,0)}\right)_{i_\sigma}^{a_\sigma} = \sum_\tau \lambda_{i_\sigma j_\tau}^{c_\sigma b_\tau\,(0,0)} (P\hat{|}c_\sigma a_\sigma) \hat{C}_P^{b_\tau j_\tau} - S_{c_\sigma a_\sigma} \sum_\tau \lambda_{k_\sigma j_\tau}^{c_\sigma b_\tau\,(0,0)} (P\hat{|}i_\sigma k_\sigma) \hat{C}_P^{b_\tau j_\tau}. \tag{B.411}$$

Contracting the doubles multipliers with the fitting coefficients in analogy to (B.401) gives rise to the intermediate

$$\tilde{A}_P^{k_\sigma c_\sigma\,(0,0)} = \sum_\tau \lambda_{k_\sigma j_\tau}^{c_\sigma b_\tau\,(0,0)} \hat{C}_P^{b_\tau j_\tau} \tag{B.412}$$

and the simplification

$$\left(\lambda_{\mu_2}^{(0,0)} A_{\mu_2\nu_1}^{(0,0)}\right)_{i_\sigma}^{a_\sigma} = \tilde{A}_P^{i_\sigma c_\sigma\,(0,0)} (P\hat{|}c_\sigma a_\sigma) - S_{c_\sigma a_\sigma} \tilde{A}_P^{k_\sigma c_\sigma\,(0,0)} (P\hat{|}i_\sigma k_\sigma). \tag{B.413}$$

B.3.2.1.4 $\Lambda_{\nu_1}^{[0,0]}$

Combining (B.399), (B.410) and (B.413) we arrive at the working equations for the residuum of the zeroth order singles multiplier equations

$$\begin{aligned} v_{i_\sigma}^{a_\sigma} =& \eta_{i_\sigma}^{a_\sigma(0,0)} + \lambda_{i_\sigma}^{c_\sigma(0,0)} \hat{f}_{c_\sigma a_\sigma} - \hat{f}_{i_\sigma k_\sigma} [S\lambda]_{k_\sigma}^{a_\sigma(0,0)} + [S\lambda]_{k_\sigma}^{a_\sigma(0,0)} Z_{i_\sigma k_\sigma}^{(0,0)} \\ &+ \tilde{C}_P^{(0,0)}(P|i_\sigma a_\sigma) + \left(\tilde{Y}_P^{k_\sigma i_\sigma(0,0)} + \Delta\tilde{Y}_P^{k_\sigma i_\sigma(0,0)} \right)(P|k_\sigma a_\sigma) \\ &+ \left(- \lambda_{k_\sigma}^{c_\sigma(0,0)} \hat{C}_P^{i_\sigma k_\sigma} + \tilde{A}_P^{i_\sigma c_\sigma(0,0)} \right)(P\hat{|}c_\sigma a_\sigma) - S_{c_\sigma a_\sigma} \tilde{A}_P^{k_\sigma c_\sigma(0,0)}(P\hat{|}i_\sigma k_\sigma). \end{aligned} \tag{B.414}$$

B.3.2.2 Zeroth order doubles multiplier equations

The zeroth order doubles multiplier equations have the following three contributions

$$\Lambda_{\nu_2}^{[0,0]} = \eta_{\nu_2}^{(0,0)} + \lambda_{\mu_1}^{(0,0)} A_{\mu_1\nu_2}^{(0,0)} + \lambda_{\mu_2}^{(0,0)} A_{\mu_2\nu_2}^{(0,0)} \stackrel{!}{=} 0. \tag{B.415}$$

B.3.2.2.1 $\eta_{\nu_2}^{(0,0)}$

Using the density fitting (B.385), (B.139) reduces to

$$\eta_{i_\sigma j_\tau}^{a_\sigma b_\tau(0,0)} = C_P^{i_\sigma a_\sigma}(P|j_\tau b_\tau) - \delta_{\sigma\tau} C_P^{i_\sigma b_\sigma}(P|j_\sigma a_\sigma). \tag{B.416}$$

Introducing the internal exchange matrix for the pair $(i_\sigma j_\tau)$

$$K_{a_\sigma b_\tau}^{i_\sigma j_\tau} = C_P^{i_\sigma a_\sigma}(P|j_\tau b_\tau) \tag{B.417}$$

this reduces to

$$\eta_{i_\sigma j_\tau}^{a_\sigma b_\tau(0,0)} = K_{a_\sigma b_\tau}^{i_\sigma j_\tau} - \delta_{\sigma\tau} K_{b_\sigma a_\sigma}^{i_\sigma j_\sigma}. \tag{B.418}$$

This is again constant during the iterations and only has to be determined once.

B.3.2.2.2 $\lambda_{\mu_1}^{(0,0)} A_{\mu_1\nu_2}^{(0,0)}$

After use of the density fitting (B.385), we get from the contraction (B.232) of the singles multipliers with the singles-doubles block of the Jacobian

$$\begin{aligned} \left(\lambda_{\mu_1}^{(0,0)} A_{\mu_1\nu_2}^{(0,0)} \right)_{i_\sigma j_\tau}^{a_\sigma b_\tau} =& \hat{f}_{j_\tau b_\tau} [S\lambda]_{i_\sigma}^{a_\sigma(0,0)} + \hat{f}_{i_\sigma a_\sigma} [S\lambda]_{j_\tau}^{b_\tau(0,0)} - \delta_{\sigma\tau} \hat{f}_{j_\sigma a_\sigma} [S\lambda]_{i_\sigma}^{b_\sigma(0,0)} \\ &- \delta_{\sigma\tau} \hat{f}_{i_\sigma b_\sigma} [S\lambda]_{j_\sigma}^{a_\sigma(0,0)} + \lambda_{i_\sigma}^{c_\sigma(0,0)} (P\hat{|}c_\sigma a_\sigma) C_P^{j_\tau b_\tau} - \delta_{\sigma\tau} \lambda_{i_\sigma}^{c_\sigma(0,0)} (P\hat{|}c_\sigma b_\sigma) C_P^{j_\sigma a_\sigma} \\ &- \delta_{\sigma\tau} \lambda_{j_\sigma}^{c_\sigma(0,0)} (P\hat{|}c_\sigma a_\sigma) C_P^{i_\sigma b_\sigma} + \lambda_{j_\tau}^{c_\tau(0,0)} (P\hat{|}c_\tau b_\tau) C_P^{i_\sigma a_\sigma} \\ &- [S\lambda]_{k_\sigma}^{a_\sigma(0,0)} (P\hat{|}i_\sigma k_\sigma) C_P^{j_\tau b_\tau} + \delta_{\sigma\tau} [S\lambda]_{k_\sigma}^{a_\sigma(0,0)} C_P^{i_\sigma b_\sigma}(P\hat{|}j_\sigma k_\sigma) \\ &+ \delta_{\sigma\tau} [S\lambda]_{k_\sigma}^{b_\sigma(0,0)} (P\hat{|}i_\sigma k_\sigma) C_P^{j_\sigma a_\sigma} - [S\lambda]_{k_\tau}^{b_\tau(0,0)} C_P^{i_\sigma a_\sigma}(P|j_\tau k_\tau). \end{aligned} \tag{B.419}$$

Introducing the intermediate

$$\tilde{B}_P^{i_\sigma a_\sigma(0,0)} = \lambda_{i_\sigma}^{c_\sigma(0,0)} (P\hat{|}c_\sigma a_\sigma) - [S\lambda]_{k_\sigma}^{a_\sigma(0,0)} (P\hat{|}i_\sigma k_\sigma) \tag{B.420}$$

reduces this to

$$\begin{aligned} \left(\lambda_{\mu_1}^{(0,0)} A_{\mu_1\nu_2}^{(0,0)} \right)_{i_\sigma j_\tau}^{a_\sigma b_\tau} =& \hat{f}_{j_\tau b_\tau} [S\lambda]_{i_\sigma}^{a_\sigma(0,0)} + \hat{f}_{i_\sigma a_\sigma} [S\lambda]_{j_\tau}^{b_\tau(0,0)} - \delta_{\sigma\tau} \hat{f}_{j_\sigma a_\sigma} [S\lambda]_{i_\sigma}^{b_\sigma(0,0)} \\ &- \delta_{\sigma\tau} \hat{f}_{i_\sigma b_\sigma} [S\lambda]_{j_\sigma}^{a_\sigma(0,0)} + \tilde{B}_P^{i_\sigma a_\sigma(0,0)} C_P^{j_\tau b_\tau} - \delta_{\sigma\tau} \tilde{B}_P^{i_\sigma b_\sigma(0,0)} C_P^{j_\sigma a_\sigma} \\ &- \delta_{\sigma\tau} \tilde{B}_P^{j_\sigma a_\sigma(0,0)} C_P^{i_\sigma b_\sigma} + \tilde{B}_P^{j_\tau b_\tau(0,0)} C_P^{i_\sigma a_\sigma}. \end{aligned} \tag{B.421}$$

B.3.2.2.3 $\lambda_{\mu_2}^{(0,0)} A_{\mu_2\nu_2}^{(0,0)}$

The contraction (B.242) of the doubles multipliers with the doubles-doubles block of the Jacobian yields

$$\begin{aligned}\left(\lambda_{\mu_2}^{(0,0)} A_{\mu_2\nu_2}^{(0,0)}\right)_{i_\sigma j_\tau}^{a_\sigma b_\tau} =& [S\lambda]_{i_\sigma j_\tau}^{a_\sigma d_\tau (0,0)} f_{d_\tau b_\tau} + f_{c_\sigma a_\sigma} [\lambda S]_{i_\sigma j_\tau}^{c_\sigma b_\tau (0,0)} \\ & - [S\lambda S]_{i_\sigma k_\tau}^{a_\sigma b_\tau (0,0)} f_{j_\tau k_\tau} - [S\lambda]_{k_\sigma j_\tau}^{a_\sigma b_\tau (0,0)} f_{i_\sigma k_\sigma}. \end{aligned} \tag{B.422}$$

B.3.2.2.4 $\Lambda_{\nu_2}^{[0,0]}$

Combining (B.418) , (B.421) and (B.422) yields the working equations for the residuum of the zeroth order doubles multiplier equations

$$\begin{aligned} v_{i_\sigma j_\tau}^{a_\sigma b_\tau} =& \eta_{i_\sigma j_\tau}^{a_\sigma b_\tau (0,0)} + \hat{f}_{j_\tau b_\tau} [S\lambda]_{i_\sigma}^{a_\sigma (0,0)} + \hat{f}_{i_\sigma a_\sigma} [S\lambda]_{j_\tau}^{b_\tau (0,0)} - \delta_{\sigma\tau} \hat{f}_{j_\sigma a_\sigma} [S\lambda]_{i_\sigma}^{b_\sigma (0,0)} \\ & - \delta_{\sigma\tau} \hat{f}_{i_\sigma b_\sigma} [S\lambda]_{j_\sigma}^{a_\sigma (0,0)} + \tilde{B}_P^{i_\sigma a_\sigma (0,0)} C_P^{j_\tau b_\tau} + \tilde{B}_P^{j_\tau b_\tau (0,0)} C_P^{i_\sigma a_\sigma} \\ & - \delta_{\sigma\tau} \tilde{B}_P^{i_\sigma b_\sigma (0,0)} C_P^{j_\sigma a_\sigma} - \delta_{\sigma\tau} \tilde{B}_P^{j_\sigma a_\sigma (0,0)} C_P^{i_\sigma b_\sigma} + [S\lambda]_{i_\sigma j_\tau}^{a_\sigma d_\tau (0,0)} f_{d_\tau b_\tau} \\ & + f_{c_\sigma a_\sigma} [\lambda S]_{i_\sigma j_\tau}^{c_\sigma b_\tau (0,0)} - [S\lambda S]_{i_\sigma k_\tau}^{a_\sigma b_\tau (0,0)} f_{j_\tau k_\tau} - [S\lambda]_{k_\sigma j_\tau}^{a_\sigma b_\tau (0,0)} f_{i_\sigma k_\sigma}. \end{aligned} \tag{B.423}$$

B.3.2.3 Zeroth order density matrix

The zeroth order density matrix is implicitly defined by the equation

$$L^{[1,0]} = h_{\mu\nu}^{(1,0)} D_{\nu\mu}^{(0,0)} = E^{(1,0)} + \lambda_\mu^{(0,0)} \Omega_\mu^{(1,0)} \tag{B.424}$$

where $D_{\nu\mu}^{(0,0)}$ is either the charge or spin density matrix in atomic orbital basis depending on the property in question. Note that on the left hand side of this equations, the indices μ and ν represent atomic orbitals whereas on the right hand side they represent excited determinants.
Starting from the left hand side of (B.424) for the spin σ yields

$$h_{\mu\nu}^{(1,0)} D_{\nu\mu}^{\sigma\ (0,0)} = h_{p_\sigma q_\sigma}^{(1,0)} D_{q_\sigma p_\sigma} \tag{B.425}$$

$$\begin{aligned} =& {}^P\Lambda_{\mu i_\sigma}^{\text{occ}} h_{\mu\nu}^{(1,0)H} \Lambda_{\nu j_\sigma}^{\text{occ}} D_{j_\sigma i_\sigma}^{(0,0)} + {}^P\Lambda_{\mu a_\sigma}^{\text{virt}} h_{\mu\nu}^{(1,0)H} \Lambda_{\nu i_\sigma}^{\text{occ}} D_{i_\sigma a_\sigma}^{(0,0)} \\ & + {}^P\Lambda_{\mu i_\sigma}^{\text{occ}} h_{\mu\nu}^{(1,0)H} \Lambda_{\nu a_\sigma}^{\text{virt}} D_{a_\sigma i_\sigma}^{(0,0)} + {}^P\Lambda_{\mu a_\sigma}^{\text{virt}} h_{\mu\nu}^{(1,0)H} \Lambda_{\nu b_\sigma}^{\text{virt}} D_{b_\sigma a_\sigma}^{(0,0)} \end{aligned} \tag{B.426}$$

where we have used the transformations (B.88), (B.89), (B.98) and (B.99) to replace the integrals in molecular orbital basis with an expression dependent on the integrals in the atomic orbital basis. The spin-specific density matrices in atomic orbital basis are then obtained by shifting the transformation from the integrals to the density matrix

$$\begin{aligned} D_{\nu\mu}^{\sigma\ (0,0)} =& {}^H\Lambda_{\nu j_\sigma}^{\text{occ}} D_{j_\sigma i_\sigma}^{(0,0)P} \Lambda_{\mu i_\sigma}^{\text{occ}} + {}^H\Lambda_{\nu i_\sigma}^{\text{occ}} D_{i_\sigma a_\sigma}^{(0,0)P} \Lambda_{\mu a_\sigma}^{\text{virt}} \\ & + {}^H\Lambda_{\nu a_\sigma}^{\text{virt}} D_{a_\sigma i_\sigma}^{(0,0)P} \Lambda_{\mu i_\sigma}^{\text{occ}} + {}^H\Lambda_{\nu b_\sigma}^{\text{virt}} D_{b_\sigma a_\sigma}^{(0,0)P} \Lambda_{\mu a_\sigma}^{\text{virt}} \end{aligned} \tag{B.427}$$

with the four blocks of the density matrix in molecular orbital basis being obtained from the right hand side of (B.424) by dropping the perturbation integrals from the previously determined expressions. The spin-specific density matrices can then be either summed to arrive at the charge density matrix relevant to spin-independent properties or subtracted from each other and scaled with the appropriate factors as discussed in appendix A to get the (normalized) spin density matrix relevant to spin dependent properties.

Since the one-electron Hartree-Fock density matrix in the atomic orbital basis is already known at the beginning of the CC2 calculation, we will ignore its contribution (see (B.134)) for now.
For the occupied-occupied, occupied-virtual and virtual-virtual blocks we have a single contribution each from (B.183)

$$D^{(0,0)}_{j_\sigma i_\sigma} = -\sum_\tau (1 - \frac{\delta_{\sigma\tau}}{2}) \lambda^{c_\tau b_\sigma\,(0,0)}_{k_\tau j_\sigma} [StS]^{k_\tau i_\sigma\,(0,0)}_{c_\tau b_\sigma} \tag{B.428}$$

$$D^{(0,0)}_{i_\sigma a_\sigma} = \lambda^{a_\sigma\,(0,0)}_{i_\sigma} \tag{B.429}$$

$$D^{(0,0)}_{b_\sigma a_\sigma} = \sum_\tau (1 - \frac{\delta_{\sigma\tau}}{2}) \lambda^{c_\tau a_\sigma\,(0,0)}_{k_\tau j_\sigma} [St]^{k_\tau j_\sigma\,(0,0)}_{c_\tau b_\sigma}. \tag{B.430}$$

For the virtual-occupied block we have one contribution from (B.134) and a second contribution from (B.183)

$$D^{(0,0)}_{a_\sigma i_\sigma} = t^{i_\sigma\,(0,0)}_{a_\sigma} + \sum_\tau [S\lambda]^{b_\tau\,(0,0)}_{j_\tau} t^{b_\tau a_\sigma\,(0,0)}_{j_\tau i_\sigma}. \tag{B.431}$$

Note that we have explicitly expanded the T_1-transformation to arrive at the contribution from (B.134). However, there are no additional terms introduced by the transformations (B.88) and (B.99), and we can safely use those transformations regardless.

B.3.2.4 Perturbed singles amplitude equations

The perturbed singles amplitudes have three contributions

$$\Omega^{[1,0]}_{\mu_1} = \Omega^{(1,0)}_{\mu_1} + A^{(0,0)}_{\mu_1\nu_1} t^{(1,0)}_{\nu_1} + A^{(0,0)}_{\mu_1\nu_2} t^{(1,0)}_{\nu_2} \stackrel{!}{=} 0. \tag{B.432}$$

B.3.2.4.1 $\Omega^{(1,0)}_{\mu_1}$

The partial derivative (B.172) of the amplitude equations with respect to the perturbation contributes

$$\Omega^{a_\sigma\,(1,0)}_{i_\sigma} = \hat{h}^{(1,0)}_{a_\sigma i_\sigma} + S_{a_\sigma c_\sigma} \sum_\tau t^{i_\sigma j_\tau\,(0,0)}_{c_\sigma b_\tau} h^{(1,0)}_{j_\tau b_\tau}. \tag{B.433}$$

Since this part does not depend on the perturbed amplitudes, we only need to evaluate it once.

B.3.2.4.2 $A^{(0,0)}_{\mu_1\nu_1} t^{(1,0)}_{\nu_1}$

Introducing the density fitting (B.385) of the two-electron integrals into the contraction

(B.265) yields

$$\begin{aligned}\left(A^{(0,0)}_{\mu_1\nu_1}t^{(1,0)}_{\nu_1}\right)^{a_\sigma}_{i_\sigma} =& t^{i_\sigma\,(1,0)}_{b_\sigma}\hat{f}_{a_\sigma b_\sigma} - [St]^{j_\sigma\,(1,0)}_{a_\sigma}\hat{f}_{j_\sigma i_\sigma} \\ &+ \sum_\tau t^{j_\tau\,(1,0)}_{b_\tau}(P|j_\tau b_\tau)\hat{C}_P^{a_\sigma i_\sigma} - t^{j_\sigma\,(1,0)}_{b_\sigma}\hat{C}_P^{j_\sigma i_\sigma}(P\hat{|}a_\sigma b_\sigma) \\ &+ S_{a_\sigma d_\sigma}\sum_\tau t^{j_\tau\,(1,0)}_{b_\tau}(P|j_\tau b_\tau)\sum_\rho t^{k_\rho i_\sigma\,(0,0)}_{c_\rho d_\sigma}C_P^{k_\rho c_\rho} \\ &- S_{a_\sigma d_\sigma}\sum_\tau t^{j_\tau\,(1,0)}_{b_\tau}(P|k_\tau b_\tau)t^{k_\tau i_\sigma\,(0,0)}_{c_\tau d_\sigma}C_P^{j_\tau c_\tau} \\ &- S_{a_\sigma d_\sigma}t^{i_\sigma\,(1,0)}_{b_\sigma}(P|j_\sigma b_\sigma)\sum_\tau t^{j_\sigma k_\tau\,(0,0)}_{d_\sigma c_\tau}C_P^{k_\tau c_\tau} \\ &- [St]^{j_\sigma\,(1,0)}_{a_\sigma}(P|j_\sigma b_\sigma)\sum_\tau t^{k_\tau i_\sigma\,(0,0)}_{c_\tau b_\sigma}C_P^{k_\tau c_\tau}. \end{aligned} \tag{B.434}$$

Useful intermediates are here the contraction $A_P^{i_\sigma a_\sigma\,(0,0)}$ of doubles amplitudes with the fitting coefficients (see (B.401)) and the contractions of the perturbed singles amplitudes with the fitting integrals

$$C_P^{(1,0)} = \sum_\tau (P|k_\tau c_\tau)t^{k_\tau\,(1,0)}_{c_\tau} \tag{B.435}$$

$$Y_P^{k_\sigma i_\sigma\,(1,0)} = -(P|k_\sigma c_\sigma)t^{i_\sigma\,(1,0)}_{c_\sigma} \tag{B.436}$$

leading us to

$$\begin{aligned}\left(A^{(0,0)}_{\mu_1\nu_1}t^{(1,0)}_{\nu_1}\right)^{a_\sigma}_{i_\sigma} =& t^{i_\sigma\,(1,0)}_{b_\sigma}\hat{f}_{a_\sigma b_\sigma} - [St]^{j_\sigma\,(1,0)}_{a_\sigma}\hat{f}_{j_\sigma i_\sigma} + C_P^{(1,0)}\hat{C}_P^{a_\sigma i_\sigma} \\ &- t^{j_\sigma\,(1,0)}_{b_\sigma}\hat{C}_P^{j_\sigma i_\sigma}(P\hat{|}a_\sigma b_\sigma) + S_{a_\sigma d_\sigma}C_P^{(1,0)}A_P^{i_\sigma d_\sigma\,(0,0)} \\ &+ S_{a_\sigma d_\sigma}\sum_\tau Y_P^{k_\tau j_\tau\,(1,0)}t^{k_\tau i_\sigma\,(0,0)}_{c_\tau d_\sigma}C_P^{j_\tau c_\tau} + S_{a_\sigma d_\sigma}Y_P^{j_\sigma i_\sigma\,(1,0)}A_P^{j_\sigma d_\sigma\,(0,0)} \\ &- [St]^{j_\sigma\,(1,0)}_{a_\sigma}(P|j_\sigma b_\sigma)A_P^{i_\sigma b_\sigma\,(0,0)}. \end{aligned} \tag{B.437}$$

Further simplification is achieved via the intermediates $Z_{j_\sigma i_\sigma}{}^{(0,0)}$ (see (B.405)) and

$$X_{k_\tau c_\tau}{}^{(1,0)} = Y_P^{k_\tau j_\tau\,(1,0)}C_P^{j_\tau c_\tau} \tag{B.438}$$

giving for the final expression

$$\begin{aligned}\left(A^{(0,0)}_{\mu_1\nu_1}t^{(1,0)}_{\nu_1}\right)^{a_\sigma}_{i_\sigma} =& t^{i_\sigma\,(1,0)}_{b_\sigma}\hat{f}_{a_\sigma b_\sigma} - [St]^{j_\sigma\,(1,0)}_{a_\sigma}\hat{f}_{j_\sigma i_\sigma} + C_P^{(1,0)}\hat{C}_P^{a_\sigma i_\sigma} \\ &- t^{j_\sigma\,(1,0)}_{b_\sigma}\hat{C}_P^{j_\sigma i_\sigma}(P\hat{|}a_\sigma b_\sigma) + S_{a_\sigma d_\sigma}C_P^{(1,0)}A_P^{i_\sigma d_\sigma\,(0,0)} \\ &+ S_{a_\sigma d_\sigma}\sum_\tau X_{k_\tau c_\tau}{}^{(1,0)}t^{k_\tau i_\sigma\,(0,0)}_{c_\tau d_\sigma} + S_{a_\sigma d_\sigma}Y_P^{j_\sigma i_\sigma\,(1,0)}A_P^{j_\sigma d_\sigma\,(0,0)} \\ &+ [St]^{j_\sigma\,(1,0)}_{a_\sigma}Z_{j_\sigma i_\sigma}{}^{(0,0)}. \end{aligned} \tag{B.439}$$

B.3.2.4.3 $A^{(0,0)}_{\mu_1\nu_2} t^{(1,0)}_{\nu_2}$

From the contraction (B.279) of the perturbed doubles amplitudes with the singles-doubles block of the Jacobian we have the contributions

$$\begin{aligned}\left(A^{(0,0)}_{\mu_1\nu_2} t^{(1,0)}_{\nu_2}\right)^{a_\sigma}_{i_\sigma} =& \sum_\tau S_{a_\sigma c_\sigma} t^{i_\sigma j_\tau\,(1,0)}_{c_\sigma b_\tau} \hat{f}_{j_\tau b_\tau} + \sum_\tau t^{j_\tau i_\sigma\,(1,0)}_{b_\tau c_\sigma} C_P^{j_\tau b_\tau}(P\hat{|}a_\sigma c_\sigma) \\ & - \sum_\tau S_{a_\sigma c_\sigma} t^{j_\tau k_\sigma\,(1,0)}_{b_\tau c_\sigma} C_P^{j_\tau b_\tau}(P\hat{|}k_\sigma i_\sigma). \end{aligned} \tag{B.440}$$

Introducing an intermediate analogous to (B.401) for the perturbed amplitudes

$$A_P^{i_\sigma a_\sigma\,(1,0)} = \sum_\tau t^{i_\sigma j_\tau\,(1,0)}_{a_\sigma b_\tau} C_P^{j_\tau b_\tau} \tag{B.441}$$

this reduces to

$$\begin{aligned}\left(A^{(0,0)}_{\mu_1\nu_2} t^{(1,0)}_{\nu_2}\right)^{a_\sigma}_{i_\sigma} =& S_{a_\sigma c_\sigma} \sum_\tau t^{i_\sigma j_\tau\,(1,0)}_{c_\sigma b_\tau} \hat{f}_{j_\tau b_\tau} + A_P^{i_\sigma c_\sigma\,(1,0)}(P\hat{|}a_\sigma c_\sigma) \\ & - \sum_\tau S_{a_\sigma c_\sigma} A_P^{k_\sigma c_\sigma\,(1,0)}(P\hat{|}k_\sigma i_\sigma). \end{aligned} \tag{B.442}$$

B.3.2.4.4 $\Omega^{[1,0]}_{\mu_1}$

Combining (B.433) , (B.439) and (B.442) we arrive at the working equation for the residuum of the perturbed singles amplitude equations

$$\begin{aligned} v^{a_\sigma}_{i_\sigma} =& \Omega^{a_\sigma\,(1,0)}_{i_\sigma} + t^{i_\sigma\,(1,0)}_{b_\sigma} \hat{f}_{a_\sigma b_\sigma} - [St]^{j_\sigma\,(1,0)}_{a_\sigma} \hat{f}_{j_\sigma i_\sigma} + [St]^{k_\sigma\,(1,0)}_{a_\sigma} Z_{k_\sigma i_\sigma}{}^{(0,0)} \\ & + S_{a_\sigma d_\sigma}\left(C_P^{(1,0)} A_P^{i_\sigma d_\sigma\,(0,0)} + Y_P^{j_\sigma i_\sigma\,(1,0)} A_P^{j_\sigma d_\sigma\,(0,0)}\right) \\ & + S_{a_\sigma d_\sigma} \sum_\tau X_{k_\tau c_\tau}{}^{(1,0)} t^{k_\tau i_\sigma\,(0,0)}_{c_\tau d_\sigma} + C_P^{(1,0)} \hat{C}_P^{a_\sigma i_\sigma} + S_{a_\sigma c_\sigma} \sum_\tau t^{i_\sigma j_\tau\,(1,0)}_{c_\sigma b_\tau} \hat{f}_{j_\tau b_\tau} \\ & + \left(A_P^{i_\sigma c_\sigma\,(1,0)} - t^{k_\sigma\,(1,0)}_{c_\sigma} \hat{C}_P^{k_\sigma i_\sigma}\right)(P\hat{|}a_\sigma c_\sigma) - \sum_\tau S_{a_\sigma c_\sigma} A_P^{k_\sigma c_\sigma\,(1,0)}(P\hat{|}k_\sigma i_\sigma), \end{aligned} \tag{B.443}$$

where we have renamed some indices and rearranged the order of terms to correspond to the documentation in the written code.

B.3.2.5 Perturbed doubles amplitude equations

For the perturbed doubles amplitude equations we have the three contributions

$$\Omega^{[1,0]}_{\mu_2} = \Omega^{(1,0)}_{\mu_2} + A^{(0,0)}_{\mu_2\nu_1} t^{(1,0)}_{\nu_1} + A^{(0,0)}_{\mu_2\nu_2} t^{(1,0)}_{\nu_2} \stackrel{!}{=} 0. \tag{B.444}$$

B.3.2.5.1 $\Omega^{(1,0)}_{\mu_2}$

The partial derivative (B.173) of the doubles amplitudes yields

$$\begin{aligned}\Omega^{a_\sigma b_\tau\,(1,0)}_{i_\sigma j_\tau} =& [St]^{i_\sigma j_\tau\,(0,0)}_{a_\sigma c_\tau} \hat{h}^{(1,0)}_{b_\tau c_\tau} + \hat{h}^{(1,0)}_{a_\sigma d_\sigma} [tS]^{i_\sigma j_\tau\,(0,0)}_{d_\sigma b_\tau} \\ & - [StS]^{a_\sigma b_\tau\,(0,0)}_{i_\sigma k_\tau} \hat{h}^{(1,0)}_{k_\tau j_\tau} - \hat{h}^{(1,0)}_{k_\sigma i_\sigma} [StS]^{a_\sigma b_\tau\,(0,0)}_{k_\sigma j_\tau}, \end{aligned} \tag{B.445}$$

which is again independent of the perturbed amplitudes and therefore invariant during the iterative solution of the perturbed amplitude equations.

B.3.2.5.2 $A^{(0,0)}_{\mu_2\nu_1} t^{(1,0)}_{\nu_1}$

Decomposing the two-electron integrals via the density fitting (B.385), the contraction (B.287) of the doubles-singles block of the Jacobian with the perturbed singles amplitudes becomes

$$\begin{aligned}\left(A^{(0,0)}_{\mu_2\nu_1} t^{(1,0)}_{\nu_1}\right)^{a_\sigma b_\tau}_{i_\sigma j_\tau} &= t^{i_\sigma\,(1,0)}_{c_\sigma}(P\hat{|}a_\sigma c_\sigma)\hat{C}^{b_\tau j_\tau}_P - \delta_{\sigma\tau} t^{i_\sigma\,(1,0)}_{c_\sigma}\hat{C}^{a_\sigma j_\sigma}_P(P\hat{|}a_\sigma c_\sigma)\\ &- \delta_{\sigma\tau} t^{j_\sigma\,(1,0)}_{c_\sigma}(P\hat{|}a_\sigma c_\sigma)\hat{C}^{b_\sigma i_\sigma}_P + t^{j_\tau\,(1,0)}_{c_\tau}(P\hat{|}b_\tau c_\tau)\hat{C}^{a_\sigma i_\sigma}_P\\ &- S_{a_\sigma c_\sigma} t^{k_\sigma\,(1,0)}_{c_\sigma}(P\hat{|}k_\sigma i_\sigma)\hat{C}^{b_\tau j_\tau}_P + \delta_{\tau\sigma} S_{a_\sigma c_\sigma} t^{k_\sigma\,(1,0)}_{c_\sigma}(P\hat{|}k_\sigma j_\sigma)\hat{C}^{b_\sigma i_\sigma}_P\\ &+ \delta_{\sigma\tau} S_{b_\sigma c_\sigma} t^{k_\sigma\,(1,0)}_{c_\sigma}(P\hat{|}k_\sigma i_\sigma)\hat{C}^{a_\sigma j_\sigma}_P - S_{b_\tau c_\tau} t^{k_\tau\,(1,0)}_{c_\tau}(P\hat{|}k_\tau j_\tau)\hat{C}^{a_\sigma i_\sigma}_P. \end{aligned} \tag{B.446}$$

Similar to the intermediate $\tilde{B}^{i_\sigma a_\sigma\,(0,0)}_P$ of the zeroth order multiplier equations (see (B.420)) we can define here

$$B^{i_\sigma a_\sigma\,(1,0)}_P = t^{i_\sigma\,(1,0)}_{c_\sigma}(P\hat{|}a_\sigma c_\sigma) - S_{a_\sigma c_\sigma} t^{k_\sigma\,(1,0)}_{c_\sigma}(P\hat{|}k_\sigma i_\sigma) \tag{B.447}$$

to arrive at the simplified expression

$$\begin{aligned}\left(A^{(0,0)}_{\mu_2\nu_1} t^{(1,0)}_{\nu_1}\right)^{a_\sigma b_\tau}_{i_\sigma j_\tau} =& B^{i_\sigma a_\sigma\,(1,0)}_P \hat{C}^{b_\tau j_\tau}_P + B^{j_\tau b_\tau\,(1,0)}_P \hat{C}^{a_\sigma i_\sigma}_P\\ &- \delta_{\sigma\tau} B^{i_\sigma b_\sigma}_P C^{a_\sigma j_\sigma}_P - \delta_{\sigma\tau} B^{j_\sigma a_\sigma}_P C^{b_\sigma i_\sigma}_P. \end{aligned} \tag{B.448}$$

B.3.2.5.3 $A^{(0,0)}_{\mu_2\nu_2} t^{(1,0)}_{\nu_2}$

The contraction (B.297) of the perturbed doubles amplitudes with the doubles-doubles block of the Jacobian yields the contribution

$$\begin{aligned}\left(A^{(0,0)}_{\mu_2\nu_2} t^{(1,0)}_{\nu_2}\right)^{a_\sigma b_\tau}_{i_\sigma j_\tau} =& [St]^{i_\sigma j_\tau\,(1,0)}_{a_\sigma d_\tau} f_{b_\tau d_\tau} + f_{a_\sigma c_\sigma}[tS]^{i_\sigma j_\tau\,(1,0)}_{c_\sigma b_\tau}\\ &- [StS]^{i_\sigma k_\tau\,(1,0)}_{a_\sigma b_\tau} f_{k_\tau j_\tau} - [StS]^{k_\sigma j_\tau\,(1,0)}_{a_\sigma b_\tau} f_{k_\sigma i_\sigma}. \end{aligned} \tag{B.449}$$

B.3.2.5.4 $\Omega^{[1,0]}_{\mu_2}$

The working equations for the residuum of the perturbed doubles equations is the sum of (B.445) , (B.448) and (B.449)

$$\begin{aligned} v^{a_\sigma b_\tau}_{i_\sigma j_\tau} = \Omega^{a_\sigma b_\tau\,(1,0)}_{i_\sigma j_\tau} &+ B^{i_\sigma a_\sigma\,(1,0)}_P \hat{C}^{b_\tau j_\tau}_P + B^{j_\tau b_\tau\,(1,0)}_P \hat{C}^{a_\sigma i_\sigma}_P\\ &- \delta_{\sigma\tau} B^{i_\sigma b_\sigma}_P C^{a_\sigma j_\sigma}_P - \delta_{\sigma\tau} B^{j_\sigma a_\sigma}_P C^{b_\sigma i_\sigma}_P\\ &+ [St]^{i_\sigma j_\tau\,(1,0)}_{a_\sigma d_\tau} f_{b_\tau d_\tau} + f_{a_\sigma c_\sigma}[tS]^{i_\sigma j_\tau\,(1,0)}_{c_\sigma b_\tau}\\ &- [StS]^{i_\sigma k_\tau\,(1,0)}_{a_\sigma b_\tau} f_{k_\tau j_\tau} - [StS]^{k_\sigma j_\tau\,(1,0)}_{a_\sigma b_\tau} f_{k_\sigma i_\sigma}. \end{aligned} \tag{B.450}$$

B.3.2.6 Perturbed singles multiplier equations

For the CC2 model with one-electron perturbations, the perturbed singles multiplier equations have the following non-zero contributions

$$\begin{aligned}\Lambda^{[1,0]}_{\nu_1} =& \eta^{(1,0)}_{\nu_1} + \xi^{(0,0)}_{\nu_1\rho_1} t^{(1,0)}_{\rho_1} + \lambda^{(0,0)}_{\mu_1} A^{(1,0)}_{\mu_1\nu_1} + \lambda^{(0,0)}_{\mu_2} A^{(1,0)}_{\mu_2\nu_1}\\ &+ \lambda^{(0,0)}_{\mu_1} B_{\mu_1\nu_1\rho_1}{}^{(0,0)} t^{(1,0)}_{\rho_1} + \lambda^{(0,0)}_{\mu_1} B_{\mu_1\nu_1\rho_2}{}^{(0,0)} t^{(1,0)}_{\rho_2} + \lambda^{(0,0)}_{\mu_2} B_{\mu_2\nu_1\rho_1}{}^{(0,0)} t^{(1,0)}_{\rho_1}\\ &+ \lambda^{(1,0)}_{\mu_1} A^{(0,0)}_{\mu_1\nu_1} + \lambda^{(1,0)}_{\mu_2} A^{(0,0)}_{\mu_2\nu_1} \stackrel{!}{=} 0. \end{aligned} \tag{B.451}$$

B.3.2.6.1 $\eta^{(1,0)}_{\nu_1}$

From the singles block of the partial energy derivative (B.140) we get the contribution

$$\eta^{a_\sigma\,(1,0)}_{i_\sigma} = h^{(1,0)}_{i_\sigma a_\sigma} \tag{B.452}$$

B.3.2.6.2 $\xi^{(0,0)}_{\nu_1\mu_1} t^{(1,0)}_{\mu_1}$

Introducing the density fitting (B.385) into the contraction (B.144) of the second derivative of the energy with respect to the amplitudes contracted with the perturbed amplitudes yields

$$\left(\xi^{(0,0)}_{\nu_1\mu_1} t^{(1,0)}_{\mu_1}\right)^{a_\sigma}_{i_\sigma} = \sum_\tau t^{j_\tau\,(1,0)}_{b_\tau} (P\hat{|}j_\tau b_\tau) C_P^{i_\sigma a_\sigma} - t^{j_\sigma\,(1,0)}_{b_\sigma} (P\hat{|}i_\sigma b_\sigma) C_P^{j_\sigma a_\sigma}. \tag{B.453}$$

Using the intermediates $C_P^{(1,0)}$ and $Y_P^{i_\sigma k_\sigma\,(1,0)}$ from the perturbed singles amplitude equations (see (B.435) and (B.436)) this reduces to

$$\left(\xi^{(0,0)}_{\nu_1\mu_1} t^{(1,0)}_{\mu_1}\right)^{a_\sigma}_{i_\sigma} = C_P^{(1,0)} C_P^{i_\sigma a_\sigma} + Y_P^{i_\sigma j_\sigma\,(1,0)} C_P^{j_\sigma a_\sigma}. \tag{B.454}$$

B.3.2.6.3 $\lambda^{(0,0)}_{\mu_1} A^{(1,0)}_{\mu_1\nu_1}$

The contraction (B.303) of the zeroth order singles multipliers with the the singles-singles block of the perturbed Jacobian contributes

$$\left(\lambda^{(0,0)}_{\mu_1} A^{(1,0)}_{\mu_1\nu_1}\right)^{a_\sigma}_{i_\sigma} = \lambda^{b_\sigma\,(0,0)}_{i_\sigma} \hat{h}^{(1,0)}_{b_\sigma a_\sigma} - \hat{h}^{(1,0)}_{i_\sigma j_\sigma} [S\lambda]^{a_\sigma\,(0,0)}_{j_\sigma}. \tag{B.455}$$

B.3.2.6.4 $\lambda^{(0,0)}_{\mu_2} A^{(1,0)}_{\mu_2\nu_1}$

From the contraction (B.312) of the zeroth order doubles multipliers with the doubles-singles block of the perturbed Jacobian we get

$$\begin{aligned}\left(\lambda^{(0,0)}_{\mu_2} A^{(1,0)}_{\mu_2\nu_1}\right)^{a_\sigma}_{i_\sigma} = &- \sum_\tau \left(\frac{1-\delta_{\sigma\tau}}{2}\right) \lambda^{c_\sigma b_\tau\,(0,0)}_{i_\sigma k_\tau} [StS]^{j_\sigma k_\tau\,(0,0)}_{c_\sigma b_\tau} h^{(1,0)}_{j_\sigma a_\sigma} \\ &- S_{a_\sigma d_\sigma} \sum_\tau \left(\frac{1-\delta_{\sigma\tau}}{2}\right) \lambda^{d_\sigma c_\tau\,(0,0)}_{k_\sigma j_\tau} [St]^{k_\sigma j_\tau\,(0,0)}_{b_\sigma c_\tau} h^{(1,0)}_{i_\sigma b_\sigma}.\end{aligned} \tag{B.456}$$

This can be simplified by reusing the occupied-occupied contribution ${D_{i_\sigma j_\sigma}}^{(0,0)}$ and the virtual-virtual contribution ${D_{b_\sigma d_\sigma}}^{(0,0)}$ to the zeroth order density, (B.428) and (B.430) respectively, to obtain

$$\left(\lambda^{(0,0)}_{\mu_2} A^{(1,0)}_{\mu_2\nu_1}\right)^{a_\sigma}_{i_\sigma} = {D_{i_\sigma j_\sigma}}^{(0,0)} h^{(1,0)}_{j_\sigma a_\sigma} - S_{a_\sigma d_\sigma} {D_{b_\sigma d_\sigma}}^{(0,0)} h^{(1,0)}_{i_\sigma b_\sigma}. \tag{B.457}$$

B.3.2.6.5 $\lambda^{(0,0)}_{\mu_1} B^{(0,0)}_{\mu_1\nu_1\rho_1} t^{(1,0)}_{\rho_1}$

The contraction (B.353) of the singles-singles-singles block of the second derivative of

the amplitude equations with respect to the amplitudes contracted with the zeroth order singles multipliers and the perturbed singles amplitudes yields

$$\begin{aligned}
\left(\lambda^{(0,0)}_{\mu_1} B^{(0,0)}_{\mu_1\nu_1\rho_1} t^{(1,0)}_{\rho_1}\right)^{a_\sigma}_{i_\sigma} =& -\hat{f}_{i_\sigma b_\sigma} t^{j_\sigma\,(1,0)}_{b_\sigma} [S\lambda^{a_\sigma}_{j_\sigma}]^{(0,0)} - [S\lambda]^{b_\sigma\,(0,0)}_{i_\sigma} t^{j_\sigma\,(1,0)}_{b_\sigma} \hat{f}_{j_\sigma a_\sigma} \\
&+ \lambda^{c_\sigma\,(0,0)}_{i_\sigma} \sum_\tau (P\hat{|}c_\sigma a_\sigma) C_P^{j_\tau b_\tau} t^{j_\tau\,(1,0)}_{b_\tau} - \lambda^{c_\sigma\,(0,0)}_{i_\sigma} (P\hat{|}c_\sigma b_\sigma) C_P^{j_\sigma a_\sigma} t^{j_\sigma\,(1,0)}_{b_\sigma} \\
&- [S\lambda]^{a_\sigma\,(0,0)}_{k_\sigma} \sum_\tau (P\hat{|}i_\sigma k_\sigma) C_P^{j_\tau b_\tau} t^{j_\tau\,(1,0)}_{b_\tau} + [S\lambda]^{a_\sigma\,(0,0)}_{k_\sigma} (P\hat{|}j_\sigma k_\sigma) C_P^{i_\sigma b_\sigma} t^{j_\sigma\,(1,0)}_{b_\sigma} \\
&+ \sum_\tau \lambda^{c_\tau\,(0,0)}_{j_\tau} (P\hat{|}c_\tau b_\tau) C_P^{i_\sigma a_\sigma} t^{j_\tau\,(1,0)}_{b_\tau} - \lambda^{c_\sigma\,(0,0)}_{j_\sigma} (P\hat{|}c_\sigma a_\sigma) C_P^{i_\sigma b_\sigma} t^{j_\sigma\,(1,0)}_{b_\sigma} \\
&- \sum_\tau [S\lambda]^{b_\tau\,(0,0)}_{k_\tau} (P\hat{|}j_\tau k_\tau) C_P^{i_\sigma a_\sigma} t^{j_\tau\,(1,0)}_{b_\tau} + [S\lambda]^{b_\sigma\,(0,0)}_{k_\sigma} C_P^{j_\sigma a_\sigma} (P\hat{|}i_\sigma k_\sigma) t^{j_\sigma\,(1,0)}_{b_\sigma}. \qquad \text{(B.458)}
\end{aligned}$$

Defining as intermediates the contraction of the zeroth order singles multipliers with the perturbed singles amplitudes over the virtual index (including the required overlap integral)

$$\bar{y}_{i_\sigma j_\sigma}{}^{(1,0)} = [S\lambda]^{b_\sigma\,(0,0)}_{i_\sigma} t^{j_\sigma\,(1,0)}_{b_\sigma} \qquad \text{(B.459)}$$

and the contraction of the perturbed singles amplitudes with the fitting coefficients

$$\bar{C}_P^{(1,0)} = \sum_\tau C_P^{j_\tau b_\tau} t^{j_\tau\,(1,0)}_{b_\tau} \qquad \text{(B.460)}$$

$$\bar{C}_P^{i_\sigma j_\sigma\,(1,0)} = C_P^{i_\sigma b_\sigma} t^{j_\sigma\,(1,0)}_{b_\sigma} \qquad \text{(B.461)}$$

this reduces to

$$\begin{aligned}
\left(\lambda^{(0,0)}_{\mu_1} B^{(0,0)}_{\mu_1\nu_1\rho_1} t^{(1,0)}_{\rho_1}\right)^{a_\sigma}_{i_\sigma} =& -\hat{f}_{i_\sigma b_\sigma} t^{j_\sigma\,(1,0)}_{b_\sigma} [S\lambda^{a_\sigma}_{j_\sigma}]^{(0,0)} - \bar{y}_{i_\sigma j_\sigma}{}^{(1,0)} \hat{f}_{j_\sigma a_\sigma} \\
&+ \lambda^{c_\sigma\,(0,0)}_{i_\sigma} (P\hat{|}c_\sigma a_\sigma) \bar{C}_P^{(1,0)} - \lambda^{c_\sigma\,(0,0)}_{i_\sigma} (P\hat{|}c_\sigma b_\sigma) C_P^{j_\sigma a_\sigma} t^{j_\sigma\,(1,0)}_{b_\sigma} \\
&- [S\lambda]^{a_\sigma\,(0,0)}_{k_\sigma} (P\hat{|}i_\sigma k_\sigma) \bar{C}_P^{(1,0)} + [S\lambda]^{a_\sigma\,(0,0)}_{k_\sigma} (P\hat{|}j_\sigma k_\sigma) \bar{C}_P^{i_\sigma j_\sigma\,(1,0)} \\
&+ \sum_\tau \lambda^{c_\tau\,(0,0)}_{j_\tau} (P\hat{|}c_\tau b_\tau) C_P^{i_\sigma a_\sigma} t^{j_\tau\,(1,0)}_{b_\tau} - \lambda^{c_\sigma\,(0,0)}_{j_\sigma} (P\hat{|}c_\sigma a_\sigma) \bar{C}_P^{i_\sigma j_\sigma\,(1,0)} \\
&- \sum_\tau [S\lambda]^{b_\tau\,(0,0)}_{k_\tau} (P\hat{|}j_\tau k_\tau) C_P^{i_\sigma a_\sigma} t^{j_\tau\,(1,0)}_{b_\tau} + [S\lambda]^{b_\sigma\,(0,0)}_{k_\sigma} C_P^{j_\sigma a_\sigma} (P\hat{|}i_\sigma k_\sigma) t^{j_\sigma\,(1,0)}_{b_\sigma} \qquad \text{(B.462)} \\
=& -\hat{f}_{i_\sigma b_\sigma} t^{j_\sigma\,(1,0)}_{b_\sigma} [S\lambda^{a_\sigma}_{j_\sigma}]^{(0,0)} - \bar{y}_{i_\sigma j_\sigma}{}^{(1,0)} \hat{f}_{j_\sigma a_\sigma} \\
&+ \bar{C}_P^{(1,0)} \left(\lambda^{c_\sigma\,(0,0)}_{i_\sigma} (P\hat{|}c_\sigma a_\sigma) - [S\lambda]^{a_\sigma\,(0,0)}_{k_\sigma} (P\hat{|}i_\sigma k_\sigma)\right) \\
&- \bar{C}_P^{i_\sigma j_\sigma\,(1,0)} \left(\lambda^{c_\sigma\,(0,0)}_{j_\sigma} (P\hat{|}c_\sigma a_\sigma) - [S\lambda]^{a_\sigma\,(0,0)}_{k_\sigma} (P\hat{|}j_\sigma k_\sigma)\right) \\
&- C_P^{j_\sigma a_\sigma} t^{j_\sigma\,(1,0)}_{b_\sigma} \left(\lambda^{c_\sigma\,(0,0)}_{i_\sigma} (P\hat{|}c_\sigma b_\sigma) - [S\lambda]^{b_\sigma\,(0,0)}_{k_\sigma} (P\hat{|}i_\sigma k_\sigma)\right) \\
&+ C_P^{i_\sigma a_\sigma} \sum_\tau t^{j_\tau\,(1,0)}_{b_\tau} \left(\lambda^{c_\tau\,(0,0)}_{j_\tau} (P\hat{|}c_\tau b_\tau) - [S\lambda]^{b_\tau\,(0,0)}_{k_\tau} (P\hat{|}j_\tau k_\tau)\right). \qquad \text{(B.463)}
\end{aligned}$$

The second equality follows from rearrangement of the terms and shows that we can reuse the intermediate $\tilde{B}_P^{i_\sigma a_\sigma (0,0)}$ (see (B.420)) used in the solution of the zeroth order multiplier equations to obtain

$$\begin{aligned}\left(\lambda_{\mu_1}^{(0,0)} B_{\mu_1\nu_1\rho_1}^{(0,0)} t_{\rho_1}^{(1,0)}\right)_{i_\sigma}^{a_\sigma} =& -\hat{f}_{i_\sigma b_\sigma} t_{b_\sigma}^{j_\sigma (1,0)} [S\lambda_{j_\sigma}^{a_\sigma}]^{(0,0)} - \bar{y}_{i_\sigma j_\sigma}{}^{(1,0)} \hat{f}_{j_\sigma a_\sigma} \\ &+ \bar{C}_P^{(1,0)} \tilde{B}_P^{i_\sigma a_\sigma (0,0)} - \bar{C}_P^{i_\sigma j_\sigma (1,0)} \tilde{B}_P^{j_\sigma a_\sigma (0,0)} \\ &- C_P^{j_\sigma a_\sigma} t_{b_\sigma}^{j_\sigma (1,0)} \tilde{B}_P^{i_\sigma b_\sigma (0,0)} + C_P^{i_\sigma a_\sigma} \sum_\tau t_{b_\tau}^{j_\tau (1,0)} \tilde{B}_P^{j_\tau b_\tau (0,0)}. \end{aligned} \tag{B.464}$$

This can be further simplified via the intermediates

$$\bar{B}_P^{i_\sigma j_\sigma (1,0)} = \tilde{B}_P^{i_\sigma b_\sigma (0,0)} t_{b_\sigma}^{j_\sigma (1,0)} \tag{B.465}$$

$$\bar{B}_P^{(1,0)} = \sum_\tau t_{b_\tau}^{j_\tau (1,0)} \tilde{B}_P^{j_\tau b_\tau (0,0)} \tag{B.466}$$

to get the expression

$$\begin{aligned}\left(\lambda_{\mu_1}^{(0,0)} B_{\mu_1\nu_1\rho_1}^{(0,0)} t_{\rho_1}^{(1,0)}\right)_{i_\sigma}^{a_\sigma} =& -\hat{f}_{i_\sigma b_\sigma} t_{b_\sigma}^{j_\sigma (1,0)} [S\lambda_{j_\sigma}^{a_\sigma}]^{(0,0)} - \bar{y}_{i_\sigma j_\sigma}{}^{(1,0)} \hat{f}_{j_\sigma a_\sigma} \\ &+ \bar{C}_P^{(1,0)} \tilde{B}_P^{i_\sigma a_\sigma (0,0)} - \bar{C}_P^{i_\sigma j_\sigma (1,0)} \tilde{B}_P^{j_\sigma a_\sigma (0,0)} \\ &+ \bar{B}_P^{(1,0)} C_P^{i_\sigma a_\sigma} - \bar{B}_P^{i_\sigma j_\sigma (1,0)} C_P^{j_\sigma a_\sigma} \end{aligned} \tag{B.467}$$

which emphasizes the similarity of the last two lines from an implementation perspective.

B.3.2.6.6 $\lambda_{\mu_1}^{(0,0)} B_{\mu_1\nu_1\rho_2}^{(0,0)} t_{\rho_2}^{(1,0)}$

Introducing the density fitting (B.385) into the contraction (B.354) of the singles-singles-doubles block of the second derivative of the amplitude equations with respect to the amplitudes contracted with the zeroth order singles multipliers and the perturbed doubles amplitudes yields

$$\begin{aligned}\left(\lambda_{\mu_1}^{(0,0)} B_{\mu_1\nu_1\rho_2}^{(0,0)} t_{\rho_2}^{(1,0)}\right)_{i_\sigma}^{a_\sigma} =& \sum_\tau [S\lambda]_{j_\tau}^{b_\tau (0,0)} \sum_\rho t_{b_\tau c_\rho}^{j_\tau k_\rho (1,0)} C_P^{k_\rho c_\rho} (P|i_\sigma a_\sigma) \\ &- \sum_\tau [S\lambda]_{j_\tau}^{b_\tau (0,0)} t_{b_\tau c_\sigma}^{j_\tau k_\sigma (1,0)} (P|k_\sigma a_\sigma) C_P^{i_\sigma c_\sigma} \\ &- [S\lambda]_{i_\sigma}^{b_\sigma (0,0)} \sum_\tau t_{b_\sigma c_\tau}^{j_\sigma k_\tau (1,0)} (P|j_\sigma a_\sigma) C_P^{k_\tau c_\tau} \\ &- [S\lambda]_{j_\sigma}^{a_\sigma (0,0)} \sum_\tau t_{b_\sigma c_\tau}^{j_\sigma k_\tau (1,0)} C_P^{k_\tau c_\tau} (P|i_\sigma b_\sigma). \end{aligned} \tag{B.468}$$

Using the contraction $A_P^{j_\tau b_\tau (1,0)}$ of the perturbed doubles amplitudes with the fitting coefficients (see (B.441)) and

$$\tilde{X}_{k_\sigma c_\sigma}^{(1,0)} = \sum_\tau [S\lambda]_{j_\tau}^{b_\tau (0,0)} t_{b_\tau c_\sigma}^{j_\tau k_\sigma (1,0)}, \tag{B.469}$$

which is a higher order analogue of (B.402), we can reduce this to

$$\begin{aligned}\left(\lambda^{(0,0)}_{\mu_1} B^{(0,0)}_{\mu_1\nu_1\rho_2} t^{(1,0)}_{\rho_2}\right)^{a_\sigma}_{i_\sigma} =& \sum_\tau [S\lambda]^{b_\tau\,(0,0)}_{j_\tau} A_P^{j_\tau b_\tau\,(1,0)}(P|i_\sigma a_\sigma) \\ &- \tilde{X}^{(1,0)}_{k_\sigma c_\sigma}(P|k_\sigma a_\sigma) C_P^{i_\sigma c_\sigma} \\ &- [S\lambda]^{b_\sigma\,(0,0)}_{i_\sigma} A_P^{j_\sigma b_\sigma\,(1,0)}(P|j_\sigma a_\sigma) \\ &- [S\lambda]^{a_\sigma\,(0,0)}_{j_\sigma} A_P^{j_\sigma b_\sigma\,(1,0)}(P|i_\sigma b_\sigma). \end{aligned} \tag{B.470}$$

Further introducing the higher order analogues of (B.405), (B.406) and (B.407)

$$Z^{(1,0)}_{i_\sigma j_\sigma} = -(P|i_\sigma c_\sigma) A_P^{j_\sigma c_\sigma\,(1,0)} \tag{B.471}$$

$$\tilde{Y}_P^{k_\sigma i_\sigma\,(1,0)} = -\tilde{X}^{(1,0)}_{k_\sigma c_\sigma} C_P^{i_\sigma c_\sigma} \tag{B.472}$$

$$\Delta\tilde{Y}_P^{j_\sigma i_\sigma\,(1,0)} = -A_P^{j_\sigma b_\sigma\,(1,0)} [S\lambda]^{b_\sigma\,(0,0)}_{i_\sigma} \tag{B.473}$$

we get the final expression for this contribution

$$\begin{aligned}\left(\lambda^{(0,0)}_{\mu_1} B^{(0,0)}_{\mu_1\nu_1\rho_2} t^{(1,0)}_{\rho_2}\right)^{a_\sigma}_{i_\sigma} =& -(P|i_\sigma a_\sigma) \sum_\tau \Delta\tilde{Y}_P^{j_\tau j_\tau\,(1,0)} + \tilde{Y}_P^{k_\sigma i_\sigma\,(1,0)}(P|k_\sigma a_\sigma) \\ &+ \Delta\tilde{Y}_P^{j_\sigma i_\sigma\,(1,0)}(P|j_\sigma a_\sigma) + [S\lambda]^{a_\sigma\,(0,0)}_{j_\sigma} Z^{(1,0)}_{i_\sigma j_\sigma} \end{aligned} \tag{B.474}$$

$$\begin{aligned} =& [S\lambda]^{a_\sigma\,(0,0)}_{j_\sigma} Z^{(1,0)}_{i_\sigma j_\sigma} - (P|i_\sigma a_\sigma) \sum_\tau \Delta\tilde{Y}_P^{j_\tau j_\tau\,(1,0)} \\ &+ \left(\tilde{Y}_P^{k_\sigma i_\sigma\,(1,0)} + \Delta\tilde{Y}_P^{k_\sigma i_\sigma\,(1,0)}\right)(P|k_\sigma a_\sigma) \end{aligned} \tag{B.475}$$

with the last equality following from renaming of summation indices.

B.3.2.6.7 $\lambda^{(0,0)}_{\mu_2} B^{(0,0)}_{\mu_2\nu_1\rho_1} t^{(1,0)}_{\rho_1}$

Using the density fitting (B.385) to decompose the two-electron integrals in the contraction (B.384) of the doubles-singles-singles block of the second derivative of the amplitude equations with respect to the amplitudes contracted with the zeroth order doubles multipliers and the perturbed singles amplitudes yields

$$\begin{aligned}\left(\lambda^{(0,0)}_{\mu_2} B^{(0,0)}_{\mu_2\nu_1\rho_1} t^{(1,0)}_{\rho_1}\right)^{a_\sigma}_{i_\sigma} =& \sum_\tau t^{j_\tau\,(1,0)}_{b_\tau} \lambda^{c_\sigma d_\tau\,(0,0)}_{i_\sigma j_\tau} (P\hat{|}c_\sigma a_\sigma)[J^{-1}]_{PQ}(Q\hat{|}d_\tau b_\tau) \\ &+ S_{d_\sigma a_\sigma} \sum_\tau [St]^{j_\tau\,(1,0)}_{b_\tau} \lambda^{d_\sigma b_\tau\,(0,0)}_{k_\sigma l_\tau} (P\hat{|}i_\sigma k_\sigma)[J^{-1}]_{PQ}(Q\hat{|}j_\tau l_\tau) \\ &- S_{d_\sigma a_\sigma} \sum_\tau t^{j_\tau\,(1,0)}_{b_\tau} \lambda^{d_\sigma c_\tau\,(0,0)}_{l_\sigma j_\tau} (P\hat{|}i_\sigma l_\sigma)[J^{-1}]_{PQ}(Q\hat{|}c_\tau b_\tau) \\ &- S_{d_\sigma a_\sigma} t^{j_\sigma\,(1,0)}_{b_\sigma} \sum_\tau \lambda^{d_\sigma c_\tau\,(0,0)}_{j_\sigma l_\tau} (P|i_\sigma b_\sigma) \hat{C}_P^{c_\tau l_\tau} \\ &- \sum_\tau [St]^{j_\tau\,(1,0)}_{b_\tau} \lambda^{d_\sigma b_\tau\,(0,0)}_{i_\sigma k_\tau} (P\hat{|}d_\sigma a_\sigma)[J^{-1}]_{PQ}(Q\hat{|}j_\tau k_\tau) \\ &- [St]^{j_\sigma\,(1,0)}_{b_\sigma} \sum_\tau \lambda^{b_\sigma d_\tau\,(0,0)}_{i_\sigma k_\tau} \hat{C}_P^{d_\tau k_\tau}(P|j_\sigma a_\sigma) \end{aligned} \tag{B.476}$$

Reusing the intermediates $\tilde{A}_P^{j_\sigma d_\sigma (0,0)}$ for contraction of the doubles multipliers with the fitting coefficients (see (B.412)), $Y_P^{i_\sigma j_\sigma (1,0)}$ for the contraction of the singles amplitudes with the fitting integrals (see (B.436)), we can simplify this to

$$\begin{aligned}
\left(\lambda_{\mu_2}^{(0,0)} B_{\mu_2\nu_1\rho_1}^{(0,0)} t_{\rho_1}^{(1,0)}\right)_{i_\sigma}^{a_\sigma} =& (P\hat{|}c_\sigma a_\sigma)[J^{-1}]_{PQ} \sum_\tau \lambda_{i_\sigma j_\tau}^{c_\sigma d_\tau (0,0)} t_{b_\tau}^{j_\tau (1,0)} (Q\hat{|}d_\tau b_\tau) \\
&+ S_{d_\sigma a_\sigma} (P\hat{|}i_\sigma k_\sigma)[J^{-1}]_{PQ} \sum_\tau \lambda_{k_\sigma l_\tau}^{d_\sigma b_\tau (0,0)} [St]_{b_\tau}^{j_\tau (1,0)} (Q\hat{|}j_\tau l_\tau) \\
&- S_{d_\sigma a_\sigma} (P\hat{|}i_\sigma l_\sigma)[J^{-1}]_{PQ} \sum_\tau \lambda_{l_\sigma j_\tau}^{d_\sigma c_\tau (0,0)} t_{b_\tau}^{j_\tau (1,0)} (Q\hat{|}c_\tau b_\tau) \\
&+ S_{d_\sigma a_\sigma} Y_P^{i_\sigma j_\sigma (1,0)} \tilde{A}_P^{j_\sigma d_\sigma (0,0)} - (P\hat{|}d_\sigma a_\sigma)[J^{-1}]_{PQ} \sum_\tau \lambda_{i_\sigma k_\tau}^{d_\sigma b_\tau (0,0)} [St]_{b_\tau}^{j_\tau (1,0)} (Q\hat{|}j_\tau k_\tau) \\
&- [St]_{b_\sigma}^{j_\sigma (1,0)} (P|j_\sigma a_\sigma) \tilde{A}_P^{i_\sigma b_\sigma (0,0)} \qquad \text{(B.477)} \\
=& (P\hat{|}c_\sigma a_\sigma)[J^{-1}]_{PQ} \sum_\tau \lambda_{i_\sigma j_\tau}^{c_\sigma b_\tau (0,0)} t_{d_\tau}^{j_\tau (1,0)} (Q\hat{|}b_\tau d_\tau) \\
&+ S_{c_\sigma a_\sigma} (P\hat{|}i_\sigma k_\sigma)[J^{-1}]_{PQ} \sum_\tau \lambda_{k_\sigma j_\tau}^{c_\sigma b_\tau (0,0)} [St]_{b_\tau}^{l_\tau (1,0)} (Q\hat{|}l_\tau j_\tau) \\
&- S_{c_\sigma a_\sigma} (P\hat{|}i_\sigma k_\sigma)[J^{-1}]_{PQ} \sum_\tau \lambda_{k_\sigma j_\tau}^{c_\sigma b_\tau (0,0)} t_{d_\tau}^{j_\tau (1,0)} (Q\hat{|}b_\tau d_\tau) \\
&+ S_{c_\sigma a_\sigma} Y_P^{i_\sigma k_\sigma (1,0)} \tilde{A}_P^{k_\sigma c_\sigma (0,0)} - (P\hat{|}c_\sigma a_\sigma)[J^{-1}]_{PQ} \sum_\tau \lambda_{i_\sigma j_\tau}^{c_\sigma b_\tau (0,0)} [St]_{b_\tau}^{l_\tau (1,0)} (Q\hat{|}l_\tau j_\tau) \\
&- [St]_{c_\sigma}^{k_\sigma (1,0)} (P|k_\sigma a_\sigma) \tilde{A}_P^{i_\sigma c_\sigma (0,0)} \qquad \text{(B.478)} \\
=& (P\hat{|}c_\sigma a_\sigma)[J^{-1}]_{PQ} \sum_\tau \lambda_{i_\sigma j_\tau}^{c_\sigma b_\tau (0,0)} \left(t_{d_\tau}^{j_\tau (1,0)} (Q\hat{|}b_\tau d_\tau) - [St]_{b_\tau}^{l_\tau (1,0)} (Q\hat{|}l_\tau j_\tau) \right) \\
&- S_{c_\sigma a_\sigma} (P\hat{|}i_\sigma k_\sigma)[J^{-1}]_{PQ} \sum_\tau \lambda_{k_\sigma j_\tau}^{c_\sigma b_\tau (0,0)} \left(t_{d_\tau}^{j_\tau (1,0)} (Q\hat{|}b_\tau d_\tau) - [St]_{b_\tau}^{l_\tau (1,0)} (Q\hat{|}l_\tau j_\tau) \right) \\
&+ S_{c_\sigma a_\sigma} Y_P^{i_\sigma k_\sigma (1,0)} \tilde{A}_P^{k_\sigma c_\sigma (0,0)} - [St]_{c_\sigma}^{k_\sigma (1,0)} (P|k_\sigma a_\sigma) \tilde{A}_P^{i_\sigma c_\sigma (0,0)} \qquad \text{(B.479)}
\end{aligned}$$

Here (B.478) follows from standardization of the indices and (B.479) from rearrangement of terms. This allows us to reuse the intermediate $B_P^{j_\tau b_\tau (1,0)}$ from the perturbed amplitude equations (see (B.447)) to obtain

$$\begin{aligned}
\left(\lambda_{\mu_2}^{(0,0)} B_{\mu_2\nu_1\rho_1}^{(0,0)} t_{\rho_1}^{(1,0)}\right)_{i_\sigma}^{a_\sigma} =& (P\hat{|}c_\sigma a_\sigma)[J^{-1}]_{PQ} \sum_\tau \lambda_{i_\sigma j_\tau}^{c_\sigma b_\tau (0,0)} B_P^{j_\tau b_\tau (1,0)} \\
&- S_{c_\sigma a_\sigma} (P\hat{|}i_\sigma k_\sigma)[J^{-1}]_{PQ} \sum_\tau \lambda_{k_\sigma j_\tau}^{c_\sigma b_\tau (0,0)} B_P^{j_\tau b_\tau (1,0)} \\
&+ S_{c_\sigma a_\sigma} Y_P^{i_\sigma k_\sigma (1,0)} \tilde{A}_P^{k_\sigma c_\sigma (0,0)} - [St]_{c_\sigma}^{k_\sigma (1,0)} (P|k_\sigma a_\sigma) \tilde{A}_P^{i_\sigma c_\sigma (0,0)}. \qquad \text{(B.480)}
\end{aligned}$$

Introducing the additional intermediates

$$V_P^{j_\tau b_\tau (1,0)} = [J^{-1}]_{PQ} B_P^{j_\tau b_\tau (1,0)} \qquad \text{(B.481)}$$

$$W_P^{i_\sigma c_\sigma (1,0)} = \sum_\tau \lambda_{i_\sigma j_\tau}^{c_\sigma b_\tau (0,0)} V_P^{j_\tau b_\tau (1,0)} \qquad \text{(B.482)}$$

$$\bar{A}_P^{i_\sigma k_\sigma (1,0)} = - \tilde{A}_P^{i_\sigma c_\sigma (0,0)} [St]_{c_\sigma}^{k_\sigma (1,0)} \qquad \text{(B.483)}$$

we finally arrive at

$$\left(\lambda_{\mu_2}^{(0,0)} B_{\mu_2\nu_1\rho_1}^{(0,0)} t_{\rho_1}^{(1,0)}\right)_{i_\sigma}^{a_\sigma} = (P|\hat{c_\sigma a_\sigma}) W_P^{i_\sigma c_\sigma (1,0)} - S_{c_\sigma a_\sigma} (P|\hat{i_\sigma k_\sigma}) W_P^{k_\sigma c_\sigma (1,0)} + S_{c_\sigma a_\sigma} Y_P^{i_\sigma k_\sigma (1,0)} \tilde{A}_P^{k_\sigma c_\sigma (0,0)} + \bar{A}_P^{i_\sigma k_\sigma (1,0)} (P|k_\sigma a_\sigma). \tag{B.484}$$

B.3.2.6.8 $\lambda_{\mu_1}^{(1,0)} A_{\mu_1\nu_1}^{(0,0)}$ and $\lambda_{\mu_2}^{(1,0)} A_{\mu_2\nu_1}^{(0,0)}$

The only difference between the contraction of the zeroth order Jacobian with either zeroth order multipliers or perturbed multipliers is the order of the multipliers. Therefore, the working equations, and by extension the actual code, are essentially the same and will not be repeated here.

B.3.2.6.9 $\zeta_{\nu_1}^{[1,0]}$

Since only the non-iterative part differs from the unperturbed case, it is convenient to introduce a new intermediate

$$\begin{aligned}\zeta_{i_\sigma}^{a_\sigma [1,0]} =& \eta_{i_\sigma}^{a_\sigma (1,0)} + \left(\xi_{\nu_1\rho_1}^{(0,0)} t_{\rho_1}{}^{(1,0)}\right)_{i_\sigma}^{a_\sigma} + \left(\lambda_{\mu_1}^{(0,0)} A_{\mu_1\nu_1}^{(1,0)}\right)_{i_\sigma}^{a_\sigma} + \left(\lambda_{\mu_2}^{(0,0)} A_{\mu_2\nu_1}^{(1,0)}\right)_{i_\sigma}^{a_\sigma} \\ &+ \left(\lambda_{\mu_1}^{(0,0)} B_{\mu_1\nu_1\rho_1}^{(0,0)} t_{\rho_1}^{(1,0)}\right)_{i_\sigma}^{a_\sigma} + \left(\lambda_{\mu_1}^{(0,0)} B_{\mu_1\nu_1\rho_2}^{(0,0)} t_{\rho_2}^{(1,0)}\right)_{i_\sigma}^{a_\sigma} \\ &+ \left(\lambda_{\mu_2}^{(0,0)} B_{\mu_2\nu_1\rho_1}^{(0,0)} t_{\rho_1}^{(1,0)}\right)_{i_\sigma}^{a_\sigma}.\end{aligned} \tag{B.485}$$

Furthermore, the sum of the first two contributions (B.452) and (B.454)

$$\bar{\eta}_{i_\sigma}^{a_\sigma (1,0)} = \eta_{i_\sigma}^{a_\sigma (1,0)} + \left(\xi_{\nu_1\rho_1}^{(0,0)} t_{\rho_1}{}^{(1,0)}\right)_{i_\sigma}^{a_\sigma} \tag{B.486}$$

$$= h_{i_\sigma a_\sigma}^{(1,0)} + C_P^{(1,0)} C_P^{i_\sigma a_\sigma} + Y_P^{i_\sigma j_\sigma (1,0)} C_P^{j_\sigma a_\sigma} \tag{B.487}$$

is a useful intermediate in its own right, since it will reoccur in the non-iterative part of the doubles equations.

Therefore, the non-iterative part of the perturbed singles multiplier equations is obtained as the sum of (B.487) , (B.455) , (B.457) , (B.467) , (B.475) and (B.484)

$$\begin{aligned}\zeta_{i_\sigma}^{a_\sigma [1,0]} =& \bar{\eta}_{i_\sigma}^{a_\sigma (1,0)} + \lambda_{i_\sigma}^{b_\sigma (0,0)} \hat{h}_{b_\sigma a_\sigma}^{(1,0)} - \hat{h}_{i_\sigma j_\sigma}^{(1,0)} [S\lambda]_{j_\sigma}^{a_\sigma (0,0)} + D_{i_\sigma j_\sigma}{}^{(0,0)} h_{j_\sigma a_\sigma}^{(1,0)} \\ &- S_{a_\sigma d_\sigma} D_{b_\sigma d_\sigma}{}^{(0,0)} h_{i_\sigma b_\sigma}^{(1,0)} - \hat{f}_{i_\sigma b_\sigma} t_{b_\sigma}^{j_\sigma (1,0)} [S\lambda_{j_\sigma}^{a_\sigma}]^{(0,0)} - \bar{y}_{i_\sigma j_\sigma}{}^{(1,0)} \hat{f}_{j_\sigma a_\sigma} \\ &+ \bar{C}_P^{(1,0)} \tilde{B}_P^{i_\sigma a_\sigma (0,0)} - \bar{C}_P^{i_\sigma j_\sigma (1,0)} \tilde{B}_P^{j_\sigma a_\sigma (0,0)} + \bar{B}_P^{(1,0)} C_P^{i_\sigma a_\sigma} \\ &- \bar{B}_P^{i_\sigma j_\sigma (1,0)} C_P^{j_\sigma a_\sigma} + [S\lambda]_{j_\sigma}^{a_\sigma (0,0)} Z_{i_\sigma j_\sigma}^{(1,0)} - (P|i_\sigma a_\sigma) \sum_\tau \Delta\tilde{Y}_P^{j_\tau j_\tau (1,0)} \\ &+ \left(\tilde{Y}_P^{k_\sigma i_\sigma (1,0)} + \Delta\tilde{Y}_P^{k_\sigma i_\sigma (1,0)}\right)(P|k_\sigma a_\sigma) + (P|\hat{c_\sigma a_\sigma}) W_P^{i_\sigma c_\sigma (1,0)} \\ &- S_{c_\sigma a_\sigma} (P|\hat{i_\sigma k_\sigma}) W_P^{k_\sigma c_\sigma (1,0)} + S_{c_\sigma a_\sigma} Y_P^{i_\sigma k_\sigma (1,0)} \tilde{A}_P^{k_\sigma c_\sigma (0,0)} \\ &+ \bar{A}_P^{i_\sigma k_\sigma (1,0)} (P|k_\sigma a_\sigma).\end{aligned} \tag{B.488}$$

Replacing $\eta_{i_\sigma}^{a_\sigma (0,0)}$ with $\zeta_{i_\sigma}^{a_\sigma [1,0]}$ in the residuum (B.414) for the zeroth order singles multiplier equations will on solution yield the perturbed multipliers.

B.3.2.7 Perturbed doubles multiplier equations

For the CC2 model with one-electron perturbations, the perturbed doubles multiplier equations have only the following non-zero contributions

$$\Lambda_{\nu_2}^{[1,0]} = \lambda_{\mu_1}^{(0,0)} A_{\mu_1\nu_2}^{(1,0)} + \lambda_{\mu_2}^{(0,0)} A_{\mu_2\nu_2}^{(1,0)} + \lambda_{\mu_1}^{(0,0)} B_{\mu_1\nu_2\rho_1}^{(0,0)} t_{\rho_1}^{(1,0)} + \lambda_{\mu_1}^{(1,0)} A_{\mu_1\nu_2}^{(0,0)} + \lambda_{\mu_2}^{(1,0)} A_{\mu_2\nu_2}^{(0,0)} \stackrel{!}{=} 0. \tag{B.489}$$

B.3.2.7.1 $\lambda_{\mu_1}^{(0,0)} A_{\mu_1\nu_2}^{(1,0)}$

The contraction (B.313) of the zeroth order singles multipliers with the singles-doubles block of the perturbed Jacobian contributes

$$\begin{aligned}\left(\lambda_{\mu_1}^{(0,0)} A_{\mu_1\nu_2}^{(1,0)}\right)_{i_\sigma j_\tau}^{a_\sigma b_\tau} =& h_{j_\tau b_\tau}^{(1,0)} [S\lambda]_{i_\sigma}^{a_\sigma (0,0)} + h_{i_\sigma a_\sigma}^{(1,0)} [S\lambda]_{j_\tau}^{b_\tau (0,0)} \\ & - \delta_{\sigma\tau} h_{j_\sigma a_\sigma}^{(1,0)} [S\lambda]_{i_\sigma}^{b_\sigma (0,0)} - \delta_{\sigma\tau} h_{i_\sigma b_\sigma}^{(1,0)} [S\lambda]_{j_\sigma}^{a_\sigma (0,0)}..\end{aligned} \tag{B.490}$$

B.3.2.7.2 $\lambda_{\mu_2}^{(0,0)} A_{\mu_2\nu_2}^{(1,0)}$

From the contraction (B.314) of the zeroth order doubles multipliers with the doubles-doubles block of the perturbed Jacobian we get the contribution

$$\begin{aligned}\left(\lambda_{\mu_2}^{(0,0)} A_{\mu_2\nu_2}^{(1,0)}\right)_{i_\sigma j_\tau}^{a_\sigma b_\tau} =& [S\lambda]_{i_\sigma j_\tau}^{a_\sigma d_\tau (0,0)} \hat{h}_{d_\tau b_\tau}^{(1,0)} + \hat{h}_{c_\sigma a_\sigma}^{(1,0)} [\lambda S]_{i_\sigma j_\tau}^{c_\sigma b_\tau (0,0)} \\ & - [S\lambda S]_{i_\sigma k_\tau}^{a_\sigma b_\tau (0,0)} \hat{h}_{j_\tau k_\tau}^{(1,0)} - [S\lambda S]_{k_\sigma j_\tau}^{a_\sigma b_\tau (0,0)} \hat{h}_{i_\sigma k_\sigma}^{(1,0)}.\end{aligned} \tag{B.491}$$

B.3.2.7.3 $\lambda_{\mu_1}^{(0,0)} B_{\mu_1\nu_2\rho_1}^{(0,0)} t_{\rho_1}^{(1,0)}$

On introduction of the density fitting (B.385), the contraction (B.365) of the singles-doubles-singles block of the second derivative of the amplitude equations with respect to the amplitudes contracted with the zeroth order singles multipliers and the perturbed singles amplitudes yields

$$\begin{aligned}\left(\lambda_{\mu_1}^{(0,0)} B_{\mu_1\nu_2\rho_1}^{(0,0)} t_{\rho_1}^{(1,0)}\right)_{i_\sigma j_\tau}^{a_\sigma b_\tau} =& [S\lambda]_{j_\tau}^{b_\tau (0,0)} \left(\sum_\rho t_{c_\rho}^{k_\rho (1,0)} (P|k_\rho c_\rho) C_P^{i_\sigma a_\sigma} - t_{c_\sigma}^{k_\sigma (1,0)} (P|i_\sigma c_\sigma) C_P^{k_\sigma a_\sigma} \right) \\ & + [S\lambda]_{i_\sigma}^{a_\sigma (0,0)} \left(\sum_\rho t_{c_\rho}^{k_\rho (1,0)} (P|k_\rho c_\rho) C_P^{j_\tau b_\tau} - t_{c_\tau}^{k_\tau (1,0)} (P|j_\tau c_\tau) C_P^{k_\tau b_\tau} \right) \\ & - \delta_{\sigma\tau} [S\lambda]_{i_\sigma}^{b_\sigma (0,0)} \left(\sum_\rho t_{c_\rho}^{k_\rho (1,0)} (P|k_\rho c_\rho) C_P^{j_\sigma a_\sigma} - t_{c_\sigma}^{k_\sigma (1,0)} (P|j_\sigma c_\sigma) C_P^{k_\sigma a_\sigma} \right) \\ & - \delta_{\sigma\tau} [S\lambda]_{j_\sigma}^{a_\sigma (0,0)} \left(\sum_\rho t_{c_\rho}^{k_\rho (1,0)} (P|k_\rho c_\rho) C_P^{i_\sigma b_\sigma} - t_{c_\sigma}^{k_\sigma (1,0)} (P|i_\sigma c_\sigma) C_P^{k_\sigma b_\sigma} \right) \\ & - [S\lambda]_{j_\tau}^{c_\tau (0,0)} t_{c_\tau}^{k_\tau (1,0)} C_P^{i_\sigma a_\sigma} (P|k_\tau b_\tau) + \delta_{\sigma\tau} [S\lambda]_{j_\sigma}^{c_\sigma (0,0)} t_{c_\sigma}^{k_\sigma (1,0)} C_P^{i_\sigma b_\sigma} (P\|k_\sigma a_\sigma) \\ & + \delta_{\sigma\tau} [S\lambda]_{i_\sigma}^{c_\sigma (0,0)} t_{c_\sigma}^{k_\sigma (1,0)} C_P^{j_\sigma a_\sigma} (P|k_\sigma b_\sigma) - [S\lambda]_{i_\sigma}^{c_\sigma (0,0)} t_{c_\sigma}^{k_\sigma (1,0)} C_P^{j_\tau b_\tau} (P|k_\sigma a_\sigma) \\ & - [S\lambda]_{k_\tau}^{b_\tau (0,0)} t_{c_\tau}^{k_\tau (1,0)} C_P^{i_\sigma a_\sigma} (P|j_\tau c_\tau) + \delta_{\sigma\tau} [S\lambda]_{k_\sigma}^{b_\sigma (0,0)} t_{c_\sigma}^{k_\sigma (1,0)} C_P^{j_\sigma a_\sigma} (P|i_\sigma c_\sigma) \\ & + \delta_{\sigma\tau} [S\lambda]_{k_\sigma}^{a_\sigma (0,0)} t_{c_\sigma}^{k_\sigma (1,0)} C_P^{i_\sigma b_\sigma} (P|j_\sigma c_\sigma) - [S\lambda]_{k_\sigma}^{a_\sigma (0,0)} t_{c_\sigma}^{k_\sigma (1,0)} C_P^{j_\tau b_\tau} (P|i_\sigma c_\sigma).\end{aligned} \tag{B.492}$$

Fortunately, this can be greatly simplified by use of the intermediates $\bar{y}_{i_\sigma j_\sigma}^{(1,0)}$ for the contraction of singles amplitudes and multipliers (see (B.459)) and the intermediates

$C_P^{(1,0)}$ and $Y_P^{i_\sigma k_\sigma (1,0)}$ for the contraction of the singles amplitudes with the fitting integrals (see (B.435) and (B.436)). Doing so, we obtain

$$\begin{aligned}
\left(\lambda_{\mu_1}^{(0,0)} B_{\mu_1\nu_2\rho_1}^{(0,0)} t_{\rho_1}^{(1,0)}\right)_{i_\sigma j_\tau}^{a_\sigma b_\tau} &= [S\lambda]_{j_\tau}^{b_\tau (0,0)} \left(C_P^{(1,0)} C_P^{i_\sigma a_\sigma} + Y_P^{i_\sigma k_\sigma (1,0)} C_P^{k_\sigma a_\sigma}\right) \\
&+ [S\lambda]_{i_\sigma}^{a_\sigma (0,0)} \left(C_P^{(1,0)} C_P^{j_\tau b_\tau} + Y_P^{j_\tau k_\tau (1,0)} C_P^{k_\tau b_\tau}\right) \\
&- \delta_{\sigma\tau} [S\lambda]_{i_\sigma}^{b_\sigma (0,0)} \left(C_P^{(1,0)} C_P^{j_\sigma a_\sigma} + Y_P^{j_\sigma k_\sigma (1,0)} C_P^{k_\sigma a_\sigma}\right) \\
&- \delta_{\sigma\tau} [S\lambda]_{j_\sigma}^{a_\sigma (0,0)} \left(C_P^{(1,0)} C_P^{i_\sigma b_\sigma} + Y_P^{i_\sigma k_\sigma (1,0)} C_P^{k_\sigma b_\sigma}\right) \\
&- \bar{y}_{j_\tau k_\tau}{}^{(1,0)} C_P^{i_\sigma a_\sigma} (P|k_\tau b_\tau) + \delta_{\sigma\tau} \bar{y}_{j_\sigma k_\sigma}{}^{(1,0)} C_P^{i_\sigma b_\sigma} (P\|k_\sigma a_\sigma) \\
&+ \delta_{\sigma\tau} \bar{y}_{i_\sigma k_\sigma}{}^{(1,0)} C_P^{j_\sigma a_\sigma} (P|k_\sigma b_\sigma) - \bar{y}_{i_\sigma k_\sigma}{}^{(1,0)} C_P^{j_\tau b_\tau} (P|k_\sigma a_\sigma) \\
&+ [S\lambda]_{k_\tau}^{b_\tau (0,0)} Y_P^{j_\tau k_\tau (1,0)} C_P^{i_\sigma a_\sigma} - \delta_{\sigma\tau} [S\lambda]_{k_\sigma}^{b_\sigma (0,0)} Y_P^{i_\sigma k_\sigma (1,0)} C_P^{j_\sigma a_\sigma} \\
&- \delta_{\sigma\tau} [S\lambda]_{k_\sigma}^{a_\sigma (0,0)} Y_P^{j_\sigma k_\sigma (1,0)} C_P^{i_\sigma b_\sigma} + [S\lambda]_{k_\sigma}^{a_\sigma (0,0)} Y_P^{i_\sigma k_\sigma (1,0)} C_P^{j_\tau b_\tau}.
\end{aligned} \tag{B.493}$$

Further simplification is obtained by reusing the intermediate $(\xi_{\nu_1\rho_1} t_{\rho_1}^{(1,0)})_{i_\sigma}^{a_\sigma}$ from the singles problem (see (B.454)) and rearranging the second half of the equation to get

$$\begin{aligned}
\left(\lambda_{\mu_1}^{(0,0)} B_{\mu_1\nu_2\rho_1}^{(0,0)} t_{\rho_1}^{(1,0)}\right)_{i_\sigma j_\tau}^{a_\sigma b_\tau} &= [S\lambda]_{j_\tau}^{b_\tau (0,0)} \left(\xi_{\nu_1\rho_1}^{(0,0)} t_{\rho_1}^{(1,0)}\right)_{i_\sigma}^{a_\sigma} + [S\lambda]_{i_\sigma}^{a_\sigma (0,0)} \left(\xi_{\nu_1\rho_1}^{(0,0)} t_{\rho_1}^{(1,0)}\right)_{j_\tau}^{b_\tau} \\
&- \delta_{\sigma\tau} [S\lambda]_{i_\sigma}^{b_\sigma (0,0)} \left(\xi_{\nu_1\rho_1}^{(0,0)} t_{\rho_1}^{(1,0)}\right)_{j_\sigma}^{a_\sigma} - \delta_{\sigma\tau} [S\lambda]_{j_\sigma}^{a_\sigma (0,0)} \left(\xi_{\nu_1\rho_1}^{(0,0)} t_{\rho_1}^{(1,0)}\right)_{i_\sigma}^{b_\sigma} \\
&+ C_P^{i_\sigma a_\sigma} \left([S\lambda]_{k_\tau}^{b_\tau (0,0)} Y_P^{j_\tau k_\tau (1,0)} - \bar{y}_{j_\tau k_\tau}{}^{(1,0)} (P|k_\tau b_\tau)\right) \\
&- \delta_{\sigma\tau} C_P^{i_\sigma b_\sigma} \left([S\lambda]_{k_\sigma}^{a_\sigma (0,0)} Y_P^{j_\sigma k_\sigma (1,0)} - \bar{y}_{j_\sigma k_\sigma}{}^{(1,0)} (P\|k_\sigma a_\sigma)\right) \\
&- \delta_{\sigma\tau} C_P^{j_\sigma a_\sigma} \left([S\lambda]_{k_\sigma}^{b_\sigma (0,0)} Y_P^{i_\sigma k_\sigma (1,0)} - \bar{y}_{i_\sigma k_\sigma}{}^{(1,0)} (P|k_\sigma b_\sigma)\right) \\
&+ C_P^{j_\tau b_\tau} \left([S\lambda]_{k_\sigma}^{a_\sigma (0,0)} Y_P^{i_\sigma k_\sigma (1,0)} - \bar{y}_{i_\sigma k_\sigma}{}^{(1,0)} (P|k_\sigma a_\sigma)\right).
\end{aligned} \tag{B.494}$$

Defining the intermediate

$$\bar{V}_P^{i_\sigma a_\sigma (1,0)} = [S\lambda]_{k_\sigma}^{a_\sigma (0,0)} Y_P^{i_\sigma k_\sigma (1,0)} - \bar{y}_{i_\sigma k_\sigma}{}^{(1,0)} (P|k_\sigma a_\sigma) \tag{B.495}$$

we finally arrive at

$$\begin{aligned}
\left(\lambda_{\mu_1}^{(0,0)} B_{\mu_1\nu_2\rho_1}^{(0,0)} t_{\rho_1}^{(1,0)}\right)_{i_\sigma j_\tau}^{a_\sigma b_\tau} &= [S\lambda]_{j_\tau}^{b_\tau (0,0)} \left(\xi_{\nu_1\rho_1}^{(0,0)} t_{\rho_1}^{(1,0)}\right)_{i_\sigma}^{a_\sigma} + [S\lambda]_{i_\sigma}^{a_\sigma (0,0)} \left(\xi_{\nu_1\rho_1}^{(0,0)} t_{\rho_1}^{(1,0)}\right)_{j_\tau}^{b_\tau} \\
&- \delta_{\sigma\tau} [S\lambda]_{i_\sigma}^{b_\sigma (0,0)} \left(\xi_{\nu_1\rho_1}^{(0,0)} t_{\rho_1}^{(1,0)}\right)_{j_\sigma}^{a_\sigma} - \delta_{\sigma\tau} [S\lambda]_{j_\sigma}^{a_\sigma (0,0)} \left(\xi_{\nu_1\rho_1}^{(0,0)} t_{\rho_1}^{(1,0)}\right)_{i_\sigma}^{b_\sigma} \\
&+ C_P^{i_\sigma a_\sigma} \bar{V}_P^{j_\tau b_\tau (1,0)} - \delta_{\sigma\tau} C_P^{i_\sigma b_\sigma} \bar{V}_P^{j_\sigma a_\sigma (1,0)} \\
&- \delta_{\sigma\tau} C_P^{j_\sigma a_\sigma} \bar{V}_P^{i_\sigma b_\sigma (1,0)} + C_P^{j_\tau b_\tau} \bar{V}_P^{i_\sigma a_\sigma (1,0)}.
\end{aligned} \tag{B.496}$$

B.3.2.7.4 $\lambda^{(1,0)}_{\mu_1} A^{(0,0)}_{\mu_1\nu_2}$ and $\lambda^{(1,0)}_{\mu_2} A^{(0,0)}_{\mu_2\nu_2}$

Contraction of the perturbed multipliers with the unperturbed Jacobian is again identical to the contractions of the zeroth order multipliers with the unperturbed Jacobian except for the order of multipliers. Since the code is easily shared with the unperturbed multiplier equations, no explicit expression will be given here.

B.3.2.7.5 $\zeta^{[1,0]}_{\nu_2}$

The non-iterative part of the perturbed doubles equations is obtained by combining (B.490) , (B.491) and (B.496)

$$\begin{aligned}
\zeta^{a_\sigma b_\tau\,[1,0]}_{i_\sigma j_\tau} =& h^{(1,0)}_{j_\tau b_\tau}[S\lambda]^{a_\sigma\,(0,0)}_{i_\sigma} + h^{(1,0)}_{i_\sigma a_\sigma}[S\lambda]^{b_\tau\,(0,0)}_{j_\tau} - \delta_{\sigma\tau} h^{(1,0)}_{j_\sigma a_\sigma}[S\lambda]^{b_\sigma\,(0,0)}_{i_\sigma} \\
& - \delta_{\sigma\tau} h^{(1,0)}_{i_\sigma b_\sigma}[S\lambda]^{a_\sigma\,(0,0)}_{j_\sigma} + [S\lambda]^{a_\sigma d_\tau\,(0,0)}_{i_\sigma j_\tau}\hat{h}^{(1,0)}_{d_\tau b_\tau} + \hat{h}^{(1,0)}_{c_\sigma a_\sigma}[\lambda S]^{c_\sigma b_\tau\,(0,0)}_{i_\sigma j_\tau} \\
& - [S\lambda S]^{a_\sigma b_\tau\,(0,0)}_{i_\sigma k_\tau}\hat{h}^{(1,0)}_{j_\tau k_\tau} - [S\lambda S]^{a_\sigma b_\tau\,(0,0)}_{k_\sigma j_\tau}\hat{h}^{(1,0)}_{i_\sigma k_\sigma} + [S\lambda]^{b_\tau\,(0,0)}_{j_\tau}\left(\xi_{\nu_1\rho_1} t^{(1,0)}_{\rho_1}\right)^{a_\sigma}_{i_\sigma} \\
& + [S\lambda]^{a_\sigma\,(0,0)}_{i_\sigma}\left(\xi_{\nu_1\rho_1} t^{(1,0)}_{\rho_1}\right)^{b_\tau}_{j_\tau} - \delta_{\sigma\tau}[S\lambda]^{b_\sigma\,(0,0)}_{i_\sigma}\left(\xi_{\nu_1\rho_1} t^{(1,0)}_{\rho_1}\right)^{a_\sigma}_{j_\sigma} \\
& - \delta_{\sigma\tau}[S\lambda]^{a_\sigma\,(0,0)}_{j_\sigma}\left(\xi_{\nu_1\rho_1} t^{(1,0)}_{\rho_1}\right)^{b_\sigma}_{i_\sigma} + C_P^{i_\sigma a_\sigma}\bar{V}_P^{j_\tau b_\tau\,(1,0)} - \delta_{\sigma\tau} C_P^{i_\sigma b_\sigma}\bar{V}_P^{j_\sigma a_\sigma\,(1,0)} \\
& - \delta_{\sigma\tau} C_P^{j_\sigma a_\sigma}\bar{V}_P^{i_\sigma b_\sigma\,(1,0)} + C_P^{j_\tau b_\tau}\bar{V}_P^{i_\sigma a_\sigma\,(1,0)} \qquad \text{(B.497)} \\
=& [S\lambda]^{a_\sigma\,(0,0)}_{i_\sigma}\left(h^{(1,0)}_{j_\tau b_\tau} + \left(\xi_{\nu_1\rho_1} t^{(1,0)}_{\rho_1}\right)^{b_\tau}_{j_\tau}\right) \\
& + [S\lambda]^{b_\tau\,(0,0)}_{j_\tau}\left(h^{(1,0)}_{i_\sigma a_\sigma} + \left(\xi_{\nu_1\rho_1} t^{(1,0)}_{\rho_1}\right)^{a_\sigma}_{i_\sigma}\right) \\
& - \delta_{\sigma\tau}[S\lambda]^{b_\sigma\,(0,0)}_{i_\sigma}\left(h^{(1,0)}_{j_\sigma a_\sigma} + \left(\xi_{\nu_1\rho_1} t^{(1,0)}_{\rho_1}\right)^{a_\sigma}_{j_\sigma}\right) \\
& - \delta_{\sigma\tau}[S\lambda]^{a_\sigma\,(0,0)}_{j_\sigma}\left(h^{(1,0)}_{i_\sigma b_\sigma} + \left(\xi_{\nu_1\rho_1} t^{(1,0)}_{\rho_1}\right)^{b_\sigma}_{i_\sigma}\right) \\
& + [S\lambda]^{a_\sigma d_\tau\,(0,0)}_{i_\sigma j_\tau}\hat{h}^{(1,0)}_{d_\tau b_\tau} + \hat{h}^{(1,0)}_{c_\sigma a_\sigma}[\lambda S]^{c_\sigma b_\tau\,(0,0)}_{i_\sigma j_\tau} - [S\lambda S]^{a_\sigma b_\tau\,(0,0)}_{i_\sigma k_\tau}\hat{h}^{(1,0)}_{j_\tau k_\tau} \\
& - [S\lambda S]^{a_\sigma b_\tau\,(0,0)}_{k_\sigma j_\tau}\hat{h}^{(1,0)}_{i_\sigma k_\sigma} + C_P^{i_\sigma a_\sigma}\bar{V}_P^{j_\tau b_\tau\,(1,0)} - \delta_{\sigma\tau} C_P^{i_\sigma b_\sigma}\bar{V}_P^{j_\sigma a_\sigma\,(1,0)} \\
& - \delta_{\sigma\tau} C_P^{j_\sigma a_\sigma}\bar{V}_P^{i_\sigma b_\sigma\,(1,0)} + C_P^{j_\tau b_\tau}\bar{V}_P^{i_\sigma a_\sigma\,(1,0)}. \qquad \text{(B.498)}
\end{aligned}$$

Using the intermediate $\bar{\eta}^{a_\sigma\,(1,0)}_{i_\sigma}$ defined in (B.487) we obtain

$$\begin{aligned}
\zeta^{a_\sigma b_\tau\,[1,0]}_{i_\sigma j_\tau} =& [S\lambda]^{a_\sigma\,(0,0)}_{i_\sigma}\bar{\eta}^{b_\tau\,(1,0)}_{j_\tau} + [S\lambda]^{b_\tau\,(0,0)}_{j_\tau}\bar{\eta}^{a_\sigma\,(1,0)}_{i_\sigma} - \delta_{\sigma\tau}[S\lambda]^{b_\sigma\,(0,0)}_{i_\sigma}\bar{\eta}^{a_\sigma\,(1,0)}_{j_\sigma} \\
& - \delta_{\sigma\tau}[S\lambda]^{a_\sigma\,(0,0)}_{j_\sigma}\bar{\eta}^{b_\sigma\,(1,0)}_{i_\sigma} + [S\lambda]^{a_\sigma d_\tau\,(0,0)}_{i_\sigma j_\tau}\hat{h}^{(1,0)}_{d_\tau b_\tau} + \hat{h}^{(1,0)}_{c_\sigma a_\sigma}[\lambda S]^{c_\sigma b_\tau\,(0,0)}_{i_\sigma j_\tau} \\
& - [S\lambda S]^{a_\sigma b_\tau\,(0,0)}_{i_\sigma k_\tau}\hat{h}^{(1,0)}_{j_\tau k_\tau} - [S\lambda S]^{a_\sigma b_\tau\,(0,0)}_{k_\sigma j_\tau}\hat{h}^{(1,0)}_{i_\sigma k_\sigma} + C_P^{i_\sigma a_\sigma}\bar{V}_P^{j_\tau b_\tau\,(1,0)} \\
& - \delta_{\sigma\tau} C_P^{i_\sigma b_\sigma}\bar{V}_P^{j_\sigma a_\sigma\,(1,0)} - \delta_{\sigma\tau} C_P^{j_\sigma a_\sigma}\bar{V}_P^{i_\sigma b_\sigma\,(1,0)} + C_P^{j_\tau b_\tau}\bar{V}_P^{i_\sigma a_\sigma\,(1,0)}. \qquad \text{(B.499)}
\end{aligned}$$

Replacing $\eta^{a_\sigma b_\tau\,(0,0)}_{i_\sigma j_\tau}$ with $\zeta^{a_\sigma b_\tau\,[1,0]}_{i_\sigma j_\tau}$ in the residuum (B.423) of the zeroth order doubles multipliers yields on solution the perturbed multipliers.

B.3.2.8 Perturbed density matrices

The perturbed one-electron density matrix is implicitly defined by the equation

$$h^{(0,1)}_{\mu\nu} D^{(1,0)}_{\nu\mu} = \eta^{(0,1)}_{\nu} t^{(1,0)}_{\nu} + \lambda^{(1,0)}_{\mu} \Omega^{(0,1)}_{\mu} + \lambda^{(0,0)}_{\mu} A^{(0,1)}_{\mu\nu} t^{(1,0)}_{\nu} \tag{B.500}$$

where $D^{(1,0)}_{\nu\mu}$ is either the charge or spin density matrix in atomic orbital basis depending on the property in question. Note that on the left hand side of this equations, the indices μ and ν represent atomic orbitals whereas on the right hand side they represent "excited" determinants.
Just like we did for the unperturbed density matrix in (B.427), the perturbed density matrices in molecular orbital basis can be separated into four blocks. Except for the orders on integrals, amplitudes and multipliers, the contributions from $\eta^{(0,1)}_{\nu} t^{(1,0)}_{\nu}$ and $\lambda^{(1,0)}_{\mu} \Omega^{(0,1)}_{\mu}$ to the perturbed density matrices are identical to those from $E^{(1,0)}$ and $\lambda^{(0,0)}_{\mu} \Omega^{(1,0)}_{\mu}$ to the unperturbed density matrix (see (B.134), (B.142) and (B.183)). Only the contraction (B.327) of zeroth order multipliers and perturbed amplitudes with the perturbed Jacobian leads to new terms.
The simplest block is the occupied-virtual block with a single contribution from (B.183)

$$D^{(1,0)}_{i_\sigma a_\sigma} = \lambda^{a_\sigma\,(1,0)}_{i_\sigma}. \tag{B.501}$$

The occupied-occupied block has two contributions from (B.327) and a single contribution from (B.183)

$$\begin{aligned} D^{(1,0)}_{j_\sigma i_\sigma} = &-[St]^{i_\sigma\,(1,0)}_{c_\sigma} \lambda^{c_\sigma\,(0,0)}_{j_\sigma} - \sum_\tau (1 - \frac{\delta_{\sigma\tau}}{2}) \lambda^{c_\tau b_\sigma\,(1,0)}_{k_\tau j_\sigma} [StS]^{k_\tau i_\sigma\,(0,0)}_{c_\tau b_\sigma} \\ &- \sum_\tau (1 - \frac{\delta_{\sigma\tau}}{2}) [S\lambda S]^{c_\tau b_\sigma\,(0,0)}_{k_\tau j_\sigma} t^{k_\tau i_\sigma\,(1,0)}_{c_\tau b_\sigma}, \end{aligned} \tag{B.502}$$

where the contractions of the doubles quantities with the overlap are chosen to allow the use of the same code for both contributions. The same holds for the virtual-virtual block

$$\begin{aligned} D^{(1,0)}_{b_\sigma a_\sigma} = &\, t^{k_\sigma\,(1,0)}_{b_\sigma} \lambda^{a_\sigma\,(0,0)}_{k_\sigma} + \sum_\tau (1 - \frac{\delta_{\sigma\tau}}{2}) [S\lambda]^{c_\tau a_\sigma\,(0,0)}_{k_\tau j_\sigma} t^{k_\tau j_\sigma\,(1,0)}_{c_\tau b_\sigma} \\ &+ \sum_\tau (1 - \frac{\delta_{\sigma\tau}}{2}) \lambda^{c_\tau a_\sigma\,(1,0)}_{k_\tau j_\sigma} [St]^{k_\tau j_\sigma\,(0,0)}_{c_\tau b_\sigma}. \end{aligned} \tag{B.503}$$

Finally, the virtual-occupied block has one contribution from (B.142), one contribution from (B.183) and three contributions from (B.327)

$$\begin{aligned} D^{(1,0)}_{a_\sigma i_\sigma} = &\, t^{i_\sigma\,(1,0)}_{a_\sigma} + \sum_\tau [S\lambda]^{b_\tau\,(1,0)}_{j_\tau} t^{b_\tau a_\sigma\,(0,0)}_{j_\tau i_\sigma} + \sum_\tau [S\lambda]^{b_\tau\,(0,0)}_{j_\tau} t^{b_\tau a_\sigma\,(1,0)}_{j_\tau i_\sigma} \\ &- [St]^{i_\sigma\,(1,0)}_{c_\sigma} \sum_\tau (1 - \frac{\delta_{\sigma\tau}}{2}) \lambda^{b_\tau c_\sigma\,(0,0)}_{j_\tau k_\sigma} [tS]^{j_\tau k_\sigma\,(0,0)}_{b_\tau a_\sigma} \\ &- t^{k_\sigma\,(1,0)}_{a_\sigma} \sum_\tau (1 - \frac{\delta_{\sigma\tau}}{2}) \lambda^{b_\tau d_\sigma\,(0,0)}_{j_\tau k_\sigma} [StS]^{j_\tau i_\sigma\,(0,0)}_{b_\tau d_\sigma} \end{aligned} \tag{B.504}$$

$$\begin{aligned} = &\, t^{i_\sigma\,(1,0)}_{a_\sigma} + \sum_\tau [S\lambda]^{b_\tau\,(1,0)}_{j_\tau} t^{b_\tau a_\sigma\,(0,0)}_{j_\tau i_\sigma} + \sum_\tau [S\lambda]^{b_\tau\,(0,0)}_{j_\tau} t^{b_\tau a_\sigma\,(1,0)}_{j_\tau i_\sigma} \\ &- [St]^{i_\sigma\,(1,0)}_{c_\sigma} D^{(0,0)}_{a_\sigma c_\sigma} + t^{k_\sigma\,(1,0)}_{a_\sigma} D^{(0,0)}_{k_\sigma i_\sigma}, \end{aligned} \tag{B.505}$$

where we have used the virtual-virtual and occupied-occupied blocks (B.430) and (B.428) of the zeroth order density matrix as intermediates.
The density matrices in atomic orbital basis can again be obtained by the transformation (B.427) followed by addition of the perturbed spin-specific density matrices to obtain the perturbed charge density matrices or subtraction and multiplication of appropriate factors to obtain the (normalized) perturbed spin density matrices.

Appendix C

Tables

Table C.1: Diagonal elements of the g-shifts and isotropic g-shifts [ppm] calculated with Z_{eff}-GIAO-CCSD at the aug-cc-pVTZ level for their benchmark set by Gauss *et al.*[33]

Molecule	Δg_{xx}	Δg_{yy}	Δg_{zz}	Δg_{iso}
BO	-1870	-1870	-60	-1267
CH_3	-84	646	646	403
CN	-2151	-2151	-124	-1475
CO^+	-2598	-2598	-125	-1774
CO_2^-	840	-5104	-779	-1681
H_2CO^+	6172	144	721	2346
H_2O^+	-188	16667	4940	7140
NF_2	-699	6704	3766	3257
NF_3^+	3766	-2010	5178	2311
NH	1465	1465	-105	942
NO_2	3596	-11728	-762	-2965
OH^+	4119	4119	-173	2688
O_2	2669	2669	-199	1713
O_3^-	-706	18062	10668	9341

Table C.2: Diagonal elements of the g-shifts and isotropic g-shifts [ppm] calculated by Glasbrenner *et al.*[36] with Z_{eff}-GIAO-B3LYP at the aug-cc-pVTZ level for the benchmark set of Gauss *et al.*[33]

Molecule	Δg_{xx}	Δg_{yy}	Δg_{zz}	Δg_{iso}
BO	-1840	-1840	-68	-1249
CH_3	-89	653	653	406
CN	-2173	-2173	-134	-1493
CO^+	-2620	-2620	-134	-1791
CO_2^-	951	-5142	-724	-1638
H_2CO^+	5927	86	249	2087
H_2O^+	-189	13654	4701	6055
NF_2	-669	7010	4147	3496
NH	1369	1369	-106	877
NO_2	3643	-11873	-697	-2976
OH^+	3722	3722	-173	2424
O_2	2686	2686	-200	1724
O_3^-	-554	18459	11084	9663

Table C.3: Diagonal elements of the g-shifts and isotropic g-shifts [ppm] calculated by Glasbrenner *et al.*[36] with SOMF-GIAO-B3LYP at the aug-cc-pVTZ level for the benchmark set of Gauss *et al.*[33]

Molecule	Δg_{xx}	Δg_{yy}	Δg_{zz}	Δg_{iso}
BO	-1699	-1699	-68	-1155
CH_3	-90	520	520	317
CN	-2029	-2029	-134	-1397
CO^+	-2451	-2451	-134	-1679
CO_2^-	914	-4636	-677	-1466
H_2CO^+	5458	80	212	1917
H_2O^+	-189	12300	4152	5421
NF_2	-619	6376	3757	3171
NH	1214	1214	-106	774
NO_2	3444	-10851	-656	-2688
OH^+	3389	3389	-173	2202
O_2	2498	2498	-200	1599
O_3^-	-526	17026	10174	8891

Table C.4: Experimentally determined diagonal elements of the g-shifts and isotropic g-shifts [ppm] assembled by Perera *et al.*[34] for comparison to their benchmark set.

Molecule	Δg_{xx}	Δg_{yy}	Δg_{zz}	Δg_{iso}
BO	-800	-800	-110	-570
BS(I)	-8100	-8100	-700	-5633
BS(II)	-8900	-8900	-800	-6200
CF_3Br^-	4700	4700	-200	3067
CF_3Cl^-	1300	1300	18900	7167
CHO	1500	0	-7500	-2000
CH_4^+	600	600	0	400
CN	-2000	-2000	-800	-1600
CO^+(I)	-2400	-2400	-1200	-2000
CO^+(II)	-3000	-3000	-1400	-2467
CO_2^-	700	-4800	-500	-1533
C_3H_5	0	400	800	400
ClO_2(I)	1300	16000	6500	7933
ClO_2(II)	300	14000	11000	8433
H_2CO^+	4600	-800	200	1333
H_2O^+	200	18800	4800	7933
MgF	-1300	-1300	-300	-967
NF_2	-100	6200	2800	2967
NF_3^+	1000	1000	7000	3000
NO_2	3900	-11300	-300	-2567
NO_3^{2-}	3400	3400	-800	2000
O_2H	-800	40000	5600	14933
O_3^-(I)	200	14700	9700	8200
O_3^-(II)	1300	16400	10000	9233
SO_2^-	-400	9700	3400	4233
SiH_3	1000	1000	5000	2333

Table C.5: Energies and isotropic g-shifts [ppm] for the g-tensor calculations with GIAO-CCSD at the aug-cc-pVTZ level for their benchmark set by Perera *et al.*[34] as provided by Perera and Morales in private communication.[108]

Molecule	E_{HF} [Hartree]	E_{corr} [Hartree]	Δg^{ZKE}	$\Delta g_{iso}^{1el-DSO}$	$\Delta g_{iso}^{2el-DSO}$	$\Delta g_{iso}^{1el-PSO}$	$\Delta g_{iso}^{2el-PSO}$	Δg_{iso}
BO	-99.557393	-0.332805	-88	100	-77	-1808	688	-1185
BS	-422.188569	-0.301280	-100	136	-106	-7370	1593	-5847
CF_3Br^-	-2908.795810	-1.273412	-308	187	-694	20206	-1686	17705
CF_3Cl^-	-795.699043	-1.266603	-389	234	-461	293	190	-132
CHO	-113.292120	-0.412644	-200	153	-136	-3061	1379	-1866
CH_3	-39.577973	-0.198634	-123	87	-99	780	-365	279
CH_4^+	-39.773584	-0.206547	-119	86	-89	1186	-569	494
CN	-92.235674	-0.345674	-165	141	-109	-2162	880	-1414
COH	-113.242854	-0.397869	-154	129	-137	-6955	3269	-3848
CO^+	-112.303624	-0.358051	-170	150	-99	-2480	920	-1678
CO_2^-	-187.661020	-0.667814	-207	164	-205	-2322	1019	-1550
C_3H_5	-116.510653	-0.561176	-131	134	-169	699	-270	263
ClO_2	-609.055004	-0.768563	-361	296	-305	15085	-4122	10594
H_2CO^+	-113.568295	-0.391772	-296	188	-182	3557	-1097	2169
H_2O^+	-75.638782	-0.236482	-316	174	-153	10463	-3749	6419
MgF	-299.146470	-0.322550	-68	127	-97	-1601	483	-1155
NCl	-513.909002	-0.405571	-236	205	-214	4100	-840	3015
NF	-153.838063	-0.433672	-263	178	-185	1737	-443	1023
NF_2	-253.267263	-0.739045	-317	213	-295	4640	-1327	2914
NF_3^+	-352.251055	-1.014307	-387	269	-354	7203	-2094	4636
NH	-54.982561	-0.171652	-202	121	-108	1639	-584	865
NO_2	-204.113035	-0.712004	-321	225	-246	-4091	1735	-2698
NO_3^{2-}	-278.779036	-1.007643	-285	197	-337	3235	-955	1855
OH^+	-75.004259	-0.176734	-322	174	-137	4127	-1273	2570
O_2	-149.676552	-0.472894	-362	223	-214	2742	-813	1575
O_2H	-150.238348	-0.497444	-345	215	-221	22534	-7842	14341
O_3^-	-224.444872	-0.785686	-372	239	-282	13638	-4646	8576
PH	-341.297937	-0.174255	-151	155	-144	3600	-736	2723
SH^+	-397.768037	-0.176921	-233	203	-177	7026	-1334	5486
SO	-472.399624	-0.448980	-275	241	-228	4203	-1000	2941
SO_2^-	-547.316377	-0.743812	-295	264	-288	6332	-1696	4318
S_2	-795.095373	-0.416926	-239	265	-246	10620	-1890	8509
SiH_3	-290.640489	-0.206058	-114	133	-129	1631	-343	1178

Table C.6: Miscellaneous data and isotropic g-shifts [ppm] for the g-tensor calculations with Z_{eff}-SDC-DF-LUCC2 at the aug-cc-pVTZ/DF-QZ level with DF-UHF reference, extended domains and full pair lists for the benchmark set of Perera *et al.*[34]

Molecule	E_{HF} [Hartree]	E_{corr} [Hartree]	$< S^2 >_{HF}$	$\frac{N_{pairs\ included}}{N_{all\ pairs}}$ [%]	N_{AO}	$t_{CPU}^{DF-LUCC2}$ [sec]	Δg^{ZKE}	$\Delta g_{iso}^{1el-DSO}$	$\Delta g_{iso}^{2el-DSO}$	$\Delta g_{iso}^{1el-PSO}$	$\Delta g_{iso}^{2el-PSO}$	Δg_{iso}
BO	-99.557305	-0.312369	0.80	100.0	92	38.20	-91	108	-45	-1835	579	-1284
BS	-422.188506	-0.239333	0.86	100.0	96	40.34	-97	121	-43	-7459	1237	-6241
CF_3Br^-	-2908.795707	-1.110197	0.76	100.0	243	894.59	-305	211	-50	19443	-208	19091
CF_3Cl^-	-795.698970	-1.196188	0.79	100.0	234	1197.73	-367	163	-50	189	-82	-146
CHO	-113.292046	-0.385861	0.77	100.0	115	62.89	-195	160	-54	-2795	916	-1968
CH_3	-39.577973	-0.161235	0.76	100.0	115	43.71	-124	87	-33	748	-295	382
CH_4^+	-39.773583	-0.167693	0.76	100.0	138	51.65	-118	86	-29	1136	-446	627
CN	-92.235591	-0.313528	1.16	100.0	92	43.15	-169	153	-59	-2023	712	-1386
COH	-113.242806	-0.360749	0.76	100.0	115	65.61	-156	128	-45	-6167	2239	-4002
CO^+	-112.303500	-0.335490	0.96	100.0	92	41.92	-177	156	-59	-2616	817	-1880
CO_2^-	-187.660921	-0.648176	0.76	100.0	138	138.21	-193	175	-60	-2051	651	-1477
C_3H_5	-116.510629	-0.472963	0.97	100.0	253	392.50	-131	135	-54	678	-267	361
ClO_2	-609.063612	-0.728793	0.78	100.0	142	194.24	-339	289	-66	10188	-2748	7323
H_2CO^+	-113.568241	-0.345111	0.79	100.0	138	73.12	-292	193	-59	3934	-1153	2622
H_2O^+	-75.638777	-0.208904	0.76	100.0	92	37.17	-319	175	-52	9959	-2979	6784
MgF	-299.146439	-0.293276	0.75	100.0	96	41.23	-65	142	-18	-1798	275	-1464
NCl	-513.908958	-0.337367	2.04	100.0	96	48.75	-237	192	-52	3049	-711	2241
NF	-153.838027	-0.405233	2.02	100.0	92	43.97	-267	168	-54	1511	-399	959
NF_2	-253.267184	-0.704098	0.76	100.0	138	163.16	-320	206	-63	3976	-1060	2738
NF_3^+	-352.249619	-0.979373	0.77	100.0	184	404.64	-386	285	-84	6150	-1575	4390
NH	-54.982558	-0.140629	2.02	100.0	69	27.05	-204	122	-42	1554	-544	885
NO_2	-204.112925	-0.706715	0.77	100.0	138	133.16	-309	234	-75	-3403	1077	-2477
NO_3^{2-}	-278.761774	-1.034479	0.75	100.0	184	540.91	-20	83	-26	-168	50	-80
OH^+	-75.004253	-0.146661	2.01	100.0	69	34.17	-324	175	-52	3954	-1187	2566
O_2	-149.676485	-0.455943	2.05	100.0	92	44.88	-352	219	-66	2587	-776	1613
O_2H	-150.238306	-0.469231	0.76	100.0	115	73.42	-342	211	-63	19519	-5853	13471
O_3^-	-224.444794	-0.780618	0.79	100.0	138	174.87	-343	230	-69	11074	-3322	7570
PH	-341.297934	-0.109531	2.03	100.0	73	29.91	-152	155	-21	3136	-431	2687
SH^+	-397.768037	-0.117895	2.02	100.0	73	27.68	-234	203	-30	6297	-945	5291
SO	-472.399520	-0.401246	2.06	100.0	96	49.72	-265	239	-48	3640	-854	2713
SO_2^-	-547.316203	-0.706723	0.79	100.0	142	177.16	-277	258	-55	5020	-1324	3621
S_2	-795.095287	-0.326177	2.06	100.0	100	51.53	-235	263	-39	9462	-1419	8030
SiH_3	-290.640479	-0.119492	0.76	100.0	119	44.90	-115	172	-21	919	-115	841

Table C.7: Diagonal elements of the g-shifts [ppm] calculated with Z_{eff}-SDC-DF-LUCC2 at the aug-cc-pVTZ/DF-QZ level with DF-UHF reference, extended domains and full pair lists for the benchmark set of Perera *et al.*[34]

Molecule	$\Delta g_{xx}^{1el-DSO}$	$\Delta g_{yy}^{1el-DSO}$	$\Delta g_{zz}^{1el-DSO}$	$\Delta g_{xx}^{2el-DSO}$	$\Delta g_{yy}^{2el-DSO}$	$\Delta g_{zz}^{2el-DSO}$	$\Delta g_{xx}^{1el-PSO}$	$\Delta g_{yy}^{1el-PSO}$	$\Delta g_{zz}^{1el-PSO}$	$\Delta g_{xx}^{2el-PSO}$	$\Delta g_{yy}^{2el-PSO}$	$\Delta g_{zz}^{2el-PSO}$	Δg_{xx}	Δg_{yy}	Δg_{zz}
BO	136	136	51	-55	-55	-24	-2752	-2752	0	868	868	-0	-1894	-1894	-63
BS	161	161	40	-53	-53	-22	-11189	-11189	-0	1856	1856	0	-9322	-9322	-79
CF_3Br^-	233	233	166	-60	-60	-30	29403	29403	-477	-369	-369	115	28902	28902	-531
CF_3Cl^-	158	158	174	-49	-49	-52	-511	-511	1588	69	69	-383	-699	-699	961
CHO	204	115	162	-69	-40	-54	3077	-1113	-10350	-955	357	3346	2062	-876	-7091
CH_3	47	107	107	-20	-40	-40	29	1107	1107	-11	-437	-437	-79	613	613
CH_4^+	102	102	53	-34	-34	-19	1744	1717	-54	-687	-676	24	1007	990	-115
CN	195	195	70	-75	-75	-28	-3034	-3034	-0	1068	1068	0	-2015	-2015	-127
COH	162	89	132	-57	-30	-49	1022	-626	-18898	-370	194	6892	601	-529	-12079
CO^+	195	195	78	-73	-73	-32	-3924	-3924	0	1225	1225	-0	-2754	-2754	-131
CO_2^-	217	105	204	-75	-36	-70	990	-1749	-5393	-336	551	1739	604	-1323	-3713
C_3H_5	107	124	175	-45	-47	-69	-57	1128	963	25	-448	-379	-102	626	559
ClO_2	226	335	305	-50	-77	-72	-647	17524	13687	109	-4515	-3838	-701	12928	9742
H_2CO^+	199	140	240	-60	-43	-75	1910	813	9078	-487	-243	-2730	1271	375	6221
H_2O^+	103	211	211	-31	-63	-62	111	12241	17525	-34	-3663	-5240	-170	8408	12115
MgF	169	169	89	-22	-22	-11	-2697	-2697	-0	413	413	0	-2203	-2203	13
NCl	191	191	193	-50	-50	-56	4573	4573	0	-1067	-1067	-0	3411	3411	-100
NF	158	158	188	-50	-50	-61	2266	2266	-0	-598	-598	0	1509	1509	-140
NF_2	137	239	241	-42	-74	-74	-564	5802	6690	145	-1524	-1801	-644	4122	4735
NF_3^+	341	341	172	-100	-100	-51	9604	9604	-758	-2463	-2463	201	6996	6996	-822
NH	108	108	149	-37	-37	-51	2331	2331	0	-816	-816	-0	1381	1381	-106
NO_2	295	159	248	-95	-51	-80	4624	-2903	-11930	-1444	908	3766	3071	-2197	-8304
NO_3^{2-}	79	85	85	-25	-27	-27	-211	-146	-146	64	43	43	-113	-64	-64
OH^+	156	156	212	-46	-46	-63	5931	5931	-0	-1781	-1781	0	3936	3936	-174
O_2	214	214	230	-64	-64	-69	3881	3881	-0	-1164	-1164	0	2515	2515	-191
O_2H	144	253	235	-43	-76	-70	-43	15883	42716	13	-4764	-12808	-272	10954	29731
O_3^-	171	265	254	-51	-80	-76	-761	15143	18840	228	-4543	-5652	-756	10443	13022
PH	135	135	194	-18	-18	-26	4704	4704	0	-647	-647	-0	4022	4022	16
SH^+	178	178	252	-26	-26	-37	9446	9446	-0	-1417	-1417	0	7946	7946	-19
SO	236	236	246	-47	-47	-50	5461	5460	-0	-1281	-1281	0	4104	4103	-68
SO_2^-	192	294	289	-41	-63	-62	-394	7301	8153	54	-1901	-2126	-467	5354	5977
S_2	261	261	266	-39	-39	-40	14193	14193	-0	-2129	-2129	0	12050	12050	-10
SiH_3	219	219	79	-26	-26	-10	1392	1392	-28	-174	-174	4	1296	1296	-70

Table C.8: Miscellaneous data and isotropic g-shifts [ppm] for the g-tensor calculations with Z_{eff}-SDC-DF-LUCC2 at the aug-cc-pVTZ/DF-QZ level with DF-ROHF reference, extended domains and full pair lists for the benchmark set of Perera *et al.*[34]

Molecule	E_{HF} [Hartree]	E_{corr} [Hartree]	$< S^2 >_{HF}$	$\frac{N_{pairs\ included}}{N_{all\ pairs}}$ [%]	N_{AO}	$t_{CPU}^{DF-LUCC2}$ [sec]	Δg^{ZKE}	$\Delta g_{iso}^{1el-DSO}$	$\Delta g_{iso}^{2el-DSO}$	$\Delta g_{iso}^{1el-PSO}$	$\Delta g_{iso}^{2el-PSO}$	Δg_{iso}
BO	-99.553926	-0.316814	0.75	100.0	92	39.80	-87	108	-44	-1583	507	-1099
BS	-422.184218	-0.245037	0.75	100.0	96	40.66	-100	125	-43	-6173	1060	-5133
CF_3Br^-	-2908.791024	-1.115109	0.75	100.0	243	894.89	-311	213	-50	18964	-214	18601
CF_3Cl^-	-795.690495	-1.206811	0.75	100.0	234	1198.61	-367	163	-49	493	-114	125
CHO	-113.286376	-0.392355	0.75	100.0	115	62.53	-197	161	-55	-2759	907	-1943
CH_3	-39.573445	-0.165969	0.75	100.0	115	38.22	-127	87	-33	750	-296	381
CH_4^+	-39.769453	-0.172100	0.75	100.0	138	47.43	-121	86	-29	1155	-454	636
CN	-92.218384	-0.346670	0.75	100.0	92	43.30	-176	156	-60	-1925	694	-1310
COH	-113.237536	-0.366385	0.75	100.0	115	66.17	-159	128	-46	-6293	2294	-4076
CO^+	-112.292586	-0.352902	0.75	100.0	92	40.14	-174	157	-60	-2232	715	-1594
CO_2^-	-187.656161	-0.653794	0.75	100.0	138	166.16	-196	176	-61	-2083	662	-1502
C_3H_5	-116.485495	-0.503873	0.75	100.0	253	374.23	-133	134	-53	662	-262	348
ClO_2	-609.041983	-0.762177	0.75	100.0	142	217.25	-334	286	-66	10704	-2697	7893
H_2CO^+	-113.560458	-0.353632	0.75	100.0	138	81.18	-296	194	-59	3710	-1090	2458
H_2O^+	-75.632933	-0.214950	0.75	100.0	92	39.99	-323	176	-52	10167	-3041	6926
MgF	-299.146313	-0.293368	0.75	100.0	96	42.22	-67	142	-18	-1773	269	-1447
NCl	-513.897499	-0.350099	2.00	100.0	96	45.42	-241	193	-52	3281	-754	2427
NF	-153.827879	-0.416280	2.00	100.0	92	44.96	-272	170	-54	1530	-405	969
NF_2	-253.260352	-0.711598	0.75	100.0	138	131.00	-326	207	-63	4032	-1076	2774
NF_3^+	-352.243466	-0.986388	0.75	100.0	184	410.25	-392	286	-84	5888	-1512	4186
NH	-54.974735	-0.148656	2.00	100.0	69	28.43	-208	123	-42	1588	-556	904
NO_2	-204.103798	-0.717754	0.75	100.0	138	160.91	-314	236	-76	-3469	1096	-2527
NO_3^{2-}	-278.761672	-1.034566	0.75	100.0	184	701.23	-19	83	-26	-151	45	-68
OH^+	-74.995610	-0.155413	2.00	100.0	69	33.95	-329	176	-52	4036	-1212	2618
O_2	-149.652744	-0.482752	2.00	100.0	92	44.14	-358	221	-66	2585	-775	1606
O_2H	-150.231421	-0.476824	0.75	100.0	115	77.55	-348	212	-63	19768	-5928	13641
O_3^-	-224.433594	-0.794021	0.75	100.0	138	180.21	-352	232	-70	11181	-3354	7637
PH	-341.290713	-0.117296	2.00	100.0	73	28.60	-147	153	-21	3223	-443	2766
SH^+	-397.760110	-0.126241	2.00	100.0	73	29.29	-228	201	-30	6447	-967	5423
SO	-472.381325	-0.424137	2.00	100.0	96	48.88	-264	239	-48	4016	-901	3042
SO_2^-	-547.307254	-0.717723	0.75	100.0	142	177.00	-277	259	-55	5270	-1334	3862
S_2	-795.079884	-0.344239	2.00	100.0	100	48.00	-229	261	-39	9597	-1439	8150
SiH_3	-290.638823	-0.121147	0.75	100.0	119	47.12	-109	171	-21	884	-110	814

Table C.9: Diagonal elements of the g-shifts [ppm] calculated with Z_{eff}-SDC-DF-LUCC2 at the aug-cc-pVTZ/DF-QZ level with DF-ROHF reference, extended domains and full pair lists for the benchmark set of Perera *et al.*[34]

Molecule	$\Delta g_{xx}^{1el-DSO}$	$\Delta g_{yy}^{1el-DSO}$	$\Delta g_{zz}^{1el-DSO}$	$\Delta g_{xx}^{2el-DSO}$	$\Delta g_{yy}^{2el-DSO}$	$\Delta g_{zz}^{2el-DSO}$	$\Delta g_{xx}^{1el-PSO}$	$\Delta g_{yy}^{1el-PSO}$	$\Delta g_{zz}^{1el-PSO}$	$\Delta g_{xx}^{2el-PSO}$	$\Delta g_{yy}^{2el-PSO}$	$\Delta g_{zz}^{2el-PSO}$	Δg_{xx}	Δg_{yy}	Δg_{zz}
BO	137	137	50	-55	-55	-23	-2375	-2375	0	761	761	-0	-1618	-1618	-60
BS	166	166	42	-54	-54	-22	-9260	-9260	-0	1590	1590	0	-7659	-7659	-80
CF_3Br^-	235	235	168	-60	-60	-30	28659	28659	-426	-373	-373	103	28150	28150	-496
CF_3Cl^-	158	158	174	-48	-48	-52	49	49	1380	-4	-4	-333	-214	-214	802
CHO	204	115	163	-70	-40	-55	2986	-910	-10354	-931	300	3353	1992	-731	-7090
CH_3	47	107	107	-20	-40	-40	9	1120	1120	-4	-442	-442	-94	619	619
CH_4^+	102	102	53	-34	-34	-19	1759	1739	-34	-693	-685	16	1013	1001	-106
CN	199	199	71	-76	-76	-28	-2887	-2887	0	1041	1041	-0	-1898	-1898	-133
COH	163	90	132	-58	-31	-49	1072	-486	-19466	-388	153	7117	631	-433	-12425
CO^+	197	197	77	-74	-74	-32	-3348	-3348	0	1073	1073	-0	-2326	-2326	-129
CO_2^-	218	105	204	-75	-37	-70	866	-1670	-5446	-301	529	1757	512	-1269	-3750
C_3H_5	105	124	174	-44	-47	-68	-80	1157	909	34	-460	-359	-119	641	522
ClO_2	224	326	307	-50	-76	-72	-587	15671	17028	117	-3898	-4309	-630	11689	12619
H_2CO^+	199	141	241	-60	-43	-75	1731	175	9225	-438	-58	-2775	1136	-81	6319
H_2O^+	104	212	212	-31	-63	-62	45	12498	17958	-14	-3740	-5369	-220	8584	12415
MgF	169	169	89	-22	-22	-11	-2660	-2660	0	404	404	-0	-2176	-2176	12
NCl	192	192	194	-50	-50	-56	4922	4922	-0	-1131	-1131	0	3692	3692	-103
NF	160	160	189	-51	-51	-61	2295	2295	-0	-607	-607	0	1525	1525	-144
NF_2	139	240	242	-42	-74	-74	-517	5857	6757	135	-1540	-1822	-611	4157	4777
NF_3^+	343	343	173	-100	-100	-51	9104	9104	-545	-2342	-2342	148	6613	6613	-667
NH	109	109	150	-38	-38	-51	2382	2382	0	-834	-834	-0	1411	1411	-109
NO_2	297	160	250	-95	-52	-80	4418	-2855	-11970	-1386	895	3780	2920	-2166	-8335
NO_3^{2-}	79	85	85	-25	-27	-27	-193	-130	-130	58	38	38	-100	-52	-52
OH^+	157	157	213	-47	-47	-63	6054	6054	-0	-1818	-1818	0	4017	4017	-179
O_2	216	216	231	-65	-65	-69	3878	3877	0	-1163	-1163	-0	2508	2507	-196
O_2H	146	254	237	-44	-76	-70	-82	16068	43319	25	-4819	-12989	-304	11078	30149
O_3^-	174	267	255	-52	-80	-77	-619	15271	18890	186	-4581	-5667	-664	10525	13050
PH	134	134	192	-18	-18	-26	4835	4835	-0	-665	-665	0	4139	4139	19
SH^+	177	177	250	-26	-26	-37	9670	9670	-0	-1451	-1451	0	8142	8142	-15
SO	236	236	245	-47	-47	-50	6024	6023	-0	-1351	-1351	0	4598	4597	-68
SO_2^-	193	294	289	-41	-63	-62	-445	7556	8699	90	-1909	-2182	-481	5601	6466
S_2	259	259	264	-39	-39	-40	14396	14396	-0	-2159	-2159	0	12228	12228	-5
SiH_3	217	217	78	-26	-26	-10	1361	1361	-71	-170	-170	9	1273	1273	-103

Table C.10: Miscellaneous data and isotropic g-shifts [ppm] for the g-tensor calculations with Z_{eff}-SDC-DF-LUCC2 at the aug-cc-pVTZ/DF-DZ level with DF-UHF reference, extended domains and full pair lists for the benchmark set of Perera *et al.*[34]

Molecule	E_{HF} [Hartree]	E_{corr} [Hartree]	$< S^2 >_{HF}$	$\frac{N_{pairs\ included}}{N_{all\ pairs}}$ [%]	N_{AO}	$t_{CPU}^{DF-LUCC2}$ [sec]	Δg^{ZKE}	$\Delta g_{iso}^{1el-DSO}$	$\Delta g_{iso}^{2el-DSO}$	$\Delta g_{iso}^{1el-PSO}$	$\Delta g_{iso}^{2el-PSO}$	Δg_{iso}
BO	-99.557305	-0.314138	0.80	100.0	92	36.35	-90	108	-44	-1834	579	-1282
BS	-422.188506	-0.241449	0.86	100.0	96	33.65	-97	121	-43	-7445	1235	-6228
CF_3Br^-	-2908.795707	-1.118020	0.76	100.0	243	806.40	-305	211	-50	19345	-206	18994
CF_3Cl^-	-795.698970	-1.205443	0.79	100.0	234	1088.01	-367	163	-50	186	-81	-148
CHO	-113.292046	-0.387528	0.77	100.0	115	52.85	-195	160	-54	-2800	918	-1972
CH_3	-39.577973	-0.161172	0.76	100.0	115	38.94	-124	87	-33	748	-295	382
CH_4^+	-39.773583	-0.167495	0.76	100.0	138	36.80	-118	86	-29	1136	-447	628
CN	-92.235591	-0.314920	1.16	100.0	92	39.45	-169	153	-59	-2024	713	-1386
COH	-113.242806	-0.362323	0.76	100.0	115	51.78	-156	128	-45	-6164	2237	-4001
CO^+	-112.303500	-0.337130	0.96	100.0	92	38.08	-176	155	-59	-2616	817	-1879
CO_2^-	-187.660921	-0.651790	0.76	100.0	138	102.80	-193	176	-60	-2056	653	-1481
C_3H_5	-116.510629	-0.473209	0.97	100.0	253	305.86	-131	135	-54	678	-267	361
ClO_2	-609.063612	-0.734328	0.78	100.0	142	171.78	-339	289	-66	10121	-2732	7272
H_2CO^+	-113.568241	-0.346223	0.79	100.0	138	57.01	-292	193	-59	3924	-1151	2616
H_2O^+	-75.638777	-0.209792	0.76	100.0	92	36.23	-319	175	-52	9956	-2978	6783
MgF	-299.146439	-0.295635	0.75	100.0	96	39.20	-65	142	-18	-1797	275	-1463
NCl	-513.908958	-0.341196	2.04	100.0	96	42.16	-237	192	-52	3037	-708	2231
NF	-153.838027	-0.408358	2.02	100.0	92	41.20	-267	168	-54	1507	-397	956
NF_2	-253.267184	-0.708837	0.76	100.0	138	104.31	-320	206	-63	3966	-1058	2731
NF_3^+	-352.249619	-0.985618	0.77	100.0	184	383.35	-386	285	-84	6128	-1569	4374
NH	-54.982558	-0.141665	2.02	100.0	69	33.74	-204	122	-42	1552	-543	885
NO_2	-204.112925	-0.710331	0.77	100.0	138	100.51	-309	234	-75	-3406	1078	-2478
NO_3^{2-}	-278.761774	-1.039609	0.75	100.0	184	495.60	-20	83	-26	-167	50	-80
OH^+	-75.004253	-0.147818	2.01	100.0	69	26.87	-324	175	-52	3951	-1187	2564
O_2	-149.676485	-0.458845	2.05	100.0	92	41.87	-352	219	-66	2583	-775	1610
O_2H	-150.238306	-0.471658	0.76	100.0	115	59.19	-342	211	-63	19494	-5845	13454
O_3^-	-224.444794	-0.784840	0.79	100.0	138	131.58	-343	230	-69	11050	-3315	7553
PH	-341.297934	-0.110955	2.03	100.0	73	33.14	-152	155	-21	3128	-430	2679
SH^+	-397.768037	-0.119533	2.02	100.0	73	34.29	-234	203	-30	6282	-943	5278
SO	-472.399520	-0.404896	2.06	100.0	96	43.57	-265	239	-48	3628	-851	2704
SO_2^-	-547.316203	-0.711923	0.79	100.0	142	131.73	-277	259	-55	4989	-1318	3597
S_2	-795.095287	-0.330617	2.06	100.0	100	44.56	-236	263	-39	9407	-1411	7984
SiH_3	-290.640479	-0.119401	0.76	100.0	119	34.83	-115	172	-21	919	-115	840

Table C.11: Diagonal elements of the g-shifts [ppm] calculated with Z_{eff}-SDC-DF-LUCC2 at the aug-cc-pVTZ/DF-DZ level with DF-UHF reference, extended domains and full pair lists for the benchmark set of Perera *et al.*[34]

Molecule	$\Delta g_{xx}^{1el-DSO}$	$\Delta g_{yy}^{1el-DSO}$	$\Delta g_{zz}^{1el-DSO}$	$\Delta g_{xx}^{2el-DSO}$	$\Delta g_{yy}^{2el-DSO}$	$\Delta g_{zz}^{2el-DSO}$	$\Delta g_{xx}^{1el-PSO}$	$\Delta g_{yy}^{1el-PSO}$	$\Delta g_{zz}^{1el-PSO}$	$\Delta g_{xx}^{2el-PSO}$	$\Delta g_{yy}^{2el-PSO}$	$\Delta g_{zz}^{2el-PSO}$	Δg_{xx}	Δg_{yy}	Δg_{zz}
BO	136	136	51	-55	-55	-23	-2751	-2751	0	868	868	-0	-1892	-1892	-63
BS	161	161	40	-53	-53	-22	-11167	-11167	0	1853	1853	-0	-9302	-9302	-79
CF_3Br^-	233	233	166	-60	-60	-30	29256	29256	-478	-367	-367	115	28756	28756	-531
CF_3Cl^-	158	158	174	-49	-49	-52	-511	-511	1579	69	69	-381	-699	-699	954
CHO	203	115	162	-69	-40	-54	3073	-1114	-10360	-953	357	3349	2059	-876	-7098
CH_3	47	107	107	-20	-40	-40	29	1107	1107	-11	-437	-437	-80	613	613
CH_4^+	102	102	53	-34	-34	-19	1744	1718	-54	-687	-677	24	1007	991	-115
CN	195	195	70	-75	-75	-28	-3036	-3036	-0	1069	1069	0	-2016	-2016	-127
COH	162	89	132	-57	-30	-49	1020	-629	-18883	-370	195	6885	600	-532	-12071
CO^+	194	194	78	-73	-73	-32	-3924	-3924	0	1225	1225	-0	-2753	-2753	-131
CO_2^-	218	105	204	-75	-36	-70	989	-1751	-5405	-335	551	1743	604	-1325	-3721
C_3H_5	107	124	175	-45	-47	-69	-57	1128	963	25	-448	-379	-102	626	558
ClO_2	227	324	316	-50	-75	-74	-649	12642	18370	109	-3471	-4835	-702	9081	13438
H_2CO^+	199	140	240	-60	-43	-75	1880	816	9077	-478	-244	-2730	1249	377	6221
H_2O^+	103	211	211	-31	-63	-62	111	12240	17518	-34	-3663	-5238	-170	8407	12111
MgF	169	169	89	-22	-22	-11	-2695	-2695	-0	412	412	0	-2201	-2201	13
NCl	191	191	193	-50	-50	-56	4555	4555	0	-1062	-1062	-0	3397	3397	-100
NF	158	158	188	-50	-50	-61	2260	2260	-0	-596	-596	0	1504	1504	-140
NF_2	137	239	241	-42	-74	-74	-565	5788	6674	145	-1521	-1797	-644	4113	4724
NF_3^+	341	341	172	-100	-100	-51	9572	9572	-760	-2455	-2455	202	6973	6973	-824
NH	108	108	149	-37	-37	-51	2328	2328	0	-815	-815	-0	1380	1380	-106
NO_2	295	159	248	-95	-51	-80	4614	-2903	-11929	-1441	908	3766	3064	-2196	-8303
NO_3^{2-}	79	85	85	-25	-27	-27	-210	-146	-146	63	43	43	-112	-64	-64
OH^+	156	156	212	-46	-46	-63	5927	5927	-0	-1780	-1780	0	3933	3933	-174
O_2	214	214	230	-64	-64	-69	3875	3875	-0	-1163	-1163	0	2510	2510	-191
O_2H	144	253	235	-43	-76	-70	-43	15864	42660	13	-4758	-12791	-271	10941	29692
O_3^-	171	265	254	-51	-80	-76	-761	15109	18801	228	-4533	-5640	-756	10419	12995
PH	135	135	194	-18	-18	-26	4692	4692	-0	-645	-645	0	4011	4011	16
SH^+	178	178	252	-26	-26	-37	9423	9423	-0	-1414	-1414	0	7927	7927	-19
SO	236	236	246	-47	-47	-50	5443	5442	-0	-1277	-1277	0	4090	4089	-68
SO_2^-	192	294	290	-41	-63	-62	-401	7258	8109	55	-1892	-2116	-472	5320	5943
S_2	261	261	266	-39	-39	-40	14111	14111	-0	-2117	-2117	0	11981	11981	-10
SiH_3	219	219	79	-26	-26	-10	1393	1393	-30	-174	-174	4	1296	1296	-71

Table C.12: Miscellaneous data and isotropic g-shifts [ppm] for the g-tensor calculations with Z_{eff}-SDC-DF-LUCC2 at the aug-cc-pVTZ/DF-TZ level with DF-UHF reference, extended domains and full pair lists for the benchmark set of Perera *et al.*[34]

Molecule	E_{HF} [Hartree]	E_{corr} [Hartree]	$< S^2 >_{HF}$	$\frac{N_{pairs\ included}}{N_{all\ pairs}}$ [%]	N_{AO}	$t_{CPU}^{DF-LUCC2}$ [sec]	Δg^{ZKE}	$\Delta g_{iso}^{1el-DSO}$	$\Delta g_{iso}^{2el-DSO}$	$\Delta g_{iso}^{1el-PSO}$	$\Delta g_{iso}^{2el-PSO}$	Δg_{iso}
BO	-99.557305	-0.312379	0.80	100.0	92	37.22	-91	108	-45	-1835	579	-1284
BS	-422.188506	-0.239351	0.86	100.0	96	41.45	-97	121	-43	-7459	1237	-6240
CF_3Br^-	-2908.795707	-1.110198	0.76	100.0	243	730.45	-305	211	-50	19441	-208	19089
CF_3Cl^-	-795.698970	-1.196197	0.79	100.0	234	974.66	-367	163	-50	188	-81	-147
CHO	-113.292046	-0.385865	0.77	100.0	115	56.04	-195	160	-54	-2795	916	-1968
CH_3	-39.577973	-0.161227	0.76	100.0	115	34.36	-124	87	-33	748	-295	382
CH_4^+	-39.773583	-0.167682	0.76	100.0	138	41.93	-118	86	-29	1135	-446	627
CN	-92.235591	-0.313534	1.16	100.0	92	38.41	-169	153	-59	-2023	712	-1386
COH	-113.242806	-0.360741	0.76	100.0	115	54.61	-156	128	-45	-6168	2239	-4003
CO^+	-112.303500	-0.335503	0.96	100.0	92	41.75	-176	155	-59	-2616	817	-1880
CO_2^-	-187.660921	-0.648188	0.76	100.0	138	134.66	-193	175	-60	-2051	651	-1477
C_3H_5	-116.510629	-0.472933	0.97	100.0	253	311.76	-131	135	-54	678	-267	361
ClO_2	-609.063612	-0.728886	0.78	100.0	142	162.98	-339	289	-66	10183	-2747	7320
H_2CO^+	-113.568241	-0.345104	0.79	100.0	138	63.41	-292	193	-59	3933	-1153	2622
H_2O^+	-75.638777	-0.208892	0.76	100.0	92	36.33	-319	175	-52	9958	-2979	6784
MgF	-299.146439	-0.293267	0.75	100.0	96	40.79	-65	142	-18	-1798	275	-1464
NCl	-513.908958	-0.337390	2.04	100.0	96	40.46	-237	192	-52	3049	-711	2240
NF	-153.838027	-0.405236	2.02	100.0	92	42.38	-267	168	-54	1511	-399	959
NF_2	-253.267184	-0.704098	0.76	100.0	138	114.27	-320	206	-63	3976	-1060	2738
NF_3^+	-352.249619	-0.979381	0.77	100.0	184	340.11	-386	285	-84	6150	-1575	4390
NH	-54.982558	-0.140626	2.02	100.0	69	37.71	-204	122	-42	1553	-544	885
NO_2	-204.112925	-0.706733	0.77	100.0	138	112.23	-309	234	-75	-3403	1077	-2477
NO_3^{2-}	-278.761774	-1.034490	0.75	100.0	184	447.68	-20	83	-26	-167	50	-80
OH^+	-75.004253	-0.146660	2.01	100.0	69	26.78	-324	175	-52	3953	-1187	2566
O_2	-149.676485	-0.455968	2.05	100.0	92	42.93	-352	219	-66	2587	-776	1612
O_2H	-150.238306	-0.469232	0.76	100.0	115	63.49	-342	211	-63	19517	-5852	13470
O_3^-	-224.444794	-0.780638	0.79	100.0	138	176.10	-343	230	-69	11073	-3322	7569
PH	-341.297934	-0.109531	2.03	100.0	73	35.55	-152	155	-21	3136	-431	2687
SH^+	-397.768037	-0.117887	2.02	100.0	73	34.96	-234	203	-30	6297	-945	5292
SO	-472.399520	-0.401294	2.06	100.0	96	45.06	-265	239	-48	3639	-854	2712
SO_2^-	-547.316203	-0.706792	0.79	100.0	142	179.98	-277	258	-55	5018	-1324	3620
S_2	-795.095287	-0.326240	2.06	100.0	100	47.98	-235	263	-39	9459	-1419	8028
SiH_3	-290.640479	-0.119480	0.76	100.0	119	43.11	-115	172	-21	918	-115	841

Table C.13: Diagonal elements of the g-shifts [ppm] calculated with Z_{eff}-SDC-DF-LUCC2 at the aug-cc-pVTZ/DF-TZ level with DF-UHF reference, extended domains and full pair lists for the benchmark set of Perera *et al.*[34]

Molecule	$\Delta g_{xx}^{1el-DSO}$	$\Delta g_{yy}^{1el-DSO}$	$\Delta g_{zz}^{1el-DSO}$	$\Delta g_{xx}^{2el-DSO}$	$\Delta g_{yy}^{2el-DSO}$	$\Delta g_{zz}^{2el-DSO}$	$\Delta g_{xx}^{1el-PSO}$	$\Delta g_{yy}^{1el-PSO}$	$\Delta g_{zz}^{1el-PSO}$	$\Delta g_{xx}^{2el-PSO}$	$\Delta g_{yy}^{2el-PSO}$	$\Delta g_{zz}^{2el-PSO}$	Δg_{xx}	Δg_{yy}	Δg_{zz}
BO	136	136	51	-55	-55	-24	-2752	-2752	0	868	868	-0	-1894	-1894	-63
BS	161	161	40	-53	-53	-22	-11188	-11188	-0	1856	1856	0	-9320	-9320	-79
CF_3Br^-	233	233	166	-60	-60	-30	29400	29400	-477	-369	-369	115	28899	28899	-531
CF_3Cl^-	158	158	174	-49	-49	-52	-511	-511	1587	69	69	-382	-700	-700	960
CHO	204	115	162	-69	-40	-54	3077	-1113	-10350	-955	357	3346	2062	-876	-7091
CH_3	47	107	107	-20	-40	-40	29	1107	1107	-11	-437	-437	-79	613	613
CH_4^+	102	102	53	-34	-34	-19	1744	1716	-54	-687	-676	24	1007	990	-115
CN	195	195	70	-75	-75	-28	-3034	-3034	-0	1068	1068	0	-2015	-2015	-127
COH	162	89	132	-57	-30	-49	1022	-626	-18901	-370	194	6893	601	-529	-12081
CO^+	194	194	78	-73	-73	-32	-3924	-3924	0	1225	1225	-0	-2754	-2754	-131
CO_2^-	217	105	204	-75	-36	-70	990	-1749	-5393	-336	551	1739	604	-1323	-3713
C_3H_5	107	124	175	-45	-47	-69	-57	1128	963	25	-448	-379	-102	626	559
ClO_2	226	335	305	-50	-77	-72	-648	17519	13679	109	-4514	-3837	-702	12924	9737
H_2CO^+	199	140	240	-60	-43	-75	1909	813	9078	-487	-243	-2730	1269	375	6221
H_2O^+	103	211	211	-31	-63	-62	111	12240	17524	-34	-3663	-5240	-170	8408	12115
MgF	169	169	89	-22	-22	-11	-2697	-2697	-0	413	413	0	-2203	-2203	13
NCl	191	191	193	-50	-50	-56	4573	4573	0	-1067	-1067	-0	3410	3410	-100
NF	158	158	188	-50	-50	-61	2266	2266	-0	-598	-598	0	1509	1509	-140
NF_2	137	239	241	-42	-74	-74	-564	5802	6690	145	-1524	-1801	-644	4122	4735
NF_3^+	341	341	172	-100	-100	-51	9604	9604	-758	-2463	-2463	201	6996	6996	-822
NH	108	108	149	-37	-37	-51	2330	2330	0	-816	-816	-0	1381	1381	-106
NO_2	295	159	248	-95	-51	-80	4624	-2903	-11930	-1444	908	3766	3071	-2197	-8304
NO_3^{2-}	79	85	85	-25	-27	-27	-210	-146	-146	63	43	43	-113	-64	-64
OH^+	156	156	212	-46	-46	-63	5930	5930	-0	-1781	-1781	0	3936	3936	-174
O_2	214	214	230	-64	-64	-69	3881	3881	-0	-1164	-1164	0	2514	2514	-191
O_2H	144	253	235	-43	-76	-70	-44	15882	42712	13	-4763	-12807	-272	10953	29729
O_3^-	171	265	254	-51	-80	-76	-762	15142	18839	228	-4543	-5652	-756	10442	13021
PH	135	135	194	-18	-18	-26	4704	4704	-0	-647	-647	0	4022	4022	16
SH^+	178	178	252	-26	-26	-37	9446	9446	-0	-1417	-1417	0	7947	7947	-19
SO	236	236	246	-47	-47	-50	5459	5458	-0	-1281	-1281	0	4102	4101	-68
SO_2^-	192	294	289	-41	-63	-62	-395	7299	8149	54	-1901	-2125	-467	5352	5974
S_2	261	261	266	-39	-39	-40	14188	14188	-0	-2128	-2128	0	12047	12047	-10
SiH_3	219	219	79	-26	-26	-10	1392	1392	-29	-174	-174	4	1296	1296	-70

Table C.14: Miscellaneous data and isotropic g-shifts [ppm] for the g-tensor calculations with Z_{eff}-SDC-DF-LUCC2 at the aug-cc-pVTZ/DF-QZ level with DF-UHF reference, Boughton-Pulay domains and full pair lists for the benchmark set of Perera *et al.*[34]

Molecule	E_{HF} [Hartree]	E_{corr} [Hartree]	$< S^2 >_{HF}$	$\frac{N_{pairs\ included}}{N_{all\ pairs}}$ [%]	N_{AO}	$t_{CPU}^{DF-LUCC2}$ [sec]	Δg^{ZKE}	$\Delta g_{iso}^{1el-DSO}$	$\Delta g_{iso}^{2el-DSO}$	$\Delta g_{iso}^{1el-PSO}$	$\Delta g_{iso}^{2el-PSO}$	Δg_{iso}
BO	-99.557305	-0.311890	0.80	100.0	92	35.76	-89	107	-44	-1819	574	-1271
BS	-422.188506	-0.238821	0.86	100.0	96	39.98	-96	120	-43	-7415	1231	-6203
CF_3Br^-	-2908.795707	-1.106847	0.76	100.0	243	697.53	-305	210	-49	19103	-201	18758
CF_3Cl^-	-795.698970	-1.192004	0.79	100.0	234	722.72	-368	162	-49	115	-62	-202
CHO	-113.292046	-0.384453	0.77	100.0	115	55.77	-195	160	-55	-2785	913	-1961
CH_3	-39.577973	-0.158913	0.76	100.0	115	34.90	-124	87	-33	746	-294	381
CH_4^+	-39.773583	-0.166266	0.76	100.0	138	43.74	-118	86	-29	1134	-446	626
CN	-92.235591	-0.313236	1.16	100.0	92	37.93	-169	153	-59	-2022	712	-1385
COH	-113.242806	-0.355519	0.76	100.0	115	52.81	-155	127	-45	-6040	2192	-3922
CO^+	-112.303500	-0.335253	0.96	100.0	92	37.10	-176	155	-59	-2615	816	-1879
CO_2^-	-187.660921	-0.646487	0.76	100.0	138	128.43	-194	178	-61	-2049	651	-1476
C_3H_5	-116.510629	-0.468262	0.97	100.0	253	252.40	-131	135	-54	675	-266	359
ClO_2	-609.063612	-0.726428	0.78	100.0	142	180.29	-339	289	-67	10190	-2744	7330
H_2CO^+	-113.568241	-0.343337	0.79	100.0	138	65.85	-292	193	-59	3937	-1154	2624
H_2O^+	-75.638777	-0.203231	0.76	100.0	92	29.14	-319	175	-52	10040	-3003	6841
MgF	-299.146439	-0.293052	0.75	100.0	96	36.27	-65	142	-18	-1781	272	-1451
NCl	-513.908958	-0.336456	2.04	100.0	96	41.57	-237	191	-52	3050	-711	2242
NF	-153.838027	-0.404492	2.02	100.0	92	38.61	-267	168	-54	1504	-397	955
NF_2	-253.267184	-0.701556	0.76	100.0	138	108.47	-320	205	-63	3938	-1051	2709
NF_3^+	-352.249619	-0.975875	0.77	100.0	184	297.35	-386	284	-84	6031	-1546	4299
NH	-54.982558	-0.136481	2.02	100.0	69	26.48	-204	122	-42	1573	-551	898
NO_2	-204.112925	-0.705284	0.77	100.0	138	124.11	-309	234	-75	-3368	1066	-2453
NO_3^{2-}	-278.761774	-1.032724	0.75	100.0	184	469.78	-20	83	-26	-189	56	-95
OH^+	-75.004253	-0.144222	2.01	100.0	69	26.64	-323	175	-52	3984	-1197	2587
O_2	-149.676485	-0.455098	2.05	100.0	92	38.85	-352	219	-66	2585	-775	1611
O_2H	-150.238306	-0.463921	0.76	100.0	115	59.18	-343	211	-63	19332	-5797	13340
O_3^-	-224.444794	-0.777453	0.79	100.0	138	148.87	-344	230	-69	10925	-3277	7464
PH	-341.297934	-0.109213	2.03	100.0	73	28.18	-152	155	-21	3139	-431	2689
SH^+	-397.768037	-0.117626	2.02	100.0	73	27.76	-234	203	-30	6299	-945	5292
SO	-472.399520	-0.400596	2.06	100.0	96	45.77	-265	239	-48	3636	-852	2710
SO_2^-	-547.316203	-0.704655	0.79	100.0	142	149.76	-278	259	-55	5060	-1327	3658
S_2	-795.095287	-0.325698	2.06	100.0	100	45.98	-235	263	-39	9445	-1417	8015
SiH_3	-290.640479	-0.118835	0.76	100.0	119	39.33	-115	173	-21	911	-114	835

Table C.15: Diagonal elements of the g-shifts [ppm] calculated with Z_{eff}-SDC-DF-LUCC2 at the aug-cc-pVTZ/DF-QZ level with DF-UHF reference, Boughton-Pulay domains and full pair lists for the benchmark set of Perera *et al.*[34]

Molecule	$\Delta g_{xx}^{1el-DSO}$	$\Delta g_{yy}^{1el-DSO}$	$\Delta g_{zz}^{1el-DSO}$	$\Delta g_{xx}^{2el-DSO}$	$\Delta g_{yy}^{2el-DSO}$	$\Delta g_{zz}^{2el-DSO}$	$\Delta g_{xx}^{1el-PSO}$	$\Delta g_{yy}^{1el-PSO}$	$\Delta g_{zz}^{1el-PSO}$	$\Delta g_{xx}^{2el-PSO}$	$\Delta g_{yy}^{2el-PSO}$	$\Delta g_{zz}^{2el-PSO}$	Δg_{xx}	Δg_{yy}	Δg_{zz}
BO	136	136	50	-55	-55	-23	-2728	-2728	-0	861	861	0	-1875	-1875	-62
BS	161	161	39	-53	-53	-22	-11123	-11123	0	1847	1847	-0	-9265	-9265	-79
CF_3Br^-	232	232	166	-59	-59	-30	28895	28895	-482	-360	-360	118	28403	28403	-533
CF_3Cl^-	156	156	173	-48	-48	-52	-537	-537	1419	78	78	-343	-718	-718	830
CHO	204	115	162	-70	-40	-55	3075	-1110	-10319	-954	356	3336	2060	-874	-7070
CH_3	47	107	107	-20	-40	-40	27	1105	1105	-11	-436	-436	-81	612	612
CH_4^+	102	102	53	-34	-34	-19	1742	1714	-54	-686	-675	24	1005	989	-115
CN	195	195	70	-75	-75	-28	-3033	-3033	0	1068	1068	-0	-2014	-2014	-127
COH	162	89	131	-57	-30	-49	1043	-605	-18559	-376	187	6766	616	-515	-11866
CO^+	194	194	78	-73	-73	-32	-3922	-3922	0	1224	1224	-0	-2753	-2753	-131
CO_2^-	221	105	207	-76	-36	-71	991	-1750	-5389	-336	551	1738	606	-1325	-3709
C_3H_5	107	124	175	-45	-47	-69	-56	1124	956	24	-446	-377	-101	624	555
ClO_2	227	325	316	-51	-76	-74	-613	12756	18428	101	-3483	-4849	-675	9183	13482
H_2CO^+	199	140	240	-60	-43	-75	1926	815	9069	-492	-243	-2728	1282	376	6215
H_2O^+	103	211	211	-31	-63	-62	110	12345	17666	-34	-3694	-5282	-171	8481	12214
MgF	169	169	89	-22	-22	-11	-2672	-2672	0	408	408	-0	-2183	-2183	13
NCl	190	190	192	-50	-50	-56	4575	4575	0	-1066	-1066	-0	3413	3413	-100
NF	158	158	188	-50	-50	-61	2256	2256	-0	-595	-595	0	1502	1502	-140
NF_2	137	238	241	-42	-74	-74	-558	5747	6625	143	-1511	-1786	-640	4080	4686
NF_3^+	341	341	171	-100	-100	-51	9473	9473	-854	-2432	-2432	225	6896	6896	-894
NH	108	108	149	-37	-37	-51	2360	2360	0	-827	-827	-0	1400	1400	-106
NO_2	295	159	248	-95	-51	-80	4613	-2884	-11833	-1441	902	3736	3063	-2183	-8238
NO_3^{2-}	79	85	85	-25	-27	-27	-234	-166	-166	70	49	49	-129	-78	-78
OH^+	156	156	212	-46	-46	-63	5976	5976	-0	-1795	-1795	0	3967	3967	-174
O_2	214	214	230	-64	-64	-69	3877	3877	-0	-1163	-1163	0	2512	2512	-191
O_2H	144	253	236	-43	-76	-70	-46	15794	42248	14	-4737	-12668	-274	10891	29404
O_3^-	171	266	254	-51	-80	-76	-756	14980	18550	227	-4494	-5565	-753	10328	12818
PH	135	135	194	-18	-18	-26	4708	4708	0	-647	-647	-0	4025	4025	16
SH^+	178	178	252	-26	-26	-37	9448	9448	-0	-1417	-1417	0	7948	7948	-19
SO	236	236	246	-47	-47	-50	5453	5454	-0	-1278	-1278	0	4099	4100	-68
SO_2^-	192	295	290	-41	-63	-62	-391	7351	8219	53	-1903	-2131	-464	5401	6037
S_2	261	261	266	-39	-39	-40	14167	14167	-0	-2125	-2125	0	12028	12028	-10
SiH_3	220	220	79	-26	-26	-10	1382	1382	-30	-173	-173	4	1288	1288	-71

Table C.16: Miscellaneous data and isotropic g-shifts [ppm] for the g-tensor calculations with Z_{eff}-SDC-DF-LUCC2 at the aug-cc-pVTZ/DF-QZ level with DF-UHF reference, extended domains and pair lists restricted using $|E_{IJ}| > 3.0 \cdot 10^{-5}$ Hartree for the benchmark set of Perera *et al.*[34]

Molecule	E_{HF} [Hartree]	E_{corr} [Hartree]	$< S^2 >_{HF}$	$\frac{N_{pairs\ included}}{N_{all\ pairs}}$ [%]	N_{AO}	$t_{CPU}^{DF-LUCC2}$ [sec]	Δg^{ZKE}	$\Delta g_{iso}^{1el-DSO}$	$\Delta g_{iso}^{2el-DSO}$	$\Delta g_{iso}^{1el-PSO}$	$\Delta g_{iso}^{2el-PSO}$	Δg_{iso}
BO	-99.557305	-0.312369	0.80	100.0	92	36.46	-91	108	-45	-1835	579	-1284
BS	-422.188506	-0.239333	0.86	100.0	96	37.67	-97	121	-43	-7459	1237	-6240
CF_3Br^-	-2908.795707	-1.107241	0.76	77.1	243	1021.39	-306	205	-50	16949	-192	16607
CF_3Cl^-	-795.698970	-1.192923	0.79	82.0	234	1453.77	-367	162	-49	111	-61	-204
CHO	-113.292046	-0.385861	0.77	100.0	115	63.58	-195	160	-54	-2795	916	-1968
CH_3	-39.577973	-0.161235	0.76	100.0	115	37.86	-124	87	-33	748	-295	382
CH_4^+	-39.773583	-0.167693	0.76	100.0	138	47.53	-118	86	-29	1136	-446	627
CN	-92.235591	-0.313528	1.16	100.0	92	36.81	-169	153	-59	-2023	712	-1386
COH	-113.242806	-0.360749	0.76	100.0	115	66.78	-156	128	-45	-6167	2239	-4002
CO^+	-112.303500	-0.335490	0.96	100.0	92	37.79	-177	156	-59	-2616	817	-1880
CO_2^-	-187.660921	-0.648071	0.76	99.0	138	188.23	-193	175	-60	-2052	652	-1478
C_3H_5	-116.510629	-0.472963	0.97	100.0	253	476.74	-131	135	-54	678	-267	361
ClO_2	-609.063612	-0.728599	0.78	98.1	142	260.14	-339	289	-67	10129	-2735	7278
H_2CO^+	-113.568241	-0.345111	0.79	100.0	138	77.18	-292	193	-59	3934	-1153	2622
H_2O^+	-75.638777	-0.208904	0.76	100.0	92	33.09	-319	175	-52	9959	-2979	6784
MgF	-299.146439	-0.293276	0.75	100.0	96	37.83	-65	142	-18	-1798	275	-1464
NCl	-513.908958	-0.337367	2.04	100.0	96	44.52	-237	192	-52	3049	-711	2241
NF	-153.838027	-0.405233	2.02	100.0	92	42.03	-267	168	-54	1511	-399	959
NF_2	-253.267184	-0.703854	0.76	95.4	138	181.42	-320	206	-63	3975	-1060	2737
NF_3^+	-352.249619	-0.978962	0.77	96.1	184	548.52	-386	285	-84	6132	-1570	4376
NH	-54.982558	-0.140629	2.02	100.0	69	27.12	-204	122	-42	1554	-544	885
NO_2	-204.112925	-0.706660	0.77	99.5	138	184.26	-309	234	-75	-3398	1075	-2473
NO_3^{2-}	-278.761774	-1.034347	0.75	99.3	184	744.13	-20	83	-26	-184	55	-92
OH^+	-75.004253	-0.146661	2.01	100.0	69	27.03	-324	175	-52	3954	-1187	2566
O_2	-149.676485	-0.455943	2.05	100.0	92	42.03	-352	219	-66	2587	-776	1613
O_2H	-150.238306	-0.469231	0.76	100.0	115	78.51	-342	211	-63	19519	-5853	13471
O_3^-	-224.444794	-0.780618	0.79	100.0	138	214.94	-343	230	-69	11074	-3322	7570
PH	-341.297934	-0.109531	2.03	100.0	73	28.58	-152	155	-21	3136	-431	2687
SH^+	-397.768037	-0.117895	2.02	100.0	73	28.59	-234	203	-30	6297	-945	5291
SO	-472.399520	-0.401246	2.06	100.0	96	46.66	-265	239	-48	3640	-854	2713
SO_2^-	-547.316203	-0.706419	0.79	96.9	142	236.45	-277	258	-55	5002	-1320	3608
S_2	-795.095287	-0.326177	2.06	100.0	100	48.39	-235	263	-39	9462	-1419	8030
SiH_3	-290.640479	-0.119492	0.76	100.0	119	41.84	-115	172	-21	919	-115	841

Table C.17: Diagonal elements of the g-shifts [ppm] calculated with Z_{eff}-SDC-DF-LUCC2 at the aug-cc-pVTZ/DF-QZ level with DF-UHF reference, extended domains and pair lists restricted using $|E_{IJ}| > 3.0 \cdot 10^{-5}$ Hartree for the benchmark set of Perera *et al.*[34]

Molecule	$\Delta g_{xx}^{1el-DSO}$	$\Delta g_{yy}^{1el-DSO}$	$\Delta g_{zz}^{1el-DSO}$	$\Delta g_{xx}^{2el-DSO}$	$\Delta g_{yy}^{2el-DSO}$	$\Delta g_{zz}^{2el-DSO}$	$\Delta g_{xx}^{1el-PSO}$	$\Delta g_{yy}^{1el-PSO}$	$\Delta g_{zz}^{1el-PSO}$	$\Delta g_{xx}^{2el-PSO}$	$\Delta g_{yy}^{2el-PSO}$	$\Delta g_{zz}^{2el-PSO}$	Δg_{xx}	Δg_{yy}	Δg_{zz}
BO	136	136	51	-55	-55	-24	-2752	-2752	-0	868	868	0	-1894	-1894	-63
BS	161	161	40	-53	-53	-22	-11189	-11189	0	1856	1856	-0	-9321	-9321	-79
CF_3Br^-	225	225	166	-60	-60	-30	25734	25575	-463	-345	-345	114	25249	25090	-518
CF_3Cl^-	157	157	172	-48	-48	-51	-564	-564	1462	85	85	-352	-737	-738	863
CHO	204	115	162	-69	-40	-54	3077	-1113	-10350	-955	357	3346	2062	-876	-7091
CH_3	47	107	107	-20	-40	-40	29	1107	1107	-11	-437	-437	-79	613	613
CH_4^+	102	102	53	-34	-34	-19	1744	1717	-54	-687	-676	24	1007	990	-115
CN	195	195	70	-75	-75	-28	-3034	-3034	0	1068	1068	-0	-2015	-2015	-127
COH	162	89	132	-57	-30	-49	1022	-626	-18898	-370	194	6892	601	-529	-12079
CO^+	195	195	78	-73	-73	-32	-3924	-3924	0	1225	1225	-0	-2754	-2754	-131
CO_2^-	217	105	204	-75	-36	-70	984	-1748	-5393	-334	550	1739	600	-1322	-3713
C_3H_5	107	124	175	-45	-47	-69	-57	1128	963	25	-448	-379	-102	626	559
ClO_2	227	324	316	-51	-76	-74	-640	12747	18280	108	-3493	-4819	-694	9164	13365
H_2CO^+	199	140	240	-60	-43	-75	1910	813	9078	-487	-243	-2730	1271	375	6221
H_2O^+	103	211	211	-31	-63	-62	111	12241	17525	-34	-3663	-5240	-170	8408	12115
MgF	169	169	89	-22	-22	-11	-2697	-2697	0	413	413	-0	-2203	-2203	13
NCl	191	191	193	-50	-50	-56	4573	4573	0	-1067	-1067	-0	3411	3411	-100
NF	158	158	188	-50	-50	-61	2266	2266	-0	-598	-598	0	1509	1509	-140
NF_2	137	239	241	-42	-74	-74	-564	5801	6688	145	-1524	-1801	-644	4122	4734
NF_3^+	342	342	172	-100	-100	-51	9579	9579	-763	-2456	-2456	203	6977	6978	-826
NH	108	108	149	-37	-37	-51	2331	2331	0	-816	-816	-0	1381	1381	-106
NO_2	295	159	248	-95	-51	-80	4626	-2891	-11928	-1445	904	3765	3072	-2188	-8303
NO_3^{2-}	78	85	85	-25	-27	-27	-225	-164	-164	68	49	49	-123	-77	-77
OH^+	156	156	212	-46	-46	-63	5931	5931	-0	-1781	-1781	0	3936	3936	-174
O_2	214	214	230	-64	-64	-69	3881	3881	-0	-1164	-1164	0	2515	2515	-191
O_2H	144	253	235	-43	-76	-70	-43	15883	42716	13	-4764	-12808	-272	10954	29731
O_3^-	171	265	254	-51	-80	-76	-761	15143	18840	228	-4543	-5652	-756	10443	13022
PH	135	135	194	-18	-18	-26	4704	4704	0	-647	-647	-0	4022	4022	16
SH^+	178	178	252	-26	-26	-37	9446	9446	-0	-1417	-1417	0	7946	7946	-19
SO	236	236	246	-47	-47	-50	5460	5461	-0	-1281	-1281	0	4103	4104	-68
SO_2^-	192	294	289	-41	-63	-62	-376	7266	8116	51	-1893	-2118	-451	5327	5947
S_2	261	261	266	-39	-39	-40	14193	14193	-0	-2129	-2129	0	12050	12050	-10
SiH_3	219	219	79	-26	-26	-10	1392	1392	-28	-174	-174	4	1296	1296	-70

Table C.18: Miscellaneous data and isotropic g-shifts [ppm] for the g-tensor calculations with Z_{eff}-SDC-DF-LUCC2 at the aug-cc-pVTZ/DF-QZ level with DF-UHF reference, extended domains and pair lists restricted using $|E_{IJ}| > 3.0 \cdot 10^{-3}$ Hartree for the benchmark set of Perera *et al.*[34]

Molecule	E_{HF} [Hartree]	E_{corr} [Hartree]	$< S^2 >_{HF}$	$\frac{N_{pairs\ included}}{N_{all\ pairs}}$ [%]	N_{AO}	$t_{CPU}^{DF-LUCC2}$ [sec]	Δg^{ZKE}	$\Delta g_{iso}^{1el-DSO}$	$\Delta g_{iso}^{2el-DSO}$	$\Delta g_{iso}^{1el-PSO}$	$\Delta g_{iso}^{2el-PSO}$	Δg_{iso}
BO	-99.557305	-0.292561	0.80	75.0	92	52.90	-81	105	-44	-1696	535	-1182
BS	-422.188506	-0.215719	0.86	71.4	96	54.13	-91	117	-43	-6704	1117	-5604
CF_3Br^-	-2908.795707	-0.998316	0.76	21.5	243	384.93	-302	186	-55	9741	-134	9434
CF_3Cl^-	-795.698970	-1.071671	0.79	22.0	234	478.69	-380	156	-48	-581	125	-728
CHO	-113.292046	-0.354777	0.77	69.4	115	71.82	-196	161	-55	-2152	708	-1534
CH_3	-39.577973	-0.145780	0.76	81.8	115	53.16	-125	87	-33	723	-285	367
CH_4^+	-39.773583	-0.163468	0.76	93.9	138	67.37	-120	86	-29	1104	-434	607
CN	-92.235591	-0.292736	1.16	82.1	92	55.13	-164	152	-59	-1908	672	-1308
COH	-113.242806	-0.332809	0.76	65.9	115	71.92	-156	126	-45	-4794	1742	-3127
CO^+	-112.303500	-0.315617	0.96	78.6	92	53.74	-164	149	-58	-2462	768	-1767
CO_2^-	-187.660921	-0.573392	0.76	44.2	138	114.79	-200	185	-64	-1887	598	-1367
C_3H_5	-116.510629	-0.381477	0.97	37.0	253	240.00	-131	139	-56	637	-251	339
ClO_2	-609.063612	-0.603406	0.78	40.6	142	137.56	-356	281	-66	10162	-2705	7316
H_2CO^+	-113.568241	-0.305563	0.79	60.0	138	80.44	-303	198	-60	4070	-1196	2709
H_2O^+	-75.638777	-0.208904	0.76	100.0	92	33.41	-319	175	-52	9959	-2979	6784
MgF	-299.146439	-0.284430	0.75	75.0	96	54.84	-63	142	-18	-1786	267	-1459
NCl	-513.908958	-0.285823	2.04	53.5	96	56.10	-233	179	-51	2568	-615	1847
NF	-153.838027	-0.364641	2.02	56.4	92	55.33	-260	163	-53	1334	-355	829
NF_2	-253.267184	-0.630942	0.76	39.5	138	104.82	-312	197	-61	3383	-909	2298
NF_3^+	-352.249619	-0.867684	0.77	31.6	184	213.50	-377	278	-83	4735	-1221	3331
NH	-54.982558	-0.138409	2.02	95.7	69	45.06	-204	122	-42	1553	-544	885
NO_2	-204.112925	-0.608076	0.77	48.1	138	112.46	-316	239	-77	-2934	929	-2159
NO_3^{2-}	-278.761774	-0.825219	0.75	30.5	184	268.80	-15	77	-24	-286	88	-160
OH^+	-75.004253	-0.138548	2.01	87.0	69	44.13	-323	175	-52	3949	-1186	2563
O_2	-149.676485	-0.444450	2.05	76.2	92	56.18	-354	220	-66	2463	-739	1525
O_2H	-150.238306	-0.436951	0.76	62.5	115	77.72	-344	207	-62	16676	-5001	11477
O_3^-	-224.444794	-0.696568	0.79	46.4	138	132.54	-370	234	-70	8844	-2653	5985
PH	-341.297934	-0.098699	2.03	73.9	73	44.50	-152	155	-21	2940	-404	2517
SH^+	-397.768037	-0.110002	2.02	82.6	73	45.55	-234	203	-30	6108	-917	5130
SO	-472.399520	-0.366032	2.06	65.3	96	56.03	-268	239	-48	3118	-745	2297
SO_2^-	-547.316203	-0.604294	0.79	36.8	142	126.68	-283	260	-54	3972	-1033	2862
S_2	-795.095287	-0.289011	2.06	66.3	100	59.50	-239	263	-39	8217	-1233	6969
SiH_3	-290.640479	-0.093253	0.76	36.4	119	54.85	-114	175	-21	728	-91	676

Table C.19: Diagonal elements of the g-shifts [ppm] calculated with Z_{eff}-SDC-DF-LUCC2 at the aug-cc-pVTZ/DF-TZ level with DF-UHF reference, extended domains and pair lists restricted using $|E_{IJ}| > 3.0 \cdot 10^{-3}$ Hartree for the benchmark set of Perera *et al.*[34]

Molecule	$\Delta g_{xx}^{1el-DSO}$	$\Delta g_{yy}^{1el-DSO}$	$\Delta g_{zz}^{1el-DSO}$	$\Delta g_{xx}^{2el-DSO}$	$\Delta g_{yy}^{2el-DSO}$	$\Delta g_{zz}^{2el-DSO}$	$\Delta g_{xx}^{1el-PSO}$	$\Delta g_{yy}^{1el-PSO}$	$\Delta g_{zz}^{1el-PSO}$	$\Delta g_{xx}^{2el-PSO}$	$\Delta g_{yy}^{2el-PSO}$	$\Delta g_{zz}^{2el-PSO}$	Δg_{xx}	Δg_{yy}	Δg_{zz}
BO	134	134	47	-55	-55	-23	-2544	-2544	-0	802	802	0	-1745	-1745	-57
BS	159	159	34	-54	-54	-21	-10056	-10056	0	1676	1676	-0	-8366	-8366	-79
CF_3Br^-	202	202	154	-67	-67	-32	14866	14866	-510	-264	-264	125	14434	14434	-565
CF_3Cl^-	150	150	168	-47	-47	-51	-1229	-1229	714	273	273	-170	-1234	-1233	282
CHO	205	116	163	-70	-40	-54	2837	-1049	-8245	-878	335	2668	1898	-835	-5665
CH_3	47	107	107	-20	-40	-40	30	1069	1069	-12	-422	-422	-79	590	590
CH_4^+	102	102	53	-34	-34	-19	1698	1668	-54	-669	-657	24	978	959	-117
CN	194	194	67	-75	-75	-27	-2862	-2862	0	1008	1008	-0	-1899	-1899	-125
COH	160	87	132	-57	-30	-49	1173	-551	-15004	-421	169	5478	699	-481	-9598
CO^+	188	188	72	-72	-72	-31	-3693	-3693	0	1152	1152	-0	-2589	-2589	-123
CO_2^-	233	102	221	-80	-36	-76	657	-1690	-4627	-233	533	1495	377	-1291	-3188
C_3H_5	114	123	181	-49	-47	-72	-65	1049	927	28	-416	-364	-102	578	541
ClO_2	209	344	289	-47	-80	-70	-1114	13085	18515	210	-3171	-5154	-1099	9822	13224
H_2CO^+	205	144	245	-61	-44	-76	2871	812	8528	-784	-244	-2561	1929	366	5833
H_2O^+	103	211	211	-31	-63	-62	111	12241	17525	-34	-3663	-5240	-170	8408	12115
MgF	170	170	87	-22	-22	-11	-2679	-2679	0	400	400	-0	-2195	-2195	14
NCl	176	176	186	-48	-48	-57	3852	3852	0	-923	-923	-0	2823	2823	-104
NF	152	152	186	-49	-49	-61	2001	2001	-0	-533	-533	0	1311	1311	-135
NF_2	127	231	234	-39	-72	-73	-580	4950	5779	146	-1305	-1569	-658	3491	4060
NF_3^+	337	337	159	-100	-100	-48	7516	7516	-828	-1940	-1940	216	5436	5436	-878
NH	108	108	149	-37	-37	-51	2330	2330	0	-816	-816	-0	1381	1381	-106
NO_2	301	159	256	-97	-51	-82	3897	-2615	-10084	-1227	821	3193	2559	-2002	-7033
NO_3^{2-}	69	80	82	-22	-25	-26	-302	-303	-252	90	94	80	-180	-169	-131
OH^+	156	156	212	-46	-46	-63	5924	5924	-0	-1779	-1779	0	3931	3931	-174
O_2	215	215	231	-64	-64	-69	3694	3694	-0	-1108	-1108	0	2383	2383	-192
O_2H	138	249	235	-42	-75	-70	-21	14392	35657	6	-4317	-10691	-261	9906	24787
O_3^-	170	270	263	-51	-81	-79	-811	12441	14901	243	-3732	-4470	-818	8528	10245
PH	135	135	195	-18	-18	-26	4410	4410	0	-606	-606	-0	3768	3768	16
SH^+	178	178	252	-26	-26	-37	9162	9162	-0	-1375	-1375	0	7705	7705	-19
SO	235	235	248	-47	-47	-50	4677	4678	0	-1117	-1117	-0	3480	3481	-70
SO_2^-	186	299	296	-39	-62	-62	-469	5763	6623	88	-1497	-1690	-518	4221	4884
S_2	260	260	269	-39	-39	-40	12326	12326	0	-1849	-1849	-0	10459	10459	-10
SiH_3	223	223	78	-26	-26	-10	1087	1087	9	-136	-136	-1	1033	1033	-37

Table C.20: Miscellaneous data and isotropic g-shifts [ppm] for the g-tensor calculations with Z_{eff}-SDC-DF-LUCC2 at the aug-cc-pVTZ/DF-DZ level with DF-UHF reference, Boughton-Pulay domains and and pair lists restricted using $|E_{IJ}| > 3.0 \cdot 10^{-5}$ Hartree for the benchmark set of Perera *et al.*[34]

Molecule	E_{HF} [Hartree]	E_{corr} [Hartree]	$< S^2 >_{HF}$	$\frac{N_{pairs\ included}}{N_{all\ pairs}}$ [%]	N_{AO}	$t_{CPU}^{DF-LUCC2}$ [sec]	Δg^{ZKE}	$\Delta g_{iso}^{1el-DSO}$	$\Delta g_{iso}^{2el-DSO}$	$\Delta g_{iso}^{1el-PSO}$	$\Delta g_{iso}^{2el-PSO}$	Δg_{iso}
BO	-99.557305	-0.313636	0.80	100.0	92	39.36	-89	107	-44	-1818	574	-1270
BS	-422.188506	-0.240902	0.86	100.0	96	35.67	-96	120	-43	-7401	1229	-6190
CF_3Br^-	-2908.795707	-1.111558	0.76	75.5	243	411.65	-306	206	-49	16696	-184	16363
CF_3Cl^-	-795.698970	-1.197922	0.79	81.2	234	438.63	-369	161	-49	58	-46	-245
CHO	-113.292046	-0.386141	0.77	100.0	115	44.97	-195	160	-55	-2790	914	-1965
CH_3	-39.577973	-0.158781	0.76	100.0	115	33.79	-124	87	-33	746	-294	381
CH_4^+	-39.773583	-0.166075	0.76	100.0	138	38.40	-118	86	-29	1134	-446	627
CN	-92.235591	-0.314666	1.16	100.0	92	39.90	-169	153	-59	-2023	713	-1386
COH	-113.242806	-0.357147	0.76	100.0	115	43.37	-155	127	-45	-6037	2191	-3920
CO^+	-112.303500	-0.336918	0.96	100.0	92	42.58	-176	155	-59	-2614	816	-1878
CO_2^-	-187.660921	-0.650001	0.76	99.0	138	113.32	-195	178	-61	-2055	653	-1480
C_3H_5	-116.510629	-0.468540	0.97	100.0	253	151.31	-131	135	-54	675	-266	359
ClO_2	-609.063612	-0.731741	0.78	97.7	142	156.42	-340	290	-67	10087	-2719	7252
H_2CO^+	-113.568241	-0.344477	0.79	100.0	138	48.87	-292	193	-59	3928	-1151	2618
H_2O^+	-75.638777	-0.204214	0.76	100.0	92	29.82	-319	175	-52	10037	-3003	6839
MgF	-299.146439	-0.295411	0.75	100.0	96	43.32	-65	142	-18	-1780	272	-1449
NCl	-513.908958	-0.340291	2.04	100.0	96	38.23	-237	191	-52	3037	-707	2233
NF	-153.838027	-0.407629	2.02	100.0	92	37.06	-267	168	-54	1500	-396	951
NF_2	-253.267184	-0.706101	0.76	95.4	138	96.62	-320	205	-63	3928	-1049	2702
NF_3^+	-352.249619	-0.981732	0.77	96.1	184	233.80	-386	285	-84	5994	-1537	4272
NH	-54.982558	-0.137578	2.02	100.0	69	28.64	-204	122	-42	1571	-551	897
NO_2	-204.112925	-0.708849	0.77	99.5	138	116.95	-309	234	-75	-3366	1065	-2451
NO_3^{2-}	-278.761774	-1.037697	0.75	99.3	184	361.59	-20	83	-26	-204	61	-106
OH^+	-75.004253	-0.145442	2.01	100.0	69	28.79	-323	175	-52	3981	-1195	2585
O_2	-149.676485	-0.458014	2.05	100.0	92	37.09	-352	219	-66	2581	-774	1608
O_2H	-150.238306	-0.466417	0.76	100.0	115	49.07	-343	211	-63	19304	-5788	13321
O_3^-	-224.444794	-0.781692	0.79	100.0	138	107.82	-344	230	-69	10901	-3270	7448
PH	-341.297934	-0.110636	2.03	100.0	73	34.95	-152	155	-21	3131	-431	2681
SH^+	-397.768037	-0.119264	2.02	100.0	73	28.96	-234	203	-30	6283	-943	5280
SO	-472.399520	-0.404238	2.06	100.0	96	42.06	-265	239	-48	3624	-849	2702
SO_2^-	-547.316203	-0.709582	0.79	96.9	142	142.55	-278	259	-55	5012	-1317	3621
S_2	-795.095287	-0.330138	2.06	100.0	100	41.09	-236	263	-39	9391	-1409	7969
SiH_3	-290.640479	-0.118742	0.76	100.0	119	34.39	-115	173	-21	911	-114	835

Table C.21: Diagonal elements of the g-shifts [ppm] calculated with Z_{eff}-SDC-DF-LUCC2 at the aug-cc-pVTZ/DF-DZ level with DF-UHF reference, Boughton-Pulay domains and and pair lists restricted using $|E_{IJ}| > 3.0 \cdot 10^{-5}$ Hartree for the benchmark set of Perera *et al.*[34]

Molecule	$\Delta g_{xx}^{1el-DSO}$	$\Delta g_{yy}^{1el-DSO}$	$\Delta g_{zz}^{1el-DSO}$	$\Delta g_{xx}^{2el-DSO}$	$\Delta g_{yy}^{2el-DSO}$	$\Delta g_{zz}^{2el-DSO}$	$\Delta g_{xx}^{1el-PSO}$	$\Delta g_{yy}^{1el-PSO}$	$\Delta g_{zz}^{1el-PSO}$	$\Delta g_{xx}^{2el-PSO}$	$\Delta g_{yy}^{2el-PSO}$	$\Delta g_{zz}^{2el-PSO}$	Δg_{xx}	Δg_{yy}	Δg_{zz}
BO	136	136	50	-55	-55	-23	-2727	-2727	-0	861	861	0	-1874	-1874	-62
BS	161	161	39	-53	-53	-22	-11102	-11102	0	1844	1844	-0	-9246	-9246	-79
CF_3Br^-	226	226	166	-59	-59	-30	25353	25217	-482	-337	-336	120	24877	24742	-531
CF_3Cl^-	156	156	172	-48	-48	-52	-573	-573	1320	90	90	-319	-744	-744	752
CHO	204	115	162	-70	-40	-55	3071	-1111	-10330	-953	356	3340	2058	-875	-7077
CH_3	47	107	107	-20	-40	-40	28	1105	1105	-11	-436	-436	-81	612	612
CH_4^+	102	102	53	-34	-34	-19	1742	1715	-54	-686	-676	24	1006	989	-115
CN	195	195	69	-75	-75	-28	-3035	-3035	0	1069	1069	-0	-2015	-2015	-127
COH	162	89	131	-57	-30	-49	1042	-608	-18546	-376	188	6760	616	-517	-11859
CO^+	194	194	78	-73	-73	-32	-3921	-3922	0	1224	1224	-0	-2752	-2752	-131
CO_2^-	221	105	208	-76	-36	-71	985	-1750	-5399	-334	551	1741	602	-1325	-3716
C_3H_5	107	124	175	-46	-47	-69	-56	1124	956	25	-446	-376	-101	623	554
ClO_2	227	326	316	-51	-76	-74	-597	12704	18155	98	-3470	-4786	-661	9144	13272
H_2CO^+	199	140	240	-60	-43	-75	1897	818	9068	-483	-244	-2727	1261	378	6214
H_2O^+	103	211	211	-31	-63	-62	110	12343	17658	-34	-3694	-5280	-170	8479	12208
MgF	169	169	89	-22	-22	-11	-2670	-2670	0	408	408	-0	-2180	-2180	13
NCl	191	191	192	-50	-50	-56	4556	4556	0	-1061	-1061	-0	3399	3399	-100
NF	158	158	188	-50	-50	-61	2250	2250	-0	-594	-594	0	1497	1497	-140
NF_2	137	238	241	-42	-74	-74	-559	5733	6609	143	-1508	-1781	-640	4071	4674
NF_3^+	341	341	172	-100	-100	-51	9420	9420	-859	-2418	-2418	226	6857	6857	-898
NH	108	108	149	-37	-37	-51	2357	2357	0	-826	-826	-0	1398	1398	-106
NO_2	295	159	249	-95	-51	-80	4604	-2872	-11829	-1438	898	3734	3057	-2175	-8234
NO_3^{2-}	78	85	85	-24	-27	-27	-246	-183	-183	74	55	54	-138	-90	-90
OH^+	156	156	212	-46	-46	-63	5971	5971	-0	-1793	-1793	0	3964	3964	-174
O_2	214	214	230	-64	-64	-69	3872	3872	-0	-1161	-1161	0	2508	2508	-191
O_2H	144	253	236	-43	-76	-70	-45	15773	42184	14	-4731	-12648	-274	10877	29359
O_3^-	171	266	254	-51	-80	-76	-755	14948	18511	227	-4484	-5553	-753	10305	12791
PH	135	135	194	-18	-18	-26	4696	4696	0	-646	-646	-0	4014	4014	16
SH^+	178	178	252	-26	-26	-37	9425	9425	-0	-1414	-1414	0	7929	7929	-19
SO	236	236	246	-47	-47	-50	5436	5437	-0	-1274	-1274	0	4086	4087	-68
SO_2^-	192	295	290	-41	-63	-62	-379	7275	8139	51	-1887	-2114	-455	5342	5975
S_2	261	261	266	-39	-39	-40	14086	14086	-0	-2113	-2113	0	11959	11959	-10
SiH_3	220	220	79	-26	-26	-10	1382	1382	-31	-173	-173	4	1288	1288	-72

Table C.22: Eigenvalues of the g-shifts and isotropic g-shifts [ppm] calculated with SOMF-SDC-B3LYP at the def2-TZVP level for their benchmark set of small molecules by Glasbrenner *et al.*[35]

Molecule	Δg_{diag1}	Δg_{diag2}	Δg_{diag3}	Δg_{iso}
AsO_3^{2-}	10627	10627	3371	8208
BO	-69	-1733	-1733	-1178
BS	-84	-9322	-9322	-6243
BeH	-40	-154	-154	-116
CF_3Br^-	51125	51125	-479	33924
CF_3Cl^-	12155	12155	-508	7934
CH	1256	-164	-15142	-4683
$CHCH_2$	517	-114	-682	-93
CHO	2256	-224	-7245	-1738
CH_2	198	173	-70	100
CH_2CH_3	678	503	-106	358
CH_2OH	2175	929	-168	979
CH_3	551	551	-89	338
CH_4^+	24221	2487	-91	8872
$COCH_3$	2200	-275	-6536	-1537
CO^+	-135	-2514	-2514	-1721
CO_2^-	1283	-668	-5144	-1510
CO_3^-	11731	11731	2912	8791
C_2H	167	167	-127	69
C_3H_5	590	559	-103	349
ClO_2	16238	12888	-548	9526
ClO_3	7325	7325	953	5201
GeH_3	16501	16501	-116	10962
H_2CO^+	5517	249	75	1947
KrF	36640	36640	-304	24325
MgF	-3	-1651	-1651	-1102
NF_2	6548	3960	-679	3276
NF_3^+	6975	6975	-602	4449
NH	1240	1240	-107	791
NH_2	4900	1453	-151	2067
NH_3^+	1600	1600	-153	1016
NO	3300	-402	-112426	-36509
NO_2	3787	-652	-11142	-2669
NO_3	14978	14978	257	10071
OCH_3	47755	5894	-213	17812
OH	56561	5406	-213	20585
ONO	3559	-638	-10980	-2686
O_2H	27277	5401	-300	10793
O_3^-	17795	10623	-557	9287
PH_2	15250	5044	-18	6759
SO_2^-	8942	5544	-369	4706
SO_3^-	2612	2612	227	1817
SiH_2	1224	1031	-511	581
SiH_3	2294	2294	-81	1502

Table C.23: Miscellaneous data and isotropic g-shifts [ppm] for the g-tensor calculations with Z_{eff}-SDC-DF-LUCC2 at the def2-TZVP/DF-QZ level with DF-UHF reference, extended domains and full pair lists for the benchmark set of small molecules used by Glasbrenner *et al.*[35]

Molecule	E_{HF} [Hartree]	E_{corr} [Hartree]	$< S^2 >_{HF}$	$\frac{N_{pairs\ included}}{N_{all\ pairs}}$ [%]	N_{AO}	$t_{CPU}^{DF-LUCC2}$ [sec]	Δg^{ZKE}	$\Delta g_{iso}^{1el-DSO}$	$\Delta g_{iso}^{2el-DSO}$	$\Delta g_{iso}^{1el-PSO}$	$\Delta g_{iso}^{2el-PSO}$	Δg_{iso}
AsO_3^{2-}	-2458.678238	-0.920531	0.81	100.0	141	305.76	-275	444	-22	2075	-1369	853
BO	-99.559843	-0.306955	0.80	100.0	62	36.75	-91	57	-26	-1817	569	-1308
BS	-422.183983	-0.232106	0.86	100.0	68	37.36	-94	62	-29	-7625	1251	-6433
BeH	-15.151160	-0.027993	0.75	100.0	25	24.67	-54	39	-18	-237	117	-153
CF_3Br^-	-2908.756551	-1.074919	0.76	100.0	172	444.88	-313	193	-25	18400	-248	18009
CF_3Cl^-	-795.835778	-1.099901	0.76	100.0	161	435.61	-315	186	-54	4300	-741	3376
CH	-38.282184	-0.098425	0.76	100.0	37	33.46	-138	87	-34	-59380	23500	-35966
$CHCH_2$	-77.421564	-0.285142	0.96	100.0	80	47.88	-137	116	-43	-68	24	-109
CHO	-113.297307	-0.372805	0.77	100.0	68	40.40	-197	160	-54	-2860	936	-2015
CH_2	-38.938201	-0.113123	2.02	100.0	43	34.25	-132	92	-35	297	-120	103
CH_2CH_3	-78.628535	-0.318842	0.76	100.0	92	60.33	-130	104	-39	734	-292	378
CH_2OH	-114.466053	-0.387891	0.76	100.0	80	52.84	-183	131	-46	1384	-453	833
CH_3	-39.577740	-0.150821	0.76	100.0	49	33.54	-126	88	-33	741	-292	377
CH_4^+	-39.734830	-0.153639	0.77	100.0	55	35.27	-112	81	-26	14332	-5658	8617
$COCH_3$	-152.360574	-0.539433	0.76	100.0	111	103.32	-210	181	-64	-2561	855	-1799
CO^+	-112.306376	-0.331416	0.99	100.0	62	36.84	-177	146	-56	-2750	859	-1978
CO_2^-	-187.662674	-0.625912	0.76	100.0	93	71.97	-215	136	-47	-2055	655	-1527
CO_3^-	-262.545314	-0.899048	0.81	100.0	124	172.52	-337	256	-81	11017	-3305	7551
C_2H	-76.179617	-0.255361	1.15	100.0	68	32.75	-172	146	-58	61	-25	-49
C_3H_5	-116.422472	-0.455213	0.83	100.0	123	111.48	-136	140	-55	720	-285	384
ClO_2	-609.066339	-0.716102	0.79	100.0	99	93.18	-344	291	-66	10158	-2577	7461
ClO_3	-683.843567	-0.971646	0.81	100.0	130	333.69	-337	339	-77	5745	-1674	3996
GeH_3	-2077.068152	-0.105458	0.75	100.0	66	37.92	-116	332	29	6111	550	6906
H_2CO^+	-113.571149	-0.334384	0.79	100.0	74	43.05	-293	183	-56	3935	-1153	2616
KrF	-2851.397971	-0.382143	0.76	100.0	79	46.64	-440	274	-51	61872	-18804	42852
MgF	-299.141356	-0.281410	0.75	100.0	63	29.52	-68	78	-9	-1165	212	-952
NF_2	-253.267808	-0.693945	0.77	100.0	93	89.76	-313	197	-61	3922	-1033	2711
NF_3^+	-352.270597	-0.950368	0.77	100.0	124	187.70	-392	280	-83	4870	-1249	3427
NH	-54.982807	-0.134024	2.02	100.0	37	32.79	-206	123	-42	1537	-538	874
NH_2	-55.586804	-0.179113	0.76	100.0	43	32.57	-202	123	-42	3902	-1355	2426
NH_3^+	-55.902328	-0.172173	0.76	100.0	49	27.87	-222	132	-45	1923	-669	1119
NO	-129.302331	-0.406873	0.80	100.0	62	38.53	-289	189	-62	-178661	57221	-121602
NO_2	-204.115318	-0.696621	0.77	100.0	93	76.77	-314	198	-64	-3230	1024	-2384
NO_3	-278.916473	-0.937764	0.76	100.0	124	218.09	-353	267	-83	11415	-3426	7820
OCH_3	-114.470180	-0.364186	0.76	100.0	80	53.41	-287	178	-54	65111	-19588	45360
OH	-75.422229	-0.196627	0.76	100.0	37	33.23	-294	166	-49	168879	-50437	118265
ONO	-204.119347	-0.691254	0.77	100.0	93	70.32	-314	243	-78	-3424	1084	-2489
O_2H	-150.242958	-0.451445	0.76	100.0	68	44.43	-345	213	-64	19313	-5791	13326
O_3^-	-224.446418	-0.749795	0.78	100.0	93	85.51	-351	233	-70	11887	-3566	8133
PH_2	-341.882011	-0.130463	0.77	100.0	49	35.07	-159	159	-21	6911	-949	5940
SO_2^-	-547.320167	-0.671492	0.78	100.0	99	98.27	-290	263	-56	5625	-1421	4120
SO_3^-	-622.223409	-0.914092	0.78	100.0	130	294.73	-300	335	-71	1542	-482	1024
SiH_2	-290.019504	-0.084491	2.01	100.0	49	28.51	-117	143	-17	395	-49	353
SiH_3	-290.636855	-0.108084	0.75	100.0	55	30.07	-118	165	-20	1050	-132	946

Table C.24: Eigenvalues of the g-shifts [ppm] calculated with Z_{eff}-SDC-DF-LUCC2 at the def2-TZVP/DF-QZ level with DF-UHF reference, extended domains and full pair lists for the benchmark set of Perera *et al.*[35]

Molecule	$\Delta g_{diag1}^{1el-DSO}$	$\Delta g_{diag2}^{1el-DSO}$	$\Delta g_{diag3}^{1el-DSO}$	$\Delta g_{diag1}^{2el-DSO}$	$\Delta g_{diag2}^{2el-DSO}$	$\Delta g_{diag3}^{2el-DSO}$	$\Delta g_{diag1}^{1el-PSO}$	$\Delta g_{diag2}^{1el-PSO}$	$\Delta g_{diag3}^{1el-PSO}$	$\Delta g_{diag1}^{2el-PSO}$	$\Delta g_{diag2}^{2el-PSO}$	$\Delta g_{diag3}^{2el-PSO}$	Δg_{diag1}	Δg_{diag2}	Δg_{diag3}
AsO_3^{2-}	525	525	283	-15	-25	-25	3243	3242	-261	-704	-1702	-1702	1765	1765	-971
BO	60	60	51	-23	-27	-27	0	-2725	-2725	853	853	-0	-64	-1930	-1930
BS	74	74	39	-22	-32	-32	-0	-11437	-11437	1877	1877	0	-76	-9612	-9612
BeH	44	44	30	-14	-20	-20	-0	-356	-356	176	176	0	-38	-210	-210
CF_3Br^-	206	206	168	-22	-22	-30	27843	27843	-486	117	-430	-430	27285	27285	-544
CF_3Cl^-	211	211	136	-39	-62	-62	6690	6690	-480	128	-1176	-1176	5349	5349	-570
CH	107	105	48	-19	-41	-41	2360	-1	-180500	71441	1	-943	1343	-109	-109131
$CHCH_2$	146	144	58	-22	-54	-54	873	-71	-1006	397	27	-353	473	-145	-655
CHO	203	178	99	-34	-60	-69	3038	-359	-11259	3646	104	-943	2032	-384	-7694
CH_2	114	82	79	-31	-31	-42	484	424	-16	5	-171	-193	207	172	-71
CH_2CH_3	131	121	61	-23	-45	-48	1208	1017	-24	8	-404	-481	681	559	-106
CH_2OH	164	138	91	-33	-49	-57	2872	1333	-52	17	-472	-904	1892	766	-159
CH_3	108	108	47	-20	-40	-40	1095	1095	33	-13	-432	-432	605	605	-79
CH_4^+	100	99	44	-13	-33	-34	38964	4047	-16	7	-1607	-15374	23546	2395	-90
$COCH_3$	230	212	102	-36	-75	-81	2924	-408	-10198	3354	124	-914	1949	-429	-6917
CO^+	180	180	77	-32	-68	-68	0	-4124	-4125	1289	1288	-0	-132	-2901	-2901
CO_2^-	156	144	108	-38	-49	-54	1694	-987	-6873	2214	302	-551	1030	-831	-4780
CO_3^-	328	220	220	-69	-69	-104	14504	14504	4044	-1202	-4357	-4357	9961	9961	2730
C_2H	180	180	77	-31	-71	-71	91	91	-0	0	-38	-38	-10	-10	-126
C_3H_5	186	127	108	-45	-48	-73	1181	1036	-56	24	-409	-470	654	604	-105
ClO_2	345	301	226	-50	-70	-79	17048	14120	-694	115	-3484	-4363	12571	10559	-747
ClO_3	390	390	238	-54	-89	-89	7842	7835	1558	-553	-2235	-2236	5571	5566	852
GeH_3	419	419	159	37	37	14	9199	9199	-66	828	828	-6	10367	10367	-16
H_2CO^+	225	199	125	-37	-60	-70	9112	1891	803	-240	-481	-2739	6235	1257	356
KrF	331	331	160	-30	-61	-61	92808	92808	-0	0	-28206	-28206	64433	64433	-310
MgF	89	72	72	-8	-8	-11	-0	-1747	-1747	318	318	0	10	-1433	-1433
NF_2	232	231	128	-39	-72	-72	8077	4507	-819	209	-1094	-2214	5711	3258	-836
NF_3^+	335	335	171	-51	-99	-99	7725	7724	-839	220	-1983	-1983	5586	5586	-891
NH	150	109	109	-38	-38	-51	2306	2306	-0	0	-807	-807	1364	1364	-107
NH_2	150	150	70	-25	-50	-51	9116	2556	33	-12	-891	-3161	5853	1562	-136
NH_3^+	160	160	75	-27	-54	-54	2856	2856	57	-20	-993	-993	1747	1747	-138
NO	238	194	136	-44	-64	-78	4825	-761	-540047	172992	215	-1544	3153	-744	-367214
NO_2	241	203	151	-49	-65	-77	5428	-1001	-14116	4456	305	-1688	3590	-907	-9836
NO_3	344	230	228	-70	-71	-107	25002	9395	-151	52	-2818	-7513	17293	6382	-216
OCH_3	218	202	115	-34	-61	-66	185608	9757	-32	13	-2944	-55834	129627	6678	-226
OH	202	200	97	-29	-59	-60	497592	8997	49	-15	-2701	-148596	348845	6143	-192
ONO	308	270	151	-49	-86	-99	4867	-970	-14170	4474	295	-1516	3246	-886	-9827
O_2H	264	228	146	-44	-68	-79	49855	8134	-50	15	-2437	-14951	34719	5536	-277
O_3^-	277	249	174	-52	-75	-83	22706	13796	-842	252	-4139	-6812	15717	9501	-818
PH_2	199	195	83	-11	-26	-27	15846	4712	175	-24	-647	-2176	13680	4078	63
SO_2^-	307	289	193	-41	-62	-65	10665	6633	-424	72	-1739	-2595	8006	4844	-491
SO_3^-	404	404	197	-42	-86	-86	2259	2259	108	-92	-677	-677	1601	1601	-129
SiH_2	175	130	123	-15	-16	-21	1082	688	-585	73	-86	-135	938	598	-476
SiH_3	208	208	80	-10	-25	-25	1588	1588	-26	3	-199	-199	1455	1455	-71

Table C.25: Eigenvalues of the g-shifts and isotropic g-shifts [ppm] calculated with SOMF-GIAO-B3LYP at the def2-TZVP level for their benchmark set of molecules with a single spin-center by Glasbrenner *et al.*[35]

Molecule	Δg_{diag1}	Δg_{diag2}	Δg_{diag3}	Δg_{iso}
CH_3	550	550	-89	337
$C_{10}H_{21}$	533	460	-139	285
$C_{15}H_{31}$	533	460	-139	285
$C_{17}H_{27}O$	566	504	-122	316
$C_{19}H_{39}O$	66021	6443	-175	24096
$C_{20}H_{41}$	534	460	-139	285
$C_{21}H_{41}$	552	549	-81	340
C_2H_5	682	507	-108	360
C_3H_7	526	469	-137	286
C_4H_9	537	465	-133	290
C_5H_{11}	534	460	-138	285
C_7H_{15}	533	460	-139	285
$C_8H_{18}NO_8$	4119	1540	-151	1836
LiH^+	-36	-39	-39	-38
NaF^+	99018	68231	-288	55654
Cys-Gly_4	220519	17231	17	79256
MTSL	7084	3805	-226	3554

Table C.26: Eigenvalues of the g-shifts and isotropic g-shifts [ppm] calculated with SOMF-SDC-B3LYP at the def2-TZVP level for their benchmark set of molecules with a single spin-center by Glasbrenner *et al.*[35]

Molecule	Δg_{diag1}	Δg_{diag2}	Δg_{diag3}	Δg_{iso}
CH_3	543	543	-92	331
$C_{10}H_{21}$	566	473	-109	310
$C_{15}H_{31}$	568	474	-108	311
$C_{17}H_{27}O$	619	520	-52	362
$C_{19}H_{39}O$	65935	6494	-143	24095
$C_{20}H_{41}$	568	474	-107	312
$C_{21}H_{41}$	557	553	-28	361
C_2H_5	680	516	-100	365
C_3H_7	544	486	-112	306
C_4H_9	558	478	-106	310
C_5H_{11}	561	475	-110	309
C_7H_{15}	563	473	-111	308
$C_8H_{18}NO_8$	4137	1509	-132	1838
LiH^+	-36	-39	-39	-38
NaF^+	99018	68179	-291	55635
Cys-Gly_4	220569	17268	15	79284
MTSL	7139	3950	-163	3642

Table C.27: Miscellaneous data and isotropic g-shifts [ppm] for the g-tensor calculations with Z_{eff}-SDC-DF-LUCC2 at the def2-TZVP/DF-QZ level with DF-UHF reference, extended domains and full pair lists for the benchmark set of molecules with a single spin-center used by Glasbrenner *et al.*[35]

Molecule	E_{HF} [Hartree]	E_{corr} [Hartree]	$< S^2 >_{HF}$	$\frac{N_{pairs\ included}}{N_{all\ pairs}}$ [%]	N_{AO}	$t_{CPU}^{DF-LUCC2}$ [sec]	Δg^{ZKE}	$\Delta g_{iso}^{1el-DSO}$	$\Delta g_{iso}^{2el-DSO}$	$\Delta g_{iso}^{1el-PSO}$	$\Delta g_{iso}^{2el-PSO}$	Δg_{iso}
CH_3	-39.577690	-0.150860	0.76	100.0	49	29.71	-126	88	-33	740	-292	376
$C_{10}H_{21}$	-391.010152	-1.670817	0.76	100.0	436	14696.28	-137	131	-49	609	-242	311
$C_{15}H_{31}$	-586.248976	-2.516255	0.76	100.0	651	46204.28	-137	134	-50	606	-242	311
$C_{17}H_{27}O$	-734.590825	-2.980321	1.40	100.0	720	89477.42	-138	182	-72	605	-239	338
$C_{19}H_{39}O$	-817.324206	-3.408441	0.76	100.0	854	180721.79	-299	202	-62	102262	-30740	71363
$C_{20}H_{41}$	-781.487784	-3.361699	0.76	100.0	866	123390.20	-137	134	-51	605	-241	312
$C_{21}H_{41}$	-819.373665	-3.497836	0.98	100.0	897	146836.97	-131	161	-63	690	-272	384
C_2H_5	-78.628163	-0.318322	0.76	100.0	92	60.85	-130	107	-40	736	-293	380
C_3H_7	-117.675535	-0.486988	0.76	100.0	135	183.37	-135	120	-46	616	-245	310
C_4H_9	-156.723549	-0.656214	0.76	100.0	178	488.01	-136	119	-45	626	-249	315
C_5H_{11}	-195.771318	-0.825334	0.76	100.0	221	1082.99	-137	122	-47	617	-245	311
C_7H_{15}	-273.866852	-1.163547	0.76	100.0	307	3887.57	-137	127	-48	613	-243	311
$C_8H_{18}NO_8$	-966.929594	-3.413604	0.76	100.0	635	62791.51	-204	150	-51	3385	-1182	2097
LiH^+	-7.738130	-0.000000	0.75	nan	20	26.97	-55	19	-1	-2	1	-37
NaF^+	-261.085561	-0.164900	0.75	100.0	63	36.39	-412	222	-56	237777	-59403	178130
Cys-Gly_4	-1546.412307	-4.396686	0.76	100.0	827	278659.76	-229	226	-41	99849	-15020	84784
MTSL	-1463.419929	-2.938594	0.77	100.0	616	80323.45	-296	243	-79	5748	-1773	3843

Table C.28: Eigenvalues of the g-shifts [ppm] calculated with Z_{eff}-SDC-DF-LUCC2 at the def2-TZVP/DF-QZ level with DF-UHF reference, extended domains and full pair lists for the benchmark set of molecules with a single spin-center used by Glasbrenner *et al.*[35]

Molecule	$\Delta g_{diag1}^{1el-DSO}$	$\Delta g_{diag2}^{1el-DSO}$	$\Delta g_{diag3}^{1el-DSO}$	$\Delta g_{diag1}^{2el-DSO}$	$\Delta g_{diag2}^{2el-DSO}$	$\Delta g_{diag3}^{2el-DSO}$	$\Delta g_{diag1}^{1el-PSO}$	$\Delta g_{diag2}^{1el-PSO}$	$\Delta g_{diag3}^{1el-PSO}$	$\Delta g_{diag1}^{2el-PSO}$	$\Delta g_{diag2}^{2el-PSO}$	$\Delta g_{diag3}^{2el-PSO}$	Δg_{diag1}	Δg_{diag2}	Δg_{diag3}
CH_3	108	108	47	-20	-40	-40	1094	1094	33	-13	-432	-432	604	604	-79
$C_{10}H_{21}$	167	137	88	-34	-52	-62	976	941	-91	36	-374	-388	535	529	-132
$C_{15}H_{31}$	172	140	89	-35	-52	-64	976	937	-94	36	-373	-388	535	530	-132
$C_{17}H_{27}O$	234	170	142	-56	-69	-91	1000	983	-168	69	-388	-398	600	552	-138
$C_{19}H_{39}O$	251	220	135	-42	-68	-77	296683	10130	-26	14	-3048	-89187	207347	6957	-214
$C_{20}H_{41}$	173	141	89	-35	-53	-64	975	936	-95	36	-372	-387	536	530	-131
$C_{21}H_{41}$	199	144	141	-54	-58	-77	1095	999	-25	12	-393	-435	618	596	-61
C_2H_5	134	122	64	-25	-45	-49	1215	1021	-28	10	-405	-483	687	562	-108
C_3H_7	152	129	79	-32	-48	-57	978	950	-81	32	-377	-389	533	531	-133
C_4H_9	150	127	81	-32	-48	-56	983	968	-73	28	-384	-390	542	533	-129
C_5H_{11}	155	129	83	-33	-49	-58	978	956	-82	31	-379	-388	537	530	-133
C_7H_{15}	161	133	86	-34	-50	-60	977	948	-87	33	-376	-387	536	530	-133
$C_8H_{18}NO_8$	192	159	100	-35	-55	-65	7527	2618	9	-3	-916	-2627	4807	1616	-132
LiH^+	20	18	18	-0	-0	-2	-0	-3	-3	2	2	0	-36	-38	-38
NaF^+	268	268	131	-33	-67	-67	514188	199159	-15	7	-49869	-128347	385631	149079	-321
Cys-Gly_4	282	257	138	-27	-44	-52	282382	17046	118	-14	-2600	-42445	239922	14445	-14
MTSL	305	235	188	-61	-76	-100	11035	6299	-90	24	-1978	-3365	7525	4231	-227

Table C.29: Miscellaneous data and isotropic g-shifts [ppm] for the g-tensor calculations with Z_{eff}-SDC-DF-LUCC2 at the def2-TZVP/DF-QZ level with DF-ROHF reference, extended domains and full pair lists for the benchmark set of molecules with a single spin-center used by Glasbrenner *et al.*[35]

Molecule	E_{HF} [Hartree]	E_{corr} [Hartree]	$< S^2 >_{HF}$	$\frac{N_{pairs\ included}}{N_{all\ pairs}}$ [%]	N_{AO}	$t_{CPU}^{DF-LUCC2}$ [sec]	Δg^{ZKE}	$\Delta g_{iso}^{1el-DSO}$	$\Delta g_{iso}^{2el-DSO}$	$\Delta g_{iso}^{1el-PSO}$	$\Delta g_{iso}^{2el-PSO}$	Δg_{iso}
CH_3	-39.573178	-0.155564	0.75	100.0	49	34.91	-128	88	-33	741	-293	375
$C_{10}H_{21}$	-391.005413	-1.675854	0.75	100.0	436	10974.88	-139	129	-49	623	-248	316
$C_{15}H_{31}$	-586.244234	-2.521296	0.75	100.0	651	61603.69	-139	132	-50	621	-247	317
$C_{17}H_{27}O$	-734.561741	-3.026702	0.75	100.0	720	111115.38	-140	171	-68	616	-243	335
$C_{19}H_{39}O$	-817.318732	-3.414203	0.75	100.0	854	199987.06	-303	203	-63	122300	-36761	85377
$C_{20}H_{41}$	-781.483044	-3.366736	0.75	100.0	866	127756.02	-139	133	-50	620	-247	317
$C_{21}H_{41}$	-819.348458	-3.528930	0.75	100.0	897	191495.38	-133	158	-62	665	-264	365
C_2H_5	-78.623377	-0.323373	0.75	100.0	92	58.98	-132	107	-40	748	-298	386
C_3H_7	-117.670815	-0.491991	0.75	100.0	135	160.50	-138	121	-46	632	-251	318
C_4H_9	-156.718806	-0.661235	0.75	100.0	178	399.56	-139	119	-45	639	-254	321
C_5H_{11}	-195.766574	-0.830358	0.75	100.0	221	811.52	-139	122	-47	631	-251	317
C_7H_{15}	-273.862114	-1.168582	0.75	100.0	307	3067.66	-139	126	-47	627	-249	316
$C_8H_{18}NO_8$	-966.924104	-3.419369	0.75	100.0	635	64889.49	-207	151	-51	3449	-1205	2136
LiH^+	-7.738129	-0.000000	0.75	nan	20	27.06	-54	19	-1	-2	1	-37
NaF^+	-261.080885	-0.167801	0.75	100.0	63	35.77	-406	220	-55	728265	-181857	546167
Cys-Gly_4	-1546.406509	-4.402903	0.75	100.0	827	208534.57	-217	223	-41	120392	-18108	102249
MTSL	-1463.410017	-2.949608	0.75	100.0	616	65923.03	-300	243	-79	5842	-1800	3906

Table C.30: Eigenvalues of the g-shifts [ppm] calculated with Z_{eff}-SDC-DF-LUCC2 at the def2-TZVP/DF-QZ level with DF-ROHF reference, extended domains and full pair lists for the benchmark set of molecules with a single spin-center used by Glasbrenner *et al.*[35]

Molecule	$\Delta g_{diag1}^{1el-DSO}$	$\Delta g_{diag2}^{1el-DSO}$	$\Delta g_{diag3}^{1el-DSO}$	$\Delta g_{diag1}^{2el-DSO}$	$\Delta g_{diag2}^{2el-DSO}$	$\Delta g_{diag3}^{2el-DSO}$	$\Delta g_{diag1}^{1el-PSO}$	$\Delta g_{diag2}^{1el-PSO}$	$\Delta g_{diag3}^{1el-PSO}$	$\Delta g_{diag1}^{2el-PSO}$	$\Delta g_{diag2}^{2el-PSO}$	$\Delta g_{diag3}^{2el-PSO}$	Δg_{diag1}	Δg_{diag2}	Δg_{diag3}
CH_3	108	108	48	-20	-40	-40	1106	1106	12	-5	-437	-437	609	609	-93
$C_{10}H_{21}$	165	135	88	-35	-51	-61	995	975	-101	39	-387	-395	552	539	-142
$C_{15}H_{31}$	169	138	90	-34	-52	-63	995	971	-103	40	-386	-395	552	540	-141
$C_{17}H_{27}O$	216	159	139	-55	-63	-85	1066	952	-171	71	-377	-424	591	567	-152
$C_{19}H_{39}O$	253	221	136	-42	-68	-78	356645	10297	-41	17	-3100	-107201	249292	7069	-230
$C_{20}H_{41}$	170	139	90	-35	-52	-63	994	971	-104	40	-386	-394	552	540	-142
$C_{21}H_{41}$	197	140	137	-53	-55	-77	1128	927	-60	25	-367	-449	633	548	-87
C_2H_5	135	123	63	-25	-46	-49	1241	1042	-38	14	-414	-493	701	572	-116
C_3H_7	153	130	80	-32	-49	-57	997	987	-89	35	-391	-397	554	540	-140
C_4H_9	150	126	81	-32	-48	-56	1003	999	-84	33	-396	-398	558	542	-138
C_5H_{11}	154	129	83	-33	-49	-58	997	987	-92	36	-392	-396	553	539	-142
C_7H_{15}	159	132	86	-34	-49	-59	996	981	-97	37	-389	-395	552	539	-142
$C_8H_{18}NO_8$	192	159	100	-35	-55	-65	7701	2668	-22	7	-935	-2689	4917	1645	-156
LiH^+	20	18	18	-0	-0	-2	-0	-3	-3	2	2	0	-36	-38	-38
NaF^+	265	264	132	-33	-66	-66	1900714	284097	-17	8	-71136	-474444	1426064	212754	-316
Cys-Gly_4	279	254	136	-27	-44	-52	343693	17460	25	0	-2665	-51660	292027	14803	-83
MTSL	306	236	188	-61	-76	-100	11248	6414	-135	36	-2011	-3426	7672	4308	-263

Table C.31: Miscellaneous data and isotropic g-shifts [ppm] for the g-tensor calculations with Z_{eff}-SDC-DF-LUCC2 at the def2-TZVP/DF-TZ level with DF-UHF reference, extended domains and full pair lists for the benchmark set of molecules with a single spin-center used by Glasbrenner *et al.*[35]

Molecule	E_{HF} [Hartree]	E_{corr} [Hartree]	$< S^2 >_{HF}$	$\frac{N_{pairs\ included}}{N_{all\ pairs}}$ [%]	N_{AO}	$t_{CPU}^{DF-LUCC2}$ [sec]	Δg^{ZKE}	$\Delta g_{iso}^{1el-DSO}$	$\Delta g_{iso}^{2el-DSO}$	$\Delta g_{iso}^{1el-PSO}$	$\Delta g_{iso}^{2el-PSO}$	Δg_{iso}
CH_3	-39.577690	-0.150846	0.76	100.0	49	29.00	-126	88	-33	740	-292	376
$C_{10}H_{21}$	-391.010152	-1.670597	0.76	100.0	436	10008.48	-137	131	-49	609	-242	311
$C_{15}H_{31}$	-586.248976	-2.515921	0.76	100.0	651	30504.45	-137	134	-50	606	-242	311
$C_{17}H_{27}O$	-734.590825	-2.979967	1.40	100.0	720	62705.49	-138	182	-72	605	-239	338
$C_{19}H_{39}O$	-817.324206	-3.407998	0.76	100.0	854	120043.24	-299	202	-62	102409	-30784	71466
$C_{20}H_{41}$	-781.487784	-3.361250	0.76	100.0	866	83880.90	-137	134	-51	605	-241	312
$C_{21}H_{41}$	-819.373665	-3.497377	0.98	100.0	897	98370.73	-131	161	-63	690	-272	384
C_2H_5	-78.628163	-0.318286	0.76	100.0	92	50.43	-130	107	-40	736	-293	380
C_3H_7	-117.675535	-0.486929	0.76	100.0	135	136.01	-135	120	-46	616	-245	310
C_4H_9	-156.723549	-0.656131	0.76	100.0	178	348.79	-136	119	-45	626	-249	315
C_5H_{11}	-195.771318	-0.825229	0.76	100.0	221	757.20	-137	122	-47	617	-245	311
C_7H_{15}	-273.866852	-1.163396	0.76	100.0	307	2659.02	-137	127	-48	613	-243	311
$C_8H_{18}NO_8$	-966.929594	-3.413425	0.76	100.0	635	43559.62	-204	150	-51	3385	-1182	2097
LiH^+	-7.738130	-0.000000	0.75	nan	20	32.38	-55	19	-1	-2	1	-37
NaF^+	-261.085561	-0.164900	0.75	100.0	63	35.61	-412	222	-56	239157	-59747	179165
Cys-Gly_4	-1546.412307	-4.396400	0.76	100.0	827	192942.04	-229	226	-41	99848	-15020	84783
MTSL	-1463.419929	-2.938514	0.77	100.0	616	48794.31	-296	243	-79	5748	-1773	3843

Table C.32: Eigenvalues of the g-shifts [ppm] calculated with Z_{eff}-SDC-DF-LUCC2 at the def2-TZVP/DF-TZ level with DF-UHF reference, extended domains and full pair lists for the benchmark set of molecules with a single spin-center used by Glasbrenner *et al.*[35]

Molecule	$\Delta g_{diag1}^{1el-DSO}$	$\Delta g_{diag2}^{1el-DSO}$	$\Delta g_{diag3}^{1el-DSO}$	$\Delta g_{diag1}^{2el-DSO}$	$\Delta g_{diag2}^{2el-DSO}$	$\Delta g_{diag3}^{2el-DSO}$	$\Delta g_{diag1}^{1el-PSO}$	$\Delta g_{diag2}^{1el-PSO}$	$\Delta g_{diag3}^{1el-PSO}$	$\Delta g_{diag1}^{2el-PSO}$	$\Delta g_{diag2}^{2el-PSO}$	$\Delta g_{diag3}^{2el-PSO}$	Δg_{diag1}	Δg_{diag2}	Δg_{diag3}
CH_3	108	108	47	-20	-40	-40	1094	1094	33	-13	-432	-432	604	604	-79
$C_{10}H_{21}$	167	137	88	-34	-52	-62	976	941	-91	36	-374	-388	535	529	-132
$C_{15}H_{31}$	172	140	89	-35	-52	-64	976	937	-94	36	-373	-388	535	530	-132
$C_{17}H_{27}O$	234	170	142	-56	-69	-91	1000	983	-168	69	-388	-398	599	552	-138
$C_{19}H_{39}O$	251	220	135	-42	-68	-77	297122	10131	-25	14	-3048	-89318	207654	6958	-214
$C_{20}H_{41}$	173	141	89	-35	-53	-64	975	936	-95	36	-372	-387	536	530	-131
$C_{21}H_{41}$	199	144	141	-54	-58	-77	1095	999	-25	12	-393	-435	618	596	-61
C_2H_5	134	122	64	-25	-45	-49	1215	1021	-28	10	-405	-483	687	562	-108
C_3H_7	152	129	79	-32	-48	-57	978	950	-81	32	-377	-389	533	531	-133
C_4H_9	150	127	81	-32	-48	-56	983	968	-73	28	-384	-390	542	533	-129
C_5H_{11}	155	129	83	-33	-49	-58	978	956	-82	31	-379	-388	537	530	-133
C_7H_{15}	161	133	86	-34	-50	-60	977	948	-87	33	-376	-387	536	530	-133
$C_8H_{18}NO_8$	192	159	100	-35	-55	-65	7527	2618	9	-3	-917	-2627	4807	1616	-132
LiH^+	20	18	18	-0	-0	-2	-0	-3	-3	2	2	0	-36	-38	-38
NaF^+	268	268	131	-33	-67	-67	517800	199686	-14	7	-50001	-129248	388342	149475	-321
Cys-Gly_4	282	257	138	-27	-44	-52	282378	17048	118	-14	-2601	-42445	239918	14446	-15
MTSL	305	235	188	-61	-76	-100	11035	6299	-90	24	-1978	-3365	7525	4231	-227

Table C.33: Miscellaneous data and isotropic g-shifts [ppm] for the g-tensor calculations with Z_{eff}-SDC-DF-LUCC2 at the def2-TZVP/DF-QZ level with DF-UHF reference, Boughton-Pulay domains and full pair lists for the benchmark set of molecules with a single spin-center used by Glasbrenner *et al.*[35]

Molecule	E_{HF} [Hartree]	E_{corr} [Hartree]	$< S^2 >_{HF}$	$\frac{N_{pairs\ included}}{N_{all\ pairs}}$ [%]	N_{AO}	$t_{CPU}^{DF-LUCC2}$ [sec]	Δg^{ZKE}	$\Delta g_{iso}^{1el-DSO}$	$\Delta g_{iso}^{2el-DSO}$	$\Delta g_{iso}^{1el-PSO}$	$\Delta g_{iso}^{2el-PSO}$	Δg_{iso}
CH_3	-39.577690	-0.150378	0.76	100.0	49	29.58	-126	88	-33	741	-292	377
$C_{10}H_{21}$	-391.010152	-1.648994	0.76	100.0	436	6712.75	-137	127	-48	611	-243	310
$C_{15}H_{31}$	-586.248976	-2.482285	0.76	100.0	651	22778.93	-137	129	-49	609	-242	310
$C_{17}H_{27}O$	-734.590825	-2.940835	1.40	100.0	720	41641.71	-138	183	-73	602	-238	337
$C_{19}H_{39}O$	-817.324206	-3.363607	0.76	100.0	854	95661.61	-299	197	-61	84882	-25516	59202
$C_{20}H_{41}$	-781.487784	-3.315583	0.76	100.0	866	64707.26	-137	130	-49	609	-242	310
$C_{21}H_{41}$	-819.373665	-3.450344	0.98	100.0	897	78705.12	-131	160	-63	686	-271	382
C_2H_5	-78.628163	-0.316038	0.76	100.0	92	51.69	-130	107	-40	734	-292	379
C_3H_7	-117.675535	-0.482258	0.76	100.0	135	120.30	-135	119	-46	615	-244	309
C_4H_9	-156.723549	-0.649010	0.76	100.0	178	265.90	-136	118	-45	625	-248	314
C_5H_{11}	-195.771318	-0.815690	0.76	100.0	221	546.32	-137	121	-46	618	-245	310
C_7H_{15}	-273.866852	-1.149017	0.76	100.0	307	1801.79	-137	124	-47	614	-244	310
$C_8H_{18}NO_8$	-966.929594	-3.384625	0.76	100.0	635	26760.87	-204	150	-51	3342	-1167	2068
LiH^+	-7.738130	-0.000000	0.75	nan	20	27.02	-55	19	-1	-2	1	-37
NaF^+	-261.085561	-0.164852	0.75	100.0	63	36.12	-412	222	-56	236185	-59005	176935
Cys-Gly_4	-1546.412307	-4.355635	0.76	100.0	827	130876.26	-229	224	-40	91112	-13706	77361
MTSL	-1463.419929	-2.902317	0.77	100.0	616	32327.29	-297	242	-79	5668	-1748	3787

Table C.34: Eigenvalues of the g-shifts [ppm] calculated with Z_{eff}-SDC-DF-LUCC2 at the def2-TZVP/DF-QZ level with DF-UHF reference, Boughton-Pulay domains and full pair lists for the benchmark set of molecules with a single spin-center used by Glasbrenner *et al.*[35]

Molecule	$\Delta g_{diag1}^{1el-DSO}$	$\Delta g_{diag2}^{1el-DSO}$	$\Delta g_{diag3}^{1el-DSO}$	$\Delta g_{diag1}^{2el-DSO}$	$\Delta g_{diag2}^{2el-DSO}$	$\Delta g_{diag3}^{2el-DSO}$	$\Delta g_{diag1}^{1el-PSO}$	$\Delta g_{diag2}^{1el-PSO}$	$\Delta g_{diag3}^{1el-PSO}$	$\Delta g_{diag1}^{2el-PSO}$	$\Delta g_{diag2}^{2el-PSO}$	$\Delta g_{diag3}^{2el-PSO}$	Δg_{diag1}	Δg_{diag2}	Δg_{diag3}
CH_3	108	108	47	-20	-40	-40	1095	1095	32	-13	-432	-432	605	605	-79
$C_{10}H_{21}$	162	134	86	-34	-50	-60	977	941	-84	33	-374	-388	532	530	-131
$C_{15}H_{31}$	165	135	87	-34	-51	-61	976	938	-86	33	-373	-387	532	530	-131
$C_{17}H_{27}O$	236	172	143	-56	-70	-92	990	979	-162	67	-387	-394	599	545	-133
$C_{19}H_{39}O$	243	216	131	-41	-66	-75	244655	10004	-13	10	-3010	-73549	170954	6863	-210
$C_{20}H_{41}$	166	136	87	-34	-51	-62	976	938	-87	33	-373	-387	532	530	-131
$C_{21}H_{41}$	198	142	140	-54	-57	-78	1093	990	-24	11	-389	-435	616	592	-62
C_2H_5	134	122	64	-25	-45	-49	1210	1020	-27	9	-405	-481	684	561	-108
C_3H_7	151	128	79	-31	-49	-57	976	946	-77	30	-375	-388	530	529	-131
C_4H_9	148	126	79	-31	-48	-56	982	962	-69	26	-381	-390	537	532	-128
C_5H_{11}	153	129	81	-33	-48	-57	977	953	-77	30	-378	-388	533	530	-132
C_7H_{15}	157	131	83	-34	-49	-59	977	946	-81	31	-376	-387	532	529	-132
$C_8H_{18}NO_8$	191	158	99	-35	-55	-65	7405	2607	12	-4	-913	-2585	4728	1609	-131
LiH^+	20	18	18	-0	-0	-2	-0	-3	-3	2	2	0	-36	-38	-38
NaF^+	268	268	131	-33	-67	-67	509701	198868	-14	7	-49795	-127228	382263	148863	-321
Cys-Gly_4	279	256	135	-26	-44	-51	256543	16665	128	-14	-2542	-38562	217967	14120	-5
MTSL	305	233	188	-61	-76	-99	10871	6223	-89	24	-1955	-3313	7411	4177	-228

Table C.35: Miscellaneous data and isotropic g-shifts [ppm] for the g-tensor calculations with Z_{eff}-SDC-DF-LUCC2 at the def2-TZVP/DF-QZ level with DF-UHF reference, extended domains and pair lists restricted using $|E_{IJ}| > 3.0 \cdot 10^{-5}$ Hartree for the benchmark set of molecules with a single spin-center used by Glasbrenner *et al.*[35]

Molecule	E_{HF} [Hartree]	E_{corr} [Hartree]	$< S^2 >_{HF}$	$\frac{N_{pairs\ included}}{N_{all\ pairs}}$ [%]	N_{AO}	$t_{CPU}^{DF-LUCC2}$ [sec]	Δg^{ZKE}	$\Delta g_{iso}^{1el-DSO}$	$\Delta g_{iso}^{2el-DSO}$	$\Delta g_{iso}^{1el-PSO}$	$\Delta g_{iso}^{2el-PSO}$	Δg_{iso}
CH_3	-39.577690	-0.150860	0.76	100.0	49	35.20	-126	88	-33	740	-292	376
$C_{10}H_{21}$	-391.010152	-1.666970	0.76	47.6	436	8274.19	-137	131	-49	604	-240	308
$C_{15}H_{31}$	-586.248976	-2.509552	0.76	33.5	651	23255.57	-137	134	-50	600	-239	308
$C_{17}H_{27}O$	-734.590825	-2.969126	1.40	34.5	720	42260.12	-138	183	-72	600	-237	336
$C_{19}H_{39}O$	-817.324206	-3.398753	0.76	25.7	854	92226.05	-299	202	-62	94639	-28449	66031
$C_{20}H_{41}$	-781.487784	-3.352138	0.76	25.8	866	61085.42	-137	134	-51	598	-238	307
$C_{21}H_{41}$	-819.373665	-3.487781	0.98	25.4	897	73230.55	-131	161	-63	692	-273	386
C_2H_5	-78.628163	-0.318322	0.76	100.0	92	57.64	-130	107	-40	736	-293	380
C_3H_7	-117.675535	-0.486988	0.76	100.0	135	182.53	-135	120	-46	616	-245	310
C_4H_9	-156.723549	-0.655791	0.76	90.6	178	426.34	-136	119	-45	628	-249	316
C_5H_{11}	-195.771318	-0.824349	0.76	79.9	221	968.41	-137	122	-47	617	-245	311
C_7H_{15}	-273.866852	-1.161419	0.76	63.2	307	2632.90	-137	127	-48	610	-242	309
$C_8H_{18}NO_8$	-966.929594	-3.404050	0.76	29.9	635	34094.37	-204	150	-51	3431	-1198	2127
LiH^+	-7.738130	-0.000000	0.75	nan	20	32.62	-55	19	-1	-2	1	-37
NaF^+	-261.085561	-0.164900	0.75	100.0	63	36.21	-412	222	-56	237777	-59403	178130
Cys-Gly_4	-1546.412307	-4.377655	0.76	27.1	827	79231.73	-229	225	-41	98645	-14838	83761
MTSL	-1463.419929	-2.918002	0.77	46.2	616	34218.50	-297	242	-79	5780	-1783	3863

Table C.36: Eigenvalues of the g-shifts [ppm] calculated with Z_{eff}-SDC-DF-LUCC2 at the def2-TZVP/DF-QZ level with DF-UHF reference, extended domains and pair lists restricted using $|E_{IJ}| > 3.0 \cdot 10^{-5}$ Hartree for the benchmark set of molecules with a single spin-center used by Glasbrenner *et al.*[35]

Molecule	$\Delta g_{diag1}^{1el-DSO}$	$\Delta g_{diag2}^{1el-DSO}$	$\Delta g_{diag3}^{1el-DSO}$	$\Delta g_{diag1}^{2el-DSO}$	$\Delta g_{diag2}^{2el-DSO}$	$\Delta g_{diag3}^{2el-DSO}$	$\Delta g_{diag1}^{1el-PSO}$	$\Delta g_{diag2}^{1el-PSO}$	$\Delta g_{diag3}^{1el-PSO}$	$\Delta g_{diag1}^{2el-PSO}$	$\Delta g_{diag2}^{2el-PSO}$	$\Delta g_{diag3}^{2el-PSO}$	Δg_{diag1}	Δg_{diag2}	Δg_{diag3}
CH_3	108	108	47	-20	-40	-40	1094	1094	33	-13	-432	-432	604	604	-79
$C_{10}H_{21}$	167	137	88	-34	-52	-62	971	937	-95	37	-372	-385	532	527	-135
$C_{15}H_{31}$	172	140	89	-35	-52	-64	968	929	-98	38	-370	-385	531	527	-135
$C_{17}H_{27}O$	234	171	143	-56	-69	-91	988	983	-170	70	-390	-392	601	544	-137
$C_{19}H_{39}O$	251	219	135	-42	-67	-77	273726	10211	-19	12	-3072	-82288	191289	7014	-209
$C_{20}H_{41}$	173	141	89	-35	-53	-64	967	927	-99	38	-369	-384	530	526	-135
$C_{21}H_{41}$	199	143	141	-54	-58	-77	1095	1005	-25	11	-395	-435	618	600	-61
C_2H_5	134	122	64	-25	-45	-49	1215	1021	-28	10	-405	-483	687	562	-108
C_3H_7	152	129	79	-32	-48	-57	978	950	-81	32	-377	-389	533	531	-133
C_4H_9	150	126	81	-32	-48	-56	983	975	-75	29	-386	-390	546	531	-130
C_5H_{11}	154	129	83	-33	-49	-58	976	960	-84	32	-381	-387	539	528	-134
C_7H_{15}	161	133	86	-34	-50	-60	972	947	-89	35	-376	-386	535	527	-135
$C_8H_{18}NO_8$	191	158	99	-35	-55	-65	7658	2615	19	-6	-915	-2673	4893	1615	-127
LiH^+	20	18	18	-0	-0	-2	-0	-3	-3	2	2	0	-36	-38	-38
NaF^+	268	268	131	-33	-67	-67	514188	199159	-15	7	-49869	-128347	385631	149079	-321
Cys-Gly_4	281	256	137	-26	-44	-52	278207	17605	124	-14	-2684	-41817	236374	14918	-8
MTSL	305	234	187	-61	-76	-100	11096	6334	-90	26	-1990	-3385	7566	4251	-227

Table C.37: Miscellaneous data and isotropic g-shifts [ppm] for the g-tensor calculations with Z_{eff}-SDC-DF-LUCC2 at the def2-TZVP/DF-QZ level with DF-UHF reference, extended domains and pair lists restricted using $|E_{IJ}| > 3.0 \cdot 10^{-3}$ Hartree for the benchmark set of molecules with a single spin-center used by Glasbrenner *et al.*[35]

Molecule	E_{HF} [Hartree]	E_{corr} [Hartree]	$< S^2 >_{HF}$	$\frac{N_{pairs\ included}}{N_{all\ pairs}}$ [%]	N_{AO}	$t_{CPU}^{DF-LUCC2}$ [sec]	Δg^{ZKE}	$\Delta g_{iso}^{1el-DSO}$	$\Delta g_{iso}^{2el-DSO}$	$\Delta g_{iso}^{1el-PSO}$	$\Delta g_{iso}^{2el-PSO}$	Δg_{iso}
CH_3	-39.577690	-0.135899	0.76	81.8	49	44.15	-126	88	-33	716	-282	361
$C_{10}H_{21}$	-391.010152	-1.234297	0.76	10.8	436	4625.68	-137	128	-49	558	-222	279
$C_{15}H_{31}$	-586.248976	-1.844687	0.76	7.3	651	16110.44	-137	131	-49	555	-221	278
$C_{17}H_{27}O$	-734.590825	-2.175706	1.40	6.4	720	30778.77	-138	194	-76	569	-226	323
$C_{19}H_{39}O$	-817.324206	-2.503896	0.76	5.4	854	62683.78	-300	197	-61	67794	-20375	47256
$C_{20}H_{41}$	-781.487784	-2.455067	0.76	5.5	866	45685.90	-137	131	-50	553	-220	278
$C_{21}H_{41}$	-819.373665	-2.559546	0.98	5.3	897	53500.09	-130	169	-66	654	-258	369
C_2H_5	-78.628163	-0.266658	0.76	50.0	92	75.47	-129	106	-40	688	-273	352
C_3H_7	-117.675535	-0.379691	0.76	33.3	135	111.80	-136	117	-45	576	-229	284
C_4H_9	-156.723549	-0.501852	0.76	25.7	178	215.69	-136	116	-44	580	-230	285
C_5H_{11}	-195.771318	-0.623938	0.76	20.9	221	386.34	-137	120	-46	571	-227	282
C_7H_{15}	-273.866852	-0.868077	0.76	15.2	307	1281.48	-137	124	-47	564	-224	280
$C_8H_{18}NO_8$	-966.929594	-2.762624	0.76	5.8	635	21690.19	-206	148	-51	3467	-1211	2147
LiH^+	-7.738130	-0.000000	0.75	nan	20	32.50	-55	19	-1	-2	1	-37
NaF^+	-261.085561	-0.164192	0.75	72.7	63	59.16	-412	222	-56	237282	-59278	177760
Cys-Gly_4	-1546.412307	-3.552710	0.76	5.3	827	71083.31	-230	223	-39	85291	-12829	72417
MTSL	-1463.419929	-2.236952	0.77	7.4	616	15006.12	-305	240	-78	4871	-1505	3223

Table C.38: Eigenvalues of the g-shifts [ppm] calculated with Z_{eff}-SDC-DF-LUCC2 at the def2-TZVP/DF-QZ level with DF-UHF reference, extended domains and pair lists restricted using $|E_{IJ}| > 3.0 \cdot 10^{-3}$ Hartree for the benchmark set of molecules with a single spin-center used by Glasbrenner *et al.*[35]

Molecule	$\Delta g_{diag1}^{1el-DSO}$	$\Delta g_{diag2}^{1el-DSO}$	$\Delta g_{diag3}^{1el-DSO}$	$\Delta g_{diag1}^{2el-DSO}$	$\Delta g_{diag2}^{2el-DSO}$	$\Delta g_{diag3}^{2el-DSO}$	$\Delta g_{diag1}^{1el-PSO}$	$\Delta g_{diag2}^{1el-PSO}$	$\Delta g_{diag3}^{1el-PSO}$	$\Delta g_{diag1}^{2el-PSO}$	$\Delta g_{diag2}^{2el-PSO}$	$\Delta g_{diag3}^{2el-PSO}$	Δg_{diag1}	Δg_{diag2}	Δg_{diag3}
CH_3	108	108	47	-20	-40	-40	1057	1057	34	-13	-417	-417	581	581	-79
$C_{10}H_{21}$	164	135	86	-34	-51	-61	928	844	-97	37	-336	-368	501	474	-139
$C_{15}H_{31}$	168	137	88	-34	-52	-62	927	838	-101	39	-334	-368	501	472	-139
$C_{17}H_{27}O$	259	187	137	-54	-75	-100	943	923	-160	65	-368	-374	588	503	-122
$C_{19}H_{39}O$	244	218	130	-40	-67	-75	193296	10097	-10	10	-3033	-58103	135042	6933	-208
$C_{20}H_{41}$	169	137	88	-34	-52	-63	926	836	-102	39	-333	-367	500	472	-139
$C_{21}H_{41}$	207	154	146	-55	-63	-80	1024	975	-37	16	-382	-407	588	578	-59
C_2H_5	134	122	63	-24	-46	-49	1125	965	-27	10	-383	-447	634	529	-107
C_3H_7	148	127	77	-31	-48	-56	935	871	-79	31	-346	-372	504	483	-135
C_4H_9	146	125	78	-31	-47	-55	938	877	-76	30	-348	-372	505	484	-135
C_5H_{11}	151	128	80	-32	-48	-57	933	867	-86	34	-344	-371	503	480	-138
C_7H_{15}	158	131	83	-33	-50	-59	930	854	-93	36	-339	-369	502	476	-139
$C_8H_{18}NO_8$	188	160	96	-33	-55	-64	7879	2496	25	-9	-873	-2752	5033	1535	-127
LiH^+	20	18	18	-0	-0	-2	-0	-3	-3	2	2	0	-36	-38	-38
NaF^+	268	268	131	-33	-67	-67	512498	199364	-15	7	-49916	-127925	384363	149238	-322
Cys-Gly_4	279	257	135	-25	-42	-50	239508	16025	341	-40	-2438	-36008	203487	13584	180
MTSL	306	228	186	-60	-74	-99	8783	5928	-98	27	-1863	-2679	5948	3967	-245

Table C.39: Miscellaneous data and isotropic g-shifts [ppm] for the g-tensor calculations with Z_{eff}-SDC-DF-LUCC2 at the def2-TZVP/DF-TZ level with DF-UHF reference, Boughton-Pulay domains and pair lists restricted using $|E_{IJ}| > 3.0 \cdot 10^{-5}$ Hartree for the benchmark set of molecules with a single spin-center used by Glasbrenner *et al.*[35]

Molecule	E_{HF} [Hartree]	E_{corr} [Hartree]	$< S^2 >_{HF}$	$\frac{N_{pairs\ included}}{N_{all\ pairs}}$ [%]	N_{AO}	$t_{CPU}^{DF-LUCC2}$ [sec]	Δg^{ZKE}	$\Delta g_{iso}^{1el-DSO}$	$\Delta g_{iso}^{2el-DSO}$	$\Delta g_{iso}^{1el-PSO}$	$\Delta g_{iso}^{2el-PSO}$	Δg_{iso}
CH_3	-39.577690	-0.150366	0.76	100.0	49	33.90	-126	88	-33	741	-292	377
$C_{10}H_{21}$	-391.010152	-1.645854	0.76	47.6	436	2300.42	-137	127	-48	607	-241	307
$C_{15}H_{31}$	-586.248976	-2.476869	0.76	33.5	651	12266.50	-137	129	-49	603	-240	307
$C_{17}H_{27}O$	-734.590825	-2.931229	1.40	34.2	720	21892.22	-138	184	-73	598	-236	334
$C_{19}H_{39}O$	-817.324206	-3.355784	0.76	25.7	854	38857.18	-299	197	-61	81390	-24467	56760
$C_{20}H_{41}$	-781.487784	-3.307890	0.76	25.8	866	26505.45	-137	130	-49	602	-240	306
$C_{21}H_{41}$	-819.373665	-3.441934	0.98	25.3	897	39422.94	-131	160	-63	688	-271	383
C_2H_5	-78.628163	-0.316009	0.76	100.0	92	46.11	-130	107	-40	734	-292	379
C_3H_7	-117.675535	-0.482209	0.76	100.0	135	83.89	-135	119	-46	615	-244	309
C_4H_9	-156.723549	-0.648609	0.76	90.6	178	190.88	-136	118	-45	626	-248	314
C_5H_{11}	-195.771318	-0.814838	0.76	79.9	221	334.04	-137	121	-46	617	-245	310
C_7H_{15}	-273.866852	-1.147246	0.76	63.2	307	786.02	-137	124	-47	611	-243	308
$C_8H_{18}NO_8$	-966.929594	-3.376837	0.76	29.9	635	9852.95	-204	150	-51	3382	-1181	2094
LiH^+	-7.738130	-0.000000	0.75	nan	20	32.58	-55	19	-1	-2	1	-37
NaF^+	-261.085561	-0.164851	0.75	100.0	63	35.26	-412	222	-56	237498	-59333	177920
Cys-Gly_4	-1546.412307	-4.338328	0.76	26.7	827	31303.51	-229	223	-40	90219	-13571	76603
MTSL	-1463.419929	-2.882853	0.77	44.4	616	10792.59	-298	242	-79	5680	-1753	3793

Table C.40: Eigenvalues of the g-shifts [ppm] calculated with Z_{eff}-SDC-DF-LUCC2 at the def2-TZVP/DF-TZ level with DF-UHF reference, Boughton-Pulay domains and pair lists restricted using $|E_{IJ}| > 3.0 \cdot 10^{-5}$ Hartree for the benchmark set of molecules with a single spin-center used by Glasbrenner *et al.*[35]

Molecule	$\Delta g_{diag1}^{1el-DSO}$	$\Delta g_{diag2}^{1el-DSO}$	$\Delta g_{diag3}^{1el-DSO}$	$\Delta g_{diag1}^{2el-DSO}$	$\Delta g_{diag2}^{2el-DSO}$	$\Delta g_{diag3}^{2el-DSO}$	$\Delta g_{diag1}^{1el-PSO}$	$\Delta g_{diag2}^{1el-PSO}$	$\Delta g_{diag3}^{1el-PSO}$	$\Delta g_{diag1}^{2el-PSO}$	$\Delta g_{diag2}^{2el-PSO}$	$\Delta g_{diag3}^{2el-PSO}$	Δg_{diag1}	Δg_{diag2}	Δg_{diag3}
CH_3	108	108	47	-20	-40	-40	1095	1095	32	-13	-432	-432	605	605	-79
$C_{10}H_{21}$	162	133	86	-34	-50	-60	971	936	-87	34	-372	-386	528	526	-133
$C_{15}H_{31}$	165	135	87	-34	-51	-61	970	930	-90	34	-370	-385	527	526	-133
$C_{17}H_{27}O$	236	173	142	-56	-70	-92	982	975	-164	68	-388	-389	599	538	-135
$C_{19}H_{39}O$	243	216	131	-41	-66	-75	234096	10080	-6	7	-3032	-70376	163568	6916	-204
$C_{20}H_{41}$	166	136	87	-34	-51	-61	968	928	-90	35	-369	-385	526	526	-134
$C_{21}H_{41}$	198	142	140	-54	-57	-78	1090	1000	-25	12	-393	-433	614	597	-62
C_2H_5	134	122	64	-25	-45	-49	1210	1020	-27	9	-405	-481	684	561	-108
C_3H_7	151	128	79	-31	-49	-57	976	946	-77	30	-375	-388	530	529	-131
C_4H_9	148	126	79	-31	-48	-55	982	967	-70	27	-383	-389	540	531	-129
C_5H_{11}	152	129	81	-33	-48	-57	975	955	-79	30	-379	-387	535	528	-133
C_7H_{15}	157	131	83	-33	-49	-59	973	944	-84	32	-375	-386	531	527	-133
$C_8H_{18}NO_8$	191	159	99	-35	-55	-65	7521	2606	19	-7	-912	-2625	4802	1608	-127
LiH^+	20	18	18	-0	-0	-2	-0	-3	-3	2	2	0	-36	-38	-38
NaF^+	268	268	131	-33	-67	-67	513151	199358	-14	7	-49917	-128089	384852	149230	-321
Cys-Gly_4	279	255	135	-26	-43	-51	253353	17160	145	-15	-2616	-38081	215256	14541	12
MTSL	304	232	188	-61	-76	-99	10856	6278	-93	25	-1973	-3310	7398	4213	-232

Table C.41: Eigenvalues of the g-shifts and isotropic g-shifts [ppm] calculated with SOMF-GIAO-B3LYP at the def2-TZVP level for their benchmark set of molecules with multiple spin-centers by Glasbrenner *et al.*[35]

Molecule	Δg_{diag1}	Δg_{diag2}	Δg_{diag3}	Δg_{iso}
$C_7H_{14}NOS$	138658	20575	2805	54013
$C_{19}FH_{26}$	3704	1518	-155	1689
$NHCH_2$	2196	901	-39	1019
$NHCH_2CH_2$	2623	996	-78	1180
$NH[CH_2O]_7CH_2S$	108747	9710	-100	39452
$NH[CH_2]_{14}CH_2$	2378	928	143	1150
$NH[CH_2]_2CH_2$	2468	948	112	1176
$NH[CH_2]_3CH_2$	2564	897	-15	1149
$NH[CH_2]_4CH_2$	2376	931	143	1150
$NH[CH_2]_9CH_2$	2579	927	-57	1150
$OC[CH_2]_{17}C_2$	1353	-118	-3253	-673
$O[CH_2]_{18}NH$	34749	3795	561	13035
Ala-Gly_2-Lys	2632	887	-32	1162

Table C.42: Eigenvalues of the g-shifts and isotropic g-shifts [ppm] calculated with SOMF-SDC-B3LYP at the def2-TZVP level for their benchmark set of molecules with multiple spin-centers by Glasbrenner *et al.*[35]

Molecule	Δg_{diag1}	Δg_{diag2}	Δg_{diag3}	Δg_{iso}
$C_7H_{14}NOS$	138718	20968	2975	54220
$C_{19}FH_{26}$	4197	1786	-28	1985
$NHCH_2$	2288	890	-7	1057
$NHCH_2CH_2$	2764	978	-28	1238
$NH[CH_2O]_7CH_2S$	108742	9710	-100	39451
$NH[CH_2]_{14}CH_2$	3289	913	456	1553
$NH[CH_2]_2CH_2$	2646	943	178	1256
$NH[CH_2]_3CH_2$	2818	899	67	1261
$NH[CH_2]_4CH_2$	2692	915	255	1287
$NH[CH_2]_9CH_2$	3178	949	129	1419
$OC[CH_2]_{17}C_2$	1487	-96	-3248	-619
$O[CH_2]_{18}NH$	35002	4513	1110	13542
Ala-Gly_2-Lys	3149	1032	111	1431

Table C.43: Miscellaneous data and isotropic g-shifts [ppm] for the g-tensor calculations with Z_{eff}-SDC-DF-LUCC2 at the def2-TZVP/DF-QZ level with DF-UHF reference, extended domains and full pair lists for the benchmark set of molecules with multiple spin-centers used by Glasbrenner *et al.*[35]

Molecule	E_{HF} [Hartree]	E_{corr} [Hartree]	$< S^2 >_{HF}$	$\frac{N_{pairs\ included}}{N_{all\ pairs}}$ [%]	N_{AO}	$t_{CPU}^{DF-LUCC2}$ [sec]	Δg^{ZKE}	$\Delta g_{iso}^{1el-DSO}$	$\Delta g_{iso}^{2el-DSO}$	$\Delta g_{iso}^{1el-PSO}$	$\Delta g_{iso}^{2el-PSO}$	Δg_{iso}
$C_7H_{14}NOS$	-800.105371	-1.677787	3.79	100.0	400	21567.68	-240	327	-95	90647	-18259	72380
$C_{19}FH_{26}$	nan	nan	2.28	100.0	807	nan	nan	nan	nan	nan	nan	nan
$NHCH_2$	-133.048391	-0.479310	2.03	100.0	123	174.76	-173	146	-52	1998	-712	1206
$NHCH_2CH_2$	-172.096539	-0.647868	2.02	100.0	166	510.07	-169	171	-61	2247	-800	1387
$NH[CH_2O]_7CH_2S$	-1288.974399	-3.310315	2.03	100.0	635	81907.07	-211	467	-131	48912	-7716	41320
$NH[CH_2]_{14}CH_2$	-679.717560	-2.846345	2.03	100.0	725	123102.18	-173	526	-181	2021	-721	1472
$NH[CH_2]_2CH_2$	-211.144381	-0.816902	2.02	100.0	209	1195.64	-169	191	-67	2232	-795	1390
$NH[CH_2]_3CH_2$	-250.191957	-0.986242	2.03	100.0	252	1862.86	-172	225	-80	2169	-771	1371
$NH[CH_2]_4CH_2$	-289.239793	-1.155391	2.03	100.0	295	3353.46	-172	250	-88	2158	-768	1380
$NH[CH_2]_9CH_2$	-484.478731	-2.000896	2.03	100.0	510	25213.77	-173	390	-135	2088	-743	1426
$OC[CH_2]_{17}C_2$	-852.152000	-3.482651	2.34	100.0	855	168842.96	-192	971	-359	-1849	618	-810
$O[CH_2]_{18}NH$	-832.695350	-3.400707	2.02	100.0	842	206400.95	-253	636	-207	52939	-16002	37113
Ala-Gly_2-Lys	-1152.663605	-4.250003	2.03	100.0	851	184981.74	-176	463	-162	1929	-685	1369

Table C.44: Eigenvalues of the g-shifts [ppm] calculated with Z_{eff}-SDC-DF-LUCC2 at the def2-TZVP/DF-QZ level with DF-UHF reference, extended domains and full pair lists for the benchmark set of molecules with multiple spin-centers used by Glasbrenner *et al.*[35]

Molecule	$\Delta g^{1el-DSO}_{diag1}$	$\Delta g^{1el-DSO}_{diag2}$	$\Delta g^{1el-DSO}_{diag3}$	$\Delta g^{2el-DSO}_{diag1}$	$\Delta g^{2el-DSO}_{diag2}$	$\Delta g^{2el-DSO}_{diag3}$	$\Delta g^{1el-PSO}_{diag1}$	$\Delta g^{1el-PSO}_{diag2}$	$\Delta g^{1el-PSO}_{diag3}$	$\Delta g^{2el-PSO}_{diag1}$	$\Delta g^{2el-PSO}_{diag2}$	$\Delta g^{2el-PSO}_{diag3}$	Δg_{diag1}	Δg_{diag2}	Δg_{diag3}
$C_7H_{14}NOS$	390	308	283	-80	-89	-118	202289	65558	4093	-1155	-15353	-38269	166305	47897	2937
$C_{19}FH_{26}$	nan	nan	nan	nan	nan	nan	nan	nan	nan	nan	nan	nan	nan	nan	nan
$NHCH_2$	184	132	122	-43	-48	-66	4219	1644	131	-59	-595	-1483	2667	967	-15
$NHCH_2CH_2$	221	151	140	-50	-55	-79	4958	1762	20	-9	-639	-1752	3163	1060	-63
$NH[CH_2O]_7CH_2S$	641	538	222	-53	-158	-181	136281	10696	-242	75	-2094	-21128	115301	8659	1
$NH[CH_2]_{14}CH_2$	748	709	120	-42	-243	-257	4714	1416	-68	2	-511	-1655	3288	930	197
$NH[CH_2]_2CH_2$	228	208	135	-48	-74	-80	4691	1688	317	-129	-609	-1648	3011	1017	144
$NH[CH_2]_3CH_2$	296	255	125	-46	-90	-104	4896	1543	69	-30	-554	-1729	3157	948	8
$NH[CH_2]_4CH_2$	335	295	120	-43	-104	-117	4568	1621	286	-120	-586	-1597	2980	987	174
$NH[CH_2]_9CH_2$	546	499	124	-45	-172	-189	4996	1437	-170	56	-516	-1770	3341	950	-13
$OC[CH_2]_{17}C_2$	1472	1416	25	-9	-522	-545	611	-180	-5977	1978	51	-174	1139	-301	-3269
$O[CH_2]_{18}NH$	901	851	155	-48	-278	-295	151874	6702	241	-78	-2097	-45832	106039	4951	348
Ala-Gly_2-Lys	670	643	75	-28	-225	-233	4771	1161	-145	48	-417	-1688	3246	880	-20

Bibliography

[1] C. M. Marian. Spin-orbit coupling in molecules. *Rev. Comp. Chem*, 17:99, 2001.

[2] W. Gerlach and O. Stern. Der experimentelle Nachweis des magnetischen Moments des Silberatoms. *Z. Phys*, 8:110, 1922.

[3] W. Gerlach and O. Stern. Der experimentelle Nachweis der Richtungsquantelung im Magnetfeld. *Z. Phys*, 9:349, 1922.

[4] W. Pauli. Zur Quantenmechanik des magnetischen Elektrons. *Z. Phys*, 43:601, 1927.

[5] E. Zavoisky. Spin-magnetic resonance in paramagnetics. *J. Phys. USSR*, 9:211, 1945.

[6] F. Neese and M. L. Munzarová. Historical Aspects of EPR Parameter Calculations. In M. Kaupp, M. Bühl, and V. G. Malkin, editors, *Calculation of NMR and EPR Parameters. Theory and Application.* Wiley-VCH Verlag GmbH & Co. KGaA, Weinheim, Germany, 2004.

[7] W. B. Mims and J. Peisach. *Advanced EPR: Applications in Biology and Biochemistry.* Elsevier, Amsterdam, Netherlands, 1989.

[8] C. S. Sunandana. Techniques and applications of electron spin resonance. *Bull. Mater. Sci.*, 21:1, 1998.

[9] A. Schweiger and G. Jeschke. *Principles of Pulse Electron Paramagnetic Resonance.* Oxford University Press, Oxford, United Kingdom, 2001.

[10] R. McWeeny. On the origin of Spin-Hamiltonian Parameters. *J. Chem. Phys.*, 42:1717, 1965.

[11] W. H. Moores and R. McWeeny. The calculation of spin-orbit splitting and g tensors for small molecules and radicals. *Proc. R. Soc. Lon. A*, 332:365, 1973.

[12] J. E. Harriman. *Theoretical foundations of Electron Spin Resonance.* Academic Press, New York, New York, 1978.

[13] G. H. Lushington, P. Bündgen, and F. Grein. Ab initio study of molecular g-tensors. *Int. J. Quant. Chem.*, 55:377, 1995.

[14] P. J. Bruna, G. H. Lushington, and F. Grein. Electron-spin g-factors of H2-. An ab initio study. *Chem. Phys. Lett.*, 258:427, 1996.

[15] G. H. Lushington and F. Grein. Complete to second-order ab initio level calculations of electronic g-tensors. *Theor. Chim. Acta*, 93:259, 1996.

[16] G. H. Lushington and F. Grein. The electronic g-tensor of MgF: A comparison of ROHF and MRD-CI level results. *Int. J. Quant. Chem.*, 60:1679, 1996.

[17] G. H. Lushington and F. Grein. Multireference configuration interaction calculations of electronic g-tensors for NO2, H2O+, and CO+. *J. Chem. Phys.*, 106:3292, 1997.

[18] G. H. Lushington. Small Closed-Form CI Expansions for Electronic g-Tensor Calculations. *J. Phys. Chem.*, 104:2969, 2000.

[19] O. Vahtras, B. Minaev, and H. Ågren. Ab initio calculations of electronic g-factors by means of multiconfiguration response theory. *Chem. Phys. Lett.*, 281:186, 1997.

[20] M. Engström, B. Minaev, O. Vahtras, and H. Ågren. Linear response calculations of electronic g-factors and spin-rotational coupling constants for diatomic molecules with a triplet ground state. *Chem. Phys. Lett.*, 237:149, 1998.

[21] M. Engström, O. Vahtras, and H. Ågren. Hartree-Fock linear response calculations of g-tensors of substituted benzene radicals. *Chem. Phys. Lett.*, 243:263, 1999.

[22] M. Engström, F. Himo, and H. Ågren. Ab initio g-tensor calculations of the thioether substituted tyrosyl radical in galactose oxidase. *Chem. Phys. Lett*, 319:191, 2000.

[23] M. Engström, F. Himo, A. Gräslund, B. Minaev, O. Vahtras, and H. Ågren. Hydrogen Bonding to Tyrosyl Radical Analyzed by Ab Initio g-Tensor Calculations. *J. Phys. Chem*, 104:5149, 2000.

[24] M. Engström, O. Vahtras, and H. Ågren. MCSCF and DFT calculations of EPR parameters of sulfur centered radicals. *Chem. Phys. Lett.*, 328:483, 2000.

[25] M. Engström, R. Owenius, and O. Vahtras. Ab initio g-tensor calculations of hydrogen bond effects on a nitroxide spin label. *Chem. Phys. Letters*, 338:407, 2001.

[26] G. Schreckenbach and T. Ziegler. Calculation of the G-Tensor of Electron Paramagnetic Resonance Spectroscopy Using Gauge-Including Atomic Orbitals and Density Functional Theory. *J. Phys. Chem. A*, 101:3388, 1997.

[27] G. Schreckenbach and T. Ziegler. Density functional calculations of NMR chemical shifts and ESR g-tensors. *Theor. Chem. Acc.*, 99:71, 1998.

[28] S. Patchkovskii and T. Ziegler. Prediction of electron paramagnetic resonance g-tensors of transition metal complexes using density functional theory: First applications to some axial d 1 MEX 4 systems. *J. Chem. Phys.*, 111:5730, 1999.

[29] S. Patchkovskii and T. Ziegler. Structural Origin of Two Paramagnetic Species in Six-Coordinated Nitrosoiron(II) Porphyrins Revealed by Density Functional Theory Analysis of the g Tensors. *Inorg. Chem.*, 39:5354, 2000.

[30] S. Patchkovskii and T. Ziegler. Prediction of EPR g Tensors in Simple d 1 Metal Porphyrins with Density Functional Theory. *J. Am. Chem. Soc.*, 122:3506, 2000.

[31] S. Patchkovskii and T. Ziegler. Calculation of the EPR g-Tensors of High-Spin Radicals with Density Functional Theory. *J. Phys. Chem.*, 105:5490, 2001.

[32] J. Autschbach and T. Ziegler. Double perturbation theory: a powerful tool in computational coordination chemistry. *Coord. Chem. Rev*, 238:83, 2002.

[33] J. Gauss, M. Kállay, and F. Neese. Calculation of Electronic g-Tensors using Coupled Cluster Theory. *J. Phys. Chem. A*, 113:11541, 2009.

[34] A. Perera, J. Gauss, P. Verma, and J. A. Morales. Benchmark coupled-cluster g-tensor calculations with full inclusion of the two-particle spin-orbit contributions. *J. Chem. Phys.*, 146:164104, 2017.

[35] M. Glasbrenner, S. Vogler, and C. Ochsenfeld. Gauge-origin dependence in electronic g-tensor calculations. *J. Chem. Phys.*, 148:214101, 2018.

[36] M. Glasbrenner, S. Vogler, and C. Ochsenfeld. Linear and sublinear scaling computation of the electronic g-tensor at the density functional theory level. *J. Chem. Phys.*, 150:024104, 2019.

[37] I. Malkin, O. L. Malkina, V. G. Malkin, and M. Kaupp. Relativistic two-component calculations of electronic g-tensors that include spin polarization. *J. Chem. Phys.*, 123:244103, 2005.

[38] S. Komorovský, M. Repiský, O. L. Malkina, V. G. Malkin, I. Malkin, and M. Kaupp. Resolution of identity Dirac-Kohn-Sham method using the large component only: Calculations of g-tensor and hyperfine tensor. *J. Chem. Phys.*, 124:084108, 2006.

[39] P. Hrobárik, O. L. Malkina, V. G. Malkin, and M. Kaupp. Relativistic two-component calculations of electronic g-tensor for oxo-molybdenum(V) and oxo-tungsten(V) complexes: The important role of higher-order spin-orbit contributions. *Chem. Phys.*, 356:229, 2009.

[40] P. Hrobárik, M. Repiský, S. Komorovský, V. Hrobáriková, and M. Kaupp. Assessment of higher-order spin–orbit effects on electronic g-tensors of d^1 transition-metal complexes by relativistic two- and four-component methods. *Theor. Chem. Acc.*, 129:715, 2011.

[41] S. Gohr, P. Hrobárik, M. Repiský, S. Komorovský, K. Ruud, and M. Kaupp. Four-Component Relativistic Density Functional Theory Calculations of EPR g- and Hyperfine-Coupling Tensors Using Hybrid Functionals: Validation on Transition-Metal Complexes with Large Tensor Anisotropies and Higher-Order Spin-Orbit Effects. *J. Phys. Chem. A*, 119:12892, 2015.

[42] A. Wodyński and M. Kaupp. Density Functional Calculations of Electron Paramagnetic Resonance g- and Hyperfine-Coupling Tensors Using the Exact Two-Component (X2C) Transformation and Efficient Approximations to the Two-Electron Spin–Orbit Terms. *J. Phys. Chem. A*, 123:5660, 2019.

[43] S. Saebø and P. Pulay. Local treatment of electron correlation. *Annu. Rev. Phys. Chem.*, 44:213, 1993.

[44] T. Korona, D. Kats, M. Schütz, T.B. Adler, Y. Liu, and H.-J. Werner. Local approximations for an efficient and accurate treatment of electron correlation and electron excitations in molecules. In R. Zalesny, M. Papadopoulos, P. Mezey, and J. Leszczynski, editors, *Linear-Scaling Techniques in Computational Chemistry and Physics. Challenges and Advances in Computational Chemistry and Physics*, volume 13. Springer, 2011.

[45] D. Kats, T. Korona, and M. Schütz. Local CC2 electronic excitation energies for large molecules with density fitting. *J. Chem. Phys.*, 125:104106, 2006.

[46] D. Kats, T. Korona, and M. Schütz. Transition strengths and first-order properties of excited states from local coupled cluster CC2 response theory with density fitting. *J. Chem. Phys.*, 127:064107, 2007.

[47] D. Kats and M. Schütz. A multistate local coupled cluster CC2 response method based on the Laplace transform. *J. Chem. Phys*, 131:124117, 2009.

[48] D. Kats and M. Schütz. Local Time-Dependent Coupled Cluster Response for Properties of Excited States in Large Molecules. *Z. Phys. Chem*, 224:601, 2010.

[49] K. Freundorfer, D. Kats, T. Korona, and M. Schütz. Local CC2 response method for triplet states based on Laplace transform: Excitation energies and first-order properties. *J. Chem. Phys.*, 133:244110, 2010.

[50] K. Ledermüller, D. Kats, and M. Schütz. Local CC2 response method based on the Laplace transform: Orbital-relaxed first-order properties for excited states. *J. Chem. Phys*, 139:084111, 2013.

[51] K. Ledermüller and M. Schütz. Local CC2 response method based on the Laplace transform: Analytic energy gradients for ground and excited states. *J. Chem. Phys.*, 140:164113, 2014.

[52] S. Loibl and M. Schütz. NMR shielding tensors for density fitted local second-order Møller-Plesset perturbation theory using gauge including atomic orbitals. *J. Chem. Phys.*, 137:084107, 2012.

[53] S. Loibl and M. Schütz. Magnetizability and rotational g tensors for density fitted local second-order Møller-Plesset perturbation theory using gauge-including atomic orbitals. *J. Chem. Phys.*, 141:024108, 2014.

[54] G. Wälz, D. Usvyat, T. Korona, and M. Schütz. A hierarchy of local coupled cluster singles and doubles response methods for ionization potentials. *J. Chem. Phys.*, 144:084117, 2016.

[55] David David. *Development of local Coupled Cluster response methods for high-spin open-shell molecules*. PhD thesis, 2018.

[56] J. Čížek. On the Correlation Problem in Atomic and Molecular Systems. Calculation of Wavefunction Components in Ursell-Type Expansion Using Quantum-Field Theoretical Methods. *J. Chem. Phys.*, 45:4256, 1966.

[57] J. Čížek. On the Use of the Cluster Expansion and the Technique of Diagrams in Calculations of Correlation Effects in Atoms and Molecules. *Adv. in Chem. Phys.*, 14:35, 1969.

[58] G. D. Purvis and R. J. Bartlett. A full coupled-cluster singles and doubles model: The inclusion of disconnected triples. *J. Chem. Phys*, 76:1910, 1982.

[59] G. E. Scuseria and H. F. Schaefer. Is coupled cluster singles and doubles (CCSD) more computationally intensive than quadratic configuration interaction (QCISD)? *J. Chem. Phys.*, 90:3700, 1998.

[60] I. Shavitt and R. J. Bartlett. *Many-Body Methods in Chemistry and Physics: MBPT and Coupled-Cluster Theory*. Cambridge University Press, Cambridge, United Kingdom, 2009.

[61] J. Autschbach. Orbitals: Some Fiction and Some Facts. *J. Chem. Educ.*, 89:1032, 2012.

[62] O. Christiansen, H. Koch, and P. Jørgensen. The second-order approximate coupled cluster singles and doubles model CC2. *Chem. Phys. Lett.*, 243:409, 1995.

[63] J. A. Pople and R. K. Nesbet. Self-Consistent Orbitals for Radicals. *J. Chem. Phys.*, 22:571, 1954.

[64] C. C. J. Roothaan. Self-Consistent Field Theory for Open Shells of Electronic Systems. *Rev. Mod. Phys.*, 32:179, 1960.

[65] P. J. Knowles, J. S. Andrews, R. D. Amos, and N. C. Handy. Restricted Møller-Plesset theory for open-shell molecules. *Chem. Phys. Lett.*, 186:130, 1991.

[66] J. Pipek and P. G. Mezey. A fast intrinsic localization procedure applicable for ab initio and semiempirical linear combination of atomic orbital wave functions. *J. Chem. Phys.*, 90:4916, 1989.

[67] S. F. Boys. Construction of Some Molecular Orbitals to Be Approximately Invariant for Changes from One Molecule to Another. *Rev. Mod. Phys.*, 32:296, 1960.

[68] J. M. Foster and S. F. Boys. Canonical Configurational Interaction Procedure. *Rev. Mod. Phys.*, 32:300, 1960.

[69] S. F. Boys. Quantum Theory of Atoms, Molecules, and the Solid State. *Academic Press, New York, NY*, page 253, 1966.

[70] G. Knizia. Intrinsic Atomic Orbitals: An Unbiased Bridge between Quantum Theory and Chemical Concepts. *J. Chem. Theory Comput.*, 9:4834, 2013.

[71] W. Meyer. Ionization energies of water from PNO-CI calculations. *Int. J. Quant. Chem.*, 5:341, 1971.

[72] F. Neese, F. Wennmohs, and A. Hansen. Efficient and accurate local approximations to coupled-electron pair approaches: An attempt to revive the pair natural orbital method. *J. Chem. Phys.*, 130:114108, 2009.

[73] J. Yang, Y. Kurashige, F. Manby, and G. K. L. Chan. Tensor factorizations of local second-order Møller-Plesset theory. *J. Chem. Phys*, 134:044123, 2011.

[74] C. Hampel and H.-J. Werner. Local treatment of electron correlation in coupled cluster theory. *J. Chem. Phys.*, 104:6286, 1996.

[75] M. Schuetz and H.-J. Werner. Low-order scaling local electron correlation methods. iv. linear scaling local coupled-cluster (lccsd). *J. Chem. Phys*, 114:661, 2001.

[76] D. Kats, D. Usvyat, and M. Schütz. On the use of the laplace transform in local correlation methods. *Phys. Chem. Chem. Phys*, 10:3430, 2008.

[77] J. W. Boughton and P. Pulay. Comparison of the boys and Pipek–Mezey localizations in the local correlation approach and automatic virtual basis selection. *J. Comput. Chem.*, 14:736, 1993.

[78] H.-J. Werner, F. R. Manby, and P. J. Knowles. Fast linear scaling second-order Møller-Plesset perturbation theory (MP2) using local and density fitting approximations. *J. Chem. Phys.*, 118:8149, 2003.

[79] B. I. Dunlap, J. W. D. Connolly, and J. R. Sabin. On some approximations in applications of Xα theory. *J. Chem. Phys.*, 71:3396, 1979.

[80] B. I. Dunlap. Robust and variational fitting. *Phys. Chem. Chem. Phys.*, 2:2113, 2000.

[81] B. I. Dunlap. Robust and variational fitting: Removing the four-center integrals from center stage in quantum chemistry. *J. Mol. Struc. (Theochem)*, 529:37, 2000.

[82] T. Helgaker, S. Coriani, P. Jørgensen, K. Kristensen, J. Olsen, and K. Ruud. Recent Advances in Wave Function-Based Methods of Molecular-Property Calculations. *Chem. Rev.*, 112:543, 2012.

[83] National Institute of Standards and Technology. CODATA Internationally recommended 2018 values of the fundamental physical constants. `https://physics.nist.gov/cuu/Constants/index.html`, 2018. Accessed: 2020-10-11.

[84] R. McWeeny. *Methods of Molecular Quantum Mechanics (Second Edition).* Academic Press, London, United Kingdom, 1992.

[85] S. Koseki, M. S. Gordon, M. W. Schmidt, and N. Matsunaga. Main Group Effective Nuclear Charges for Spin-Orbit Calculations. *J. Phys. Chem.*, 99:12764, 1995.

[86] S. Koseki, M. W. Schmidt, and M. S. Gordon. Effective Nuclear Charges for the First- through Third-Row Transition Metal Elements in Spin-Orbit Calculations. *J. Phys. Chem. A*, 102:10430, 1998.

[87] B. A. Heß, C. M. Marian, U. Wahlgren, and O. Gropen. A mean-field spin-orbit method applicable to correlated wavefunctions. *Chem. Phys. Lett.*, 251:365, 1996.

[88] A. Berning, M. Schweizer, H.-J. Werner, P. J. Knowles, and P. Palmieri. Spin-orbit matrix elements for internally contracted multireference configuration interaction wavefunctions. *Mol. Phys.*, 98:1823, 2000.

[89] F. Neese. Efficient and accurate approximations to the molecular spin-orbit coupling operator and their use in molecular g-tensor calculations. *J. Chem. Phys*, 122:034107, 2005.

[90] T. Helgaker and P. Jørgensen. An electronic Hamiltonian for origin independent calculations of magnetic properties. *J. Chem. Phys.*, 95:2595, 1991.

[91] F. London. Quantum theory of interatomic currents in aromatic compounds. *J. Phys. Radium*, 8:397, 1937.

[92] T. Helgaker, M. Jaszuński, and K. Ruud. Ab Initio Methods for the Calculation of NMR Shielding and Indirect Spin-Spin Coupling Constants. *Chem. Rev.*, 99:293, 1999.

[93] S. Loibl, F.R. Manby, and M. Schütz. Density fitted, local Hartree–Fock treatment of NMR chemical shifts using London atomic orbitals. *Mol. Phys.*, 108:1362, 2010.

[94] P. Pulay. Convergence acceleration of iterative sequences. The case of SCF iteration. *Chem. Phys. Lett.*, 73:393.

[95] P. Pulay. Improved SCF convergence acceleration. *J. Comput. Chem.*, 3:556, 1982.

[96] O. Christiansen, P. Jørgensen, and C. Hattig. Response Functions from Fourier Component Variational Perturbation Theory Applied to a Time-Averaged Quasienergy. *Int. J. Quant. Chem.*, 68:1, 1998.

[97] H.-J. Werner, P. J. Knowles, G. Knizia, F. R. Manby, and M. Schütz. Molpro: a general-purpose quantum chemistry program package. *WIREs Comput Mol Sci 2*, page 242, 2012.

[98] H.-J. Werner, P. J. Knowles, G. Knizia, F. R. Manby, M. Schütz, P. Celani, W. Györffy, D. Kats, T. Korona, R. Lindh, A. Mitrushenkov, G. Rauhut, K. R. Shamasundar, T. B. Adler, R. D. Amos, S. J. Bennie, A. Bernhardsson, A. Berning, D. L. Cooper, M. J. O. Deegan, A. J. Dobbyn, F. Eckert, E. Goll, C. Hampel, A. Hesselmann, G. Hetzer, T. Hrenar, G. Jansen, C. Köppl, S. J. R. Lee, Y. Liu, A. W. Lloyd, Q. Ma, R. A. Mata, A. J. May, S. J. McNicholas, W. Meyer, T. F. Miller III, M. E. Mura, A. Nicklass, D. P. O'Neill, P. Palmieri, D. Peng, K. Pflüger, R. Pitzer, M. Reiher, T. Shiozaki, H. Stoll, A. J. Stone, R. Tarroni, T. Thorsteinsson, M. Wang, and M. Welborn. MOLPRO, version 2019.2, a package of ab initio programs. `https://www.molpro.net`.

[99] R. Polly, H.-J. Werner, F. R. Manby, and Peter J. Knowles. Fast Hartree–Fock theory using local density fitting approximations. *Mol. Phys.*, 102:2311, 2004.

[100] W. Győrffy, T. Shiozakia, G. Knizia, and H.-J. Werner. Analytical energy gradients for second-order multireference perturbation theory using density fitting. *J. Chem. Phys.*, 138:104104, 2013.

[101] J. D. Hunter. Matplotlib: A 2D graphics environment. *Comput. Sci. & Engin.*, 9:90, 2007.

[102] N. B. Balabanov and K. A. Peterson. Systematically convergent basis sets for transition metals. I. All-electron correlation consistent basis sets for the 3d elements Sc-Zn. *J. Chem. Phys.*, 123:064107, 2005.

[103] T. H. Dunning. Gaussian basis sets for use in correlated molecular calculations. I. the atoms boron through neon and hydrogen. *J. Chem. Phys.*, 90:1007, 1989.

[104] R. A. Kendall, T. H. Dunning, and R. J. Harrison. Electron affinities of the first-row atoms revisited. Systematic basis sets and wave functions. *J. Chem. Phys.*, 96:6796, 1992.

[105] B. P . Prascher, D. E. Woon, K. A. Peterson, T. H. Dunning, and A. K. Wilson. Gaussian basis sets for use in correlated molecular calculations. VII. Valence, core-valence, and scalar relativistic basis sets for Li, Be, Na, and Mg. *Theor. Chem. Acc.*, 128:69, 2011.

[106] A. K. Wilson, D. E. Woon, K. A. Peterson, and T. H. Dunning. Gaussian basis sets for use in correlated molecular calculations. IX. the atoms gallium through krypton. *J. Chem. Phys.*, 110:7667, 1999.

[107] D. E. Woon and T. H. Dunning. Gaussian basis sets for use in correlated molecular calculations. IV. Calculation of static electrical response properties. *J. Chem. Phys.*, 100:2975, 1994.

[108] A. Perera and J. A. Morales. Private communication, 2020.

[109] F. Weigend and R. Ahlrichs. Balanced basis sets of split valence, triple zeta valence and quadruple zeta valence quality for H to Rn: Design and assessment of accuracy. *Phys. Chem. Chem. Phys.*, 7:3297, 2005.

[110] F. Weigend, A. Köhn, and C. Hättig. Efficient use of the correlation consistent basis sets in resolution of the identity MP2 calculations. *J. Chem. Phys.*, 116:3175, 2002.

[111] F. Weigend. A fully direct RI-HF algorithm: Implementation, optimised auxiliary basis sets, demonstration of accuracy and efficiency. *Phys. Chem. Chem. Phys.*, 4:4285, 2002.

[112] C. Hättig. Optimization of auxiliary basis sets for RI-MP2 and RI-CC2 calculations: Core–valence and quintuple-ζ basis sets for H to Ar and QZVPP basis sets for Li to Kr. *Phys. Chem. Chem. Phys.*, 7:59, 2005.

[113] F. Weigend. Hartree–Fock exchange fitting basis sets for H to Rn. *J. Comput. Chem*, 29:167, 2008.

[114] F. Weigend, M. Häser, H. Patzelt, and R. Ahlrichs. RI-MP2: optimized auxiliary basis sets and demonstration of efficiency. *Chem. Phys. Lett.*, 294:143, 1998.

[115] A. Hellweg, C. Hättig, S. Höfener, and W. Klopper. Optimized accurate auxiliary basis sets for RI-MP2 and RI-CC2 calculations for the atoms Rb to Rn. *Theor. Chem. Acc.*, 117:587, 2007.

[116] D. Kats and F. Manby. Sparse tensor framework for implementation of general local correlation methods. *J. Chem. Phys.*, 138:144101, 2013.

[117] E. P. Wigner. *Group Theory and its Application to the Quantum Mechanics of Atomic Spectra*. Academic Press, New York, New York, 1959.

[118] C. Eckart. The Application of Group theory to the Quantum Dynamics of Monoatomic Systems. *Rev. Mod. Phys.*, 2:305, 1930.

[119] T. Helgaker P. Jørgensen and J. Olsen. *Molecular Electronic-Structure Theory*. John Wiley & Sons Ltd., Chichester, United Kingdom, 2000.